
THE UNIVERSITY of ADELAIDE

# The Role of Colloidal Silver Synthesized from *Corymbia Maculata* in Eradicating Infection in Chronic Rhinosinusitis

**Sholeh Feizi**

BSc Animal Biology, MSc Biochemistry

A thesis submitted for the degree of Doctor of Philosophy at

The University of Adelaide in 2021

School of Medicine

## Table of Contents

**Thesis declaration**

I certify that this work contains no material which has been accepted for the award of any other degree or diploma in my name, in any university or other tertiary institution and, to the best of my knowledge and belief, contains no material previously published or written by another person, except where due reference has been made in the text. In addition, I certify that no part of this work will, in the future, be used in a submission in my name, for any other degree or diploma in any university or other tertiary institution without the prior approval of the University of Adelaide and where applicable, any partner institution responsible for the joint-award of this degree.

The author acknowledges that copyright of published works contained within the thesis resides with the copyright holder(s) of those works.

I also give permission for the digital version of my thesis to be made available on the web, via the University's digital research repository, the Library Search and also through web search engines, unless permission has been granted by the University to restrict access for a period of time.

Sholeh Feizi

28.10.2021

**Acknowledgements**

This thesis would not have been possible without the inspiration and support of a number of wonderful individuals, my thanks and appreciation to all of them for being part of this journey and making this thesis possible.

There are no proper words to convey my deep gratitude and respect for my thesis and research supervisors, Associate Professor Sarah Vreugde, Professor Peter-John Wormald and Professor Alkis James Psaltis. They have inspired me to become an independent researcher and helped me realize the power of critical reasoning. They also demonstrated what a brilliant and hard-working scientist can accomplish. They generously gave their time to offer me valuable comments toward improving my work and provided me constructive criticism which helped me develop a broader perspective to my thesis. Without their enthusiasm, encouragement, support and continuous optimism this thesis would hardly have been completed.

I am forever thankful to Dr. Clare Cooksley for her insight into addressing problems. She has immensely influenced this research. I would like to show my appreciation to all ENT group members at the University of Adelaide for sharing their expertise and experiences, and for providing valuable feedback throughout this research.

Finally, my deep and sincere gratitude to my family for their continuous and unparalleled love, help and support. I am forever indebted to my parents for giving me the opportunities and experiences that have made me who I am. I am grateful to my brother and sister who offered invaluable support and humor over the years. They selflessly encouraged me to explore new directions in life and seek my own destiny. This journey would not have been possible if not for them, and I dedicate this milestone to them.

**Financial Support**

I am writing to express my sincere gratitude to The University of Adelaide for making the Fee Scholarship possible. I am deeply appreciative of your support.

I appreciate the Hospital Research Foundation (THRF) at the Queen Elizabeth Hospital and the ENT group at the University of Adelaide for their financial support for my life expenses during the course of my research. I value the support you've given me.

**Publications Arising during this Thesis**

- Sholeh Feizi, Clare M Cooksley, George S Bouras, Clive A Prestidge, Tom Coenye, Alkis James Psaltis, Peter-John Wormald, Sarah Vreugde. ''Colloidal Silver combating Pathogenic *Pseudomonas aeruginosa* and MRSA in Chronic Rhinosinusitis'', Colloids and Surfaces B: Biointerfaces, 2021.

- Sholeh Feizi, Clare M Cooksley, Roshan Nepal, Alkis James Psaltis, Peter-John Wormald, Sarah Vreugde. ''Silver Nanoparticles as a Bioadjuvant of Antibiotics against Biofilm-Mediated Infections with MRSA and *P. aeruginosa* in Chronic Rhinosinusitis Patients'', Pathology, 2021.

- Sholeh Feizi, Shari Javadiyan, Clare M Cooksley, Gohar Shaghayegh, Alkis J Psaltis, Peter-John Wormald, Sarah Vreugde. ''Green Synthesized Colloidal Silver Is Devoid of Toxic Effects on Primary Human Nasal Epithelial Cells in Vitro'', Food and Chemical Toxicology, 2021

**Peer-Reviewed Presentations Arising from this Thesis**

**Oral Presentations**

2021

- ‘‘Safety of Green Synthesized Colloidal Silver to Primary Human Nasal Epithelial Cells’’
  The Queen Elizabeth Hospital Research Expo, October, Adelaide, Australia

2020

- ‘’Treatment of bacterial infections in chronic rhinosinusitis with bio synthesized colloidal silver’’
  The Queen Elizabeth Hospital Research Expo, October, Adelaide, Australia

2019

- ‘’Treatment of bacterial airway infections with green synthesized silver/silver chloride nanoparticle’’
  The Queen Elizabeth Hospital Research Expo, October, Adelaide, Australia

**Poster Presentation**

2020

- Treatment of bacterial infections in chronic rhinosinusitis with bio synthesized colloidal silver, Florey Postgraduate Research Conference, Adelaide, Australia (Virtual)

**Abbreviations**

| | |
|---|---|
| **CRS** | Chronic rhinosinusitis |
| **CRSsNP** | Chronic rhinosinusitis without nasal polyps |
| **CRSwNP** | Chronic rhinosinusitis with nasal polyps |
| **EPOS** | European Position Paper on Rhinosinusitis and Nasal Polyps |
| **COPD** | Chronic Obstructive Pulmonary Disease |
| **QoL** | Quality-of-life |
| **MH** | Manuka honey |
| **MGO** | Methylglyoxal |
| **PDT** | Photodynamic therapy |
| **EDTA** | Methylene blue/ethylene-diamine tetra acetic acid |
| **NO** | Nitric oxide |
| **SNOT – 22** | Sino - Nasal Outcome Test-22 |
| **TR** | Taste receptors |
| **CFTR** | Cystic fibrosis transmembrane conductance regulator |
| **ICAR** | International Consensus Statement on Allergy and Rhinology |
| **INCS** | Intranasal corticosteroids |
| **NPs** | Nanoparticles |
| **Ag NPs** | Silver Nanoparticles |
| **AMR** | Antimicrobial resistance |
| **MDR** | Multidrug-resistant |
| **WHO** | World Health Organization |
| **MRSA** | *Methicillin resistant Staphylococcus aureus* |
| **ROS** | Reactive oxygen species |
| **NADPH** | Niacinamide adenine dinucleotide phosphate |
| **MDA** | Malondialdehyde |
| **ssDBPs** | Single-stranded DNA binding proteins |
| **UDP** | Uridine diphosphate |
| **IUPAC** | International Union of Pure and Applied Chemistry |

| | |
|---|---|
| **EPS** | Extracellular Polymeric Substances |
| **TT** | Toxicity threshold |
| **FBS** | Fetal bovine serum |
| **BSA** | Bovine serum albumin |
| **HAS** | Human serum albumin |
| **GSH** | Reduced glutathione |

List of Tables

List of Figures

**Aims and Thesis Summary**

The purpose of this thesis is to report on the synthesis of silver nanoparticles (Ag NPs) [ also named colloidal silver (CS)] using plant extracts in a biocompatible way and examine its safety and efficacy against human nasal epithelial cells (HNECs) and clinical isolates separated from chronic rhinosinusitis (CRS) patients, respectively.

The work describes the synthesis and extensive characterization of Ag NPs manufactured using plant extracts as biocompatible reducing agents. Their safety and efficacy were then evaluated through *in vitro* and *in vivo* experiments. Focus was given to the synthesis of CS in an efficient way as it is a significant issue in the realm of topical therapy of infection in CRS by CS.

The thesis itself is composed of four chapters which deal with synthesis of Ag NPs and evaluating its safety and efficacy.

Chapter 1 serves as an introductory chapter and briefly explores the core concepts that underpin the subsequent chapters. It is subdivided into three sections. The first deals with chronic rhinosinusitis treatment, the second describes the antibacterial mechanism of CS and the third explains its mechanism of toxicity.

Chapter 2 is a peer-reviewed publication, describing the production of CS using gum tree fresh leaves and examining its efficacy and safety *in vitro* and *in vivo*.

Chapter 3 is a peer-reviewed publication, explaining the efficacy of CS once combined with antibiotics.

Chapter 4 is a peer-reviewed publication, elaborating the safety of CS to HNECs.

Chapter 5 is conclusions and reflections on future directions for this body of research.

## Chapter 1: Literature Review

### Chronic rhinosinusitis

The paranasal sinuses are comprised of four pairs of hollow cavities located near but apart from the nasal cavity. They are named following the skull bones from which they originate. They include the frontal, maxillary, ethmoid, and sphenoid sinuses which are in the low center of the forehead, the cheekbones, between the eyes and in bones behind the nose, respectively. The mucosa of the nasal passages is in continuity with the mucosa of sinuses. Rhinosinusitis refers to the inflammation of the sinus and nasal mucosal lining and can result in mucosal edema, sinus ostia obstruction, and mucociliary dysfunction (Figure 1.1) [1].

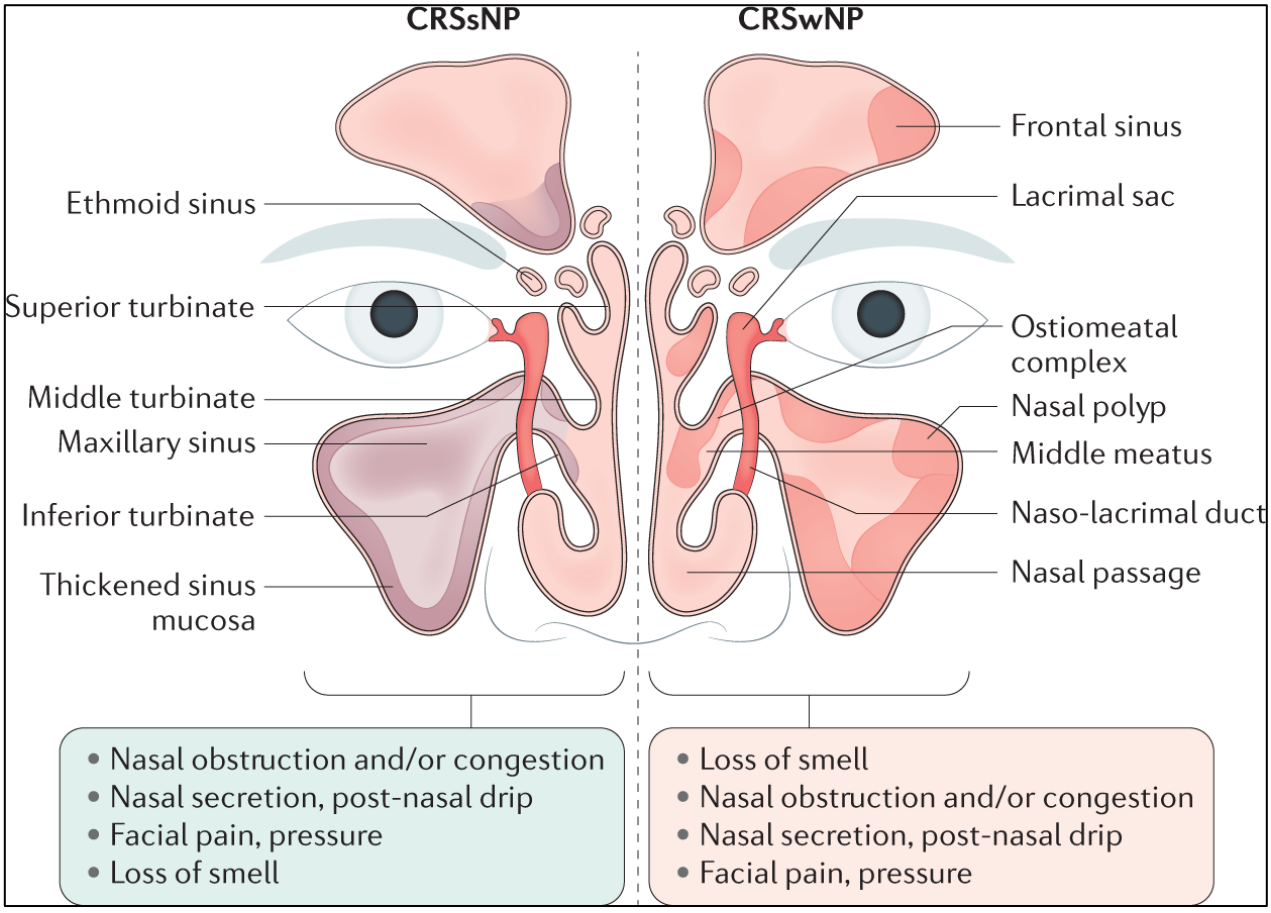


**Figure 1.1** Anatomy of the paranasal sinuses and the nasal passage.

Manifestations of chronic rhinosinusitis without nasal polyps (CRSsNP) and chronic rhinosinusitis with nasal polyps (CRSwNP) are illustrated [1].

According to the duration of the symptoms, rhinosinusitis is categorized into four different groups including acute rhinosinusitis, subacute rhinosinusitis, chronic rhinosinusitis (CRS), and recurrent acute

rhinosinusitis. The symptom duration of acute rhinosinusitis is less than four weeks; subacute rhinosinusitis is 4 to 12 weeks and CRS is more than 12 weeks. In contrast, recurrent acute rhinosinusitis describes recurrent infections lasting less than 4 weeks without persistent symptoms in between episodes [2-4]. Based on the endoscopic findings, CRS can be divided phenotypically into two groups including CRS with nasal polyps (CRSwNP) and CRS without nasal polyps (CRSsNP). These two groups typically have different associated inflammatory responses, can manifest differently in terms of symptoms and signs, and often have different responses to medical treatments [5]. Disease severity, the number of surgeries and medication use is often more frequent in CRSwNP in comparison to CRSsNP [6, 7]. Moreover, the probability of having other diseases such as asthma in patients with CRSwNP is also higher [8]

**Epidemiology of Chronic rhinosinusitis**

CRS is considered one of the most prevalent chronic diseases which places a significant cost on both people and society. It is diagnosed based on symptom profile with objective evidence of sinonasal inflammation on CT imaging or nasal endoscopy. Diagnostic criteria are clearly defined in the European Position Paper on Rhinosinusitis and Nasal Polyps (EPOS) paper published in 2020 [9]. However, most CRS cases (16% CRS reported cases) are reported by patients themselves rather than otolaryngologists [10-12]. The prevalence of CRS seems dependent on geographical variations based on population-based studies. According to Global Allergy and Asthma European Network, 57,128 CRS cases were reported in 12 European countries with the an average of 10.9% of the population per country [12]. Likewise, a prevalence of 12.1% was reported by a national health interview survey in the USA [13]. In Canada, the prevalence depends on age and was reported as 3.4% and 5.7% among 73,364 in females and males, respectively [10]. According to another survey, 10% of the population is affected by sinusitis in Australia [14, 15]. The frequency of CRS is higher than other chronic respiratory diseases such as hay fever (8.9%), chronic asthma (10.9%) and Chronic Obstructive Pulmonary Disease (COPD, 2.6%).

The direct cost of CRS can be related to health output such as outpatient visits (bearing the largest cost), followed by prescription medical therapy and surgical operations to manage the disease which cost 10$-13$ Billion in 2016 [16]. The financial cost per patient can reach $800 per year. However, the indirect cost of CRS is much greater, contributing to a high frequency of employee absenteeism and other social impacts. Research suggests the frequency of missed work days or absenteeism is 57% [16], followed by 13.3% activity limitation, 12% work limitation, 9% social limitation and 6% perceived cognitive limitations [17, 18]. Generally, the indirect cost of CRS is estimated to be more than $20 billion in the USA [19].

Symptoms arising from the inflammation caused by CRS include nasal congestion, anosmia, facial pain/pressure as well as anterior and posterior rhinorrhea. The symptoms are not just limited to the sinonasal passages; CRS can contribute to poor sleep quality [20], fatigue [21], bodily pain [22] and depression [23-25]. In general, CRS patients reported a severe deficiency in their quality-of-life (QoL) [26-28].

## Mechanism/Pathophysiology of chronic rhinosinusitis

### The epithelium and remodelling

The nasal epithelium acts as a physical and immunological barrier that is responsible for maintaining the balance of water and electrolytes along with the removal, degradation and neutralization of environmental particles and toxins. Secreted mucus and the mucociliary blanket also protect the nasal epithelial surface by trapping and removing environmental toxins. The epithelial cells themselves can protect against pathogens through different mechanisms including the production of enzymes, peptides, proteins, lipids and ions. Furthermore, they play a role in the activation of pattern recognition receptors that facilitate a response to microbial pathogens [29, 30].

### The microbiome of chronic rhinosinusitis

Man et al [31] demonstrated that different microorganisms such as bacteria, fungi and viruses live on healthy sinus mucosa. They not only interact with the mucosal immune system but also are important in the physiological maturation of the mucosa. In the disease state certain factors can influence the microbial ecology of the paranasal sinuses resulting in inflammation. Pathophysiological factors include the external and host environments, along with microbes, while pathological factors include changes in the microbiota (the group of microorganisms existing in a specific environment), lack of balance of the local or systemic immune system, allergens, toxins, and genetic predisposition [9, 32-35].

A recent multicentered study was conducted to characterize the sinonasal microbiome using 16S rRNA sequencing in a large group worldwide [36]. Based on the results, the core microbiome of the sinonasal tract was comprised of five different genera of bacteria, *Corynebacterium* (44.02%), *Staphylococcus* (27.34%), *Moraxella*, *Streptococcus* and *Haemophilus. Corynebacterium* and *Staphylococcus* were shown to be the most common and frequent genera in healthy control patients and could potentially function as essential commensal bacteria required to maintain the sinonasal physiology. *Streptococcus, Moraxella* and *Haemophilus* comprised the second most abundant group. The study further demonstrated a significant reduction of *Corynebacterium* in CRSwNP patients (40.29%) compared to healthy controls (50.43%), proposing its key role in the conversion of *S. aureus* from commensal to virulent bacteria [36].

Early studies revealed that the microbiomes of healthy control and CRS patients are different and introduced the dysbiosis theory of CRS [37, 38]. This theory suggests that sinus mucosal inflammation in CRS is initiated, propagated, or maintained by changes in sinus microbial communities away from "normal" or "healthy" microbes. Dysbiosis has either an intrinsic or environmental cause, but the source is currently unknown [39]. Different studies have reported varying changes in diversity. For example, Aurora et al., 2013 reported an increase in alpha diversity (the diversity of the species within one sample) in CRS patients [40], while other researchers reported lower bacterial diversity [37, 41, 42]. Cleland et al., 2016 [43] and Ramakrishnan and Frank, 2015 [44] found no difference in alpha diversity.

The sinuses were originally thought to be a sterile environment; however, recent studies revealed the presence of bacterial species in healthy sinuses which are referred to as the gate-keeping commensal bacteria. They include *S. epidermidis*, *Propionibacterium spp*., *Corynebacterium spp*. [45] and recently identified *Lactobacillus spp.* [46]. They provide stability to the healthy microbiome, rendering it more resistant to dysbiosis [45]. The collapse or reduction of these species interferes with not only the abundance, but also the conversion of a proportion of the non-pathogenic (*Staphylococcus*, *Propionibacterium* and *Corynebacterium spp*.) to pathogenic bacteria (*S. aureus, P. aeruginosa, Haemophilus spp.* and *S.* pneumoniae*)* amongst CRS patients [40, 45, 47, 48].

*S. aureus* and *P. aeruginosa* are reported to be involved in many cases of CRS [49-51] and are generally related to more severe disease, medical and surgical recalcitrance, post-operative complications and higher surgical revision rates [52-55]. These pathogenic species cause inflammation and injury to the sinuses in CRS patients through different mechanisms, one of which is the formation of biofilm [56-58].

*S. aureus* is the most prevalent species isolated from CRS patients at the time of sinus surgery [59]. The pathogenesis of *S. aureus* is associated with biofilm formation and intracellular residency within the epithelium [60] which allows the bacteria to escape the immune system and persist before initial infection. Once an opportunity presents, they arise to induce acute exacerbations and worsen current inflammation [61]. *S. aureus* can further contribute to CRS by working together with other organisms in multi microbial environments [62, 63]. Under normal circumstances, *S. aureus* has a significant impact on keeping the sinuses in a healthy condition and have been found in a high prevalence and relative abundance in control patients. In contrast, they exhibit greater virulence in CRS patients [64]. By forming biofilms, *S. aureus* can increase its resistance to antibiotics, impair the host immune system and increase its tolerance to nutritional deprivation [65]. Immune evasion is facilitated by the sequestered proteins originating from the bacterial biofilm and the Agr quorum sensing system [65].

## Medical therapies for chronic rhinosinusitis

### Bacteriophage cocktails

The use of topical delivery of bacteriophages for CRS treatment dates back to the 20th century. With the development of antibiotics around the same time, the application of phages in Western Medicine decreased however [66]. Bacteriophages are viruses that attach to a strain specific bacterial host and infect the bacteria through one of the lytic or lysogenic cycles. In the lytic cycle, bacteriophages both lyse host bacteria and infect other bacteria [67]. Non-antibiotic topical delivery of bacteriophages is a promising treatment for CRS given that they are species specific in their bactericidal action, meaning that commensal bacteria and host cells remain unaffected. They have been shown to penetrate bacterial biofilms, and have antibiofilm activity [68]. The application of phage cocktails instead of single phage isolates can improve their range of activity against bacteria and reduce the formation of phage resistant colonies [68, 69].

Safety and efficiency studies have been performed *in vitro* (Table 1.1) and *in vivo* in animal studies (Table 2.1) and human clinical trials (Table 3.1).

**Table 1.1** Overview of *in vitro* studies demonstrating the sensitivity and efficacy of phages or phage-derived enzymes to *ex vivo* isolates from CRS patients [70].

| Isolates from Sinonasal Swabs | Included CRS Patients | Phage | Phage Sensitivity | Efficacy |
|---|---|---|---|---|
| *S. aureus* [71] | 66 | CT-SA, cocktail<br>SA1, single phage | 94%<br>90% | Biofilm mass reduction: 80% after CT-SA application |
| *S. aureus* [72] | NS | P128, bacteriophage derived muralytic enzyme | NS | Biofilm mass reduction: 95.5% |
| *P. aeruginosa* [69] | 47 [1] | Pa193, single phage<br>Pa204, single phage<br>Pa222, single phage<br>Pa223, single phage<br>CT-PA, cocktail | 73%<br>53%<br>73%<br>71%<br>85% | Significant biofilm mass reduction after CT-PA, Pa222 and Pa223 |
| *S. aureus* [73] | 61 | P68, single phage | 74%<br>59% | NS |

| | | | | | |
|---|---|---|---|---|---|
| | | | K710, single phage<br>NOV012, cocktail | 85% | |
| *S. aureus* [74] | 9 [2] | | ISP, single phage | NS | Reduced IL-5 levels after 24 and 72 h, no significant changes compared to antibiotics |
| *S. aureus* [75] | 65 | | Sa83, single phage<br>Sa87, single phage | 69%<br>71% | NS |
| Different pathogen [3] [76] | 50 | | Sensitive phage from collection Biophage Pharma, NS | 80% | NS |
| *S. aureus* [77] | 15 | | AB-SA01, cocktail | 80% | NS |

NS = not specified. [1] CRS patients with or without cystic fibrosis. [2] Samples collected during functional endoscopic sinus surgery. [3] Different pathogen include *S. aureus*, *S. epidermidis*, *P. aeruginosa* and *H. influenzae*.

**Table 2.1** Overview of animal studies investigating the safety and efficacy of bacteriophages or phage-derived enzymes in the treatment of chronic rhinosinusitis [70].

| Pathogen | Animal Model + Application Method | Included Subjects | Phage | Safety | Efficacy |
|---|---|---|---|---|---|
| *S. aureus* [78] | Mice, intranasal instillation | 14 | Phage lysin CHAPk from bacteriophage K | NS | Two-log reduction in S. aureus cells 1 h after single application |
| *S. aureus* [79] | Sheep, frontal rinsing via mini trephinations | 27 | CT-SA cocktail | No histological changes to frontal sinus mucosa | Significant reduction of biofilm mass |
| *S. aureus* [73] | Sheep, frontal rinsing via mini trephinations | 21 | NOV012 cocktail | No histological changes to frontal sinus mucosa | NS |
| *P. aeruginosa* [73] | Sheep, frontal rinsing via mini trephinations | 32 | CT-PA cocktail | No histological changes to frontal sinus mucosa | Significant reduction of biofilm mass |

NS = not specified.

**Table 3.1** Overview of clinical trials investigating the safety and efficacy of phages or phage-derived enzymes in the treatment of (recalcitrant) rhinosinusitis [70].

| Study Type | Participants | Pathogen | Therapeutic Regimen | Phage | Safety | Efficacy |
|---|---|---|---|---|---|---|
| OBS [80] | Recalcitrant CRS (n = 60) | *S. aureus* | Nasal nebulizer | Phage lysate A-1 and B-7 | No reported AE | Clinical improvement: Excellent: 45%, Good: 33%, Fair: 17%, Poor: 5% |
| OBS [81] | Suppurative sinusitis (n = 46) | Different pathogen [1] | Oral or nasal drops, NS | Sensitive phage from collection, NS | NS | Clinical improvement: Full recovery: 83%, Marked: 7%, No effect: 11% |
| OBS [82] | Healthy carriers (n = 21) | *S. aureus* | Oral (n = 10) or nasal application (n = 11) | Staphylococcal monophage (n = 21), Pyophage cocktail (n = 21), Placebo (n = 21) | No reported AE after nasal therapy, mild AE 2 in 4 subjects after oral therapy. No changes in blood values. | NS |
| RCT [83] | Acute maxillary sinusitis (n = 58) | Different pathogen [3] | Preoperative nasal rinsing, followed by oral treatment (n = 38); Second generation cephalosporin (n = 20) | Polyvalent Pyophage | No reported AE | Clinical improvement: Excellent: 45%, Good: 33%, Fair: 17%, Poor: 5% |
| OBS [77] | Recalcitrant CRS (n = 9) | *S. aureus* | Intranasal high-volume irrigations | AB-SA01, cocktail | Mild AE [4] in 3 patients, all of them resolved by the end of the trial. No changes in vital | Clinical improvement: Full recovery: 83%, Marked: 7%, No effect: 11% |

| | | | | | | |
|---|---|---|---|---|---|---|
| | | | | | signs or blood values | |
| OBS [84] | CRS (n = 25) | Different pathogen [5] | Nasal (n = 4) or nasal + oral application (n = 21) | Sensitive phage from collection | NS | NS |

OBS = observational study; RCT = randomized controlled trial; CRS = chronic rhinosinusitis; AE = adverse events; n = number; NS: not specified; LKS = Lund-Kennedy Score. [1] Different pathogen include *S. aureus, E. coli, Klebsiella, Proteus* and *P. aeruginosa*. [2] Mild adverse events include vomiting, loose stool, gastric acidity, mild epigastric pain and low-grade fever. [3] Different pathogens include *S. pneumoniae, S. aureus, H. influenzae* and hemolytic streptococci. [4] Mild adverse events include diarrhea, epistaxis, oropharyngeal pain, cough and rhinalgia. [5] Different pathogens include *S. aureus*, *P. aeruginosa*, *Klebsiella pneumoniae* and *E. coli*.

**Probiotic irrigations**

Probiotics are live organisms providing health benefits, eliminating pathogens, and restoring or improving the colonization of healthy commensal microorganisms. Different formulations have been applied for the treatment of allergic rhinitis, and more specifically, they have been recently used for the treatment of CRS [85]. The use of oral probiotics for CRS has been shown to have some benefits in a recent study [86, 87], however another, randomized placebo-control trial involving two weeks of topical probiotic treatments did not demonstrate any microbial or clinical benefit [88].

**Manuka honey**

Manuka honey (MH) is well-known for its wound-healing and antibacterial properties [89]. Methylglyoxal (MGO) is the active component of MH with efficacy against different bacteria including *S. aureus*, MRSA and *P. aeruginosa* demonstrated *in vitro* [90-92]. The synergistic antibiofilm effect of MH components and MGO has been observed in the treatment of CRS [93]. In addition, the synergist effect of MH and rifampicin was reported to decline the biofilm biomass and kill *S. aureus* embedded within the biofilm [94]. Perceived benefits of MH over traditional antibiotics include over the counter availability, cheap cost, low side effect profile and the unlikeliness of bacteria developing resistance [95-97]. Four clinical trials have been conducted to evaluate the efficacy of MH for the treatment of CRS with the findings demonstrating improvement of symptoms and endoscopic scores, enhancement of cytokine expression and significant improvement in microbiological profiles [98-101].

**Surfactants**

Surfactants are important constituents of the innate immune system, consisting of phospholipids that coat the mucous membrane and eliminate the surface tension and mucus viscosity in the respiratory system [102]. Surfactants can disrupt bacterial cell membrane leading to biofilm eradication in CRS [103]. *In vitro* efficacy of baby shampoo against immature biofilms of *P. aeruginosa* has been reported, however, the efficacy of baby shampoo use in clinical trials of biofilm related CRS has produced conflicting findings [104]. Topical surfactants in the *in vivo* studies in CRS revealed the lack of consistency *in vivo* or human clinical trial evidence, and the high incidence of adverse effects [104-107]. Finally, the utility of surfactant-based agents for the treatment of CRS remains limited.

**Deferiprone and gallium-protoporphyrin**

Nutritional immunity is a process in which the immune system eliminates the availability of iron, an essential element for bacterial metabolism [108, 109]. Deferiprone, an oral iron chelator, and gallium-protoporphyrin, a heme analog, have been reported to show antibiofilm activity [110]. The mechanism underlying the action of deferiprone and gallium-protoporphyrin (DG) involves the chelation of environmental iron by deferiprone, causing expression of bacterial iron transporters, thereby increasing gallium-protoporphyrin uptake. Once inside the bacteria, gallium-protoporphyrin acts as a bactericidal agent [111]. A synergistic effect of DG in combination with gentamicin and ciprofloxacin has shown efficacy in a wound-healing gel in a sheep model. The efficacy and safety of topical DG combined with chitogel have demonstrated safety and efficacy in a sinusitis sheep model [112]. However, human trials are needed to confirm the efficacy of DG as a viable treatment strategy for CRS.

**Photodynamic therapy**

Photodynamic therapy (PDT) is a process in which different photosensitizers and various wavelengths of light are applied to change oxygen to free radicals that have bactericidal activity [113-117]. PDT can also act specifically through its ability to influence organisms that absorb the photosensitizer, further leading to death through exposure to a specific wavelength of light [118, 119]. PDT can eradicate biofilms, Gram-negative bacteria and antimicrobial-resistant organisms [113, 117, 120]. The efficacy of PDT to eliminate microbial biofilm in CRS has been reported previously *in vitro* [121]. That study confirmed the safety of PDT in a living human ciliated respiratory mucosal model [122] and the efficacy of methylene blue/ethylene-diamine tetra acetic acid (EDTA) photosensitizer and 670-nm non-thermal activating light in a maxillary sinus model of *P.*

*aeruginosa* and MRSA [123]. The efficacy of PDT and chlorhexidine has been demonstrated in the reduction of MRSA and surgical site infection [124]. More studies are required to demonstrate the efficacy of PDT against resistant bacteria in CRS.

**Nitric oxide therapy**

Enhancing mucociliary clearance and destroying bacterial membranes, enzymes and DNA, nitric oxide (NO) has a vital role in the innate immune defense in the airways, preventing an increase in pathogens in the sinonasal tract. [125-127]. The amount of NO is considered a biomarker [128]. For instance, the level of NO is low, moderately low and high in CRSwNP, CRSsNP and healthy patients [129, 130]. Its level is also high in patients under medical treatments and after surgery [131, 132]. The antibiofilm activity of NO may be due to the formation of acidified nistabutrite derivatives [133, 134]. The safety and efficacy of isosorbide mononitrate liposomes containing NO were reported both *in vitro* and *in vivo* (in a sheep model) [135, 136]. It has been observed that microparticles releasing NO showed efficacy against planktonic forms of clinical isolates isolated from CRS patients [137]. However, more studies are required to develop smaller nanoparticles and to translate *in vitro* experiments to *in vivo* clinical studies.

**Xylitol**

Xylitol, a 5-carbon nonionic compound, has been shown to improve the activity of the innate immune system through the reduction of the salt concentration of airway liquid [138]. Xylitol nasal sprays have been observed to lower the staphylococcal carriage rates in healthy people [139]. When applied to a *P. aeruginosa* CRS maxillary infection in a rabbit model, Xylitol has been shown to reduce the severity of sinusitis. [140]. Xylitol efficacy in the treatment of CRS has been demonstrated through reduction of Sino - Nasal Outcome Test (SNOT - 22) scores and increased concentration of nasal NO and NO synthase mRNA in the sinuses [141]. As Xylitol is cheap and has minimum harmful effects, more clinical studies should be performed to confirm its efficacy.

**Taste receptor therapy**

Taste receptors (TR) including bitter (T2R) and sweet (T1R) receptors exist in the sinonasal epithelium and have an impact on the regulation of the innate immune system [142, 143]. T2R38, one of the isoforms of T2R, is expressed in ciliated epithelial cells and is a key mediator in sinonasal defense [126]. Molecules secreted by gram-negative bacteria activate T2R38, leading to the stimulation of NO production, mucociliary clearance, the direct killing of bacteria and antimicrobial peptide production [144]. These findings

suggest that bitter agonists which can stimulate the expression of bitter taste receptor, T2R, have promise as a topical therapy in CRS. However, the mechanism of expression of T1R and T2R seems different in human sinonasal epithelial cells. It has been observed that T1R and T2R expression is different in upper airway cells as T1R is expressed at the same time as T2R and inhibits the mechanism of action of T2R. Generally, phenotype and genotype of taste receptors vary in upper airway cells which have an important effect on the immune system and lead to their consideration as a future treatment for CRS [143, 145].

**Cystic fibrosis transmembrane conductance regulator modulator associations**

Cystic fibrosis transmembrane conductance regulator (CFTR) is a channel located on the apical surface of the sinonasal epithelium which regulates anion secretion ($Cl^-$ and $HCO_3^-$) and sinonasal mucociliary clearance which can be important in the treatment of CRS [146, 147]. Ivacaftor is an oral drug that potentiates CFTR by increasing $Cl^-$ secretion and actively increasing channel gating. Although clinically beneficial, Ivacaftor is expensive [148], therefore, other treatments are used in combination with it to lower the efficient doses and decrease the cost [149, 150]. For instance, ethanol activates CFTR leading to the stimulation of $Cl^-$ secretion and can be used as a topical aerosol in combination with CFTR activators for the treatment of CRS [151]. Resveratrol, like ethanol, can be used in combination with Ivacaftor as a CFTR potentiator as a topical treatment for CRS [152]. Ivacaftor induces the antibiofilm activity of L-methionine against *P. aeruginosa*; consequently, the combination of both as a topical delivery appears to be promising for the treatment of infection associated with *P. aeruginosa* in CRS. It has been reported that Ivacaftor-coated sinus stents enhance the antibiofilm activity of ciprofloxacin against *P. aeruginosa* biofilm [149, 153].

**Ciprofloxacin-eluting stent**

Continuous antibiotic therapy is essential for the treatment of CRS, not only for the killing of microbes, but also for the prevention of resistance development. Drug-eluting nasal stents which release antibiotics over a long period reduce the need for frequent administration of the antibiotic to patients [154]. The efficacy of ciprofloxacin-coated sinus stents has been reported in both *in vitro* and *in vivo* rabbit models [155]. No signs of inflammation were observed in maxillary sinuses after 3 weeks and the *P. aeruginosa* biofilm was eradicated through the continuous release of the drug [155, 156]. Although earlier studies noted the efficacy and safety of ciprofloxacin-coated sinus stents, there is more room for testing other antimicrobial agents and different concentrations for the treatment of CRS.

## Antibiotics

### Oral antibiotics

One of the most prescribed medications for the treatment of CRS is antibiotics (20). Despite this there is a paucity of evidence for their benefit in the treatment of this condition. The overuse of antibiotics has led to an increase in the appearance of antibiotic-resistant microorganisms [157]. Based on the International Consensus Statement on Allergy and Rhinology (ICAR), patients suffering from CRSwNP should not be prescribed long courses of non-macrolide antibiotics, however, it is still not confirmed that this approach is effective for the treatment of CRSsNP [158]. Further studies were performed to provide sufficient evidence for the efficacy of non-macrolide antibiotics in CRS patients [159]. Macrolide antibiotics have also anti-inflammatory and immune-modulatory activities. These properties have gained interest in addition to their role as anti-bacterial agents in chronic airway inflammatory diseases which require low dose and long term use of macrolides [160].

One of the most critical threats to patients' safety is antibiotic resistance, making it crucial to take efficacy and appropriate application of antibiotics into consideration. This is specifically applicable in CRS because the inappropriate use, overuse and variability in prescribing antibiotics can cause hazards to public health [161, 162]. Apart from resistance, antibiotics can induce other problems including mild (rash, nausea, diarrhea) and life-threatening (anaphylaxis) side effects [162].

### Topical antibiotics

Topical antibiotics can exhibit fewer side effects and increased efficacy This mode of treatment facilitates the administration of antibiotics at much higher concentrations than those obtained systemically. Mupirocin topical therapy was applied for the treatment of *S. aureus* infection in recalcitrant CRS patients in a double-blinded, randomized, placebo-controlled trial. The results revealed that mupirocin sinonasal rinses are an effective short-term treatment based on microbiological and selected rhinological outcomes [163]. However, the recolonization of *S. aureus* after some months was detected in these patients [164]. Topical tobramycin in a rabbit sinusitis model indicated the reduction of *P. aeruginosa* counts in a dose-dependent manner and tobramycin is the only antibiotic approved by the food and drug administration (FDA) for topical use in the airways against *P. aeruginosa* infections [165]. Recent studies evaluating the effect of topical antibiotics are shown in table 4.1 [166].

**Table 4.1** Recent literature on topical antibiotics in CRS [166].

| Study type | Frequency | Study population | Treatment | Outcomes | Results |
|---|---|---|---|---|---|

| | | | | | |
|---|---|---|---|---|---|
| DB-RCT [167] | 9 | CF patients with positive *P. aeruginosa* culture from nasal lavage | 28 days of inhalation with tobramycin (80 mg/2 mL) or 2 mL isotonic saline daily (4 minutes per nostril) using the PARI Sinus™ nebulizer | Change in number of *P. aeruginosa* colonies, SNOT-20, nasal endoscopy | No statistically significant change between groups in number of colonies, 6.67 decrease in SNOT-20 in tobramycin group vs 3.34 increase in control group ($p$ = 0.033); no change in endoscopic appearance |
| Prospective, controlled [168] | 37 | Recalcitrant CRS s/p ESS with positive culture and/or biofilm formation | Topical 0.3% ofloxacin eye drops every 8 hours for 12 weeks or no antibiotics (systemic or local) | SEM, bacteriology RSI, nasal endoscopy, CT scoring | Pretreatment: biofilm in 91% of treatment group compared; post-treatment: thin patches of biofilm in 20%; statistically significant improvement in RSI, endoscopy, and CT |
| Meta-analysis [169] | 101 (3 studies) | Prospective, retrospective cohort, or RCT evaluating mupirocin's effect on staphylococcal colonization | Mupirocin irrigation | Residual staphylococcal infections after 1 month and 6 months | 0.08 (95% CI, 0.04-0.16) residual infection at 1-month 0.53 (95% CI, 0.27-0.78) |
| Cochrane systematic review **[159]** | 0 (No studies met inclusion criteria) | RCTs | NA | NA | NA |
| Systematic review [170] | 4 systematic reviews | RCTs, systematic reviews, meta-analyses | Topical antibiotics | NA | 3 RCTs found no clinical benefit;<br><br>1 RCT showed short-term efficacy of mupirocin irrigations |
| Retrospective [171] | 69 | Patients with CRS that underwent ESS and were treated with high-volume topical antibiotic irrigations | Tobramycin (21), levofloxacin (4), Mupirocin (23), gentamicin (4) cephalosporin (3) | SNOT-20, Lund-Kennedy endoscopic score; negative culture results | No significant change in SNOT-20 for CF and non-CF;<br><br>significant improvement in endoscopic score for non-CF but not for CF,<br><br>72% of non-CF with negative post-treatment culture data, 29% of CF |

| | | | | | |
|---|---|---|---|---|---|
| | | | | | patients with negative post-treatment culture data |
| Retrospective [172] | 22 | Patients with medically and surgically refractory CRS who were treated with topical mupirocin therapy and symptomatic before and after mupirocin therapy | Twice-daily, high-volume mupirocin irrigations for at least 1 week | Culture data before and after mupirocin treatment | 19 gram-positive and 3 gram-negative before treatment vs 9 gram-positive and 13 gram-negative after therapy; *Corynebacterium* and *P. aeruginosa* were most frequently cultured after treatment |

CF = cystic fibrosis; CI = confidence interval; CRS = chronic rhinosinusitis; CRSsNP = chronic rhinosinusitis without nasal polyps; CT = computed tomography; DB-RCT = double-blinded, randomized controlled trial; ESS = endoscopic nasal surgery; RSI = Rhinosinusitis symptom inventory; SEM = scanning electron microscopy; SNOT-20 = 20-item Sino-Nasal Outcome Test; s/p = status-post.

**Corticosteroids**

CRS patients may receive corticosteroids topically or orally as part of their medical management. Corticosteroids function via either reducing eosinophil viability and activation [173-175] or by directly preventing chemotactic cytokine production by epithelial cells of the nasal mucosa and nasal polyps [176-178]. Topical intranasal corticosteroids (INCS) are beneficial in both CRSsNP and CRSwNP as they improve symptom scores and reduce symptoms, polyp size, polyp recurrence rates and improve nasal airflow [9]. The efficacy of single-modality oral or systemic steroids in CRSsNP patients is still unknown [178]. Oral steroids were used as an adjunct therapy to antibiotics or intranasal corticosteroids by CRS patients in two clinical trials. The low or very low improvement in symptom severity, polyp size and condition of the sinuses were observed, which may be because of the short-term usage. [179]. Topical delivery of corticosteroids may have side effects such as epistaxis, itching, sneezing and dry nose [9]. As oral corticosteroids are applied long term and at a high dose, the side effects are more severe such as changes in bone mineral density, fat metabolism, proximal muscle strength, appetite, glucose tolerance, early cataract formation and suppression of the pituitary-hypothalamic axis (56-3). Short-term usage of oral corticosteroids may cause an increase in insomnia and gastrointestinal or mood disturbances [179].

**Nanoparticle; Colloidal silver or Silver Nanoparticles**

We have witnessed immense changes since the advent of nanotechnology, especially in the area of Nanoparticles (NPs) affecting their unique properties and size-dependent physicochemical properties [180]. A major focus of nanomaterial research is the synthesis of NPs of various sizes, shapes, and structures for specific purposes. Apart from the differences in shape, size, and surface area, NPs can be used for applications that are somewhat different from those of bulk materials [181]. As for NP synthesis, it is divided primarily into physical, chemical, and biological methods. To make NPs by physical means, temperature, pressure, and energy will need to be maintained. Several chemical methods are used to make NPs, including laser pyrolysis, atomic or molecular condensation, sol-gel processes, chemical etching, sputtering, and spray pyrolysis [182]. Chemical concentrations and reaction conditions can alter the shape and size parameters of NPs. In the context of a specific application, precisely synthesized NPs are challenged by bioaccumulation, toxic nature, modeling factors, regeneration, reuse, and recycling [183]. Nanoparticles are divided into different groups: carbon-based NPs (such as fullerenes, carbon nanofibers, carbon nanotubes, lampblack graphene), inorganic NPs (metals like gold, silver and metal oxides like titanium dioxide, iron oxide), organic NPs (dendrimers, micelles, liposomes and polymer nanoparticles), and composite based NPs (combination of carbon based, metal based or organic based nanoparticles with any sort of metal, ceramic, or polymer bulk materials) [184, 185]. During the past decade, more attention has been paid to metallic NPs that originate from noble metals such as silver, gold, platinum, palladium, ruthenium, and rhodium, and their biomedical evaluation and reevaluation [186]. Silver Nanoparticles (Ag NPs) are unique among nanomaterials derived from noble metals for their ability to kill bacteria [187]. Chemical reduction-based NPs synthesis has its limitations, as most reducing agents have more adverse effects on the environment than bioreduction techniques [188]. Through the introduction of sustainable and green methods, green synthesis contributes significantly to reducing toxic and harmful by-products. Moreover, biosynthesized silver and gold NPs are applied for photocatalytic and biomedical purposes [189, 190].

Silver has been used as a bactericide for the treatment of burns, chronic wounds and ulcers [191, 192]. It is used in dressings and catheters in addition to its use in hygiene and personal care [193, 194]. However, due to the emergence of antibiotics, safety and the noted adverse effect of argyria, silver lost its popularity in the 20$^{th}$ century [195, 196]. With the emergence of multi-drug resistant organisms, interest in silver has re-emerged [51, 197]. Topical delivery of Ag NPs has shown good antibacterial activity with the typically observed systemic side effects [191, 198]. It has been reported that silver has efficacy against fungi, protozoa, viruses, gram-negative and gram-positive bacteria *in vitro* [199, 200]. In addition, colloidal silver can prevent the development of

antibacterial and anti-biofilm resistance in different bacteria including *S. aureus, P. aeruginosa* and *Escherichia coli* [198, 201, 202]. Colloidal silver has been used in intranasal sprays in patients with *S. aureus* infected recalcitrant CRS [201]. In *vitro* experiments, by Goggin et al [201], has shown the efficacy of commercially available colloidal silver against *S. aureus* biofilm with a later published sheep CRS model also demonstrating evidence for safety and efficacy of topical colloidal silver synthesized by commercially available generators (Coyote Zenterprise, North Carolina, USA) [203]. Richter et al, have also reported the efficacy of chemically synthesized spherical colloidal silver against biofilms of clinical isolates of *S. aureus*, *P. aeruginosa* and MRSA separated from CRS patients [198]. These promising outcomes resulted in a human trial in which the above-mentioned colloidal silver was used as a topical wash by CRSsNP patients for 2 weeks [204]. Although the safety of colloidal silver was again demonstrated, silver was not shown to have improved efficacy over oral antibiotics. Similarly, Scott et al [205] also failed to observe the efficacy of commercially available nasal spray of colloidal silver in a randomized control human trial in recalcitrant CRSsNP patients.

**Antimicrobial resistance and the development of new antimicrobial compounds**

The invention of antibiotics has been one of the major achievements of modern medicine [206]. However, this very success has led to an increase in antibiotic resistance, more generally antimicrobial resistance (AMR) [207]. The high-level appearance of AMR is due to both the misuse and overuse of antimicrobial agents with a rise in multidrug-resistant (MDR) bacteria linked mainly to the overuse of antimicrobials against harmful pathogens [208]. Pathogenic microbes that are resistant to antibiotics represent a challenge to pharmaceutical industries and medical professionals [209]. The treatment of infections caused by MDR bacteria is challenging with treatment courses that are longer, less effective, and more expensive. In addition, some pathogens have evolved to be resistant to all known antibacterial agents (multi- and pan-resistant bacteria, also known as “superbugs”), posing a global threat [210]. Several deadly diseases are caused by drug-resistant pathogens, according to the World Health Organization (WHO) [211]. Therefore, efforts have been directed in recent years towards developing new and better antimicrobial compounds [212].

**Silver Nanoparticles and their antimicrobial activity**

Antimicrobial properties of silver and Ag NPs have generally been demonstrated against a wide variety of microorganisms including bacteria, viruses, and fungi [213]. As antibiotics were discovered, silver's applications in medicine gradually decreased. With the advancement of nanomaterials with size in the nano range, the antimicrobial properties of silver and Ag NPs, in particular against antibiotic-resistant strains, have been rediscovered. Ag NPs of 10-100 nm showed indeed strong bactericidal activity against both gram-

positive and gram-negative bacteria [214]. In line with previous research, it has been shown that Ag NPs may be effective against MDR bacteria, including m*ethicillin-resistant Staphylococcus aureus* (MRSA), *Erythromycin-resistant Streptococcus pyogenes, Ampicillin-resistant Escherichia coli,* and *Vancomycin-resistant Staphylococcus aureus* [215]. Antibacterial properties of silver were applied before antibiotic therapy primarily to treat burns and open wounds [216]. A silver-based antiseptic has wide applications, and microorganisms have less tendency to become resistant to it [217]. Ag NPs possess a wide range of antibacterial and antifungal properties. It is also advantageous to use Ag NPs in clinical and therapeutic applications since it is relatively less reactive than silver ions [218].

Four mechanisms explain Ag NPs' antimicrobial activity: 1) Ag NP adhesion to cellular walls and membranes, 2) penetration of Ag NPs into the cell and destroying of the intracellular organelles such as mitochondria, vacuoles, ribosomes and biomolecules such as proteins, lipids and DNA, 3) inducement of cellular toxicity and oxidative stress through the production of reactive oxygen species (ROS) and free radicals and 4) changes in signal transduction pathways (Figure 2.1) [218].

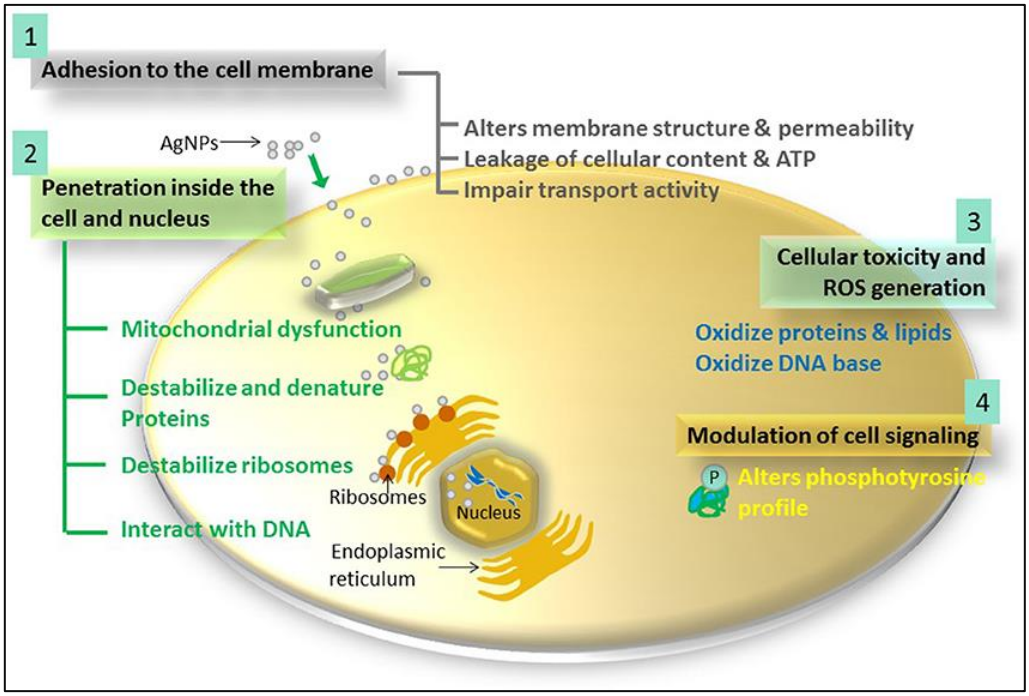


**Figure 2.1** The four most prominent routes of antimicrobial action of Ag NPs.

1, Ag NPs adhere to the microbial cell surface and results in membrane damage and altered transport activity; 2, Ag NPs penetrate inside the microbial cells and interact with cellular organelles and biomolecules, and thereby, affect respective cellular machinery; 3, Ag NPs cause an increase in ROS inside the microbial cells leading to cell damage and; 4, Ag NPs modulate cellular signal system ultimately causing cell death [218].

**Adhesion of Silver Nanoparticles onto the Surface of Cell Wall and Membrane**

Ag NPs adhere to the cell wall and the membrane of microorganisms [219]. As the cell membrane is negatively charged, the positive charge on the surface of Ag NPs provides the electrostatic attraction between the cell membrane and Ag NPs and facilitates adhesion to the cell wall. The interaction of Ag NPs with microorganisms results in morphological changes such as shrinkage of the cytoplasm and detachment of the membrane leading to the disruption of the cell wall [220]. Moreover, transmission electron microscopy images showed the disruption of the cell wall and the appearance of electron dense pits in *E. coli* after few minutes of exposure to Ag NPs [221, 222]. Furthermore, Ag NPs interact with the sulfur-containing proteins leading to disruption of the cell wall. This can affect the integrity of the lipid bilayer and the permeability of the cell membrane. The increase in membrane permeability as the result of the alternation in cell morphology hurts transportation through cell membrane and causes leakage of cellular content [223, 224]. Ag NPs are also able to modify the cells genetically through condensation of genetic materials causes cell necrosis and cell death [202, 222, 225].

The thickness and composition of the cell wall have an impact on the antimicrobial activity of Ag NPs. Gram-negative bacteria are more sensitive to Ag NPs than gram-positive bacteria. This is due to the structure of peptidoglycan in the cell wall which is thicker in gram-negative bacteria compared to gram-positive bacteria.. Furthermore, the negatively charged lipopolysaccharides (LPS) induce the attachment and deposition of positively charged Ag NPs to the membrane and promote the antibacterial activity of Ag NPs [226, 227]. Consequently, the cell wall structure, thickness, and composition as well as concentration of Ag NPs affects the antibacterial efficacy of Ag NPs.

**Silver Nanoparticles Penetration Inside the Cell and Destabilization of Intracellular Structures and Biomolecules**

The interaction of Ag NPs with microbial cell membranes results in several cellular dysfunctions. Initial Ag NP attachment only occurs at the cell membrane and results in alterations to membrane structure, permeability, and transport ability. At other times, Ag NPs may penetrate cells after adhering to cellular membranes and disturb their vital functions [228, 229]. Gram-negative bacteria uptake Ag NPs through porins, water-filled channels that exist in the outer membrane (OM) [230]. Ag NPs hinder translation and protein synthesis when they interact with ribosomes [226, 231, 232]. The interaction of Ag ions with proteins has been shown to cause the deactivation of proteins. For example, Ag ions can deactivate the proteins through binding to the thiol groups [226, 233]. The interference of Ag NPs and Ag ions with the disulfide bonds in proteins can

lead to the deactivation of the bonding sites of proteins resulting in functional disorganization [234, 235]. Ag NPs disrupt the glycolytic cycle in bacteria as a result of the inactivation of the enzyme phosphomannose isomerase, required for the conversion of mannose-6-phosphate into fructose-6-phosphate [236]. Ag NPs can also cause DNA to be sheared or denatured resulting in an interruption of cell division [237, 238]. Ag NPs damage DNA and modify DNA repair genes, making mutant strains more vulnerable to Ag NP-based antibacterial treatments [239]. Interestingly, Ag ions form complexes with nucleic acids where they interact most preferentially with nucleosides rather than with phosphate groups. Intercalation of Ag ions between purines and pyrimidine bases disrupts the H-bonds between bases of the antiparallel DNA strands, causing interruption of the double helix structure which may hinder transcription in microorganisms [231]. Ag NPs can also disturb transcription by changing the DNA structure from a relaxed to a condensed form [202]. Ag ions also inhibit bacterial cell division and reproduction [240].

**Silver Nanoparticles Induced Bactericidal effects**

Heavy metal ions, such as Ag ions, can cause toxic effects in bacteria largely due to increased oxidative stress. A considerable part of Ag NPs' antibacterial efficacy can indeed be explained by their ability to produce ROS and free radical species such as hydrogen peroxide ($H_2O_2$), superoxide anion ($O_2^-$), hydroxyl radical ($OH^•$), hypochlorous acid (HOCl) and singlet oxygen [225,241,242,243,244]. ROS are responsible for bacterial death, however, the mechanism in which Ag NPs have bactericidal activity through ROS is unclear [243]. In certain cases, toxic effects may be caused by the binding of Ag ions to the cell membrane of bacteria, which then relays signals and prevents them from performing respiration [245]. Inhibition of respiratory chain enzymes by Ag ions causes respiratory electron transport chain dysfunction through uncoupling it from oxidative phosphorylation [246]. By itself, excess amounts of generated free radicals lead to direct damage of membranes, eventually resulting in bacterial cell death. The initial step in ROS generation involves the oxidation of polyunsaturated fatty acids resulting in the formation of lipid hydroperoxides [247] and hyperoxidation of lipids, proteins, and DNA may indeed result from an increase in ROS levels in bacterial cells [248].

**Modulation of Signal Transduction Pathways**

Numerous protein substrates are phosphorylated in bacteria [249]. Signal transmission in bacteria is accomplished by phosphorylation and dephosphorylation processes, which are essential for growth and bacterial activity [250]. A useful way to study the effect of Ag NPs on bacterial signal transduction pathways is to examine the phosphotyrosine profile of bacterial proteins from both gram-positive and gram-negative

bacteria. Bacterial growth and molecular activities are affected by these signaling pathways. When protein substrates such as RNA polymerase sigma factor (RNA pol σ factor), single-stranded DNA binding proteins (ssDBPs) and Uridine diphosphate (UDP) glucose dehydrogenase are reversibly phosphorylated on the tyrosine residue, they become active [251-253]. DNA replication, recombination, metabolism, and the process of bacterial division depend on phosphorylated proteins [254]. By inhibiting phosphorylation of proteins, bacterial growth will be inhibited in turn due to decreased enzymatic activity [254]. Iniesta et al. (2006) also suggested that phosphosignaling pathways are important for bacterial cell cycle progression [254]. Several gram-positive and gram-negative bacteria have also been implicated in the process of tyrosine phosphorylation of proteins in the synthesis and transport of exopolysaccharide and capsular polysaccharide [255]. Inhibiting microbial growth is believed to be a consequence of Ag NP's activity on dephosphorylating tyrosine residues on bacterial peptide substrates and modulating cellular signaling [256]. The alternation in the profile of tyrosine phosphorylated proteins by Ag NPs is species dependent. For instance, Ag NPs change the dephosphorylation of two peptides of relative masses 150 and 110 kDa in *E. coli* and *S. typhi*, but not in *S. aureus* [257].

**Biofilm structure and properties**

Biofilm is defined as an "Aggregate of microorganisms in which cells are embedded within a self-produced matrix of extracellular polymeric substances and adhere to each other and/or to a surface" (definition by the International Union of Pure and Applied Chemistry, IUPAC) [258]. Alteration in growth rate and gene transcription make biofilm phenotypically different in comparison to the planktonic bacteria [259]. Biofilm can be found in both natural and industrial environments and is reported to be related to almost 80% of microbial infections in the human body [260]. Biofilms have various advantages for bacteria. For example, they can help bacteria to adapt to different environments and increase the rate of their survival in stressful and difficult conditions (the presence of antibiotics). Biofilms have been reported to enhance nutrient uptake and defense mechanisms in bacteria [261]. Biofilms also cause genotypic [262, 263] and phenotypic [264, 265] changes of bacteria. Bacteria can have various growth states within the biofilm, for instance fast growing/metabolic active states and slow growing/metabolic inactive states [266]; Bacteria also can get adaptive mutations [267] and changes in quorum sensing [268, 269] as wll as produce antibiotic degrading enzymes [270]; Bacteria within biofilms benefit from the removal of antimicrobials through efflux pumps [271]. Biofilms also allow for the existence of a subpopulation of multidrug resistant persister cells [272, 273]. Once within the biofilm, bacteria are preserved against fluctuations of water, oxygen, salt, nutrients, pH levels, toxicity of metals and UV intensity [274, 275]. Biofilms also promote the tolerance of bacteria to innate and

adaptive immune responses as well as decrease the susceptibility to antimicrobial agents up to 1000-fold in comparison to planktonic bacteria [272].

Biofilm formation includes four main processes, adhesion, production of Extracellular Polymeric Substances (EPS), proliferation and detachment (Figure 3.1) [276]. The first and the second steps are the irreversible attachment of planktonic bacteria to a surface or the other bacteria through pili, flagella and receptors and the release of extracellular polymeric substances. In the third step, microcolonies are formed because of the proliferation of bacteria. In this step, biofilm formation is affected by the activation of quorum sensing, cell-to-cell signalling and the transcription of specific genes [277, 278]. Mature biofilms consisting of multi-layered cell clusters are formed as the bacteria differentiate based on the nutrient supply and environmental conditions. Finally , bacteria are detached from the biofilm, which may be due to the lack of space, nutrient limitations or fluid shear and starvation, and a new biofilm life cycle is initiated [58, 279-282].

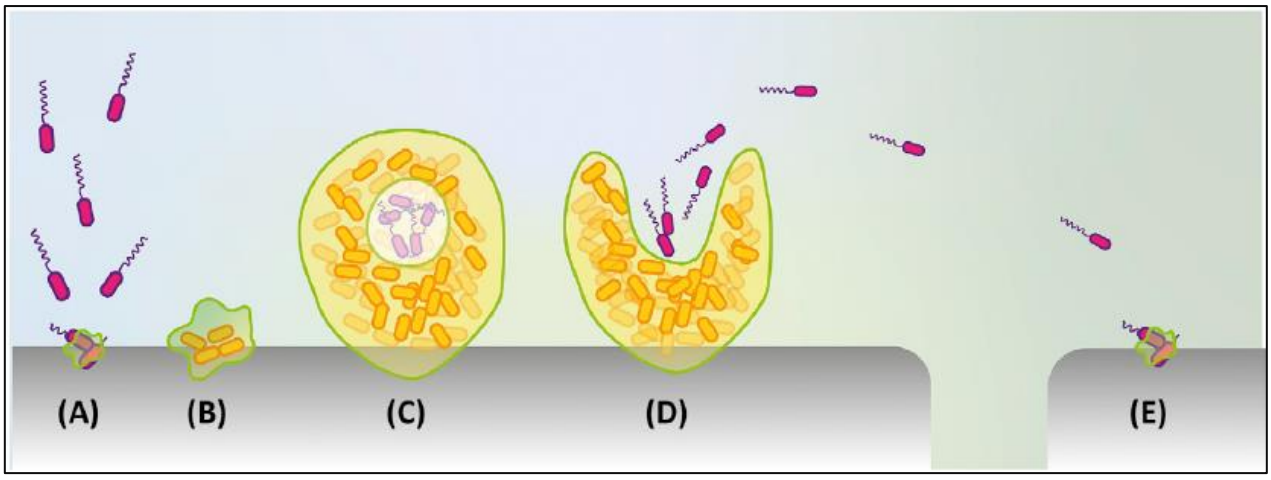


**Figure 3.1** Life Cycle of Biofilm.

(A) Attachment/adherence of the bacteria to the surface. (B) Formation of monolayer and production of extracellular polymeric substances (EPS). (C) Microcolony formation and proliferation. (D) Biofilm dispersal–detachment and reversion of planktonic cells. (E) Start of life cycle of biofilm again [276].

**Nanoparticle–Biofilm Interaction**

The emergence of multidrug-resistant strains of bacteria is a concern associated with long-term antibiotic use. Therefore, it is becoming essential to develop alternative approaches for the treatment of biofilm related infections. The NPs look like a promising alternative due to their extraordinary mechanical, chemical, electrical, and magnetic properties [276].

NP-biofilm interaction involves three main mechanisms (Figure 4.1). The first step is the transportation of NP into the biofilm-fluid interface. In the second step, NPs are deposited on the surface of the biofilm and in the third step, they migrate within the biofilm [283].

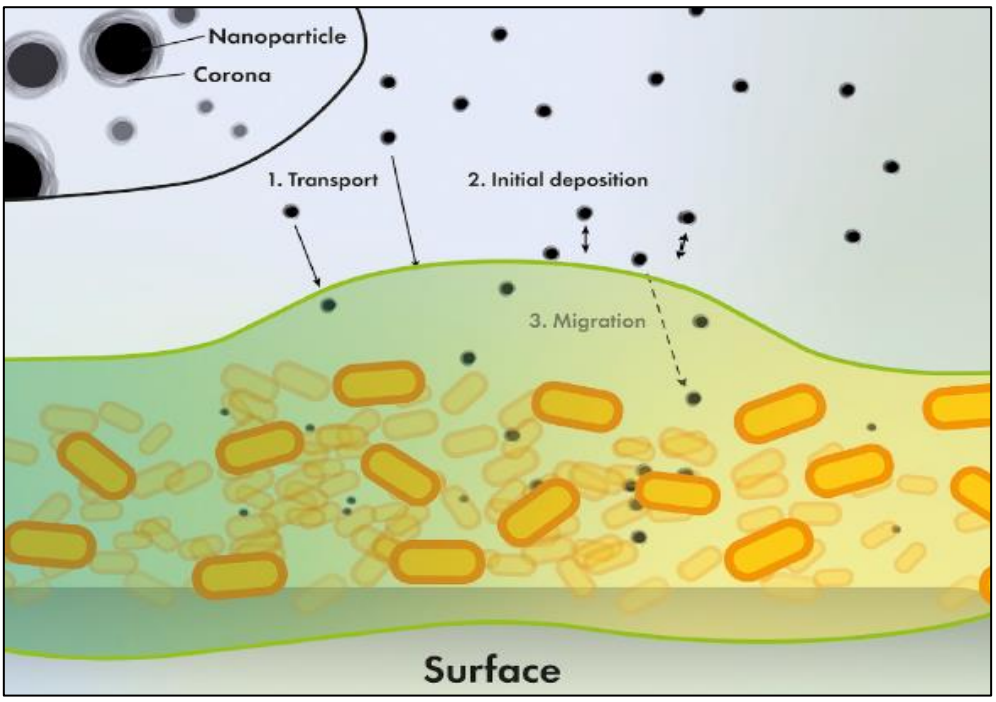


**Figure 4.1** Representation of the Stages (Transport, Initial Deposition, and Migration) Involving Nanoparticle (NP) Transport Phenomena within Bacterial Biofilms.
As NPs are incorporated in the matrix, sorption (and sometimes reactive) processes result in their surface becoming covered in biofilm matrix constituents, a corona structure [276].

The NPs remain intact for only a very short time once encountering biofilm [283, 284]. Then, they are transported within biofilm through two steps. Initially, the NPs penetrate the biofilm which depends not only on their size [285] and surface charge [286], but also on the viscosity, composition and water pores of the EPS matrix, the density of bacteria, liquid flow and external mass transfer resistance [287]. Then, the interaction of NPs with biofilm happens (Figure 5.1). Both the NPs and biofilms possess physicochemical properties that influence their interaction. It determines the amount of particle uptake, the type of interaction with biofilm matrix and surface of bacteria and the mechanism of toxicity [288]. The EPS matrix and NPs mainly interact physically, although they also interact chemically and biologically [289]. Steric interactions are the main physical interaction in the stabilization of NPs once NPs encounter biofilm. In high salinity or ionic strength media, steric stabilization can prevent NP aggregation, which is crucial for determining their interaction with biofilm EPS [289].

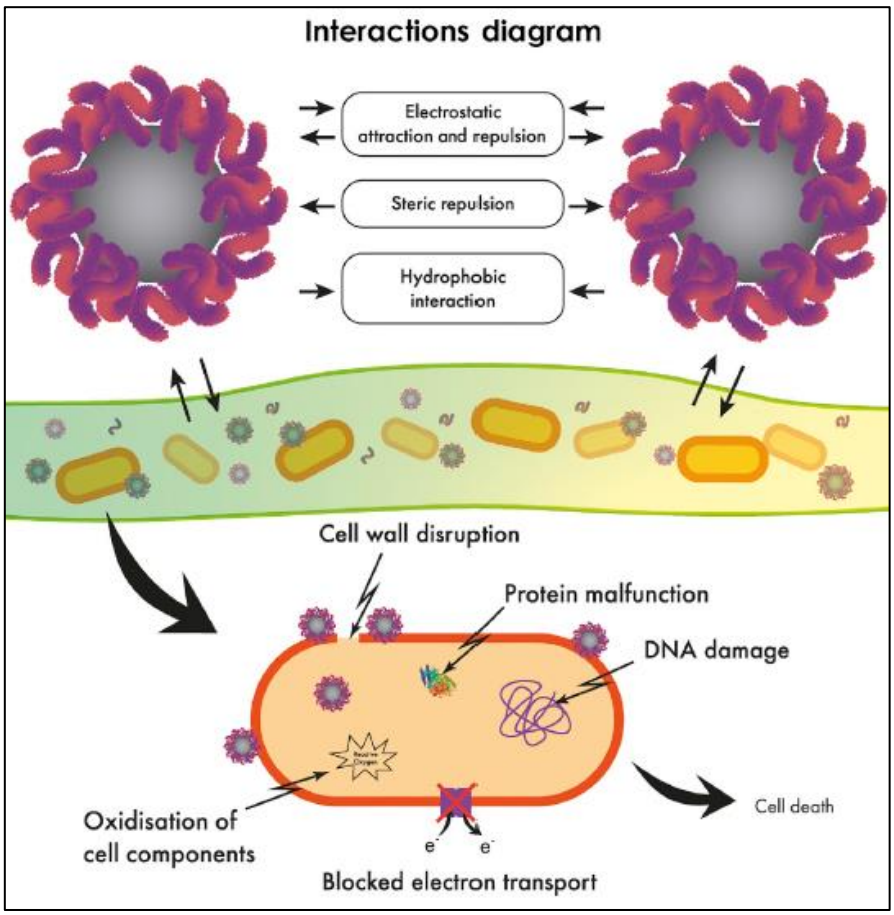


**Figure 5.1** Graphical Diagram Describing the Different Physicochemical Interactions between Nanoparticles (NPs) and Bacterial Biofilms [276].

**Silver Nanoparticles and Eradication of Biofilm**

Treatment of biofilm infections is difficult due to the complex physicochemical properties and variability of the EPS and its component interactions [290]. Biofilm EPS remains attached to biotic and abiotic surfaces even after the microbial components of a biofilm were killed or inactivated, which presents a major challenge for antimicrobials. Further colonization by other microorganisms may be facilitated by the presence of EPS matrix remnants which can lead to serious outcomes [290]. Consequently, a prudent safety evaluation of potential biofilm dispersal agents for clinical application is needed, as they should also be used alongside antibiotics to prevent recolonization [276]. The development of new therapies for biofilms, such as functional NPs seems promising for the treatment of biofilms [291].

Ag NPs demonstrate an improved ability to inhibit microbial growth, adhesion, and biofilm growth [291-295]. NP–bacterial biofilm interactions were associated with extensive sloughing of the biofilm bacteria into suspension, but the viability of the bacteria remained relatively stable [296]. The EPS matrix of biofilms can cause the aggregation of Ag NPs, which may explain why the eradication of biofilms by Ag NPs was ineffective [296]. Bacteria are protected physically by EPS; once treated with Ag NPs, the removal of loosely bound EPS causes the increase of bacterial sensitivity to Ag NPs [276]. It has been reported that the exposure time of NPs to the biofilm is important [296]. For instance, NPs (d= 5-150 nm) exposed to biofilms for 8-24 h is more effective at reducing the biofilm biomass than when exposed for less time [296]. Studies have shown that biofilms are more resistant to Ag NPs in comparison to planktonic bacteria [297]. Changes in ionic strength and interaction with components of EPS as well as limitation of Ag NPs/ions diffusion within biofilm matrix were partially responsible for this reduced action against biofilm forms of bacterial growth [298]. The diversity of bacterial species forming biofilms is also important for treatment with Ag NPs. Ag NPs are more effective against biofilm of one species rather than biofilm formed by a mixture of bacteria [276]. Ag NPs are also reported to inhibit quorum sensing in biofilm [229].

## Silver nanoparticles-induced cytotoxicity

### Effects of particle size and shape on cytotoxicity

Particle size has an impact on the cytotoxicity of Ag NPs [299]. Size-dependent effects were observed in multiple cell lines on cell viability, lactate dehydrogenase activity [299], and ROS generation [300] by Ag NPs. The particle size can greatly affect the surface area, volume, and surface reactivity [300-302]. When NPs are deposited over biological and solid surfaces, their sedimentation velocity, diffusion capacity, and attachment efficiency are influenced by their size [303-307]. Mammalian cells can also be affected by particle size [308]. Size dependent effects of Ag NPs on various cell lines are shown in table 5.1, indicating small particles are prone to cause more toxicity [309].

**Table 5.1** Size dependent effects of Ag-NPs on different cell lines [309].

| Particle sizes (nm) | Cell type | Findings | References |
|---|---|---|---|
| 15, 30, 55 | Rat Alveolar macrophages | Ag NPs induced size dependent cytotoxicity | [300] |
| 10, 50, 100 | HepG2 | Ag NPs induced size dependent toxicity through autophagy lysosomal system and inflammasome activation | [310] |

| | | | |
|---|---|---|---|
| 5, 20, 50 | A549, SGC-7901, HepG2 and MCF-7 | $EC_{50}$ values were size dependent and smaller particles can enter easily than larger particles | [307] |
| 13 ± 4.7 | HeLa and U937 | Ag NPs induced cytotoxicity in both HeLa and U937 cell lines | [311] |
| 10 | HepG2 | Cytotoxicity induced through the oxidative stress | [312] |
| 20, 80, 113 | RAW 264.7 & L929 | Ag NPs induced cytotoxicity depends on cell type and Np size | [313] |
| 5–10 | HepG2 | Ag NPs induced Oxidative changes in HepG2 cell | [314] |
| 30–50 | A431A549 | Ag NP's toxicity depends on particle size and surface potential | [315] |
| 7–20 | A431HT-1080 | Apoptosis induced in both A431 and HT-1080 cell lines | [316] |
| 15, 30, 55 | Alveolar macrophages cells | ROS and LDH generated in a size dependent manner | [317] |

The smaller Ag NPs also induce more inflammation than large ones. In certain cell types, there is a size-dependent toxicity threshold (TT) depending on particle size (Table 6.1) [309].

**Table 6.1** Effects of Ag NPs on cell viability upon 24 h incubation [309].

| Ag NP preparation technique | Particle sizes, nm | Cell type | Cytotoxicity assay | Toxicity threshold, µg/mL | Reference |
|---|---|---|---|---|---|
| Chemical reduction | 30–50 | A431<br>A549 | MTT assay | >50 | [318] |
| Unknown (commercial product) | >70 (PVP-coated) | A549 | MTT assay | 0.5 (Ag NPs) 1 (Ag+) | [319] |
| Unknown (commercial product) | 10<br>50<br>100 | HeLa | CCK-8 (WST-based assay) | 10<br>20<br>20 | [320] |
| Unknown (patented preparation) | 7–20 | A431<br>HT-1080 | XTT assay | 1.56<br>6.25 | [321] |
| Unknown (commercial product) | <10 | HepG2 | MTT assay<br>Alamarblue assay | 0.5 (Ag NPs)<br>0.1 (Ag+)<br>0.7 (Ag NPs)<br>0.7 (Ag+) | [322] |
| Unknown (commercial product) | 5–10 | HepG2 | MTT assay | 2.0 | [322, 323] |

Based on the synthesis process, different shapes of Ag NPs are produced, such as spheres, triangles, squares, cubes, circles, rods, ovals, and flowers (Figure 6.1). There is no credible evidence that the shape of particles has significant effects on the biological system from the nano-toxicological point of view. It might be influenced by more than one factor and in some synthesis processes, Ag NPs of different shapes can agglomerate in the cytoplasm of mammalian cells [309, 324].

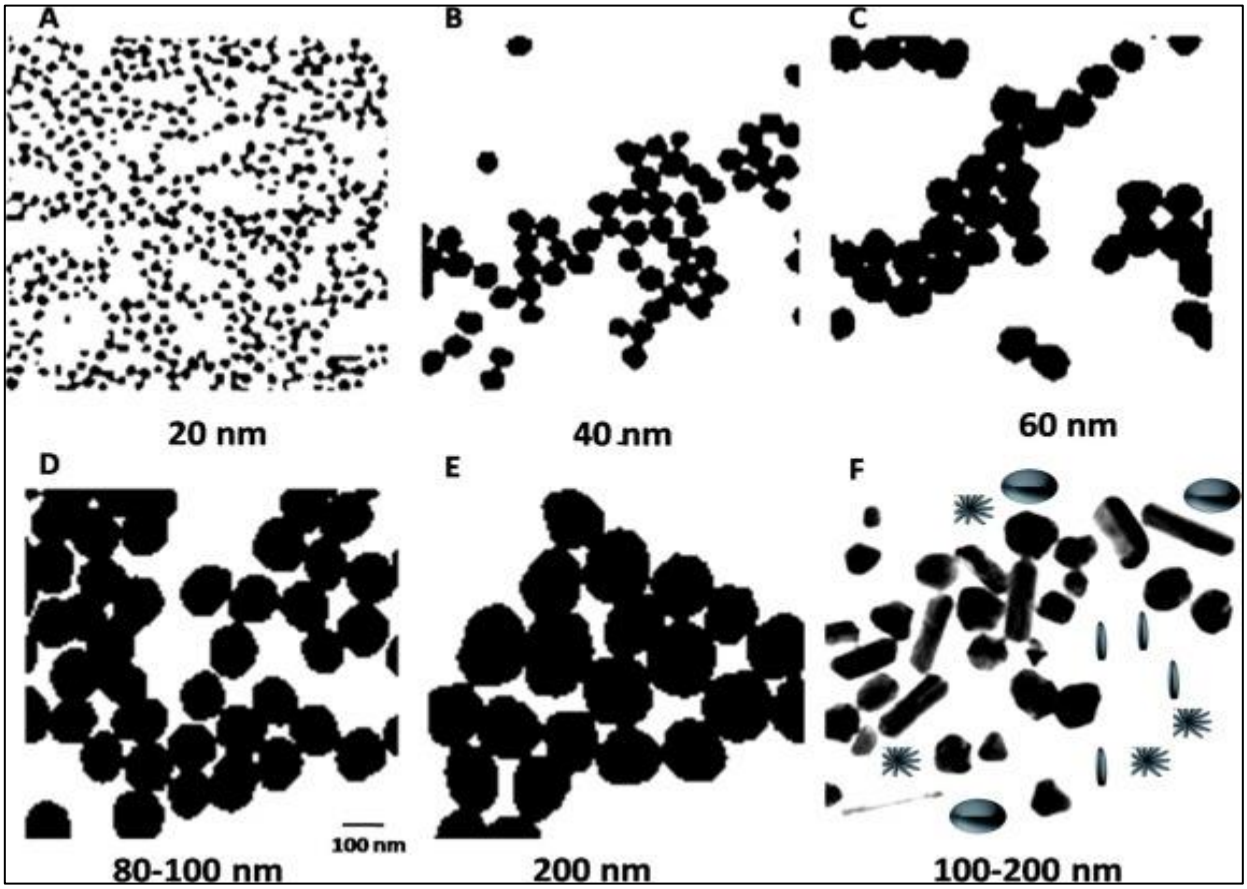


**Figure 6.1** Transmission electron microscopy (TEM) images of synthesized Ag NPs with various sizes and shapes.

(A) to (F) Spherical, oval, rod and flower shaped Ag NPs can be obtained from green synthesis. Spherical shaped Ag NPs mostly obtained by chemical synthesis. The size variability is independent of the synthesis process. Ag NPs change color as they change their size (color not shown). Scale bars are 100 nm [309].

The shape of Ag NPs can influence their uptake mechanisms, thereby modulating their cytotoxicity. Spherical particles, for instance, did not exhibit any negative effects on cytotoxic parameters in A549 cells, whereas Ag NPs in the shape of wires did [324]. The type of cell line is furthermore affecting the cytotoxicity of Ag NPs. For instance, 5–43 nm Ag NPs at 2.0 mg/L concentration is causing more toxicity in macrophages

than in A549, A498, HepG2, and neurons (Neuro 2A) [325]. Researchers found that Ag NPs internalized into macrophages through scavenger receptors, followed by cytotoxicity in the cytoplasm as a result of Ag ions release [325]. The toxicity of different sizes of Ag NPs is dependent on the pH of the environment. To give an example, in acidic phagolysosomes, Ag NPs at the size of 20 nm exhibited more toxicity rather than 110 nm as they release Ag ions easily and induce more toxicity [326].

**Effects of Ag NP concentration on toxicity**

Another important factor affecting toxicity is the concentration of NPs [313]. Understanding the minimum dosage of NPs that induces toxicity and the differentiation of its effects in different subjects is critical. For instance, a decrease in cell viability was observed in RAW 264.7, human Chang liver and rat liver cell line (BRL 3A) as the concentration of Ag NPs was increased [327]. Ag NPs cytotoxicity varies substantially from cell type to cell type, and this should be considered for their application in consumer products and in testing their effects on the environment [309]. In general, toxic concentration ranges for NPs depend on particle size, type of medium, temperature, surface functionalization, and particle crystallinity [328]. In tests with HaCaT keratinocytes, Ag NPs in the shape of nano prisms and spheres at 100 ppm concentration was not cytotoxic after 48 h [329]. In contrast, exposure of Ag NPs (0.01–10 mg/mL for 24 h) to a normal human lung bronchial epithelial cell line (BEAS-2B) induces toxicity through ROS induction, micronuclei formation, and DNA damage. The effect of different concentrations of Ag NPs on various cell lines is shown in table 7.1 [309].

**Table 7.1** Effects of Ag NPs of different ranges of concentration on different cell lines [309].

| Concentration range | Effects of Ag NPs in different ranges | References |
|---|---|---|
| 25–75 µg/mL | In rat alveolar macrophage cell line, cytotoxicity increases in a concentration dependent manner | 300 |
| 5, 15, 40, 125 µg/mL | Cytotoxicity occurred through mitochondrial depolarization | 330 |
| 10–50 g/mL | Induce cytotoxicity in BRL 3A rat liver cell through ROS generation GSH depletion and reduction of mitochondrial membrane potentiality | 327 |
| 20 µg/mL | Induce mitochondrial swelling in HSCs cell line after giving treatment for 2 days | 324 |
| 20–250 µg/mL | Apoptosis and necrosis induced in HSCs cell line | 325 |
| 40–80 µg/mL | 40 µg/mL was considered as IC50 value for MCF-7 cell line and apoptosis occurred at the concentration of 80 µg/ml. More than 80 µg/mL induce necrosis when the percentage of apoptosis being decreased | 331 |

| | | |
|---|---|---|
| 10–25 µg/mL | In MDA-MB- 231 cell line, DNA damage occurs in the presence or absence of concurrent radiation treatment | [332] |
| 50 µg/mL | Antioxidant capacity increased in Caco-2 cells | [333] |
| 1, 2, 4 µg/mL | Cell viability decreased in a concentration dependent manner | [334] |
| 10–50 µg/mL | In THP-1-derived human macrophages cell line cell viability decreased in a concentration dependent manner | [335] |
| 5 µg/mL | Promote epigenetic dysregulation in HT22 cells through cell proliferation, DNA damage response and DNA methylation | [336] |
| 0.4 and 0.8 µg/mL | Arrest G1 phase in the cell cycle in RAW 264.7 cell line | [337] |

In summary, Ag NPs display varying cytotoxicity depending on the cell type, particle size, exposure time and organism [309].

**Effects of coatings**

The coating of Ag NPs produces both electrostatic and electrosteric repulsions between the particles, and this further stabilizes the particles, preventing aggregation and reducing cytotoxicity. Cell viability was indeed significantly decreased by uncoated Ag NPs in a time-and dose-dependent manner [338]. Coating types depend on capping agent properties, such as organic capping agents (polysaccharides, citrates, polymers, proteins, etc) and inorganic capping agents (sulfide, chloride, borate, and carbonate) which can affect the cytotoxicity of Ag NPs such as the generation of ROS, the depletion of antioxidant defenses, and the loss of mitochondrial membrane potential. Shape, aggregate formation, and dissolution of Ag NPs are affected by surface coating. Ag NPs coated with polysaccharides derived from chitosan, for example, worked as antibacterial agents without toxic effects on eukaryotic cells. In general, Ag NPs induce cytotoxicity largely due to the coating materials and their characteristics [338].

**Effects of agglomeration**

NPs will often aggregate in solution or ambient air. Diffusion, gravity, and convection forces determine how NPs interact with cells [339, 340]. The pH, electrolyte or salt content, as well as the protein content in the culture medium may affect agglomeration [340]. It has been demonstrated in several studies that NPs and proteins possess different binding capacities depending on their composition [341-343]. Treatment preparation further influences the agglomeration state of Ag NPs in the medium. Ag NPs could have a

hydrodynamic diameter greater than the nominal particle size, depending on suspension preparation [314]. Last but not least, the aggregated particles have fewer adverse effects on cells [314].

Agglomeration states of NPs can affect NP localization within cells [314]. For instance, when Ag NPs are compared with titanium oxide ($TiO_2$) nanoparticles, they appear to aggregate very loosely. Hence, the agglomeration of Ag NPs was found in the cytoplasm, nucleus, and mitochondria while $TiO_2$ agglomerates were found mostly in vacuoles. This is due to the interaction of NPs with proteins and DNA which induces toxicity [314].

Because of their high surface area, Ag NPs tend to agglomerate in culture medium [344]. The agglomeration may cause toxicity, rather than ionic metals [344]. A variety of intracellular responses can be triggered by aggregation. Therefore, toxicological interests emphasize the importance of determining how agglomeration or aggregation states of NPs influence biological responses [314, 345].

**Effects of surface corona, charge, and hydrophobicity/hydrophilicity**

Different nanomaterials are used in biomedical applications. Interactions between nanomaterials and biological entities are generally considered to exert adverse effects on biological systems. [346].

The complicated interactions between Ag NPs and proteins have also attracted a lot of attention [346]. The ability of proteins to bind to the surface of NP is critical to producing coronas, and, consequently, the existence of a protein corona may profoundly affect biological activity. Corona formation is demonstrated in experimental studies *in vitro* and *in vivo* when nanoparticles interact with cellular systems [309].

There is a significant effect of the corona on biological responses. Various properties of particles such as size [332], shape [347], the composition of particle surface [348] as well as the content of biological fluids affect not only corona composition, but also the adverse effects on human health and the environment. Coronas can be categorized as hard and soft according to their surface affinity and exchange rate. Silver ions can use soft corona proteins as a vehicle, while hard corona proteins prevent ions from entering the cellular system. A variety of corona effects have been studied, examining the interactions of silver nanoparticles based on a structure with different proteins such as fetal bovine serum (FBS), bovine serum albumin (BSA), human blood plasma, human serum albumin (HSA), tubulin, ubiquitin (cytoskeletal protein), and hyaluronan-binding protein. Research in this area was aimed at measuring and understanding protein accumulation on silver nanoparticle surfaces. It has been determined that more than 500 proteins are directly related to the formation of the corona, of which 50% can be identified on the NP surface regardless of their coating or size. In studies with BSA, it was found that polymer coatings could greatly affect nanoparticles, as

could the surface charge of the particles. When electrostatically stabilized NPs are present, the BSA can exhibit a low affinity for them. This indicates the importance of electrostatic and hydrophobic interactions in the formation of protein coronas. Nanoparticles, and therefore the corona, is mainly controlled by their affinity and electrostatic stabilization. Uncoated and surfactant-free Ag NPs have the affinity to be coated by proteins because of the increased changes in entropy, however, electrostatically stabilized NPs show less potential to coating due to the limited entropy changes. Additionally, the biological activities of coronas were examined to determine their cytotoxicity and antibacterial properties. The antibacterial activity of Ag NPs depends not only on capping agents but also the method of their delivery to the organisms such as oral or intravenous administration. Particle coating reduces the toxicity of the protein corona which is induced by oxidative stress through cell surface receptors. The dissolution of Ag NPs to Ag cations is also influenced by corona impacting the toxicity. The cytotoxicity of the corona is controlled by the functional groups and charges on the particle surface [349, 350].

**Uptake mechanism of Silver Nanoparticles**

The uptake mechanism of Ag NPs is different based on cell type. This includes diffusion, phagocytosis, and endocytosis. The way Ag NPs enter human macrophages can be phagocytic or non-phagocytic [351]. Although agglomerated Ag NPs are phagocytosed by the cells, non-aggregated particles are taken up through alternative routes. The engulfment of Ag NPs by mammalian cells is also determined by the size of the particles [261, 266, 352]. Ag NPs can also be absorbed directly through the ion channel or membrane flip-flop mechanisms. The transportation of particles can occur passively or actively [335].

**ROS generation in Silver Nanoparticles induced toxicity**

Numerous *in vitro* experiments have demonstrated that ROS-mediated toxicity is primarily responsible for the cellular and biochemical changes in the cells [353]. Various mechanisms may contribute to Ag NPs-induced toxicity, including oxidative stress. Biological processes are maintained by ROS such as superoxide radicals ($O_2$*) and $H_2O_2$, respectively. In the event of excessive ROS, the antioxidant defense system may collapse, allowing DNA, proteins, and lipids to be damaged [317]. Among other consequences, ROS released by mitochondria induces oxidative stress, disrupt ATP synthesis, and induce DNA damage, leading to apoptosis [262, 353]. Increasing ROS levels cause the GSH level to drop rapidly, and simultaneously LDH levels rise, resulting in apoptosis [263]. The oxidative stress generated by Ag NPs can harm human cell lines through DNA damage [263, 353], redox homeostasis at the intracellular level, lipid peroxidation and protein carbonylation. The antioxidant enzyme activity as well as the level of glutathione and sulfhydryl

groups bound to proteins decrease resulting in apoptosis [264]. Consequently, Ag NPs are primarily cytotoxic through apoptosis-induced cell death [265, 267]. Interestingly, decreases in PARP (poly ADP ribose polymerase) expression are associated with notable increases in caspase-3, H2X, and p-p53 expressions [267]. By apoptosis, Ag NPs can activate the p53 signaling pathway (Figure 7.1)[309].

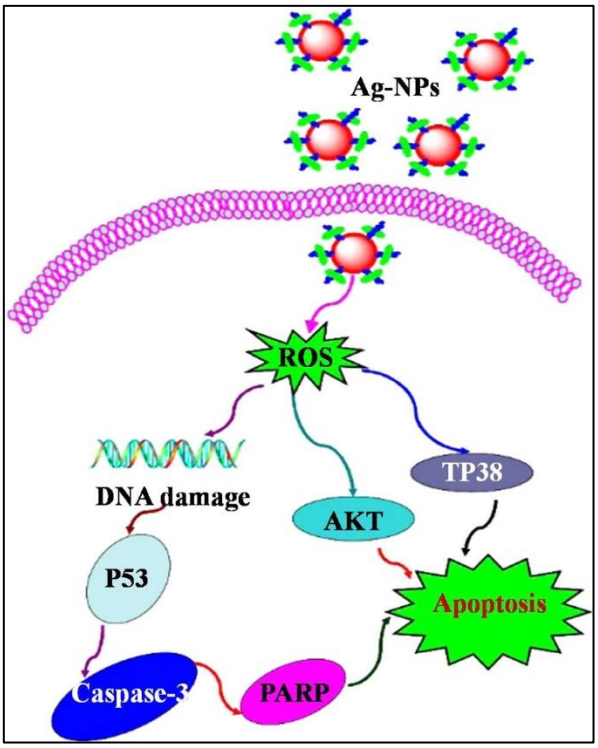


**Figure 7.1** Apoptosis inducing signaling pathway mediated by p53, AKT, MAPK activation to suppress ROS generated by Ag NPs [309].

By increasing the permeability of mitochondrial membranes, Ag NPs may result in mitochondrial dysfunction, regulating caspase-dependent apoptosis through JNK signaling [327]. As a result of loss of mitochondrial membrane potential (ΔΨ), Bcl-2 is downregulated, BAX is upregulated, and cytochrome C is released into the cytosol. By releasing cytochrome C into the cytosol, a cascade is initiated, leading to the activation of caspase 3 via apaf-1 and caspase 9 [268]. Hence, Ag NPs can cause cellular death by inducing apoptosis via mitochondria and caspase-dependent pathways which are mediated by JNK (Figure 8.1). Ag NPs can also cause epigenetic dysregulation through the reprogramming of gene expression [336]. They have also been shown to influence the cell cycle and hypermethylation of DNA which may have an epigenomic impact [336].

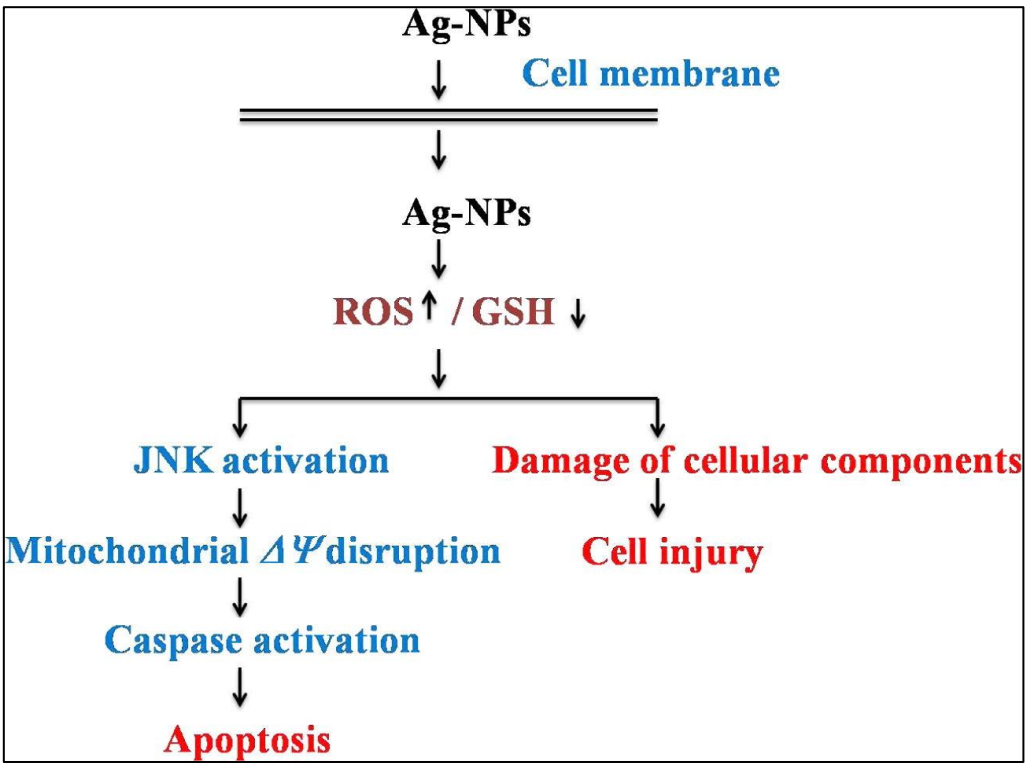


**Figure 8.1** A proposed pathway for silver nanoparticles (Ag NPs) induced reactive oxygen species (ROS) generation and intracellular reduced glutathione (GSH) depletion, damage to cellular components, and apoptosis [327].

The mechanism of toxicity in Ag NPs is compared to the Trojan-horse-type molecular pathway [313]. For example, RAW 265 cells phagocytose and make Ag NPs available in cytosol and culture medium of active cells but not in those that have been damaged. The nanoparticles released from the damaged cells may promote a 'Trojan horse-like' mechanism within the culture medium. Ag NPs are changed to Ag ions inside the damaged cells causing both damage to the cells and Ag NPs disappearing. The ROS produced as the result of phagocytosed Ag NPs induce inflammatory signaling and TNF-α secretion as well as a destruction of the cell membrane and apoptosis. This is thought to be because of the ionization of Ag NPs in the cell indicated as the Trojan-horse type mechanism [313].

Generally, three various mechanisms are involved in the penetration of Ag NPs within the cells such as diffusion, phagocytosis or endocytosis. After that, either Ag NPs or silver ions are released causing oxidative stress through ROS production. During ROS overproduction, several antiapoptotic proteins are denatured, which then leads to the expression of pro-apoptotic proteins. Thus, apoptosis signaling pathways are initiated by apoptotic proteins (Figure 9.1) [309].

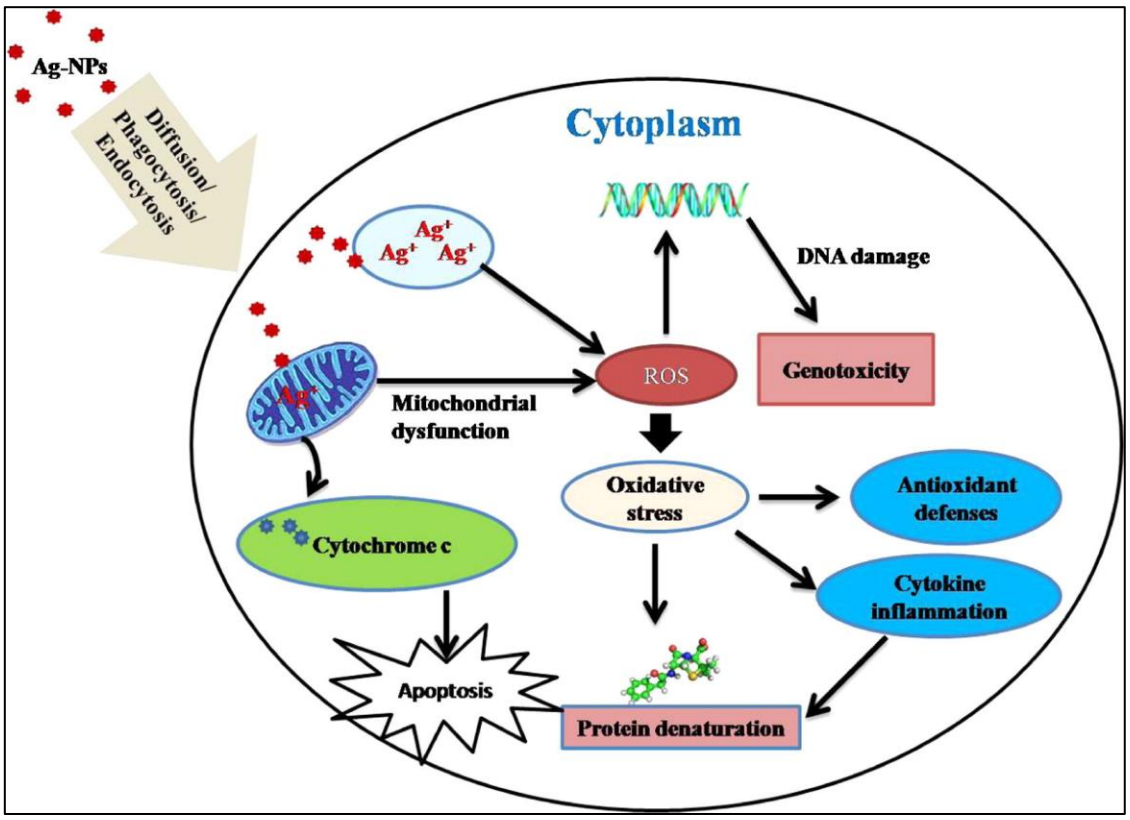


**Figure 9.1** Possible uptake process and mechanism of cytotoxicity induced by Ag NPs in different cell lines based on the metadata from several studies [309].

## Chapter 2: Colloidal Silver combating Pathogenic *Pseudomonas aeruginosa* and MRSA in Chronic Rhinosinusitis

### Statement of Authorship

| | |
|---|---|
| Title of Paper | Colloidal Silver combating Pathogenic *Pseudomonas aeruginosa* and MRSA in Chronic Rhinosinusitis |
| Publication Status | Published |
| Publication Details | Colloids and Surfaces B: Biointerfaces, https://doi.org/10.1016/j.colsurfb.2021.111675 |

### Principal Author

| | |
|---|---|
| Name of Principal Author (Candidate) | Sholeh Feizi |
| Contribution to the Paper | Project design, experimental work, data collection and analysis, manuscript preparation |
| Overall percentage (%) | 75% |
| Certification: | This paper reports on original research I conducted during the period of my Higher Degree by Research candidature and is not subject to any obligations or contractual agreements with a third party that would constrain its inclusion in this thesis. I am the primary author of this paper. |
| Signature | Date<br>28/09/2021 |

### Co-Author Contributions

| | |
|---|---|
| Name of Co-Author | Dr. Clare M Cooksley |
| Contribution to the Paper | Experimental support, manuscript preparation |
| Signature | Date<br>28/09/2021 |

| | |
|---|---|
| Name of Co-Author | George S. Bouras |
| Contribution to the Paper | Statistical analysis |
| Signature | Date<br>28/09/2021 |

| | |
|---|---|
| Name of Co-Author | Prof. Clive A Prestidge |
| Contribution to the Paper | Experimental support, manuscript preparation |
| Signature | Date<br>28/09/2021 |

| | |
|---|---|
| Name of Co-Author | Prof. Tom Coenye |
| Contribution to the Paper | Experimental support, manuscript preparation |
| Signature | Date<br>28/09/2021 |

| | |
|---|---|
| Name of Co-Author | Prof. Alkis J Psaltis |
| Contribution to the Paper | Project design, manuscript preparation |
| Signature | Date<br>28/09/2021 |

| | |
|---|---|
| Name of Co-Author | Prof. Peter-John Wormald |
| Contribution to the Paper | Project design, manuscript preparation |
| Signature | Date<br>28/09/2021 |

| | |
|---|---|
| Name of Co-Author | Associate/Prof. Sarah Vreugde |
| Contribution to the Paper | Project design, manuscript preparation |
| Signature | Date<br>28/09/2021 |

Colloidal Silver combating Pathogenic *Pseudomonas aeruginosa* and MRSA in Chronic Rhinosinusitis

Sholeh Feizi [a,b], Clare M Cooksley [a,b], George S Bouras [a,b], Clive A Prestidge [c], Tom Coenye [d], Alkis James Psaltis [a,b], Peter-John Wormald [a,b], Sarah Vreugde [a,b*]

[a] Department of Surgery-Otolaryngology Head and Neck Surgery, Basil Hetzel Institute for Translational Health Research, Central Adelaide Local Health Network, Woodville South, Australia.

[b] The University of Adelaide, Adelaide, Australia.

[c] Clinical and Health Sciences and ARC Centre of Excellence in Convergent Bio and Nano Science and Technology, University of South Australia, Adelaide, Australia

[d] Laboratory of Pharmaceutical Microbiology, Ghent University, Ghent, Belgium

*Corresponding author email address: sarah.vreugde@adelaide.edu.au

***Corresponding author postal address:** 37a Woodville Road, Woodville SA 5011, Australia

*Corresponding author phone number: +61-(0)8-8222-6928

## Graphical Abstract

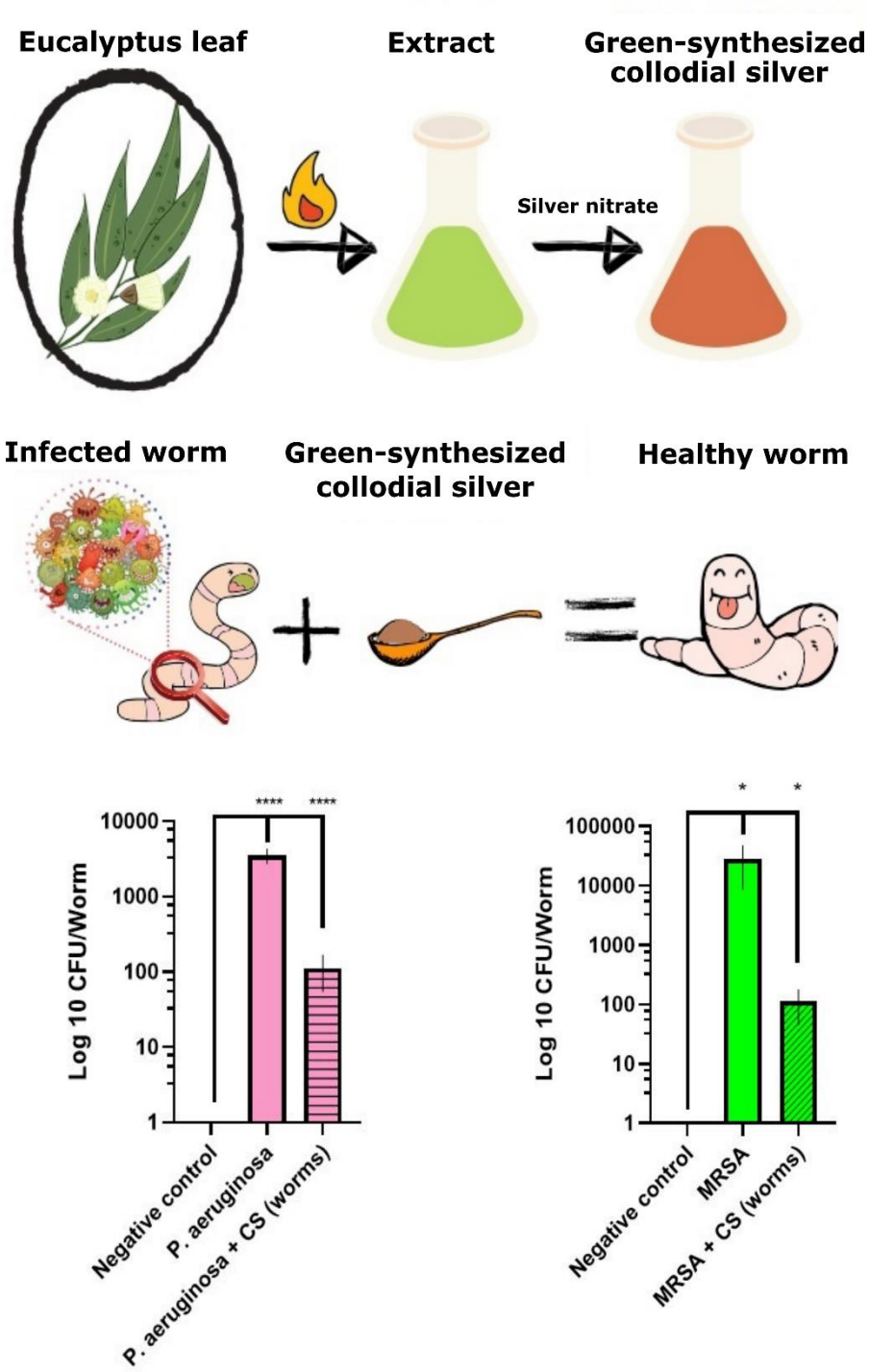

**Abstract**

The emergence of antibiotic resistant bacteria requires the development of new antimicrobial compounds one of which is colloidal silver (CS). It has strong bactericidal properties and is the most promising inorganic nanoparticles for the treatment of bacterial infectious diseases. However, their production can be slow and cumbersome. Here, we used *Corymbia maculata* aqueous leaf extract as a reducing agent to synthesize CS in a single 15-minute process. CS was physiochemically characterized for shape, size, zeta potential and stability. The Minimal Inhibitory Concentration (MIC) and Minimum Biofilm Eradication Concentration (MBEC) of CS against planktonic and biofilm forms of methicillin-resistant *Staphylococcus aureus* (MRSA, n= 5), *Pseudomonas aeruginosa (*n= 5), *Haemophilus influenzae* (n= 5) and *Streptococcus pneumoniae* (n= 3) chronic rhinosinusitis clinical isolates were investigated using the microdilution method and resazurin assay, respectively. The *in vitro* cytotoxicity on bronchial epithelial cells (Nuli-1) was analyzed by the crystal violet proliferation assay. The safety and efficacy of CS was evaluated in an *in vivo* infection model in *Caenorhabditis* elegans. CS was spherical with a diameter of between 11-16 nm (TEM analysis) in dried form and 40 nm (NanoSight) in colloidal form and was stable at room temperature and 4°C for one year. Average MIC and MBEC values varied between 11 and 44 ppm for MRSA, *H. influenzae* and *S. pneumoniae* and between 0.2 and 3 ppm for *P. aeruginosa*. CS was not toxic to Nuli-1 cells or *C. elegans* at concentrations of 44 ppm and reduced the Colony Forming Units counts by 96.9% and 99.6% in *C. elegans* for MRSA and *P. aeruginosa*, respectively. In conclusion, a novel, green synthesis of stable CS is demonstrated with good safety and efficacy profiles, particularly against *P. aeruginosa* in planktonic and biofilm forms. These CS have potential applications against clinical infections, including in the context of CRS.

**Keywords:** infection, chronic rhinosinusitis, green synthesis, eucalyptus, silver nanoparticle, *P. aeruginosa*

## Introduction

Chronic rhinosinusitis (CRS) is a heterogeneous inflammatory disease of the nasal cavity and paranasal sinuses which lasts for 12 weeks or longer [69]. Multiple factors are implicated in the etiopathogenesis of CRS including infection, obstruction of the sinus ostia and allergy [269]. Biofilms have been detected on the sinonasal mucosa of CRS patients, in particular in those patients with the refractory disease [270, 271].

Biofilms are organized communities of microbial cells embedded in a self-produced protein, nucleic acid and polysaccharide matrix, which allows the attachment of the biofilm to surfaces such as the mucosa [272, 273]. Compared to their planktonic counterparts, bacteria within biofilms are up to 1000 fold more tolerant to antibiotics due to the biofilm matrix forming a physical diffusion barrier and because of the slow rate of growth of bacterial cells within the biofilm [274, 275, 354]. Moreover, the extracellular matrix can contain enzymes that can inactivate or degrade antimicrobial agents [275].

One of the most common medical treatments for CRS is antibiotics [269]. However, bacterial resistance to antibiotics, antibiotic side effects, high health care costs and lack of evidence in support of antibiotic efficacy have resulted in the search for alternative treatment methods [157, 355].

Metallic silver has been previously used as an antimicrobial agent [356, 357]. More specifically, 10-100 nm silver nanoparticles (also termed colloidal silver-CS) have shown antibacterial activity against both Gram-negative and Gram-positive bacteria [201, 214, 358]. Importantly, CS has high antimicrobial activity against multi drug resistant bacteria including methicillin-resistant *Staphylococcus aureus* (MRSA) [359]. Binding to proteins, CS changes the structure of both bacterial cells and their nuclear membranes resulting in cellular disturbance and cell death [217]. Silver ions can also bind to thiol groups of microbial protein and lead to disruption of DNA structure and replication, finally resulting in cell death [226]. CS can also induce bacterial cell death by producing reactive oxygen species and free radicals [360].

CS can be synthesized by physical, chemical and biological methods. The toxic and harmful effects on living systems of by-products and materials used in the chemical synthesis of CS [361] and the high operational costs for the preparation of CS using physical methods have prompted efforts to produce CS through biological methods. Bio-reduction of silver ions by plant extracts reduces the use of toxic and harmful materials and has several advantages compared to physical and chemical methods [189, 190]. Plant extracts contain biochemical compounds playing the role of both reducing and stabilizing agents promoting the fast and cost-effective production of highly stable monodispersed CS particles. The easy access to plants, the production of environmentally friendly waste materials and low risk of contamination in comparison to the

production of CS by microorganisms, have recently focused the attention on the reduction of silver ions by plant extracts [355, 359, 362, 363]. However, plants and thus their extracts differ in the composition and concentration of biomolecules affecting their efficiency to facilitate the reduction process. This can affect the size, morphology, stability and antimicrobial activity of CS and thus complete characterisation of the biochemical properties as well as evaluation of toxicity and antimicrobial efficacy is required prior to using such nanoparticles in clinical application.

Previous research in our team has shown promise for CS to kill *S. aureus* (including MRSA) and *Pseudomonas aeruginosa* biofilm cells *in vitro* [201, 358] and *in vivo* [203]. Moreover, Ooi et al demonstrated the safety of twice daily CS (30 ppm) sinonasal rinses for 10 days in CRS patients. However, in those studies, CS was produced using a chemical extraction method which was ineffective and slow.

In the present study, CS was produced in a fast and cost-effective way using *Corymbia maculata* aqueous leaf extracts. CS and leaf extracts were extensively characterized, and their efficacy tested against clinical isolates of MRSA, *P. aeruginosa*, *Haemophilus influenzae* and *Streptococcus pneumoniae* in biofilm and planktonic form and in an *in vivo* model of MRSA and *P. aeruginosa* biofilms.

## Materials and methods

### Preparation of plant extracts

*Corymbia maculata* (spotted gum) fresh leaves were collected. Then they were washed three times with Milli Q water prepared in a three-stage Milli-Q Plus 185 purification system (Merck Millipore, Darmstadt, Germany) and the water was evaporated in the dark at room temperature. Afterward, they were finely cut and added to boiling water in a Meyer flask and boiled in a water bath and the extract was filtered using Whatman paper no. 1.

### Synthesis of CS and determination of reaction endpoint

The extract was added to 1 mM silver nitrate ($AgNO_3$, 99.9999% trace metals basis, Sigma-Aldrich, Steinheim, Germany) at room temperature. The color conversion from white to yellow revealed the immediate formation of CS. To determine the endpoint of the synthesis reaction of colloidal silver (CS), saturated NaCl solution (26% w/v) was used. Every 5 minutes, 3 ml of the CS and silver nitrate solution (as control) was treated with 5 µl of saturated NaCl solution and the reaction repeated until silver chloride (AgCl) precipitation in the CS ceased formation [364]. CS was centrifuged at 17000 x g, 4°C, 15 min after overnight incubation at room temperature. The supernatant was removed, and the precipitate was dissolved in Milli Q water to

concentrate the CS six times, followed by sonication in a Branson sonifier 450 (Timer: hold, Duty cycle%: 40% and Output Control: 4 (80 watts)).

**Characterization of CS**

The concentration of CS was determined by ICP-OES (Perkin Elmer Optima 8000 ICP-OES) using different concentrations of a known sample of CS ranging from 1 ppb CS to 500 ppb prepared in 2% nitric acid ($HNO_3$) along with CS diluted 1000-fold in 2% $HNO_3$. Indium was used as an internal standard. 2% $HNO_3$ solution was used as calibration blank (cal blk) and the intensity of the test samples was normalized to those values. The accuracy of the calibration curve was tested by using a second set of standards where silver was added to the solution [365].

UV–Vis extinction (absorption + scattering) spectra were recorded at 25 °C, 400-700 nm 2 hours after initiation of CS preparation by an Evolution 201 UV-Vis spectrometer to study the reduction process after particle synthesis.

Dynamic Light Scattering (DLS) measurement and surface potential of CS were analyzed using a Malvern Zetasizer Nano Series ZL at room temperature to acquire the particle size which was reported as the z-average and surface potential as zeta potential (-potential). The measurements were conducted at a scattering angle of 173° at 25 °C using a helium−neon laser with a wavelength of 633 nm. In addition, the diameter of CS in Brownian motion (diluted 1: 2500) was also measured by nanoparticle tracking analysis (NTA), a laser based optical technique, fitted with a syringe pump attachment (NanoSight NS300, Malvern, UK).

CS were spotted onto formvar/carbon 200 mesh grids (ProSciTech, Townsville, Australia) and examined. Transmission Electron Microscopy (TEM) and energy dispersive X-ray (EDXA) analysis were performed by a Tecnai G2 Spirit TWIN Transmission Electron Microscope (FEI, Hillsboro, USA), operating at 100KV, to confirm the morphology and size of CS, respectively. Then, the particle size distribution was determined using the University of Texas Health Science Center San Antonio (UTHSCSA) image tool software, version 3.00 (Image Tool Software, San Antonio, USA). CS was freeze-dried and X-ray diffraction (XRD) was performed with Cu radiation in the 2θ range of 5-80 operated at a voltage of 40 kV (Rigaku MiniFlex 600, Japan).

CS were centrifuged and resuspended in water and 5% dextrose and stored at two different temperatures (room temperature and 4°C). The stability of CS was evaluated by measuring the size of CS at various concentrations by a Malvern Zetasizer Nano Series ZL.

**Determination of reducing agents in the plant leaf extracts**

**Gas-Chromatography-Mass-Spectrometry (GC-MS)**

The extract was prepared as described [366]. Briefly, 8 ml chloroform was added to the 40 ml extract and oscillated continuously for 10 minutes. The mixture was then kept at room temperature for 24 hours followed by dehydration of the bottom extract with saturated sodium sulfate. The filtrate was analyzed using an Agilent Technologies 7891A GC system (Carrier gas (He) flow rate 1.2mL/min. Restek Sil MS column 30m, 0.25 mm I.D. 0.25 µm film thickness) coupled with an Agilent 5973N mass spectrometer. The initial column temperature (40°C) was held for 3.5 minutes, before ramping at 10 °C /min up to 280 °C which was held for a further 4 minutes. The injector temperature or inlet temperature was constant at 250°C. Identification of the compounds was performed by the analogy of mass spectra with those of the National Institute of Standards and Technology mass spectral libraries (NIST, Gaithersburg, USA).

**Colorimetric assays**

Phenolic compounds were determined by the Folin–Ciocalteau colorimetric method using gallic acid as a standard [367]. The spectrometric assay based on aluminum formation was used to quantify Flavonoid content [368]. The phenol-sulfuric acid colorimetric method was used to assess the total sugar content of the extract [369].

**Bacterial Strains and Cell Lines**

The study was approved by the human research ethics committee at the Queen Elizabeth Hospital, Woodville, South Australia, Australia (HREC/15/TQEH/132). Clinical isolates were collected from the sinonasal cavities of patients undergoing endoscopic sinus surgery for CRS or from otitis media effusions (*H. influenzae* NT 1159 and NT 176). Isolates were identified as MRSA, *S. pneumoniae, P. aeruginosa* or *H. influenzae* by an independent diagnostic microbiology laboratory (identification based on MALDI-TOF Mass Spectrometry, Adelaide Pathology, Adelaide, Australia). The bacterial reference strain *H. influenzae* ATCC 33391 was obtained from American Type Culture Collection (ATCC, Manassas, USA). The Nuli-1 cell line (derived from human airway epithelial cells) was purchased from ATCC.

**Cytotoxicity Studies**

Nuli-1 cells were grown in a serum-free bronchial epithelial growth medium (BEGM) (Lonza Australia Pty Ltd, Mount Waverley VIC, Australia). Cells were maintained in a fully humidified incubator with 5% $CO_2$

at 37 °C. Cells (10.000 cells/well) were exposed to different concentrations of CS for 1 hour, followed by the determination of cell viability by crystal violet proliferation assays.

**Crystal violet proliferation assay and *in vivo* toxicity assay**

Briefly, Nuli-1 cells were fixed in 100 µl of 10% neutral buffered formalin for 30 minutes. Following removal of formalin by flicking, the cells were stained with 100 µl of 1% crystal violet in 2% ethanol. They were then washed in distilled water 8 times. Next, 100 µl of 10% acetic acid was added to each well and the plates were placed on a rocking platform at room temperature for 1 hour to elute the crystal violet. Finally, the absorbance was read at 595 nm by a microplate reader (Imark plate reader, Bio-Rad). Cell viability percentage (CV%) was quantified according to equation 1:

$$CV\% = \frac{A_T}{A_C} \times 100\% \qquad (1)$$

Metabolic activity of cells was expressed as the Cell Viability percentage (% CV), where $A_C$ is the Absorbance of the untreated control cells (100% cell viability) and $A_T$ is the Absorbance
observed in the treated cells. Both $A_C$ and $A_T$ were subtracted from background fluorescence (medium). Viability studies were performed as three independent experiments with four wells per treatment [370].

An *in vivo* toxicity assay in *Caenorhabditis elegans* (*C. elegans*) AU37 (glp-4; sek-1) was performed to examine the safety of the synthesized CS. Briefly, to synchronize worm populations, they were collected from Nematode Growth Medium (NGM) agar plates (seeded with an *Escherichia coli* OP50 lawn and incubated at 16 °C) by washing with 0.9% saline. 4 N sodium hydroxide plus 5% sodium hypochlorite was used to lyse the worms and harvest the eggs. Thereafter, synchronized nematodes (L4 stage) were collected with OGM medium (95% M9 buffer, 5% Brain Heart Infusion (BHI) supplemented with 10 µg/ml cholesterol) and seeded in a 96-well plate containing approximately 20 worms per well. The nematodes were exposed to different concentrations of CS for 1 hour with the control group exposed to OGM medium (Richter et al. 2017). The percentage of surviving worms was calculated by counting the live worms. Viability studies were performed as three independent experiments with two wells per treatment.

**Antibacterial activity of CS**

***In vitro* antibacterial activity studies**

Clinical isolates were streaked onto nutrient agar, tryptone soy agar, chocolate agar and blood agar plates for *P. aeruginosa*, MRSA, *H. influenzae* and *S. pneumoniae,* respectively. Antibacterial activity of CS against planktonic forms of bacteria was assessed by determining the minimal inhibitory concentration (MIC)

using the microdilution method as described by the Clinical and Laboratory Standard Institute (CLSI) [371]. Briefly, one colony of bacteria was resuspended in broth medium to adjust to 0.5 ± 0.1 McFarland units (approximately 1.5 × $10^8$ Colony Forming Units (CFU)/mL). Dilutions of bacteria 1:100 in broth were prepared using nutrient broth (NB) for *P. aeruginosa*, tryptone soy broth (TSB) for MRSA and *S. pneumoniae* and supplemented BHI (sBHI) [372] for *H. influenzae*, respectively. Then, 96-well microtiter plates were inoculated with 100 µl of diluted bacterial suspensions followed by 100 µl of different concentrations of CS and incubated at 37°C for 18-24 h (with the addition of 5% $CO_2$ for *H. influenzae* and *S. pneumoniae*). Finally, the absorbance was read at 595 nm. Bacterial Growth Inhibiting percentage (BGI%) of CS was quantified according to equation 2:

$$BGI\% = 100 - (\frac{A_T}{A_C} \times 100\%) \qquad (2)$$

Antibacterial activity of CS is expressed as the BGI%, where $A_C$ is the absorbance of the untreated control bacteria (100% bacterial growth) and $A_T$ is the absorbance observed in the treated bacteria. Both $A_C$ and $A_T$ were subtracted from background absorbance (broth). The effect of CS against growth inhibition of planktonic forms of bacteria was performed as three independent experiments with three wells per treatment.

The minimum biofilm eradication concentration (MBEC) of CS was determined as described by Richter et al. 2017. Briefly, one colony of bacteria was resuspended in 0.9% saline to adjust to 1.0 ± 0.1 McFarland units (approximately 3 × $10^8$ CFU/mL). The suspension was diluted 1:15 in broth (TSB for *P. aeruginosa* and MRSA and sBHI for *H. influenzae*) and black 96-well plates (Costar, Corning Incorporated, Corning, U.S.) were inoculated with 150 µl of diluted bacterial suspensions. Suspensions were incubated at 37°C for 48 h on a rotating platform at 70 rpm in a 5% $CO_2$ incubator. Established biofilms were washed twice with phosphate buffered saline (PBS) and exposed to different concentrations of CS for 1 h at 37°C on a rotating platform at 70 rpm, in a 5% $CO_2$ incubator. Biofilms were washed twice with sterile water followed by measurement of bacterial viability via the resazurin assay (Life Technologies, Scoresby, Australia).

**Resazurin assay**

Briefly, 200 µl of a freshly prepared 10% resazurin dilution in broth medium was added and incubated at 37 °C on a rotating platform at 70 rpm (5% CO2 incubator for *H. influenzae* and *S. pneumoniae*) protected from light. The fluorescence was measured after 1 h and readings were continued hourly until reaching maximum fluorescence on a FLUOstar OPTIMA plate reader (BGM Labtech Gretenberg, Germany) at λ excitation = 530 nm/λ emission = 590 nm. Biofilm Eradication percentage (BE%) was quantified according to equation 3.

$$BE\% = 100 - (\frac{F_T}{F_C} \times 100\%) \qquad (3)$$

Antimicrobial activity of CS is expressed as BE%, where $F_C$ is the fluorescence of the untreated control biofilm (100% biofilm viability) and $F_T$ is the fluorescence observed in the treated biofilm. Both $F_C$ and $F_T$ were subtracted from background fluorescence (broth). Biofilm eradication studies were performed as three independent experiments with four wells per treatment.

### *In vivo* bacterial infection assay

To examine the efficacy of CS, age-synchronized *C. elegans* worms (glp-4; sek-1) were collected. 20 worms were seeded per well and nourished with CS, OGM medium and bacterial suspension with Optical Density (OD) three. Worms in OGM medium alone and bacterial suspension/OGM medium were considered as negative and infection control, respectively. CFU per worm was determined after 1-hour incubation at 20 °C as follows. Nematodes were collected and rinsed with M9 buffer supplemented with 1 mM sodium azide. Thereafter, they were washed with PBS before being mechanically disrupted. 1.0 mm silicon carbide beads (Biospec Products, OK, U.S.) along with worms were vortexed for 10 minutes. Finally, CFU was counted by spreading different dilutions of the lysates on Tryptic Soy Agar (TSA) plates with 7% NaCl and cetrimide agar plates for MRSA and *P. aeruginosa*, respectively [198].

### Statistical Analysis

All experiments were performed in three independent experiments with three wells per treatment and are shown as mean ± standard deviation (SD) by one-way analysis of variance (ANOVA) (GraphPad Prism version 8.00, GraphPad Software, La Jolla, U.S.). Two-way ANOVA analysis was used to test the effects of time and concentration on the size of CS. Statistical significance was estimated at the 95% confidence level and a p-value of $<0.05$ was considered statistically significant.

## Results

### Characteristics of CS particles obtained

CS was synthesized immediately after adding $AgNO_3$ solution to aqueous extracts of *Corymbia maculata* fresh leaves causing a change in colour from transparent light green to brown (Figure 1.2a) [366]. No further change in colour was observed after about 15 minutes when the reaction was considered complete. This was also indicated by the absence of AgCl precipitation after adding saturated NaCl to CS in contrast to AgCl precipitation occurring in $AgNO_3$ solution treated with saturated NaCl (Figure 1.2b).

Shape, size and dielectric constant of the CS environment cause the extinction spectra of CS with a strong peak at 430 nm (Figure 1.2c) specific for CS [373]. The single surface plasmon resonance (SPR) band in the extinction spectra is indicative of spherical CS in colloidal form according to Mie's theory [374].

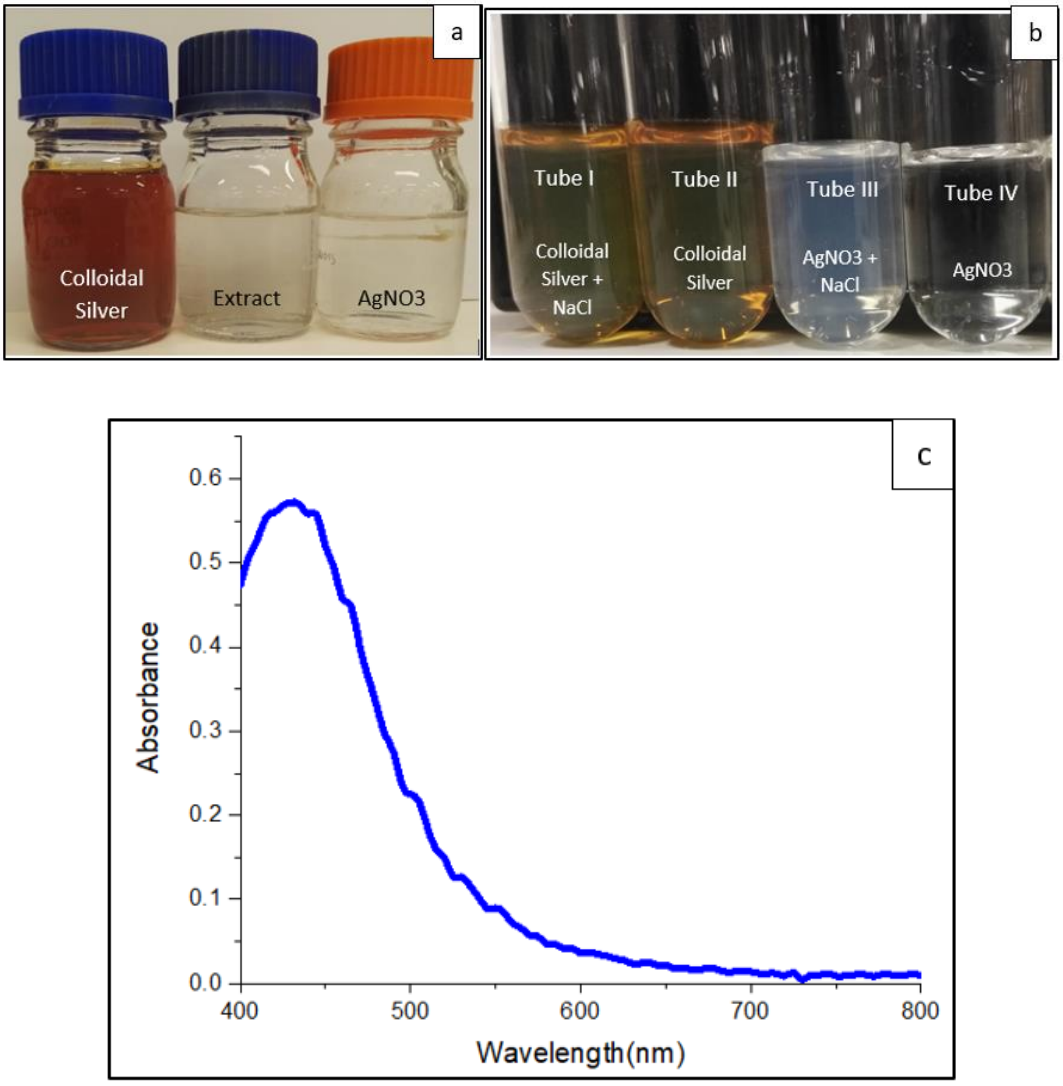


**Figure 1.2** Optical and visible spectroscopy characterization of colloidal silver (CS).

(a) Colloidal silver (brown colour), extract (transparent) and silver nitrate ($AgNO_3$) (transparent) solution, (b) The end of synthesis reaction (Tube I: CS treated with NaCl, which is similar in appearance/colour to Tube II, which is only CS). Tube III: $AgNO_3$ treated with NaCl (cloudy) in comparison to Tube IV, which is $AgNO_3$ only (c) Visible spectra of CS measured as absorbance vs wavelength (nm)

The hydrodynamic diameter (HDD) of CS was measured by NTA using the Nano Sight and DLS using Malvern zetasizer after centrifugation and resuspending CS in water. The average diameter of CS is 40 nm ± 36, which was measured by nanoparticle counting technique using Nano Sight and 70 nm ± 36

using Malvern zetasizer. There was no discrepancy between the two techniques used indicating consistent size of produced CS by both measuring the number based particle size, Nano Sight, and the intensity-based size distribution, Malvern zetasizer (Figure 2.2a and b). The zeta-potential was -20.4 mV (Figure 2.2c).

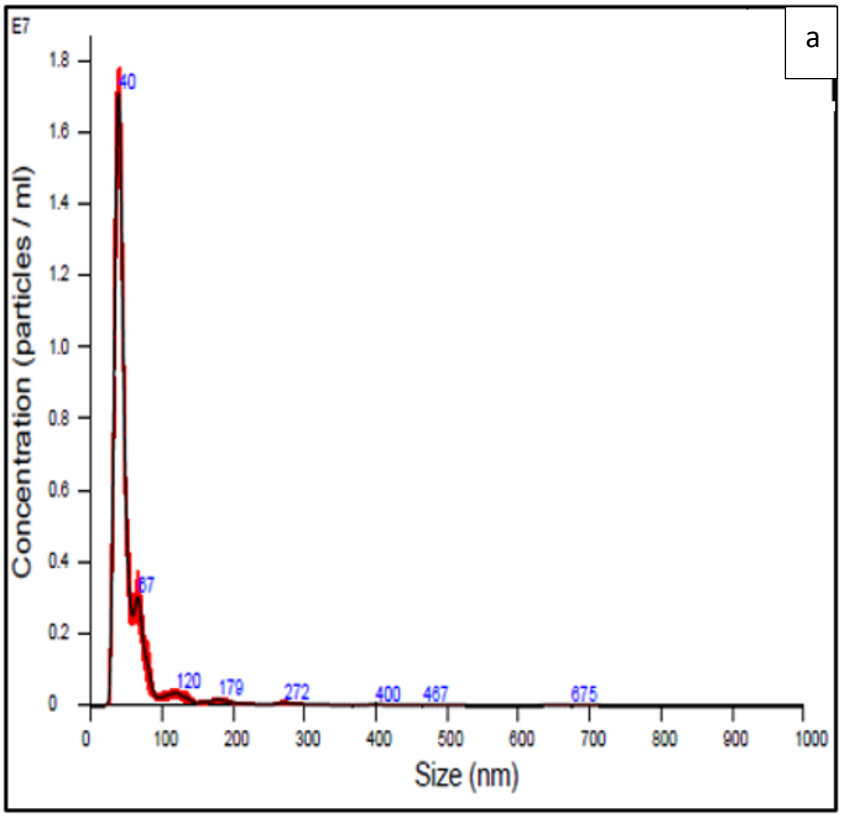


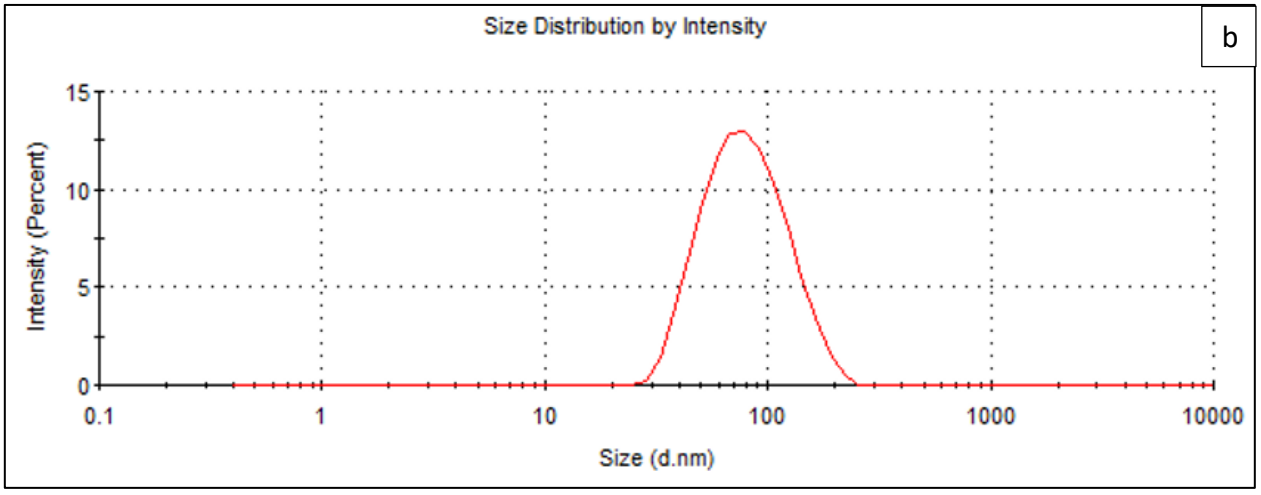

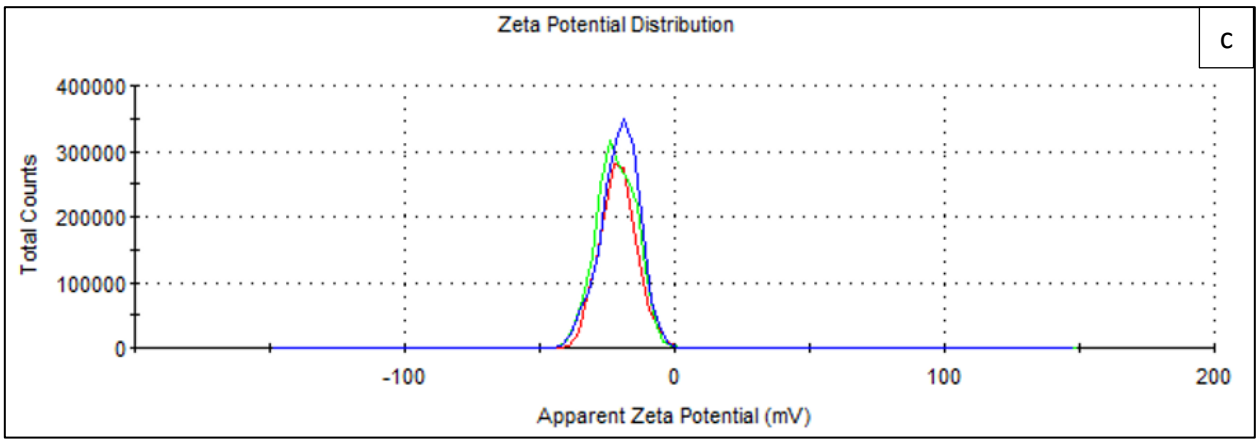


**Figure 2.2** Hydrodynamic diameter and surface charge of colloidal silver (CS).

(a) The number based particle size measuring by Nano sight and (b) the intensity-based size distribution of CS by Malvern zetasizer (c) Zeta-potential (surface charge in mV) of CS. The representative measurement from three replicates is shown (SD=6.93)

TEM images showed the presence of spherical CS (Figure 3.2a and b). They were well distributed with a size range of 1 to 60 nm most of which were between 16 and 20 nm and the mean was 25 ±10 (Figure 3.2c and d).

The EDX spectrum indicated the presence of silver and chloride atoms related to CS. Moreover, there were other peaks related to other elements such as carbon, oxygen and copper, which can be related to TEM grid and the extract (Figure 3.2e).

The crystalline structure of CS is indicated by the XRD pattern (Figure 3.2f). The Face-Centered Cubic (fcc) structure of metallic silver is reflected by the 111, 200, 220, 311, 220 and 222 Miller indices, related to 2θ= 38.32°, 44.35°, 64.52°, 67.66°, 77.43°, and 81.57°, respectively. Furthermore, 111, 200, 220 and 222 Miller indices attributed to 2θ= 28°, 32.44°, 46.44°, and 57.66°, respectively, indicating the fcc-structured AgCl-NPs [375, 376].

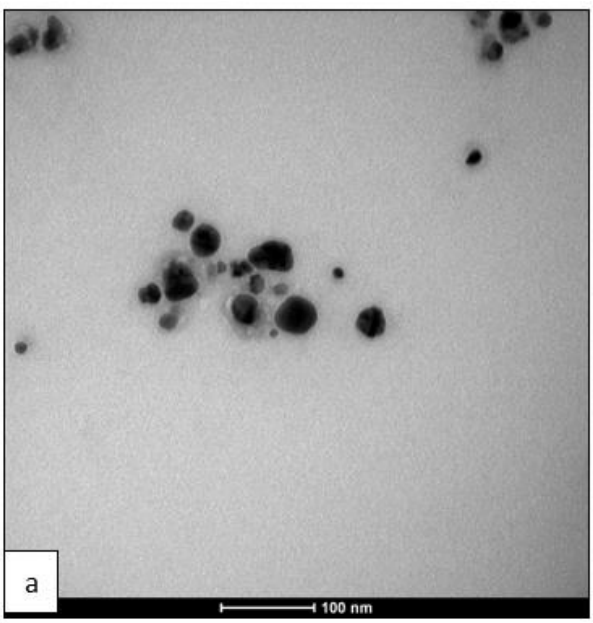
a
100 nm

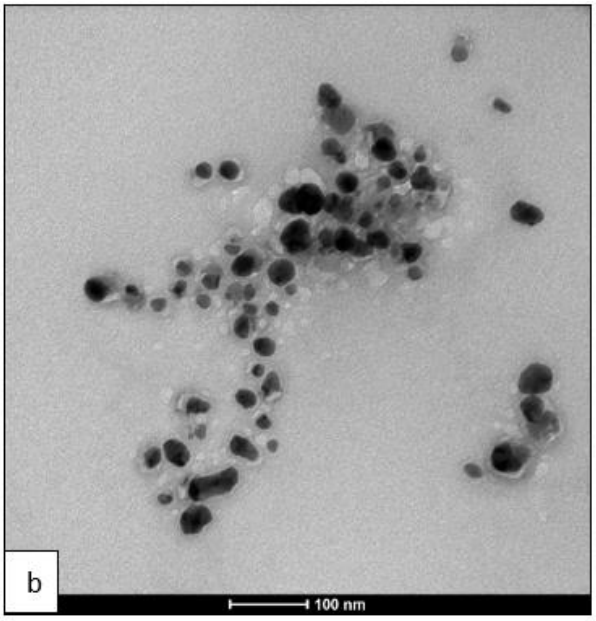
b
100 nm

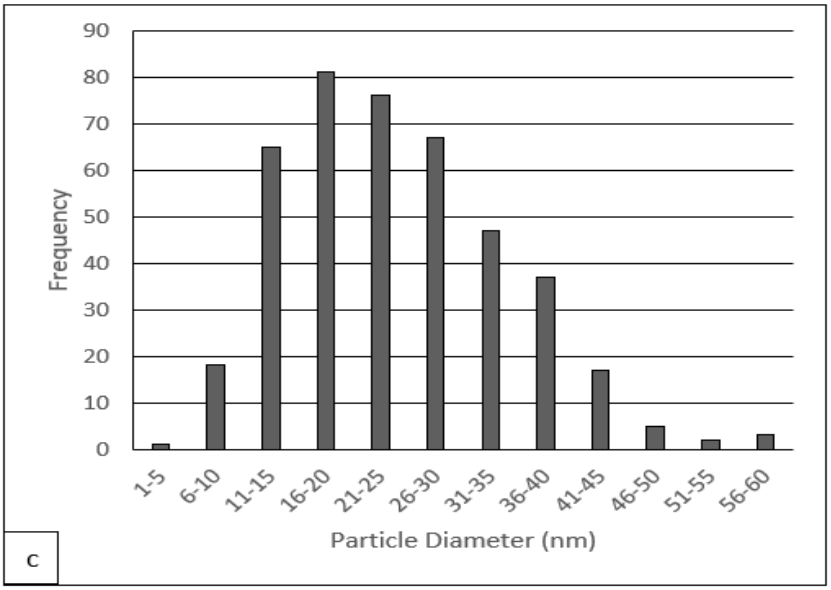
c
Frequency
90
80
70
60
50
40
30
20
10
0
1-5
6-10
11-15
16-20
21-25
26-30
31-35
36-40
41-45
46-50
51-55
56-60
Particle Diameter (nm)

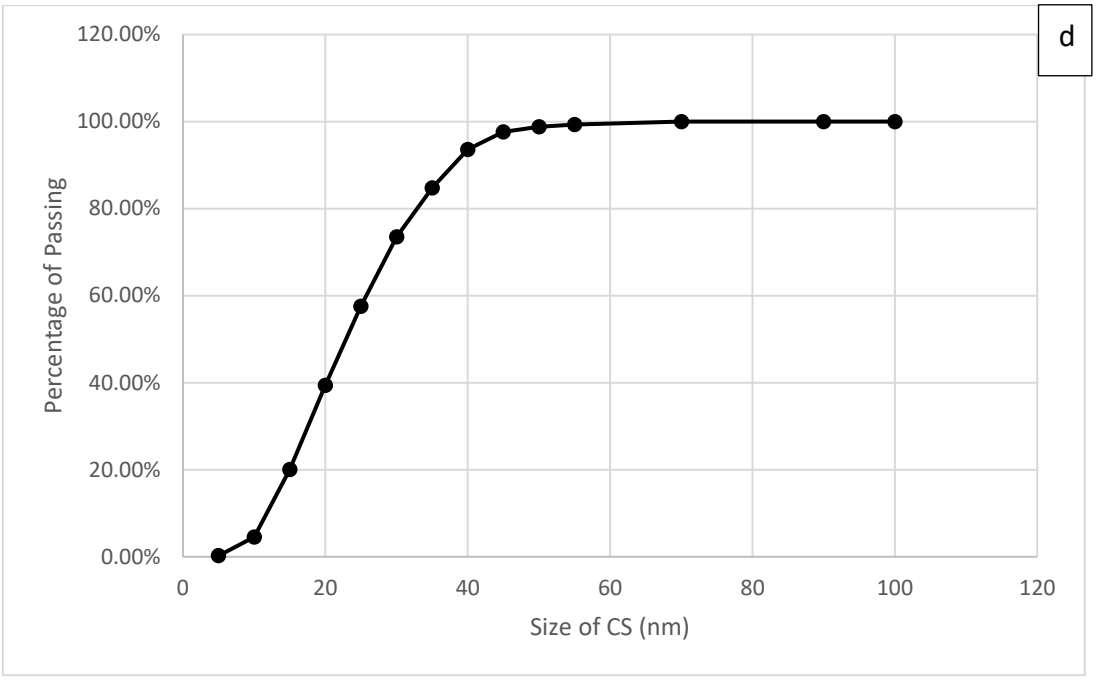
d
120.00%
100.00%
80.00%
60.00%
40.00%
20.00%
0.00%
Percentage of Passing
0
20
40
60
80
100
120
Size of CS (nm)

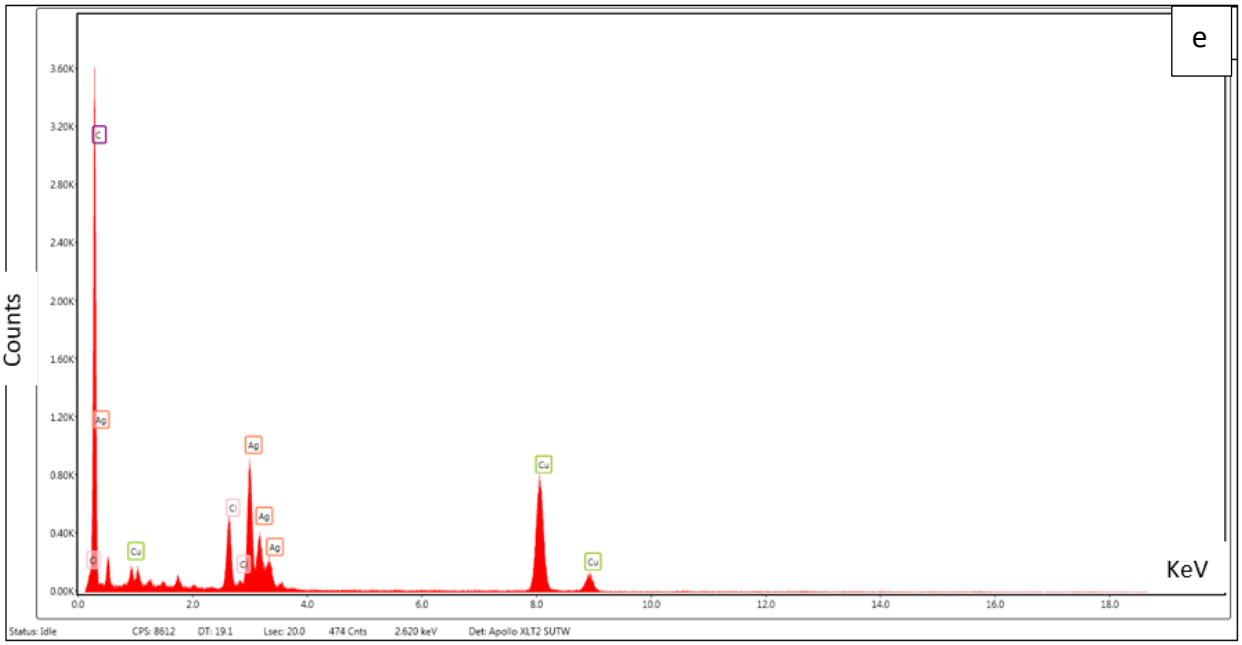
e
Counts
KeV
C
Ag
Cu
Cl
Status: Idle
CPS: 8612
DT: 19.1
Lsec: 20.0
474 Cnts
2.620 keV
Det: Apollo XLT2 SUTW

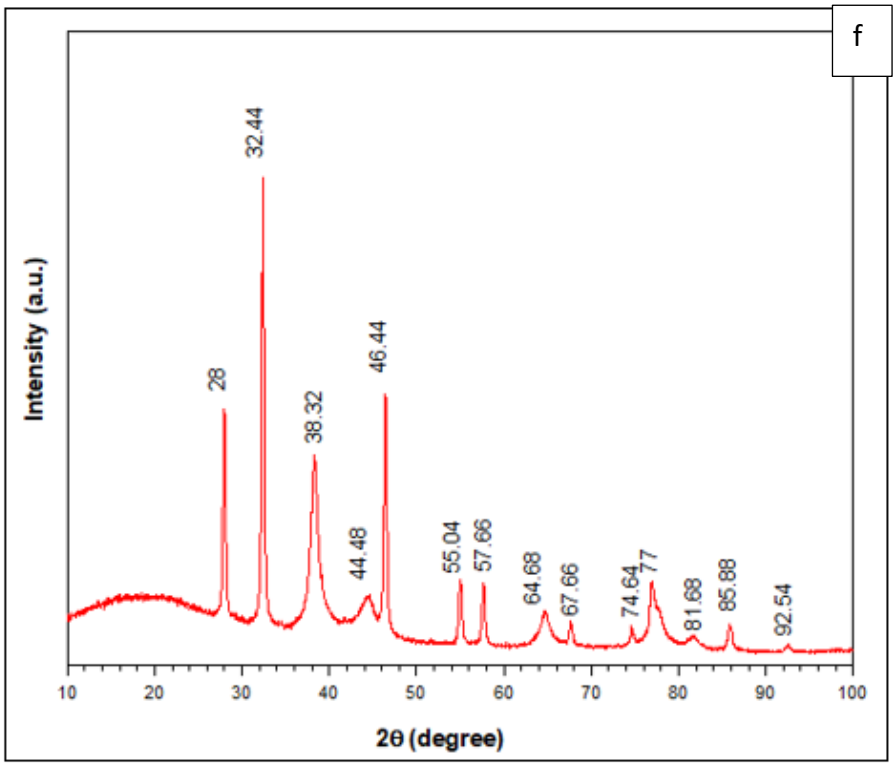


**Figure 3.2** Morphology, size distribution, elemental analysis and crystal structure of CS.

(a) and (b), Transmission electron microscopy (TEM) images of CS, (c) particle size distribution histogram, (d) size distribution curve e) energy dispersive X-ray (EDX) spectrum and (f) X-ray diffraction (XRD) pattern of CS.

Based on the result of ICP-OES, the concentration of synthesized CS was 350 ppm (Table 1.2).

**Table 1.2** ICP-OES analysis of CS.

| Sample Id | In 230.606 (IS) | Ag 328.068, ppb | Ag 338.289, ppb | Ag 328.068, ppb | Ag 338.289, ppb |
|---|---|---|---|---|---|
| | | dil 1000 times | dil 1000 times | adjusted result | adjusted result |
| | | LOD: 10 ppb | LOD: 10 ppb | | |
| cal blk | 1 | 0 | 0 | | |
| 1 ppb | 1.002562388 | 1 | 1 | | |
| 5 ppb | 1.017496569 | 5 | 5 | | |
| 10 ppb | 1.025156885 | 10 | 10 | | |
| 50 ppb | 1.003618591 | 50 | 50 | | |
| 100 ppb | 0.994348212 | 100 | 100 | | |
| 200 ppb | 0.989153277 | 200 | 200 | | |
| 500 ppb | 0.969354705 | 500 | 500 | | |

| | | | | | | |
|---|---|---|---|---|---|---|
| Blank | 0.971635331 | 1.075416952 | 1.473206177 | | | |
| 100 ppb CCV | 0.978593305 | 99.13850097 | 98.60467523 | | | |
| 100 ppb QC27 | 0.812874014 | 110.2173081 | 103.1577324 | | | |
| Blank | 0.973805914 | 1.086097102 | 1.25555434 | | | |
| 1 x 1000 | 0.971815519 | 355.2301016 | 352.5099214 | 355230.1016 | 352509.9214 | 350 |
| Blank | 0.9756107 | 1.230263281 | 1.310913517 | | | |
| Blank | 0.966588123 | 1.209807405 | 1.33460031 | | | |
| 100 ppb CCV | 0.978318423 | 99.73583126 | 99.29736119 | | | |
| 100 ppb QC27(quality control) | 0.832884465 | 107.1017336 | 100.8410938 | | | |

* Based on the table, different samples including calibration blank (2% nitric acid, cal blk), CS of known concentration from 1 ppb to 500 ppb, blank, Continuing Calibration Verifications (*CCV*), Quality Control 27 (QC) along with the CS synthesized in our study (1000 times diluted) were running on Perkin Elmer Optima 8000 ICP-OES. The results came well within the calibration range. Indium (In) was used as the internal standard and the results were given by two wavelengths (328 and 338), we can use either or. The results are given in ppb in the table, which in ppm would translate into slightly more than 350 ppm as concentration for the CS in our study. The blank, 100 ppb QC, 100 ppb CCV were injected several times as it is shown in the table to make sure that the results are accurate.

The stability of CS was assessed over one year after synthesis by measuring their size using DLS (Malvern Zetasizer) (Table 2.2 and Figure 4.2). Two-way ANOVA analysis testing the effects of Time and Concentration on Size showed that concentration had a significant effect on size. In particular, CS at a concentration of 58 ppm showed a significantly larger size than CS at higher concentrations (p-value<2e-16). Further, the effect of time on size was not significant (p-value = 0.0911) (Figure 5.2).

a

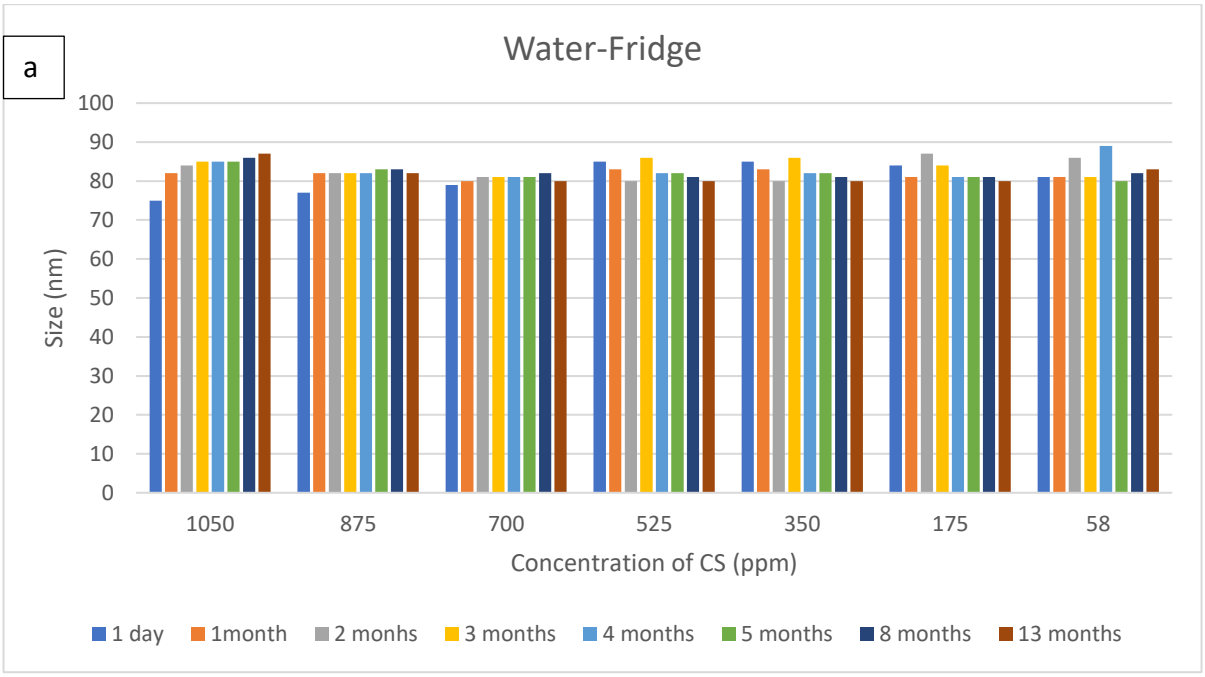
Water-Fridge
100
90
80
70
60
50
40
30
20
10
0
Size (nm)
1050
875
700
525
350
175
58
Concentration of CS (ppm)
1 day
1month
2 monhs
3 months
4 months
5 months
8 months
13 months

b

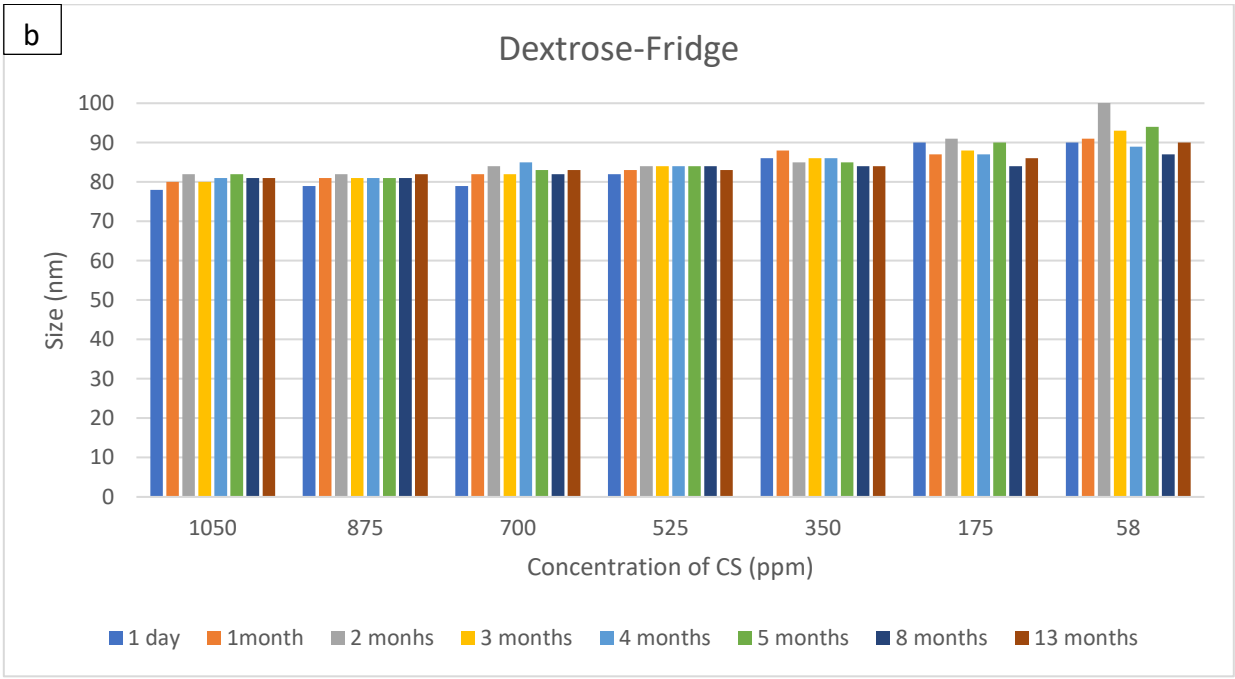
Dextrose-Fridge
100
90
80
70
60
50
40
30
20
10
0
Size (nm)
1050
875
700
525
350
175
58
Concentration of CS (ppm)
1 day
1month
2 monhs
3 months
4 months
5 months
8 months
13 months

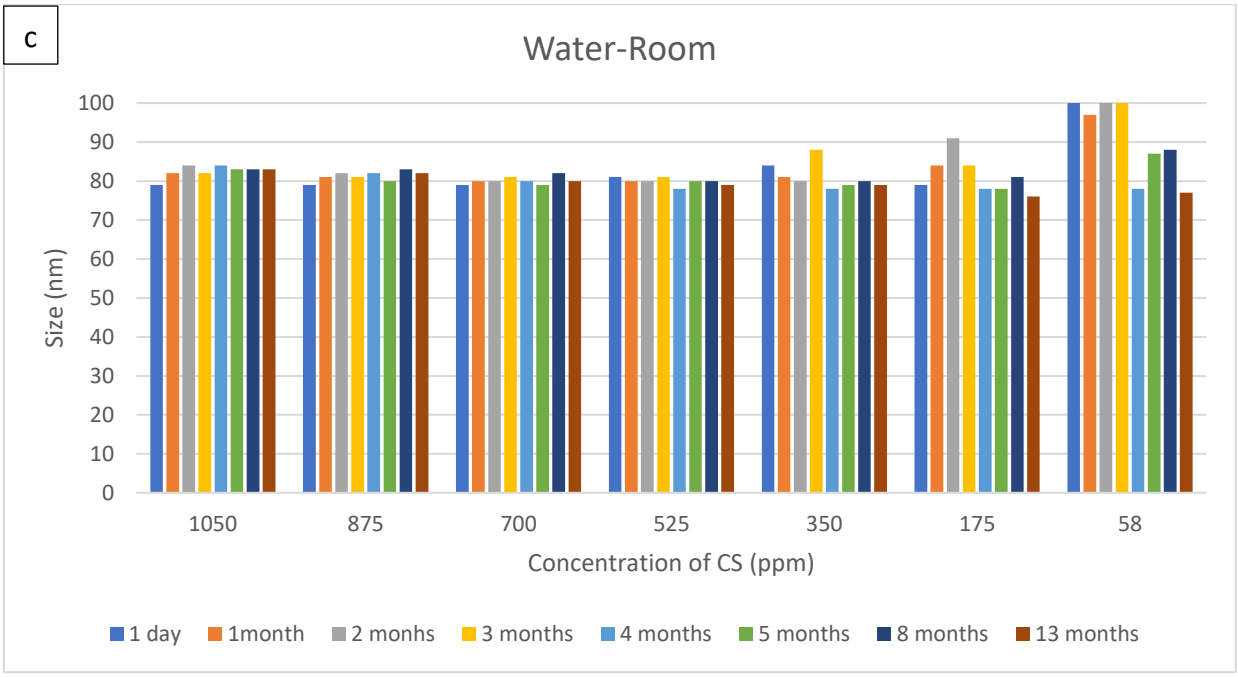


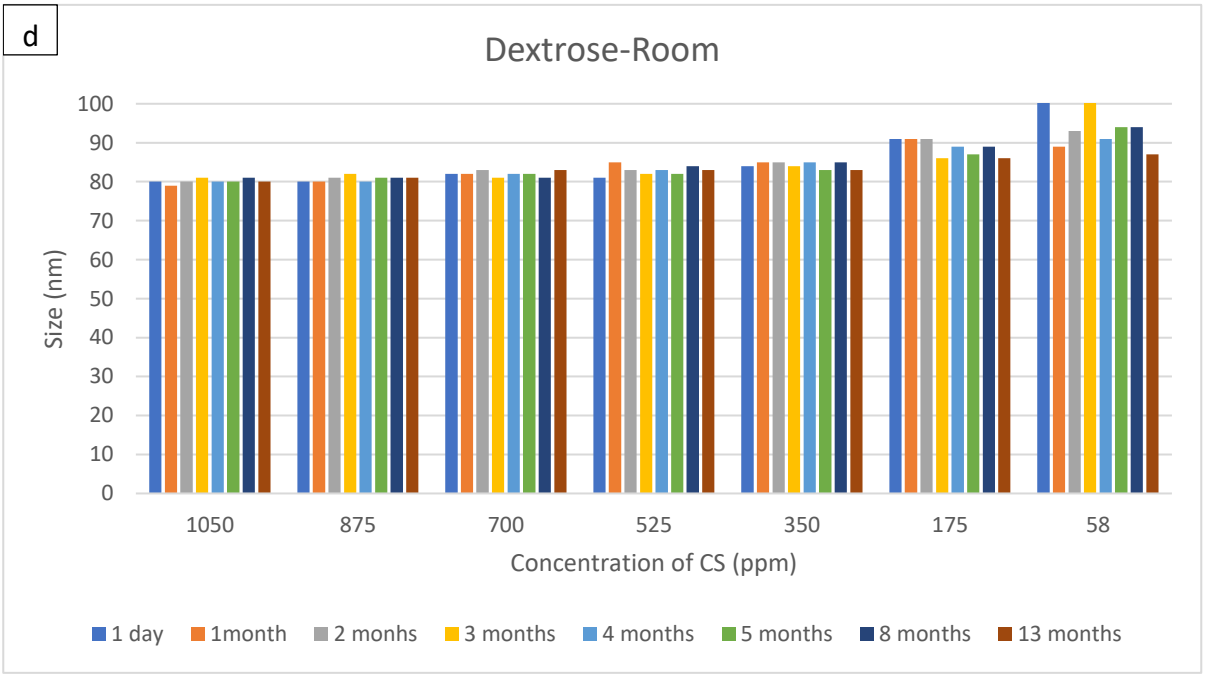


**Figure 4.2** Size of CS (using Malvern Zetasizer) at different time points.

CS size at different concentration resuspended a) in water and kept in the fridge, b) in dextrose and kept in fridge c) in water and kept at room d) in dextrose and kept at room

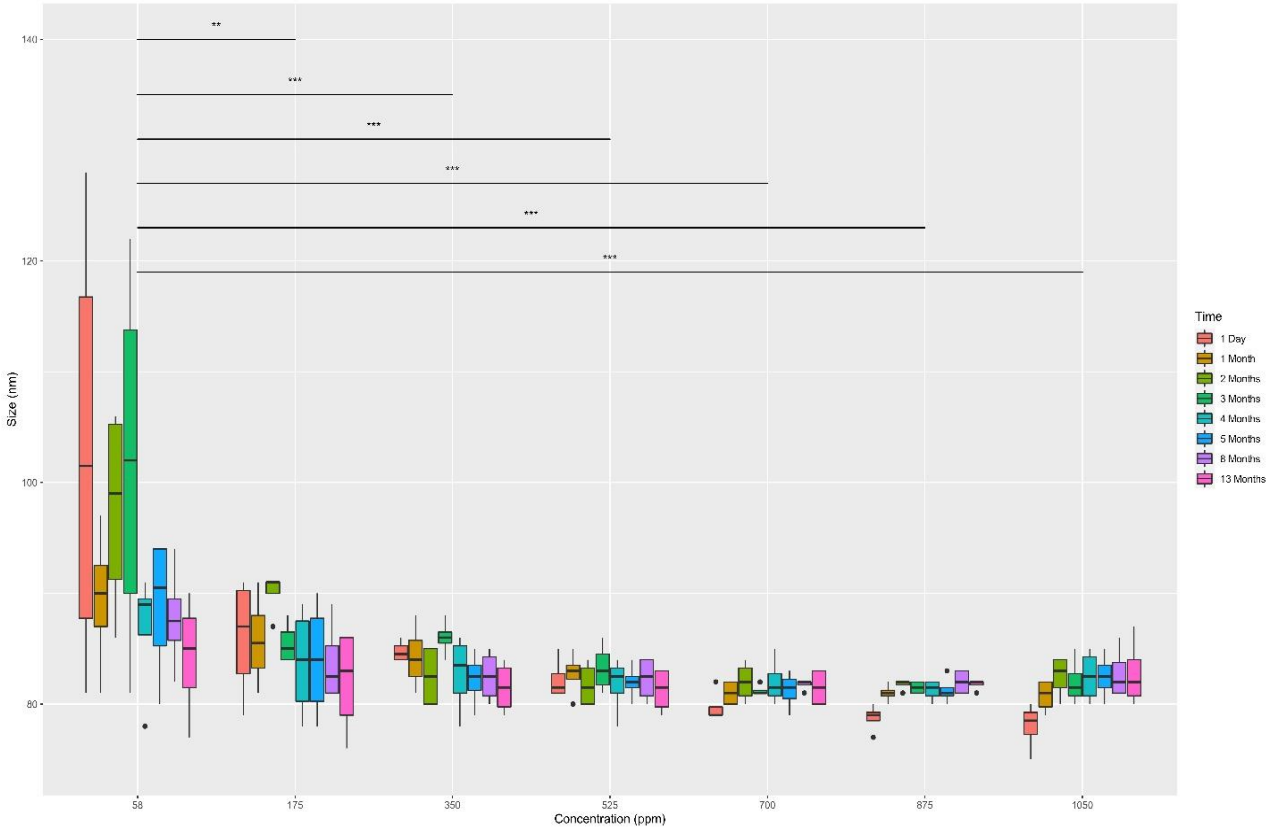


**Figure 5.2** Clustered box plot of size for different time points and concentrations.

Concentration is each group of boxes withdifferent time having different colour indicated by the legend.

### Identification of biomolecules involved in the synthesis of CS

### Gas-Chromatography-Mass-Spectrometry

Analysis of the leaf extract was performed by GC-MS to identify the reducing and capping biomolecules in the extract. The chromatogram shows the presence of fourteen biomolecules with various retention times (RT) in the leaf extract (Figure 6.2 and Table 2.2). Biomolecules such as 1,8- cineole (cineole or eucalyptol, RT-9.999 minutes), ionones or 3-buten-2-one 4-(2 6 6-trimethyl-1-cyclohexen-1-yl) (RT-18.174 minutes) and 1-cyclohexanone 2-methyl-2-(3-methyl-2-oxobutyl) (RT-19.662 minutes) can play a role in reducing silver ions to CS due to oxidation of carbon double bonds to carboxylic groups [377]. Moreover, 4-bromo-1-naphthylamine (RT-20.677 minutes) is also a probable reducing agent due to the amine or bromide group. Furthermore, the other biomolecules such as Eicosane (RT-22.183 minutes), Heneicosane (RT-23.123 minutes, RT-24.02 minutes and RT-24.89 minutes), Tetracosane (RT-25.724 minutes), Pentacosane (RT-26.527 minutes), Hexacosane (RT-27.308 minutes), Heptacosane (RT-27.308 minutes), Octacosane

(RT-29.125 minutes) and Octadecane 3-ethyl-5-(2-ethylbutyl)- (RT-30.277 minutes) can cover the CS surface and help its stability as well as acting as reducing agents [378].

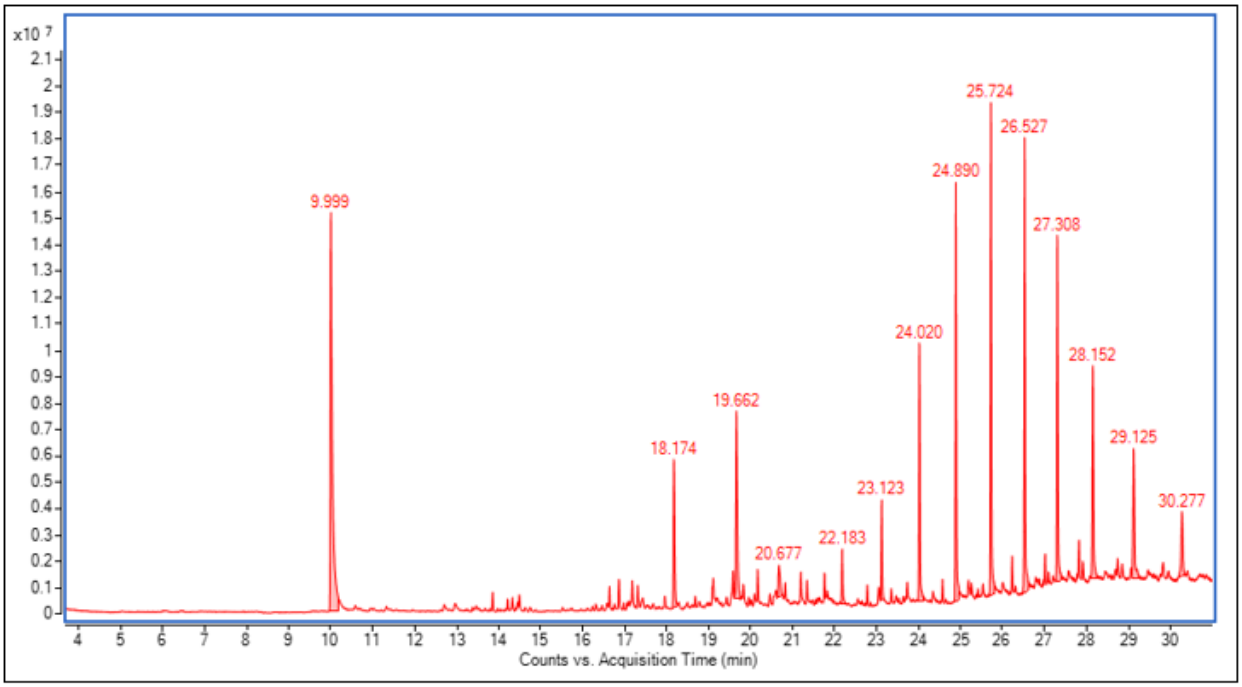


**Figure 6.2** Biomolecule analysis of spotted gum tree fresh leaf extract.

Gas-Chromatography-Mass-Spectrometry (GC-MS) spectra of spotted gum leaf extract

**Table 2.2** The classification for mass spectra of the main biomolecules in the extract.

| Function | Name/retention time (min) | Features | Information details |
|---|---|---|---|
| Reducing/ Capping agents | 1,8- cineole (cineole or eucalyptol), RT-9.999 | Monoterpene | 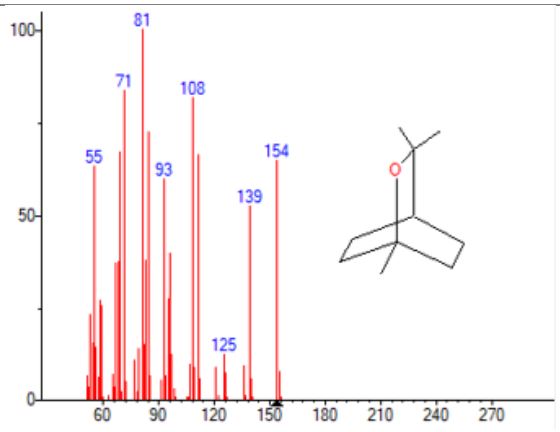 |

| | | | |
|---|---|---|---|
| Reducing/ Capping agents | Ionones or 3-buten-2-one 4-(2 6 6-trimethyl-1-cyclohexen-1-yl) RT-18.174 | Ketones | 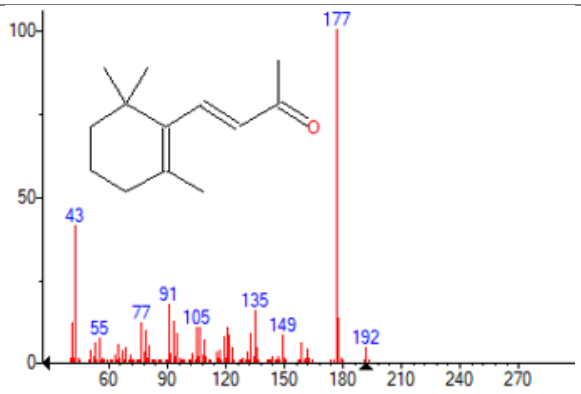 |
| Reducing/ Capping agents | 1-cyclohexanone 2-methyl-2-(3-methyl-2-oxobutyl) RT-19.662 | | 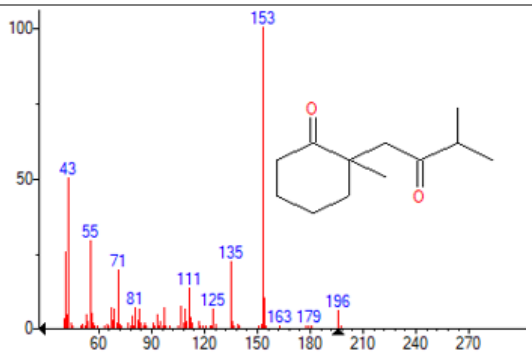 |
| Reducing/ Capping agents | 4-bromo-1-naphthylamine RT-20.677 | | 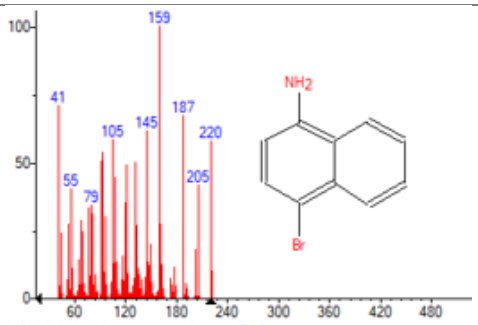 |
| Capping agent | Eicosane RT-22.183 | Alkane | 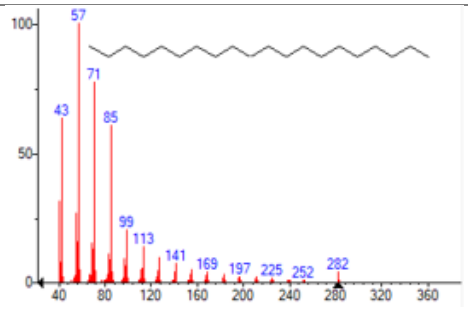 |
| Capping agent | Heneicosane RT-23.123 | Alkane | 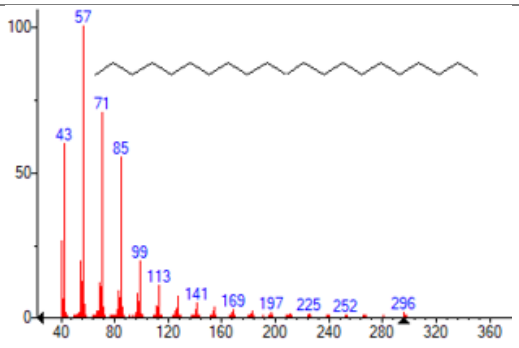 |

| | | | |
|---|---|---|---|
| Capping agent | Heneicosane RT-24.02 | Alkane | 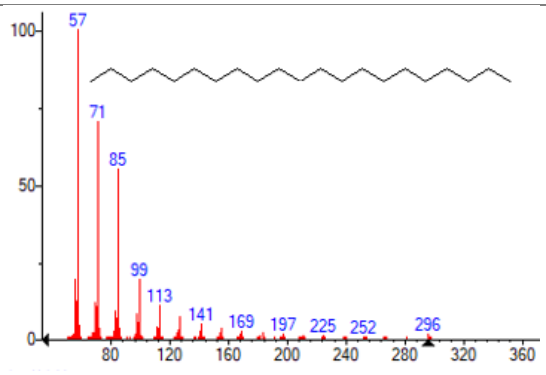 |
| Capping agent | Heneicosane RT-24.89 | Alkane | 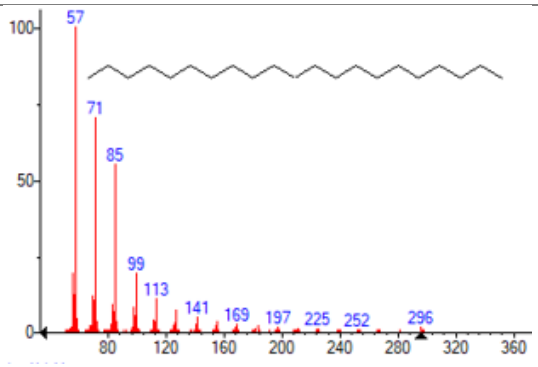 |
| Capping agent | Tetracosane RT-25.724 | Alkane | 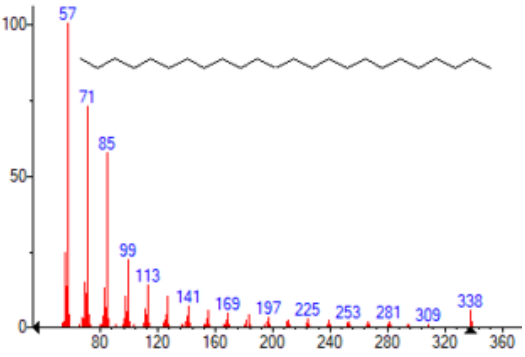 |
| Capping agent | Pentacosane RT-26.527 | Alkane | 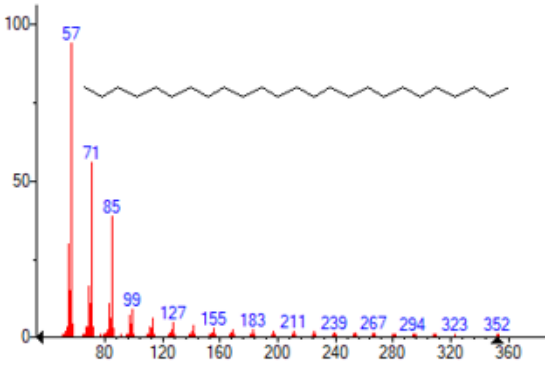 |

| | | | |
|---|---|---|---|
| Capping agent | Hexacosane RT-27.308 | Alkane | 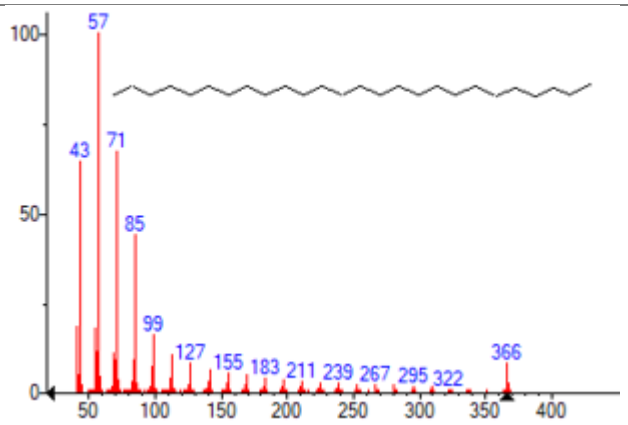  |
| Capping agent | Heptacosane RT-27.308 | Alkane | 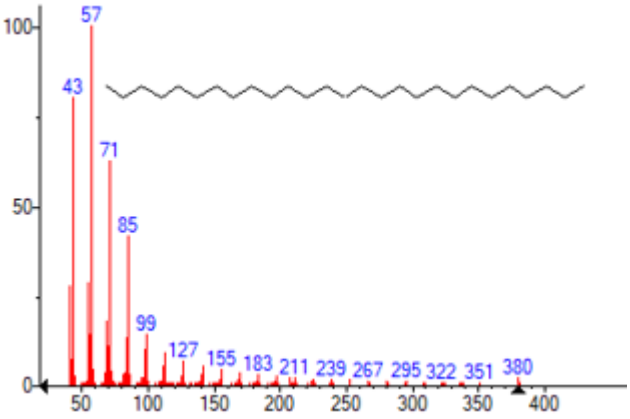  |
| Capping agent | Octacosane RT-29.125 | Alkane | 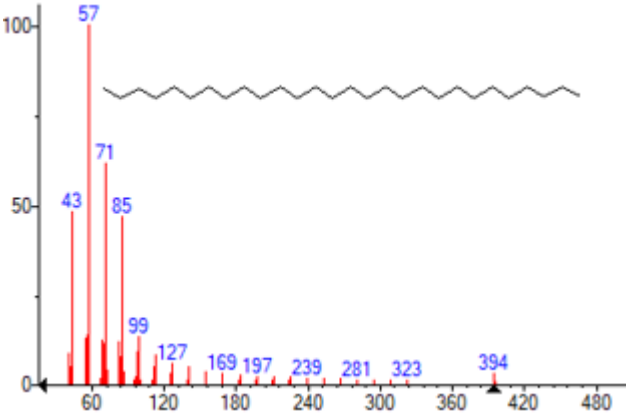  |
| Capping agent | octadecane 3-ethyl-5-(2-ethylbutyl)- RT-30.277 | Alkane | 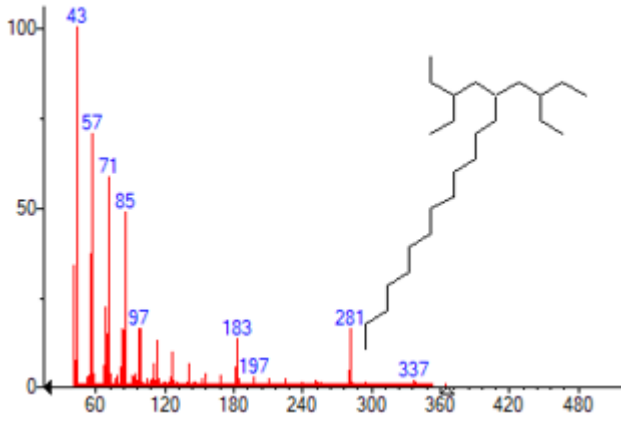  |

### Colorimetric assays

To further analyze the reducing agents in the extract, phenolic compounds, flavonoids and sugars were quantified calorimetrically. Based on this analysis, the concentrations of phenolic compounds and sugars were 9.5 ±3 and 91 ±33 ug/ml while no flavonoids were detected.

### Safety

The cell viability of Nuli-1 cells after application of different concentrations (range 0.2-175 ppm) of CS for 1 hour was similar and not significantly different from untreated cells ($p>0.05$) (Figure 7.2a). Moreover, CS did not affect the viability of nematodes for concentrations up to 87 ppm ($p>0.05$). Worm survival significantly reduced to 85% compared to the negative control for the highest (175 ppm) CS concentration tested ($p<0.0001$) (Figure 7.2b).

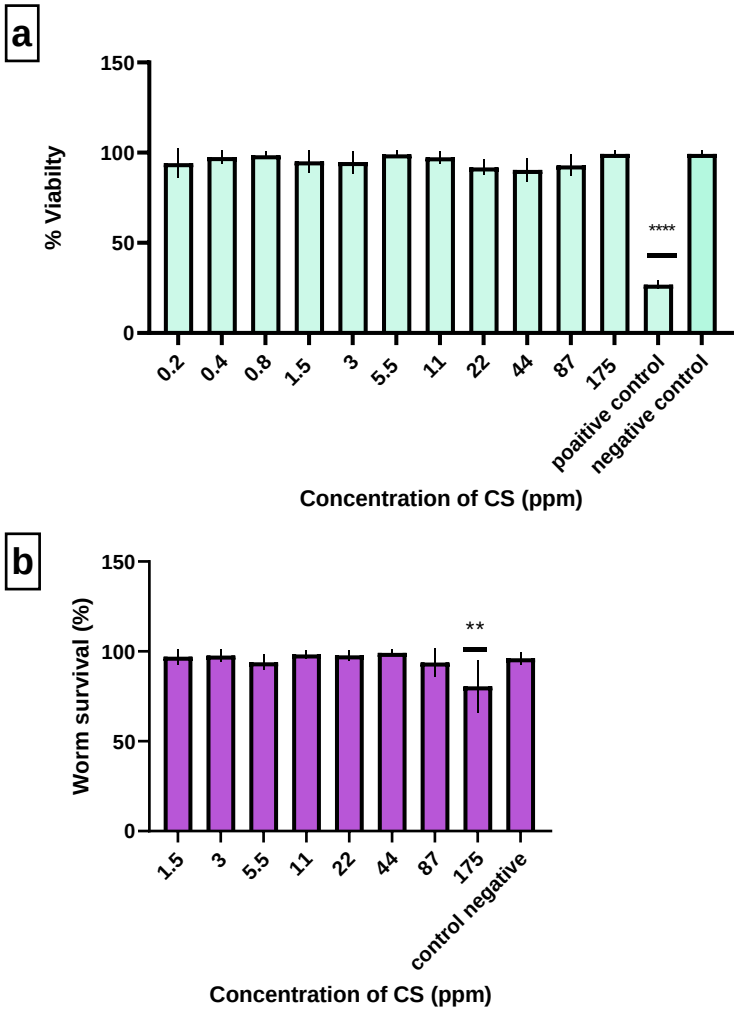


**Figure 7.2** Toxicity studies in Nuli-1 cells and *C. elegans*.

(a) Crystal violet cell viability (%) of Nuli-1 cells after 1-hour exposure to CS, at various concentrations (ppm) or positive control (Triton X-100 10%), normalized to negative control (medium). (b) *C. elegans* survival after 1-hour exposure to CS, normalized to the negative control (water). Data represent the mean ± SD of three biological replicates, one-way analysis of variance (ANOVA). Statistical comparison to the positive control (Triton X-100 10%) and non-treated worms, respectively. ****, $p < 0.0001$; SD, standard deviation.

## Antibacterial activity studies

### Planktonic assays: Minimum Inhibitory Concentration (MIC)

The MIC was tested for all bacteria for CS concentrations ranging from 0.2-44 ppm. These included clinical isolates harvested from the sinonasal cavities of patients with CRS or otitis media and reference strains (Table 3.2). The MIC of CS for all the isolates is summarized in Table 4.2. MIC values were different between bacterial species and among strains for each of the species. From the 4 species tested, *P. aeruginosa* appeared the most sensitive to CS treatment. Significant bacterial growth inhibition compared to the positive control is shown in Figure 8.2.

**Table 3.2** Bacterial isolates for MIC and MBEC assays.

| Bacterium | **Total number of bacterial strains used in MIC and MBEC assays** | **Isolate ID; isolates used in biofilm assays highlighted** | **Isolate origin** |
|---|---|---|---|
| *P. aeruginosa* | 5, 3 | 5562 | CRS patient |
| | | 1158 | CRS patient |
| | | 6776 | CRS patient |
| | | 4747 | CRS patient |
| | | 5927 | CRS patient |
| MRSA | **5, 3** | 1415 | CRS patient |
| | | 5640 | CRS patient |
| | | 5562 | CRS patient |
| | | 5743 | CRS patient |
| | | 7465 | CRS patient |
| *S. pneumoniae* | 5, 0 | 25e | CRS patient |
| | | 34e | CRS patient |
| | | 4d | CRS patient |
| | | 28d | CRS patient |
| | | 30d | CRS patient |

| | | | |
|---|---|---|---|
| *H. influenzae* | 5, 3 | 30e | CRS patient |
| | | 28e | CRS patient |
| | | 024 | ATCC 33391 |
| | | 027 | Otitis media patient |
| | | 028 | Otitis media patient |

**Table 4.2** MIC and MBEC of CS.

| Bacterium | | **MIC of CS (ppm)** | **MBEC of CS (ppm)** |
|---|---|---|---|
| *H. influenzae* | Isolate 1 | 5.5 | 1.5 |
| | Isolate 2 | 5.5 | 1.5 |
| | Isolate 3 | 5.5 | 11 |
| | Isolate 4 | 44 | - |
| | Isolate 5 | 11 | - |
| *S. pneumoniae* | Isolate 1 | 5.5 | - |
| | Isolate 2 | 22 | - |
| | Isolate 3 | 22 | - |
| | Isolate 4 | 22 | - |
| | Isolate 5 | 22 | - |
| MRSA | Isolate 1 | 5.5 | 44 |
| | Isolate 2 | 5.5 | 44 |
| | Isolate 3 | 11 | 22 |
| | Isolate 4 | 5.5 | - |
| | Isolate 5 | 11 | - |
| *P. aeruginosa* | Isolate 1 | 0.2 | 3 |
| | Isolate 2 | 0.2 | 3 |
| | Isolate 3 | 0.2 | 3 |
| | Isolate 4 | 0.08 | - |
| | Isolate 5 | 0.2 | - |

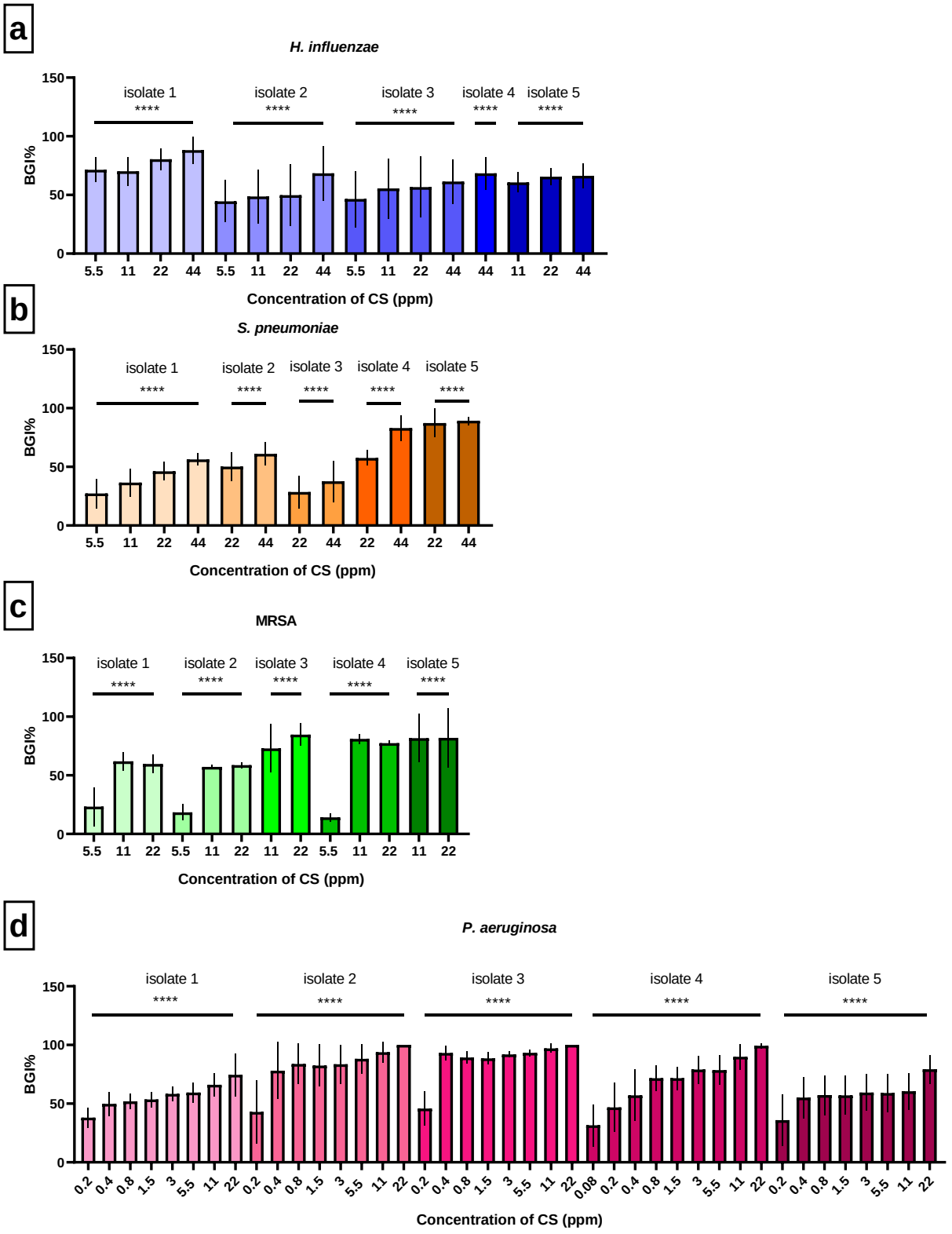


**Figure 8.2** Percentage of bacterial growth inhibition of CS.

Bacterial growth inhibition Percentage of CS in (a) *H. influenzae* (4 CIs and 1 reference strain), (b) *S. pneumoniae* (5 CIs), (c) MRSA (5 CIs) and (d) *P. aeruginosa* (5 CIs) after exposure to CS at various

concentrations (ppm). Only significant results are shown. Data represent the mean ± SD of three biological replicates, one-way analysis of variance (ANOVA). Statistical comparison to the positive control (bacteria only). ****, $p < 0.0001$; SD, standard deviation.

**Minimum biofilm eradication concentration (MBEC)**

The effect of CS (concentrations ranging from 1.5-175 ppm) on biofilm eradication *in vitro* was assessed by the resazurin viability assay. Three isolates were selected for *P. aeruginosa*, MRSA and *H. influenzae* (2 clinical isolates and 1 reference strain). *S. pneumoniae* clinical isolates did not form biofilm and were not tested in this assay. The MBEC of CS for all the isolates is summarized in Table 4.2. Significant biofilm eradication compared to the positive control (no treatment) is shown in Figure 9.2.

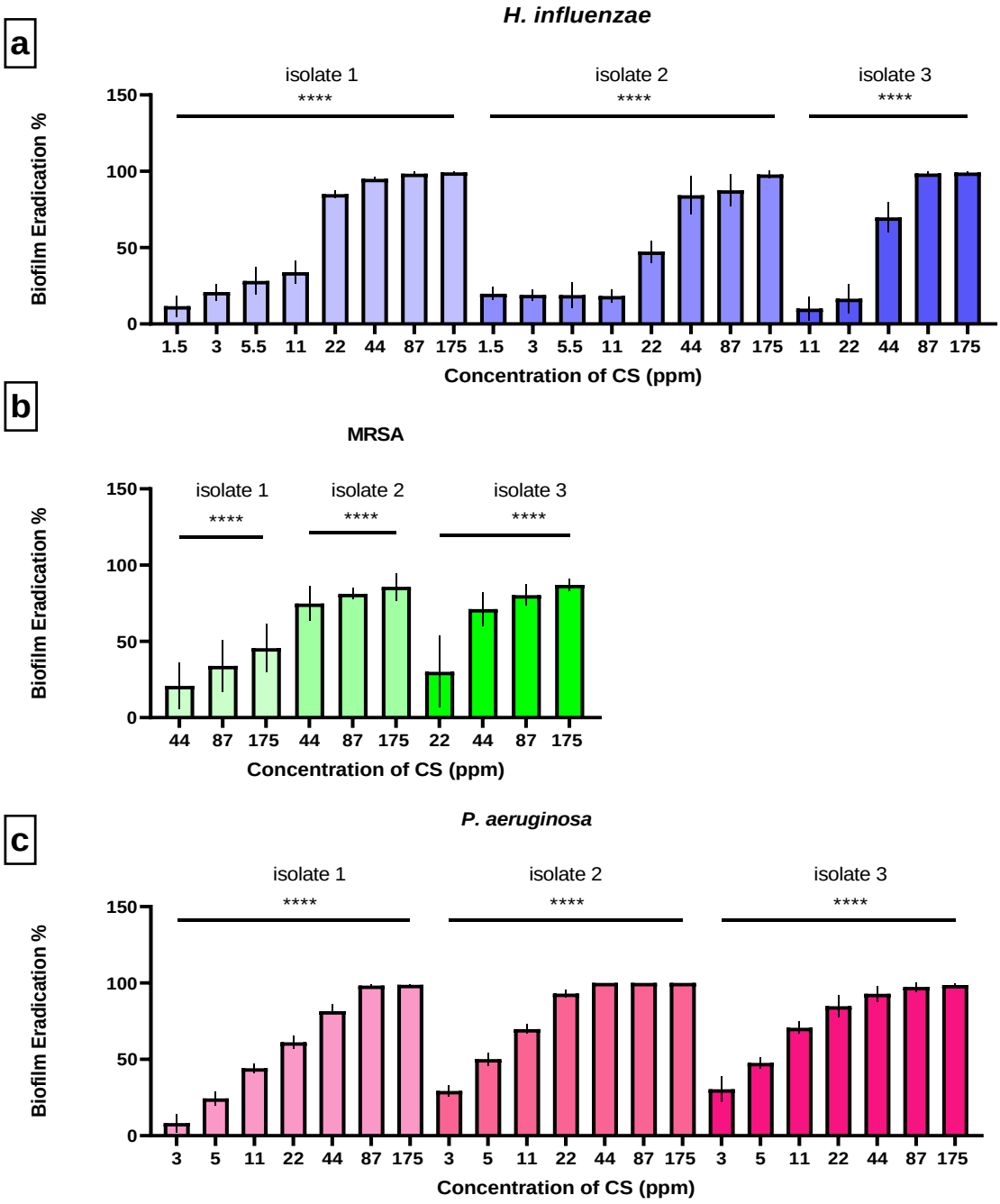


**Figure 9.2** Minimum Biofilm Eradication Concentration of CS.

Biofilm eradication (%) of CS in (a) *H. influenzae* (2 Clinical isolates and 1 reference strain), (b) MRSA (3 Clinical isolates) and (c) *P. aeruginosa* (3 Clinical isolates) biofilms after exposure to CS. Data represent the mean ± SD of three biological replicates, one-way analysis of variance (ANOVA). Statistical comparison to the positive control (bacteria only). **, $p < 0.01$; ****, $p < 0.0001$; SD, standard deviation.

### *In vivo* efficacy

We then selected one *P. aeruginosa* and one MRSA clinical isolate to infect *C. elegans* and measured the effect of 1-hour CS treatments on CFU counts. There was a significant reduction of *P. aeruginosa* and MRSA CFU per worm in the infected worms ($3.514 \times 10^3$ and $28.240 \times 10^3$ CFUs in infection control of *P. aeruginosa* and MRSA, respectively, in comparison with $0.11 \times 10^3$ (percentage of reduction or efficacy percentage = 99%) and $0.112 \times 10^3$ (percentage of reduction or efficacy percentage = 97%) CFUs in *P. aeruginosa* and MRSA infected worms treated with 44 ppm CS, respectively) (Figure 10.2a and b).

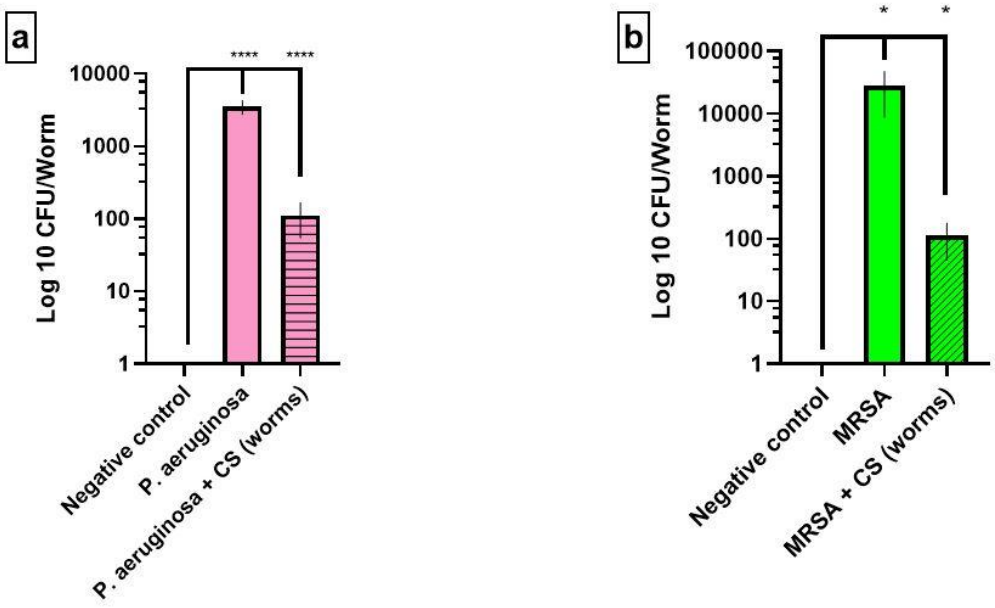


**Figure 10.2** Efficacy study of CS against MRSA and *P. aeruginosa* in *C. elegans*.
Log 10 colony forming units (CFU) per worm after 1-hour infection with (a) *P. aeruginosa* and (b) MRSA each time in the absence (infection control) and presence (treatment group) of CS (44ppm). Data represent the mean ± SEM of three biological replicates, one-way analysis of variance (ANOVA). * $p < 0.05$; ****, $p < 0.0001$; SEM, standard error of the mean.

## Discussion

In this study, *Corymbia maculata* aqueous leaf extracts were used to synthesize CS in a rapid 15-minute one-step process. The CS particles were spherical with an average size of 40 nm and were highly stable for over one year at room temperature. Planktonic and biofilm forms of *P. aeruginosa, H. influenzae*, *S. pneumoniae* (planktonic only) and MRSA were sensitive to CS at various concentrations with *P. aeruginosa* being the most sensitive. CS was not toxic when applied to airway epithelial cells *in vitro* and in an *in vivo C. elegans* model.

Nanostructured materials are of interest due to their antimicrobial properties [359]. More specifically, CS or silver nanoparticles are reported to have the strongest bactericidal properties and are the most promising inorganic nanoparticles for the treatment of bacterial infectious diseases [211]. Green chemistry synthesis of CS has gained great attention in recent years because it is easy, fast and cheap, while the process yields biologically and cytologically compatible CS [359]. Therefore, in the present study, plant mediated synthesis of CS was performed by Eucalyptus leaf extract.

Eucalyptus trees comprise over 700 species, are fast growing and are native to Australia [379]. They have been of worldwide interest due to their inherent anti-inflammatory, anti-bacterial and wound healing effects as well as their supportive role in the immune system and respiratory health [380, 381]. Leaf essential oils have a wide application in the food, medicinal and cosmetic industry and have been reported to possess antioxidant properties mostly because of 1,8- cineole (cineole or eucalyptol), the main biomolecule in the leaf oil [382, 383]. Water and steam-based extraction methods have been investigated to be the most effective way to harvest bioactive components of the eucalyptus leaves, more specifically, bioactive phenolic compounds [384]. In the present study, a water-based extraction method was used to produce bioactive components of *Corymbia maculata* leaf such as phenolic compounds and sugars which can act as reducing agents [385]. Additionally, the reducing ability of the leaf extract was confirmed by GC-MS, indicating the presence of biomolecules possessing ether, ketone, amine groups or bromide ions and double bonds which can potentially act as electron donors to silver ions and reduce them to form CS. These reducing agents in their oxidized form along with biomolecules having covalent bonds between carbon molecules can locate on the surface of CS particles and are thought to be responsible for stability of CS [378, 386].

The stability of CS nanoparticles depends not only on the chemical composition of their surface but also on environmental factors such as ionic strength, pH and background electrolytes which promote stability through three different mechanisms. These include electrostatic, steric and electrosteric stabilization [387]. While polyelectrolytes supply the electrostatic stabilization through electrostatic repulsion, uncharged polymers on the surface of CS provide steric repulsion resulting in steric stabilization. Z-potential absolute values of greater than 30 (thus more or less than Z-potential values of +30 or -30 respectively) indicate high electrostatically stabilized CS while the Z-potential value would be zero in purely sterically stabilized CS. In addition, in the case of electrosteric stabilization, stability occurs through both electrostatic and steric repulsion. Given the CS size was stable for over one year, in particular, CS at high concentration, and considering a Z-potential of -20 mV, it can be concluded that the CS produced in this study is electrosterically stabilized [387, 388].

The toxicity of CS depends on their physiochemical properties such as size, surface area, dose and the time of exposure [389]. Due to mucociliary clearance, the drug retention time in the nasal cavity is maximum of 15 minutes. Hence a maximum exposure time of 60 minutes of the silver nanoparticles was deemed sufficient to test toxicity in this study because the silver nanoparticles will be used as a nasal wash solution [390].

The size of CS has an impact on the surface to volume ratio and consequently on the surface reactivity of the nanoparticles. The size also affects the rate of precipitation, deposition and diffusion and the attachment efficiency of CS in biological environments. The smaller the NPs, the more toxic they are thought to be. Another physical property of CS is their shape, which affects toxicity by impacting their cellular uptake. Spherical silver nanoparticles have been reported to have limited cell toxicity in comparison to nanowires, star-shaped and cubic ones [309, 358, 391]. Green synthesized CS has been reported to be less toxic in comparison to chemically synthesized CS [309]. In this study, the green synthesized CS were spherical and around 40 nm in size and showed no toxic effect after 1-hour exposure to bronchial epithelial cells. Absence of toxicity was furthermore confirmed *in vivo* in a *C. elegans* model where exposure to 44 ppm CS resulted in a survival percentage of more than 93%.

The biocidal effect of CS depends on their physicochemical characteristics including size, shape, surface coating and concentration. Smaller silver nanoparticles can penetrate the bacterial membrane easily in comparison to the larger ones [392]. Surface coating is also important as the bacterial membrane is negatively charged and has strong electrostatic interactions with positively charged CS leading to easy penetration through the bacterial cell membrane [219]. Small silver nanoparticles can also release ionic silver quicker thanlarge ones, so more ionic silver will be available to interact with proteins and enzymes sulfhydryl groups or nucleosides within the DNA leading to cell death [393]. It has been reported that CS has stronger antibacterial effects on Gram-negative bacteria than Gram-positives, due to the latter's thicker cell wall [394]. However, we could not confirm this. From the 4 bacterial species tested, the Gram-negative *P. aeruginosa* in planktonic and biofilm form appeared to be the most sensitive to CS. However, *H. influenzae,* also gram-negative, had similar sensitivity to CS as gram-positive MRSA and *S. pneumoniae*.

Penetration of CS into the biofilm is affected by the size, shape and hydrophobicity of the nanoparticles, as well as by the charge and functional groups of the CS surface [283]. Moreover, biofilm matrix penetration is also influenced by environmental properties such as concentration of the media, as well as the ratio of media to CS concentration [395]. The overall charge of the bacterial cell wall and biofilm matrix is negative, therefore, positively charged nanoparticles are reported to interact strongly with the biofilm [396, 397]. In general, the concentration of CS needed for biofilm eradication is higher than the concentration of CS that

can inhibit planktonic bacterial growth which is thought to be related to the aggregation of CS particles interacting with the biofilm matrix [298]. Our results for MRSA and *P. aeruginosa* are following those findings where CS concentrations for biofilm eradication were up to 4-fold those needed for planktonic growth inhibition. In contrast, for 2 out of 3 *H. influenzae* tested, the CS concentration needed to reduce biofilm growth was 2-fold less than the CS concentration needed to inhibit the growth of planktonic forms of the bacteria. The sub-MIC value of CS needed for *H. influenzae* biofilm eradication may be due to the strong effect of CS on the Quorum Sensing (QS) system which is important for bacterial biofilm cooperative activities and physiological processes [398]. Moreover, cell death or cell surface modification in the presence of CS can prevent bacterial adhesion and growth in the biofilm matrix, leading to biofilm reduction [399, 400]. Further research evaluating more *H. influenzae* CIs in planktonic and biofilm are needed to evaluate whether this is a general feature of those species.

Other relatively easy and fast production processes have been used, for example, using sodium citrate alone or in combination with $NaBH_4$. However, those have various limitations. Sodium citrate is a weak reductant leading to the formation of relatively large polydisperse Ag NPs [401]; in contrast, silver nanoparticles produced by gum tree leaves in our study were monodispersed in addition to having an ideal size of 40 nm. Citrate-coated Ag NPs are shown to be toxic towards primary human umbilical vein endothelial cells (HUVEC) [401] and red blood cells [402]; in contrast, our silver nanoparticles were not toxic to Nuli-1 cells or *in vivo* in *C. elegans.* $NaBH_4$ acts only as a reducing agent, hence an additional capping agent is needed to have stabilized silver nanoparticles [401]; in contrast, in our study silver nanoparticles were produced by leaf extract only because the extract contains both reducing and capping agents resulting in exceptionally stable silver nanoparticles.

**Conclusions**

Highly stable spherical 40 nm CS was synthesized in an economical and fast process using *Corymbia maculata* aqueous leaf extracts. CS showed antibacterial activity against biofilm and planktonic forms of gram-positive and gram-negative clinical isolates from CRS patients in both *in vitro* and *in vivo studies*. Importantly, CS was not toxic for both airway epithelial cells and *C. elegans* within the exposure of 1 h. Future clinical studies will evaluate the potential for green synthetized CS to be used topically to treat infectious exacerbations in the context of CRS.

**Chapter 3: Silver Nanoparticles as a Bioadjuvant of Antibiotics against Biofilm-Mediated Infections with MRSA and *Pseudomonas aeruginosa* in Chronic Rhinosinusitis Patients**

## Statement of Authorship

| | |
|---|---|
| Title of Paper | Silver Nanoparticles as a Bioadjuvant of Antibiotics against Biofilm-Mediated Infections with MRSA and *Pseudomonas aeruginosa* in Chronic Rhinosinusitis Patients |
| Publication Status | Accepted |
| Publication Details | The Journal of Pathology |

## Principal Author

| | |
|---|---|
| Name of Principal Author (Candidate) | Sholeh Feizi |
| Contribution to the Paper | Project design, experimental work, data collection and analysis, manuscript preparation |
| Overall percentage (%) | 75% |
| Certification: | This paper reports on original research I conducted during the period of my Higher Degree by Research candidature and is not subject to any obligations or contractual agreements with a third party that would constrain its inclusion in this thesis. I am the primary author of this paper. |
| Signature | Date<br>28/09/2021 |

## Co-Author Contributions

| | |
|---|---|
| Name of Co-Author | Dr. Clare M Cooksley |
| Contribution to the Paper | Experimental support, manuscript preparation |
| Signature | Date<br>28/09/2021 |

| | |
|---|---|
| Name of Co-Author | Roshan Nepal |
| Contribution to the Paper | Experimental support |
| Signature | Date<br>28/09/2021 |

| | |
|---|---|
| Name of Co-Author | Prof. Alkis J Psaltis |
| Contribution to the Paper | Project design, manuscript preparation |
| Signature | Date<br>28/09/2021 |

| | |
|---|---|
| Name of Co-Author | Prof. Peter-John Wormald |
| Contribution to the Paper | Project design, manuscript preparation |
| Signature | Date<br>28/09/2021 |

| | |
|---|---|
| Name of Co-Author | Associate/Prof. Sarah Vreugde |
| Contribution to the Paper | Project design, manuscript preparation |
| Signature | Date<br>28/09/2021 |

Silver Nanoparticles as a Bioadjuvant of Antibiotics against Biofilm-Mediated Infections with MRSA and *Pseudomonas aeruginosa* in Chronic Rhinosinusitis Patients

Sholeh Feizi [a,b], Clare M Cooksley [a,b], Roshan Nepal [a,b], Alkis James Psaltis [a,b], Peter-John Wormald [a,b], Sarah Vreugde [a,b*]

[a] Department of Surgery-Otolaryngology Head and Neck Surgery, Basil Hetzel Institute for Translational Health Research, Central Adelaide Local Health Network, Woodville South, Australia.

[b] The University of Adelaide, Adelaide, Australia.

*Corresponding author email address: sarah.vreugde@adelaide.edu.au

*Corresponding author postal address: 37a Woodville Road, Woodville SA 5011, Australia

*Corresponding author phone number: +61-(0)8-8222-6928

Running title: Silver Nanoparticle as Bioadjuvant of Antibiotics

**Abstract**

Infectious diseases caused by antibiotic resistant bacteria in planktonic and biofilm form are difficult to treat with conventional antibiotics. Silver nanoparticles (Ag NPs) can be used as alternatives to antibiotics and can alter the susceptibility of bacteria to antibiotics. Here, the antibacterial properties of 16 different antibiotics and Ag NPs, alone and in combination, were tested against clinical isolates of *Pseudomonas aeruginosa* (n=3), *Staphylococcus aureus* (n=3) and methicillin resistant *Staphylococcus aureus* (MRSA) (n=2) isolated from chronic rhinosinusitis (CRS) patients. The microdilution method and resazurin assay were used to determine the minimum inhibitory concentration and minimum biofilm eradication concentration for planktonic and biofilm forms, respectively. Results showed that Ag NPs and gentamicin combinations had synergistic antibacterial activity against *P. aeruginosa* planktonic and biofilm forms and MRSA biofilms. Furthermore, additive effects against biofilms were seen for combinations of Ag NPs with tobramycin or ciprofloxacin against *P. aeruginosa*; with mupirocin against MRSA; with augmentin, doxycycline, azithromycin and clindamycin against *S. aureus*. Moreover, additive effects against planktonic forms were observed for combinations of Ag NPs with tobramycin, ciprofloxacin, imipenem, ceftazidime and aztreonam against *P. aeruginosa*; with gentamicin or linezolid against MRSA; with doxycycline or clindamycin against *S. aureus*. In conclusion, Ag NP-antibiotic combinations can result in enhanced antimicrobial action against *P. aeruginosa,* MRSA and *S. aureus* clinical isolates in planktonic and biofilm forms and can be used in the context of CRS with confirmed infection.

**Keywords:** *Corymbia maculata*, silver nanoparticles, gentamicin, synergism, *P. aeruginosa*, biofilm

## Introduction

The use of silver to control infections dates back to the 19th century when silver nitrate was used both as an antiseptic and a disinfectant, treating burns and open wounds. Although the use of silver has been less frequent since the discovery of antibiotics, there has been renewed interest in its use recently, particularly with the emerging threat of antimicrobial resistance. However, the potential for complex formation and precipitation of silver in ionic form with other ions and molecules limits its stability and use as an antimicrobial [359, 403, 404].

Silver can be used as a pharmaceutical agent in various forms including ionic, colloidal, combined or nanoparticles [405]. The bactericidal effect of silver is due to its binding to the thiol groups of proteins resulting in disruption of the cell and nuclear membrane structure leading to cell death. Moreover, silver ions can also induce bacterial cell death by disrupting the DNA structure or interfering with DNA replication and transcription [406]. Silver nanoparticles (Ag NPs) have several advantages. These include (i) a relatively long-term antimicrobial activity of Ag NPs due to the gradual release of silver ions (ii) lower toxicity to eukaryotic cells compared to silver ions and (iii) a lack of antimicrobial resistant phenotypes [407]. These factors make Ag NPs a promising alternative treatment to control infections, in particular those with multi-drug resistant bacteria.

Ag NPs not only have antibacterial activity but,can also enhance the bacterial susceptibility to conventional antibiotics. This can be due to the destabilizing and destructive effect of Ag NPs on the structure and metabolism of bacteria. Ag NPs can also form complexes with antibiotics through weak molecular interactions. This can enhance the overall antimicrobial efficacy of the antibiotics by promoting a prolonged and continuous release of antibiotics and/or Ag NPs at the site of infection. In addition, the complex formation can reduce both compounds' potential local toxicity. Consequently, the combination of Ag NPs and antibiotics can strengthen the overall antimicrobial action and can be used in particular to treat infections with bacteria resistant to antibiotics [359, 408].

Interestingly other studies have also reported a reduced antimicrobial activity when Ag NPs and antibiotics are combined, thought to be possibly due to the chemical interaction between both compounds. Studies have also shown high variability between species on whether combining antibiotics with Ag NPs results in synergistic, additive or antagonistic effects [409-412]. Therefore, before application in the clinic, a comprehensive analysis of various antibiotic-Ag NP combinations against disease-relevant clinical isolates is required.

In the present study, Ag NPs were combined with different antibiotics and the antimicrobial effectiveness of the combination treatment was determined using the fractional inhibitory concentration index.

Both planktonic and biofilm forms of *Pseudomonas aeruginosa,* methicillin resistant *S. aureus* (MRSA) and *S. aureus* isolated from chronic rhinosinusitis (CRS) patients were tested.

## Materials and Methods

### Ag NPs Synthesis

Spherical 40 nm Silver nanoparticles (Ag NPs) were synthesized from fresh leaves of *Corymbia maculata* (spotted gum) as described previously [413]. These were cut into pieces and boiled in sterile Milli Q water at 100 °C in a water bath for few minutes. Afterward, the filtrate was added to pre-warmed silver nitrate solution (1 mM Ag NO3, 99.9999% trace metals basis, Sigma-Aldrich, Steinheim, Germany) and kept at room temperature overnight. The colloidal silver was centrifuged at 38500 g 1 hour, 4 °C (Beckman Coulter's Avanti JXN-26 high-speed centrifuge) and resuspended in 18 ml Milli Q water. Finally, the solution was sonicated for 15 minutes [Branson sonifier 450 (Timer: hold, Duty cycle%: 40% and Output Control: 4 (80 watts)].

### Bacterial Strains

This study was approved by the human research ethics committee at the Queen Elizabeth Hospital, Woodville, South Australia, Australia (HREC/15/TQEH/132). Bacteria were isolated from the sinonasal cavities of CRS patients. Identification of clinical isolates (*P. aeruginosa*, *S. aureus* and MRSA) was done by an independent diagnostic microbiology laboratory using matrix assisted laser desorption ionization-time of flight mass spectrometry (MALDI-TOF MS, Bruker® MBT) (SA Pathology, Adelaide, Australia). The identification numbers of the bacterial isolates are detailed in Table 1.3.

**Table 1.3** Bacterial isolates cultured from CRS patients for Minimum Inhibitory Concentration (MIC) and Minimum Biofilm Eradication Concentration (MBEC) assays.

| Bacterial species | Number of isolates used in MIC and MBEC assays | Isolate ID |
|---|---|---|
| ***P. aeruginosa*** | 3 | C447, 5562, C449 (isolate 1, 2 and 3, respectively) |
| **MRSA** | 3 | C256, 5562 (isolate 1 and 2 respectively) |
| ***S. aureus*** | 3 | 5485, 5579, 5580 (isolate 1, 2 and 3, respectively) |

### Antimicrobial agents

The antibiotics included gentamycin, ciprofloxacin, imipenem, aztreonam, ceftazidime, linezolid, mupirocin, teicoplanin, vancomycin, cefoxitin, azithromycin, doxycycline, clindamycin, sulfamethoxazole-trimethoprim

and augmentin (amoxycillin-clavulanic acid) which were purchased and dissolved in an appropriate solvent according to table 2.3.

**Table 2.3** Antibiotics and their solvents.

| Antibiotics | Solvent |
|---|---|
| Gentamicin (Sigma Aldrich, St Louis, Missouri, the US) | Phosphate buffer, pH 6, 0.1 mol/L [371, 414] |
| Ciprofloxacin (Sigma Aldrich, St Louis, Missouri, the US) | 0.1N HCl (Sigma Aldrich) |
| Imipenem (Sigma Aldrich, St Louis, Missouri, the US) | Phosphate buffer, pH 7.2, 0.01 mol/L [414] |
| Aztreonam (Sigma Aldrich, St Louis, Missouri, the US) | Phosphate buffer Saline (PBS), pH 7.2 (Cayman chemical) |
| Ceftazidime (Sigma Aldrich, St Louis, Missouri, the US) | PBS, pH 7.2 (Cayman chemical) |
| Linezolid (Sigma Aldrich, St Louis, Missouri, the US) | Water (Sigma Aldrich) |
| Mupirocin (Sigma Aldrich, St Louis, Missouri, the US) | Dimethyl sulfoxide (DMSO, Sigma Aldrich)) |
| Teicoplanin (Sigma Aldrich, St Louis, Missouri, the US) | DMSO (Sigma Aldrich) |
| Vancomycin (Sigma Aldrich, St Louis, Missouri, the US) | Water [414] |
| Cefoxitin (Sigma Aldrich, St Louis, Missouri, the US) | Water [414] |
| Azithromycin (Sigma Aldrich, St Louis, Missouri, the US) | 95% ethanol [414] |
| Doxycycline (Sigma Aldrich, St Louis, Missouri, the US) | Water [414] |
| Clindamycin (Sigma Aldrich, St Louis, Missouri, the US) | Water [414] |
| sulfamethoxazole (Alfa Aesar, Heysham, England+ trimethoprim (Sigma Aldrich, St Louis, Missouri, the US) ratio 1:5) | Sulfamethoxazole: DMSO (Cayman chemical)<br>Trimethoprim: DMSO (Cayman chemical) |
| Augmentin (Amoxicillin (Sigma Aldrich, St Louis, Missouri, the US) + Potassium Clavulanic acid (Sigma Aldrich, St Louis, Missouri, the US) ratio 1:4) | Amoxicillin: phosphate buffer, pH 6, 0.1 mol/L [414]<br>Potassium Clavulanic acid: Water (Sigma Aldrich) |

**Antibacterial activity evaluation of Ag NPs, antibiotics and Ag NP- antibiotic on planktonic bacteria**

The minimum inhibitory concentration (MIC) of Ag NPs and antibiotics alone and in combination were determined using a broth microdilution method as previously described by our department [111]. In brief, different concentrations of Ag NPs and antibiotics alone and in combination starting from ½ MIC were inoculated with 1:100 dilution of a 0.5 McFarland solution (approximately $3 \times 10^8$ Colony Forming Unit (CFU)s/mL) of different clinical isolates. Microtiter plates were incubated under standard laboratory conditions (37°C), for 18-24 hours. The MIC of Ag NPs and antibiotics alone and in combination was determined as the lowest dilution without any visible turbidity. The experiments were performed in two independent replicates.

**Evaluation of biofilm eradication capability of Ag NPs, antibiotics and Ag NP- antibiotic**

Minimum Biofilm Eradication Concentration (MBEC) of Ag NPs and antibiotics alone and in combination were determined as detailed before [415].

Shortly, 1.0 ± 0.1 McFarland units (approximately 3 × $10^8$ CFU/mL) suspensions of the bacteria were diluted 1:15 in Tryptone Soya Broth (TSB) and 150 µl was distributed into black, clear-bottomed, 96-well microplates (Costar, Corning Incorporated, Corning, USA). Next, the plates were incubated at 37°C for 48 hours on a rotating platform at 70 rpm. Established biofilms were washed with sterile Milli Q water to remove any remaining planktonic bacteria and different concentrations of Ag NPs and antibiotics alone and in combination were added.

Following an additional 24-hour incubation at 37°C on a rotating platform at 70 rpm, biofilms were washed with Milli Q water and bacterial viability was measured using the AlamarBlue assay (Life Technologies, Scoresby, Australia). The experiments were performed in two independent replicates.

**AlamarBlue assay**

Concisely, the plates were covered with 200 µl of freshly made 10% Resazurin sodium salt in TSB (Sigma-Aldrich) and incubated on a rotating platform at 70 rpm at 37 °C protected from light. The fluorescence intensity was measured every hour until reaching maximum fluorescence intensity (FLUOstar OPTIMA plate reader, BGM Labtech Gretenberg, Germany, λ excitation = 530 nm/λ emission = 590 nm). Percentage of Biofilm Eradication (BE%) was calculated according to equation 1.

$$BE\% = 100 - (\frac{F_T}{F_C} \times 100\%) \qquad (1)$$

The MBEC of Ag NPs, antibiotics and Ag NPs in combination with antibiotics is expressed as BE%, where $F_C$ is the fluorescence of the untreated control biofilm (100% biofilm viability) and $F_T$ is the fluorescence observed in the treated biofilm. The background fluorescence of the broth medium was subtracted from both the $F_C$ and $F_T$ readings. Biofilm eradication studies were performed as three independent experiments. The MBEC was taken as 80% biofilm eradication.

To determine the interactive effect of Ag NPs and antibiotics, the fractional inhibitory concentration index (FICI) was calculated by the results of MICs and MBECs according to the following formula:

$$FICI = \frac{MIC\ or\ MBEC\ of\ ABX\ in\ combination}{MIC\ or\ MBEC\ of\ ABX\ alone} + \frac{MIC\ or\ MBEC\ of\ Ag\ NPs\ in\ combination}{MIC\ or\ MBEC\ of\ Ag\ NPs\ alone} \qquad (2)$$

FICI values of ≤0.5, 0.5 to 1.0, 1.0 to 4.0 and >4 show synergy, additivity, indifference and antagonism, respectively [416].

## Results

### MIC and MBEC

MIC and MBEC of Ag NPs and antibiotics were determined for *P. aeruginosa (n=3)*, *S. aureus* (n=3) and MRSA (n=2) clinical isolates collected from the sinonasal cavities of patients with CRS. Results are presented in tables 3.3 and 4.3, respectively. The MIC of Ag NPs against *P. aeruginosa* varied between 0.8 to 2.25 ppm and was 22 ppm for *S. aureus* and *MRSA.* The MIC values for the different antibiotics varied between different strains of each of the *P. aeruginosa*, *S. aureus* and MRSA and were classified as susceptible, intermediate and resistant according to the Clinical and Laboratory Standard Institute (CLSI) criteria in M100-S22 guidelines [414]. Moreover, MBEC values of Ag NPs in *P. aeruginosa*, *S. aureus* and *MRSA biofilms were* between 11 and 22 ppm for *P. aeruginosa* and between 22 and 44 ppm for *S. aureus* and *MRSA clinical isolates.* The MBEC of antibiotics varied between the various clinical isolates of the same strain, except for mupirocin where the MBEC value was 640 ug/ml for both clinical isolates.

**Table 3.3** MIC for Ag NPs and *antibiotics* for each organism**.**

| **Organism**<br><br>**Antimicrobial agent (Ag NPs (ppm) and antibiotics (µg/ml))** | **P. aeruginosa, isolate 1** | **P. aeruginosa, isolate 2** | **P. aeruginosa, isolate 3** | **MRSA, isolate 1** | **MRSA, isolate 2** | **S. aureus, isolate 1** | **S. aureus, isolate 2** | **S. aureus, isolate 3** |
|---|---|---|---|---|---|---|---|---|
| Ag NPs | 0.8 | 2.25 | 0.8 | 22 | 22 | 22 | 22 | 22 |
| Gentamicin | 4 (S) | 8 (I) | 32 (R) | 2 (S) | 4 (S) | | | |
| Ciprofloxacin | 0.06 (S) | 16 (R) | 0.5 (S) | | | | | |
| Imipenem | 4 (I) | 16 (R) | 8 (R) | | | | | |
| Aztreonam | 4 (S) | 4 (S) | 4 (S) | | | | | |
| Ceftazidime | 4 (S) | 4 (S) | 4 (S) | | | | | |
| Tobramycin | 4 (S) | 2 (S) | 4 (S) | | | | | |
| Linezolid | | | | 2 (S) | 2 (S) | | | |
| Mupirocin | | | | 0.3 (S) | 0.03 (S) | | | |
| Teicoplanin | | | | 0.5 (S) | 0.5 (S) | | | |
| Vancomycin | | | | 2 (S) | 4 (I) | | | |
| Cefoxitin | | | | 8 (R) | 16 (R) | | | |
| Azithromycin | | | | | | 1 (I) | 1 (I) | 1 (I) |
| Doxycycline | | | | | | 0.125 (S) | 0.125 (S) | 0.06 (S) |

| | | | |
|---|---|---|---|
| Clindamycin | 1 (R) | 1 (R) | 1 (R) |
| Trimethoprim/sulfamethoxazole | 1 (S) | 0.25 (S) | 0.25 (S) |
| Augmentin (Amoxicillin/clavulanic acid) | 1 (S) | 2 (S) | 2 (S) |

Ag NPs are shown in ppm and antibiotics are in µg/ml. Susceptible (S), Intermediate (I) and Resistant (R) based on CLSI except for mupirocin which is based on what was reported by Rajkumari et al., 2014 [417].

**Table 4.3** MBEC for Ag NPs and antibiotics for each organism.

| **Organism**<br>**Antimicrobial agent** | **P. aeruginosa, isolate 1** | **P. aeruginosa, isolate 2** | **P. aeruginosa, isolate 3** | **MRSA, isolate 1** | **MRSA, isolate 2** | **S. aureus, isolate 1** | **S. aureus, isolate 2** | **S. aureus, isolate 3** |
|---|---|---|---|---|---|---|---|---|
| Ag NPs | 11 | 22 | 11 | 22 | 22 | 44 | 44 | 22 |
| Gentamicin | 4 | 8 | 8 | 32 | 32 | | | |
| Ciprofloxacin | 16 | 32 | 64 | | | | | |
| Tobramycin | 2 | 4 | 4 | | | | | |
| Mupirocin | | | | 640 | 640 | | | |
| Azithromycin | | | | | | 128 | 256 | 128 |
| Doxycycline | | | | | | 32 | 32 | 64 |
| Clindamycin | | | | | | 1 | 2 | 1 |
| Augmentin (Amoxicillin/clavulanic acid) | | | | | | 32 | 8 | 32 |

Ag NPs are shown in ppm and antibiotics are in µg/ml.

**Antimicrobial activity of Ag NP- antibiotic against planktonic growth inhibition**

The fractional inhibitory concentration index (FICI) was calculated for each Ag NP- antibiotic combination. Synergistic, additive, indifferent and antagonistic effects are reported as FICI ≤ 0.5, 0.5 < FICI ≤1, 1 < FICI < 4 and FICI > 4, respectively [408].

None of the antibiotic- Ag NP combinations showed antagonistic effects against any of the clinical isolates tested.

Regarding *P. aeruginosa*, synergistic effects were observed when Ag NPs and gentamicin were combined for all (n=3/3) clinical isolates. Moreover, additive effects were noted when Ag NPs were combined with aztreonam, ceftazidime, ciprofloxacin, imipenem and tobramycin (n=3/3) to inhibit bacterial growth in planktonic form (Figure 1.3a).

For MRSA, additive effects were seen when Ag NPs were combined with gentamicin or linezolid to inhibit bacterial growth in planktonic form (n=2/2). Ag NPs did not enhance the antimicrobial effects of teicoplanin, vancomycin, cefoxitin and mupirocin and the combination of both compounds was indifferent (n=2/2) (Figure 1.3b).

For *S. aureus*, additive effects were detected when Ag NPs were combined with doxycycline and clindamycin (n=3/3). However, indifferent effects were seen when Ag NPs were combined with augmentin, azithromycin and sulfamethoxazole-trimethoprim (n=3/3) (Figure 1.3c).

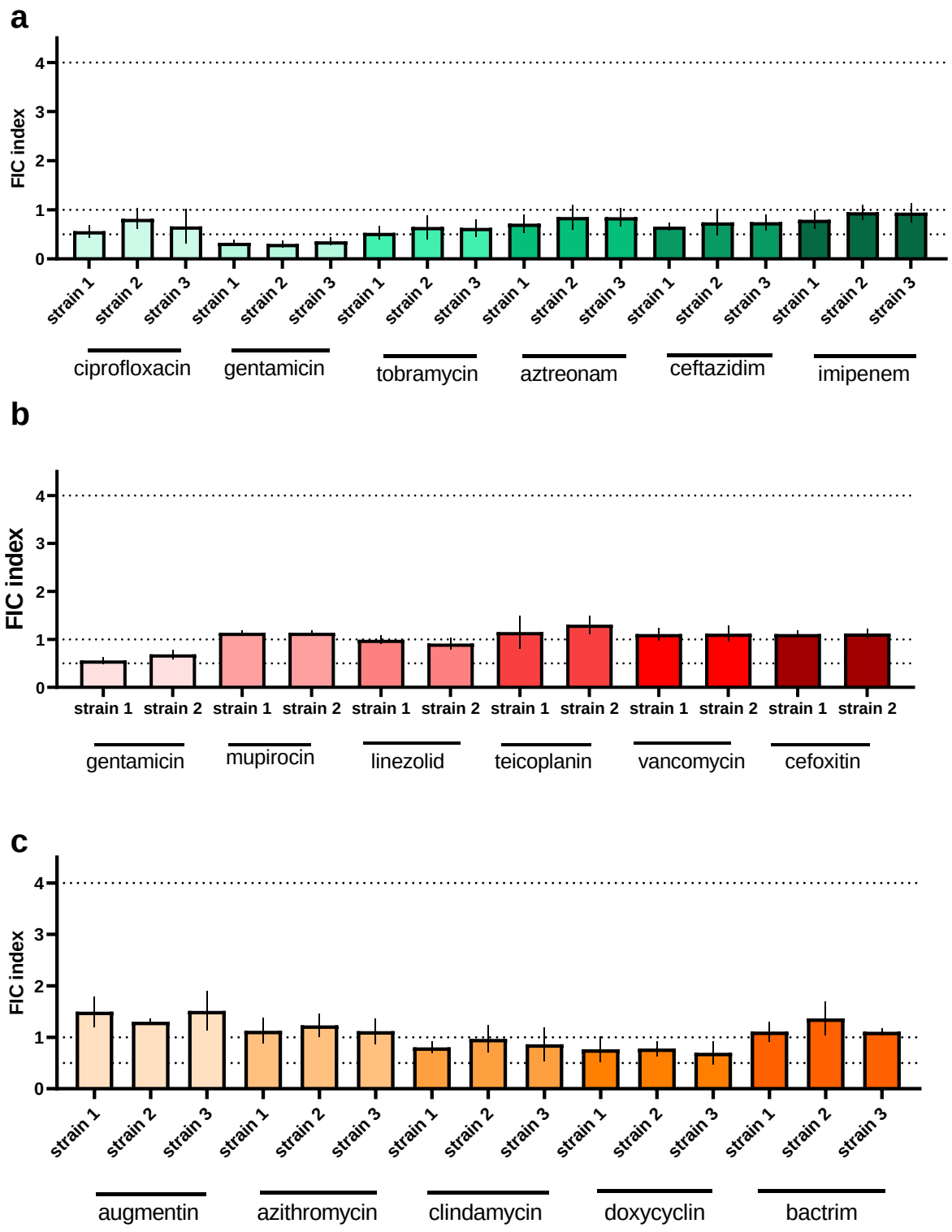


**Figure 1.3** Fractional inhibitory concentration index (FICI) for planktonic growth inhibition for various antibiotics combined with Ag NPs.

FICI for n=3 strains of each (a) P. aeruginosa (green), (b) MRSA (red) and (c) S. aureus (orange). FICI ≤ 0.5, 0.5 < FICI ≤1, 1 < FICI < 4 and FICI > 4 indicate synergistic, additive, indifferent and antagonistic effects.

**Antimicrobial activity of Ag NP-antibiotic against biofilm**

Regarding *P. aeruginosa*, synergistic effects were seen for MBEC values when Ag NPs were combined with gentamicin (n=3/3). Additive effects were seen when Ag NPs were combined with ciprofloxacin (n=3/3) and tobramycin (n=3/3) (Figure 2.3a).

Concerning MRSA, synergistic effects were discerned for MBEC values when Ag NPs were combined with gentamicin (n=2/2) whilst additive effects were seen when Ag NPs were combined with mupirocin (n=2/2) (Figure 2.3b and).

For *S. aureus*, additive effects were observed when Ag NPs were combined with augmentin, azithromycin, clindamycin and doxycycline (n=3/3) (Figure 2.3c and).

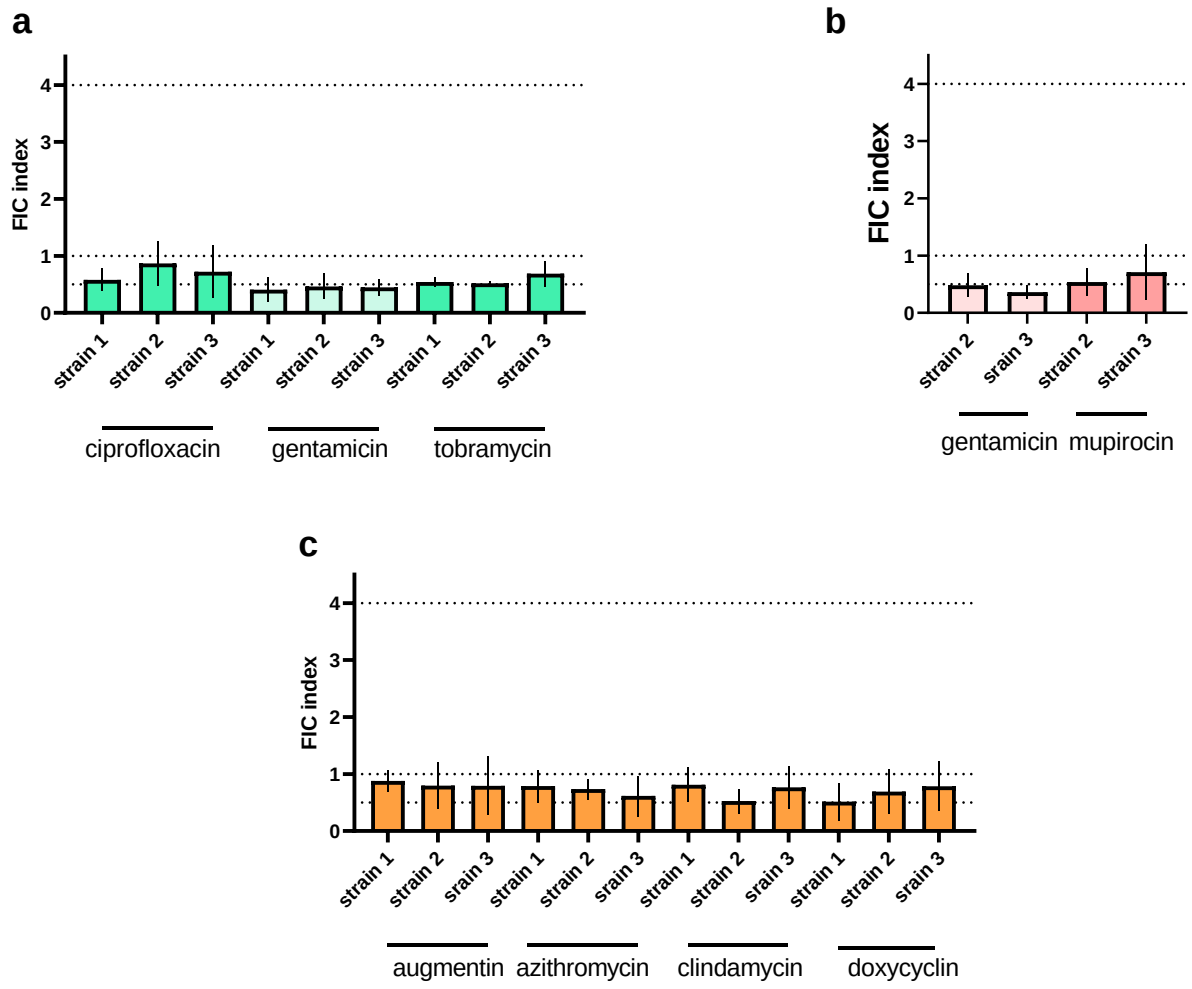


**Figure 2.3** Fractional inhibitory concentration index (FICI) for biofilm eradication for various antibiotics combined with Ag NPs.

FICI for n=3 strains of each (a) P. aeruginosa (green), (b) MRSA (red) and (c) S. aureus (orange). FICI ≤ 0.5, 0.5 < FICI ≤1, 1 < FICI < 4 and FICI > 4 indicate synergistic, additive, indifferent and antagonistic effects.

**Discussion**

In this study, Ag NPs were used as a bioadjuvant to antibiotics to improve the overall antimicrobial effect as a combination treatment. Ag NPs showed no antagonistic effects when combined with any of the antibiotics tested against clinical *S. aureus*, *P. aeruginosa* and MRSA isolates from CRS patients. Rather, Ag NPs enhanced the gentamicin antimicrobial activity through synergism to inhibit the planktonic growth of *P. aeruginosa* as well as the biofilm growth of *P. aeruginosa* and MRSA. Furthermore, Ag NPs in combination with various antibiotics had additive antimicrobial effects against *S. aureus*, *P. aeruginosa* and MRSA clinical isolates. Importantly, those synergistic and additive antimicrobial effects of the combination treatment were similar between 3 different strains for each of those species regardless of whether those strains were susceptible or resistant to antibiotics. These findings are in line with a recent study showing relatively improved effects of antibiotic-Ag NP combinations in particular in antibiotic resistant strains [418]. They support the use of antibiotics in combination with Ag NPs even in the context of bacterial infections with pathogens resistant to that antibiotic.

Fast spreading antibiotic resistant pathogenic bacteria require the development of new therapeutic means and methods, one of which is the combination therapy of antibiotics with other antimicrobials [408, 419]. Combination therapy can increase the speed of bacterial killing, expand the host range of antibiotic effectiveness, lower the effective concentration of antibiotics and therefore their side-effects and finally restrict the development of resistance in microorganisms [420].

The antimicrobial activity of plant extract-mediated synthesized Ag NPs against antibiotic susceptible and antibiotic resistant bacteria have been reported previously [356, 421]. In line with those studies, our results indicate similar MIC and MBEC values of Ag NPs against different clinical isolates for each of the different antibiotics to which the isolates were susceptible.

A proposed mechanism of action Ag NPs as a bioadjuvant to antibiotics could be that Ag NPs cause oxidative stress with increased production of reactive oxygen species leading to bacterial cell death through damage to the biomolecules inside the bacterial cell [407]. Furthermore, additive or synergistic antimicrobial effects of antibiotic-Ag NP combination treatments could be linked to the enhanced attachment and penetration of antibiotics through the bacterial cell wall in the presence of Ag NPs [408]. According to the Vazquez- Muñoz study, increased antibiotic effectiveness when combined with Ag NPs can be expected for those antibiotics that are targeting the division of the cell wall. Our findings are largely in line with that concept

where the combination of Ag NPs with aztreonam, ceftazidime, imipenem, which their target is the cell wall, had additive effects against *P. aeruginosa* planktonic growth and cefoxitin inhibiting MRSA planktonic growth through additivity [408]. Also, our results indicate a trend towards lower FIC values for Ag NP-antibiotic against planktonic forms of gram-negative bacteria in comparison to gram-positive bacteria. This is potentially linked to a thinner peptidoglycan layer in gram-negatives which makes the penetration of antibiotic-Ag NP easier [422].

Whilst important, and providing guidance on which antibiotic-Ag NP combinations could be selected to combat *P. aeruginosa* and/or *S. aureus*/MRSA infections, our study indicates additive or synergistic effects against biofilms for all antibiotics tested when combined with Ag NPs. A biofilm is a structured conglomerate of bacteria embedded in a self-produced extracellular polymer matrix (EPS) consisting of proteins, polysaccharides and extracellular DNA. Bacterial biofilms in chronic infections such as CRS are difficult to treat because bacterial cells within biofilms increase their tolerability to antibiotics [69]. This is the result of various contributing factors such as poor penetration of antibiotics through the EPS matrix and slower growth of the bacterial cells with the formation of persister cells. The antibacterial effect of antibiotics against biofilms can therefore be improved by Ag NPs as they disrupt and detach established biofilms and make the bacterial cells accessible to not only antibiotics but also Ag NPs [423]. Furthermore, the Ag NPs once combined with antibiotics appears to be able to kill bacterial persister cells as they can improve the antibacterial effect of antibiotics [424]. Moreover, antibiotic-Ag NP enhanced biofilm killing ability could be related to Ag NPs action on inhibiting oxygen metabolism and metabolic enzymes as well as antibiotics activity through protein synthesis inhibition resulting in a thinner EPS matrix [425, 426]. Together, these properties of AgNPs might explain why the FIC values for biofilm eradication of all isolates are lower than the FIC values for their planktonic counterparts [423].

This study showed consistent synergistic effects of gentamicin-Ag NPs combinations to inhibit the growth of *P. aeruginosa* planktonic cells as well as eradicate biofilms of *P. aeruginosa* and MRSA. This might be due to the higher release rate of silver ions by Ag NPs or enhancement of oxidative stress when combined with gentamicin [408, 427].

## Conclusion

Ag NPs appear to be a promising tool in the treatment of bacterial biofilms, in particular in CRS. We have shown that they improve the antibiotic bactericidal activity and are effective, in particular against clinical bacterial isolates from CRS patients. More specifically, Ag NPs did not have any antagonistic effects when

combined with different antibiotics against *P. aeruginosa,* MRSA and *S. aureus* clinical isolates from CRS patients. Gentamicin-Ag NPs were the most successful combination as they consistently eradicated biofilms of difficult-to-treat *P. aeruginosa* and MRSA clinical isolates through synergism. Future clinical studies are needed to translate these findings towards improved therapies against biofilm mediated chronic infections.

## Chapter 4: Green Synthesized Colloidal Silver Is Devoid of Toxic Effects on Primary Human Nasal Epithelial Cells *in Vitro*

### Statement of Authorship

| | |
|---|---|
| Title of Paper | Green Synthesized Colloidal Silver Is Devoid of Toxic Effects on Primary Human Nasal Epithelial Cells *in Vitro* |
| Publication Status | Published |
| Publication Details | The Journal of Food and Chemical Toxicology https://doi.org/10.1016/j.fct.2021.112606 |

### Principal Author

| | |
|---|---|
| Name of Principal Author (Candidate) | Sholeh Feizi |
| Contribution to the Paper | Project design, experimental work, data collection and analysis, manuscript preparation |
| Overall percentage (%) | 75% |
| Certification: | This paper reports on original research I conducted during the period of my Higher Degree by Research candidature and is not subject to any obligations or contractual agreements with a third party that would constrain its inclusion in this thesis. I am the primary author of this paper. |
| Signature | Date<br>28/09/2021 |

### Co-Author Contributions

| | |
|---|---|
| Name of Co-Author | Dr. Clare M Cooksley |
| Contribution to the Paper | Experimental support, manuscript preparation |
| Signature | Date<br>28/09/2021 |

| | |
|---|---|
| Name of Co-Author | Dr. Shari Javadiyan |
| Contribution to the Paper | Experimental support, manuscript preparation |
| Signature | Date<br>28/09/2021 |

| | |
|---|---|
| | |

| | |
|---|---|
| Name of Co-Author | Gohar Shaghayegh |
| Contribution to the Paper | Experimental support |
| Signature | Date<br>28/09/2021 |

| | |
|---|---|
| Name of Co-Author | Prof. Alkis J Psaltis |
| Contribution to the Paper | Project design, manuscript preparation |
| Signature | Date<br>28/09/2021 |

| | |
|---|---|
| Name of Co-Author | Prof. Peter-John Wormald |
| Contribution to the Paper | Project design, manuscript preparation |
| Signature | Date<br>28/09/2021 |

| | |
|---|---|
| Name of Co-Author | Associate/Prof. Sarah Vreugde |
| Contribution to the Paper | Project design, manuscript preparation |
| Signature | Date<br>28/09/2021 |

Green Synthesized Colloidal Silver Is Devoid of Toxic Effects on Primary Human Nasal Epithelial Cells *in Vitro*

Sholeh Feizi [a,b], Shari Javadiyan [a,b], Clare M Cooksley [a,b], Gohar Shaghayegh [a,b], Alkis James Psaltis [a,b], Peter-John Wormald [a,b], Sarah Vreugde [a,b]*

[a] Department of Surgery-Otolaryngology Head and Neck Surgery, Basil Hetzel Institute for Translational Health Research, Central Adelaide Local Health Network, Woodville South, Australia.

[b] The University of Adelaide, Adelaide, Australia. *Corresponding author email address: sarah.vreugde@adelaide.edu.au

*Corresponding author postal address: 37a Woodville Road, Woodville SA 5011, Australia

*Corresponding author phone number: +61-(0)8-8222-6928

**Abstract**

Evaluating the safety of previously fabricated and effective green synthesized colloidal silver (GSCS) on the mucosal barrier structure and function is essential before conducting human trials. The GSCS was applied to primary human nasal epithelial cells (HNECs) grown in an air-liquid interface (ALI) culture. Epithelial barrier integrity was evaluated by measuring the transepithelial electrical resistance (TEER) and fluorescein isothiocyanate (FITC)-dextran paracellular permeability. Ciliary beat frequency (CBF) was quantified. Effects of the GSCS on cell viability and inflammation were examined through lactate dehydrogenase, the 3-(4,5-Dimethylthiazol-2-yl)-2,5-Diphenyltetrazolium Bromide viability assay and interleukin 6 (IL-6) enzyme linked immunosorbent assay. The localization and transportation of GSCS within HNECs and their HNEC-ALI cultures was assessed by transmission electron microscopy and inductively coupled plasma-mass-spectrometry, respectively. Application of GSCS to HNECs-ALI cultures for up to 2 hours caused a significant reduction in the TEER values, however, it did not drop within the first 10 and 20 minutes for CRS and non-CRS control HNECs. The paracellular permeability, cell viability, IL-6 secretion and CBF remained unchanged. No GSCS was observed within or transported across HNECs. In conclusion, the application of GSCS to HNECs is devoid of toxic effects.

**Keywords:** silver nanoparticle, green synthesis, epithelial integrity, topical delivery, lactate dehydrogenase, interleukin 6

## Introduction

Dysbiosis and an overgrowth of pathogens at the sinonasal mucosa along with a defective mucociliary function can underlie the inflammatory process in the context of chronic rhinosinusitis (CRS) [428]. The cornerstone of therapy is antibiotics; however, their effectiveness is hampered by the increasing burden of antibiotic resistance. This requires treatment strategies to fight those pathogens. Silver nanoparticles (Ag NPs) or colloidal silver (CS), a non-antibiotic antimicrobial therapy, is considered as one of those treatment strategies.

The Ag NPs' toxicity depends on various factors including their size, concentration, exposure time and surface coating which influence their cellular uptake and oxidative state [429]. The Ag NPs can induce toxicity through different mechanisms resulting in morphological changes [430], DNA damage, the overexpression of metallothioneins [431], reactive oxygen species (ROS) generation, intracellular calcium influx, mitochondrial membrane potential reduction [432], profibrotic inducement [433], LDH leakage, the release of inflammatory proteins, decrease albumin synthesis [434] and increase apoptosis rate [435].

The safety and efficacy of CS have been reported before in the context of CRS both *in vitro* and *in vivo* [201, 203, 269, 358], however, their method of manufacturing was time-consuming. Goggin et al. and Chen et al. used over the counter and commercially available CS respectively [201]. Rajiv et al., and Richter et al. used commercially available generators and chemical materials, respectively, to synthesize CS which was time consuming and the use of chemical materials to manufacture CS for medical use is not desirable [203,358]. To overcome those limitations, we have recently used a unique water-based extraction single-step production process using Corymbia maculate (spotted gum tree) leaf extract reducing the time of reduction of silver ions to CS to 15 minutes. This green synthesized colloidal silver (GSCS) showed excellent *in vitro* efficacy against planktonic and biofilm *S. aureus*, MRSA and *P. aeruginosa* clinical isolates from CRS patients. Moreover, GSCS did not show toxicity when applied to an airway epithelial cell line (Nuli-1 cells) and in a *Caenorhabditis elegans in vivo* model supporting the potential use of GSCS for the treatment of infections in CRS patients [413]. However, further safety experiments, in particular, their effect on the mucosal barrier and mucociliary function are required before conducting human trials.

In this study we aimed to evaluate GSCS safety by measuring the transepithelial electrical resistance (TEER), ciliary beat frequency (CBF) and paracellular permeability after a two-hour application to primary human nasal epithelial cells (HNECs) in an air-liquid interface (ALI) culture. Moreover, their effect on inflammation and cell viability was determined.

## Materials and Methods

### Colloidal silver synthesis

Colloidal silver (CS) was synthesized as described previously [413]. In short, *Corymbia maculata* (spotted gum) leaves were cut into pieces and boiled in sterile Milli Q water. Afterward, the aqueous extract was added to pre-warmed silver nitrate solution (1 mM Ag NO3, 99.9999% trace metals basis, Sigma-Aldrich, Steinheim, Germany) and incubated at room temperature overnight. The GSCS was centrifuged at 38, 500 x *g* for 1 hour, 4 °C (Beckman Coulter's Avanti JXN-26 high-speed centrifuge) and resuspended in 18 ml Milli Q water. Finally, the solution was sonicated for 15 minutes [Branson sonifier 450 (Timer: hold, Duty cycle%: 40% and Output Control: 4 (80 watts)].

### Primary human nasal epithelial cell culture

Ethics approval for the collection and use of HNECs was granted from the Queen Elizabeth Hospital Human Research Ethics Committee (reference HREC/15/TQEH/132) and all patients gave written informed consent before the collection of HNECs. Poeple were defined as CRS patients according to the European Position Paper on Rhinosinusitis and Nasal Polyps (EPOS) guidelines [9]. Non-CRS controls were scheduled for septoplasty and had no history, signs or symptoms of CRS. Primary human nasal epithelial cells (HNECs) were collected from the inferior turbinates of CRS and non-CRS control patients and extracted from cytology brushes (McFarlane Medical Equipment Pty Ltd, Surrey Hills, VIC, Australia) as described [436]. HNECs were suspended in Roswell Park Memorial Institute (RPMI) (Gibco by Thermofisher Scientific Australia, Scoresby, Victoria) and centrifuged at 525 x *g* for 7 minutes at 4˚C. Next, the pellet was resuspended in EX+ medium (StemCell Technologies) which was comprised of PneumaCult-EX basal medium containing PneumaCult-EX 50x and 50 U/ml of penicillin, 50 µg/ml of streptomycin (150700-063, Invitrogen Life Technologies, Gaithersburg, MD, USA) and transferred to a 100-mm-diameter culture plate coated with anti-CD68 (Dako, Glostrup, Denmark) for 20 minutes to deplete monocytes. HNECs were then grown in a type I collagen coated T 75 flask (Thermo Scientific, Waltham, MA, USA) at 37 °C humidified air with 5% $CO_2$ [436].

### Air-liquid interface culture

Once the HNECs reached 80% confluency, $7 \times 10^4$ cells per well were seeded onto collagen-coated 6.5-mm permeable Transwells (Corning, NY, USA) of ALI cell culture plates. After 3-4 days, $EX^+$ medium in the basal chamber was replaced with ALI-complete medium [PneumaCult-ALI basal medium containing PneumaCult-ALI 10X Supplement, PneumaCult-ALI Maintenance Supplement, 50 U/ml of penicillin and 50 µg/ml of streptomycin (150700-063, Invitrogen Life Technologies, Gaithersburg, MD, USA)] and the medium

in the apical chamber was removed. The media in the basal chamber was changed every two days until TEER value measurements reached at least 1000 Ω/cm$^2$ (approximately 2 weeks) and cilia generation for cilia beat frequency measurements (approximately 4 weeks) [437].

**Transepithelial electrical resistance measurements**

Transepithelial electrical resistance (TEER) values were measured with the EVOM volt-ohmmeter (World Precision Instruments, Sarasota, FL). One hundred microliters (100 µl) of warmed ALI-complete medium was added into the apical chambers of all ALI cultures to measure HNECs baseline resistance. The media in the apical chamber was replaced with different concentrations of GSCS (prepared in water and diluted in medium), negative (water added to the medium in same proportions as GSCS) and positive controls (10% Triton X-100 in medium), respectively. HNECs-ALI cultures were kept on a heating platform at 37°C during measurements. The TEER values were measured every 10 minutes up to two hours after the application of test compounds [438]. The TEER measurements were normalized to the negative control. Transepithelial electrical resistance studies were carried out independently three times with two wells per treatment (n=6).

**Fluorescein isothiocyanate-dextran permeability assay**

A two-hour incubation of HNECs-ALI cultures with treatments was performed, then cells were washed with PBS and 1:10 fluorescein isothiocyanate (FITC)-dextran 0.3 mg/ml (Sigma-Aldrich, St. Louis, MO, USA) was added to the cells for two hours. The amount of FITC-dextran was quantified in the medium from the basal chamber of the Transwell by measuring fluorescence with a microplate reader (FLOUstar Optima; BMG Labtech, Ortenberg, Germany) [439]. Relative permeability measurements were compared to the negative control. Permeability studies were carried out independently three times with two wells per treatment.

**Lactate dehydrogenase cytotoxicity assay**

After exposure of the HNECs to different treatment groups for two hours followed by another two hours to FITC-dextran, the supernatants from the basal chambers were collected from all the wells. Lactate dehydrogenase (LDH) was assayed using a Cytotoxicity Detection Kit (Promega Australia, Alexandria NSW, Australia). Briefly, the supernatants were centrifuged at 250 x *g*, 4°C for 4 minutes and 50 µl aliquots were transferred into duplicate wells of a 96 well plate. Then, 50 µl of Substrate Mix dissolved in Assay Buffer was added and the plate was then incubated for 30 minutes at room temperature, in the dark. Finally, the absorbance was read at 490 nm by a microplate reader (Imark plate reader, Bio-Rad) following the addition

of a 50 µl Stop Solution. Cell viability percentage was reported after correction for the absorbance of the medium as background. Viability studies were carried out independently three times with four wells per treatment (n=12)[440].

**The 3-(4,5-Dimethylthiazol-2-yl)-2,5-Diphenyltetrazolium Bromide (MTT) cytotoxicity assay**

After exposure of the HNECs to different treatment groups for two hours and 15 minutes, the cells were washed with PBS and MTT assay was performed according to the protocol reported by Plumb, 1999 [441]. Briefly, the cells were exposed to 100 µl ALI-complete medium and 25 µl MTT (5 mg/ml) and incubated for 4 hours at 37 °C humidified air with 5% $CO_2$. Then, the supernatants were removed, and MTT-formazan crystals were dissolved by adding 200 µl Dimethyl sulfoxide (DMSO) and glycine buffer (0.1 M glycine, 0.1 M NaCl adjusted to pH 10.5 with 1 M NaOH). The plate was then incubated overnight at room temperature, in the dark on a shaking platform. Finally, the absorbance was read at 470 nm by a microplate reader (Imark plate reader, Bio-Rad). Cell viability percentage was reported after correction for the absorbance of the medium as background. Viability studies were carried out independently three times with two wells per treatment (n=6)[440].

**Interleukin 6 inflammatory marker Enzyme-Linked Immunosorbent Assay (IL-6 ELISA)**

After exposure of the HNECs to different treatment groups for two hours followed by another two hours to FITC-dextran, the basal chamber's supernatants were quantified for IL-6 concentration using an Enzyme-Linked Immunosorbent Assay (ELISA) kit (BD Biosciences, Franklin Lakes, NJ, USA) according to the manufacturer's instructions. The experiment was carried out independently three times with two wells per treatment. The concentration (pg/ml) of IL-6 was calculated using a standard curve [442].

**Ciliary beat frequency measurements**

HNEC-ALI cultures were exposed to GSCS or control for 2 hours and CBF was evaluated every 10 minutes up to two hours using a 20× objective, and magnification ×1.5 on an inverted microscope (Olympus IX70; Olympus, Tokyo, Japan) and a Model Basler acA645-100µm USB3 camera (Basler AG, Ahrensburg, Germany) was used to record videos at 100 frames per second at a resolution of 640 × 480 pixels. The recorded videos were analyzed using the Sisson-Ammons Video Analysis (SAVA) system. HNECs-ALI cultures were washed twice with PBS, then a baseline CBF was taken after applying 100 µl of media on HNECs, before exposing the cells to treatment groups, medium (negative control) and 10% Triton X-100

(positive control). The HNECs-ALI cultures were returned to the incubator at 37°C between readings. The experiments were performed in 6 replicates and the results were normalized to baseline [390].

**Morphology assessment of HNECs exposed to GSCS; Localization of GSCS in apical area and intercellular space**

To determine the distribution of GSCS once exposed to the HNECs along with the effect of GSCS on the morphology of HNECs, HNEC-ALI cultures were incubated for different periods with treatments, including media (negative control, 2 h), GSCS (44 ppm, 15 min and 2 h) and 10% Triton x-100 (positive control, 2 h). Following washing with 5% dextrose (3 times), the HNEC-ALI cultures were fixed overnight at 40 °C in a solution of 4% paraformaldehyde, 1.25% glutaraldehyde in phosphate buffer pH7.2 to which 4% sucrose had been added. They were then washed in phosphate buffer and post fixed in Osmium tetroxide for 1 h. After that, they were dehydrated through a series of ethanols followed by propylene oxide and epon/araldite resin before being placed in embedding molds with fresh resin and set in an oven at 60 °C for 48 h. One-micron survey sections were cut on a Leica UC7 ultramicrotome, mounted on glass slides and stained with 0.05% toluidine blue made up in borax buffer then imaged with a light microscope. When a suitable area was found, 90 nm sections were cut using a diamond knife and collected onto 200 mesh copper grids. These unstained grids were examined with a Tecnai G2 spirit 120kV TEM (FEI, Hillsboro, USA) and digital images recorded with AMT Nanosprint 15 MKII (AMT Imaging Direct, Woburn, USA). For TEM images, GSCS were spotted onto formvar/carbon 200 mesh grids (ProSciTech, Townsville, Australia) and TEM was performed by a Tecnai G2 Spirit TWIN Transmission Electron Microscope (FEI, Hillsboro, USA), operating at 100KV, to confirm the morphology and size of GSCS, respectively.

**Transportation of GSCS from apical to basal chamber across HNEC-ALI cultures**

HNECs grown in ALI-culture Transwell plates were incubated for different periods with treatments, including media (negative control, 2 h), GSCS (treatment groups, 44 ppm, 15 min and 2 h) and 10% Triton x-100 (positive control, 2 h). Then the media was collected at the basal chamber to evaluate the presence of GSCS. The GSCS concentration was determined by inductively coupled plasma mass-spectrometry (ICP-MS, Perkin Elmer Nexion 350D). A silver (Ag) calibration was made in 2% $HNO_3$ ranging from 0.01 ppb to 20 ppb. The samples were diluted 10 and 20 times in 2% $HNO_3$ and Iridium were used as internal standard. All results were corrected for the internal standards. A calibration curve was created from the calibrants (0,01 ppb-20 ppb) and the cal blank was used representing 0% Ag. The intensities (counts) from the samples were then compared to the calibration curve with known concentrations. The accuracy of the calibration curve was tested by using a known concentration of Ag (1 ppb of QC27) from another source. The accuracy of the

calibration throughout the run was tested by checking a specific concentration from the calibration, in this case, the 1 ppb standard was used, a few times during the run, and at the end of the run, to make sure the calibration was still valid

### Statistical Analysis

GraphPad Prism (version 8.00, GraphPad Software, La Jolla, U.S.) was used for data analysis and graphing. Data were presented as the mean ± standard error of the mean (SEM) using analysis of variance (ANOVA), with Tukey honestly significant difference (HSD) post hoc test to evaluate significance between treatment groups.

## Results

### Transepithelial electrical resistance

Primary human nasal epithelial cell air liquid interface (HNEC-ALI) cultures were established from 3 CRS and 3 non-CRS control patients. The GSCS reduced the TEER values of HNEC-ALI cultures in a dose dependent way in cells derived from both patient groups after 10-20 . TEER values remained low for the remainder of the two hours of incubation (figure 1.4).

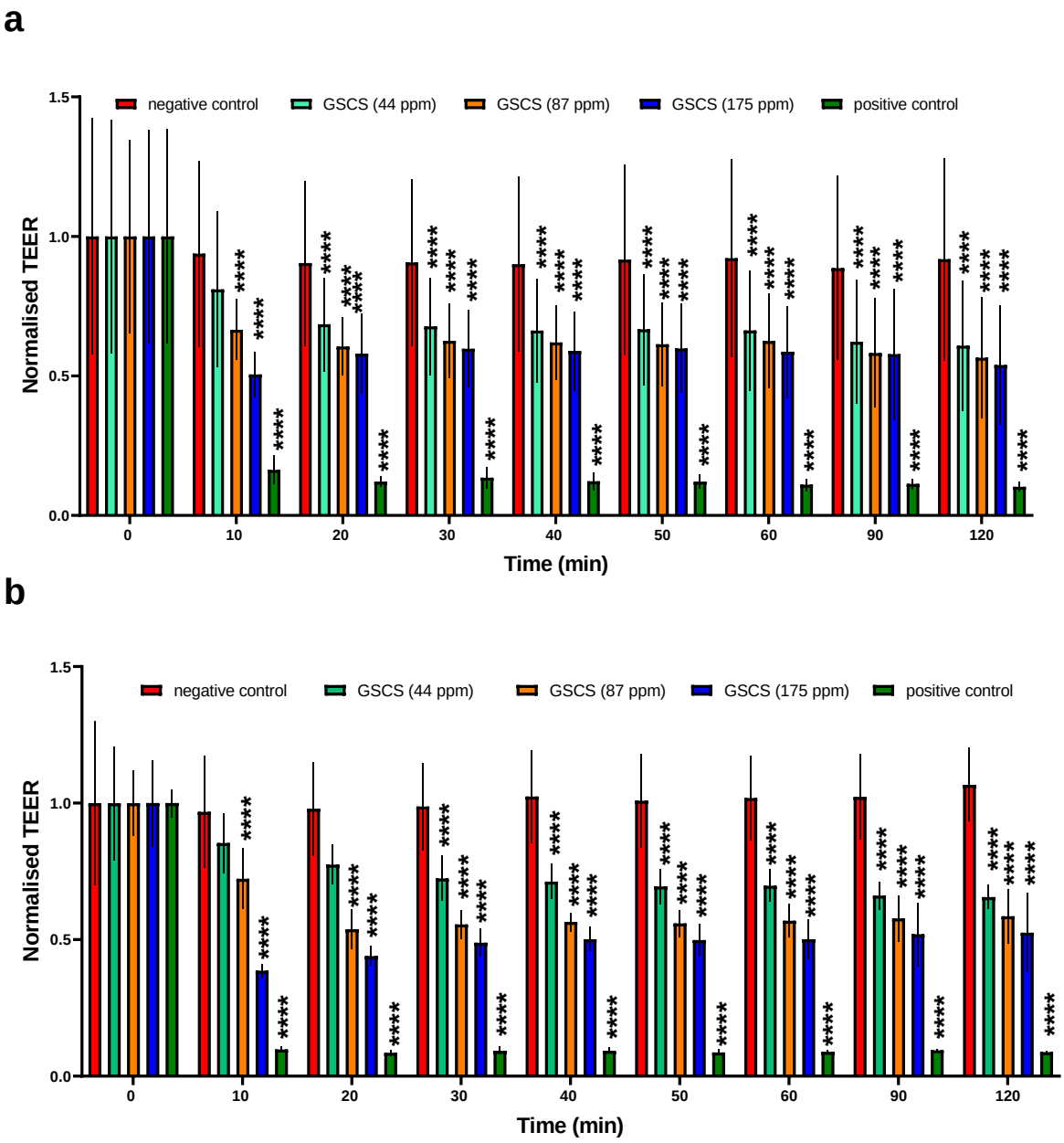


**Figure 1.4** Transepithelial electrical resistance of HNECs-ALI cultures derived from CRS and non-CRS control patients exposed to GSCS after two hours.

Transepithelial electrical resistance was quantified after a two-hour exposure of GSCS at 44, 87 and 175 ppm on HNEC-ALI cultures from (a) non-CRS control patients and (b) CRS patients. Negative and positive controls were medium and 10 % Triton X-100, respectively. The values are shown as means ± SEM for n = 6 ANOVA followed by Tukey HSD post hoc test. ****p < 0.0001. HNECs = human nasal epithelial cells; ALI; air-liquid interface; CRS; chronic rhinosinusitis; GSCS; green synthesized colloidal silver

**Paracellular permeability**

Application of GSCS for 2 hours did not have a significant effect on the paracellular permeability of FITC-dextran in HNEC-ALI cultures compared to the negative control, measured 4 hours after application of the test compounds (Figure 2.4).

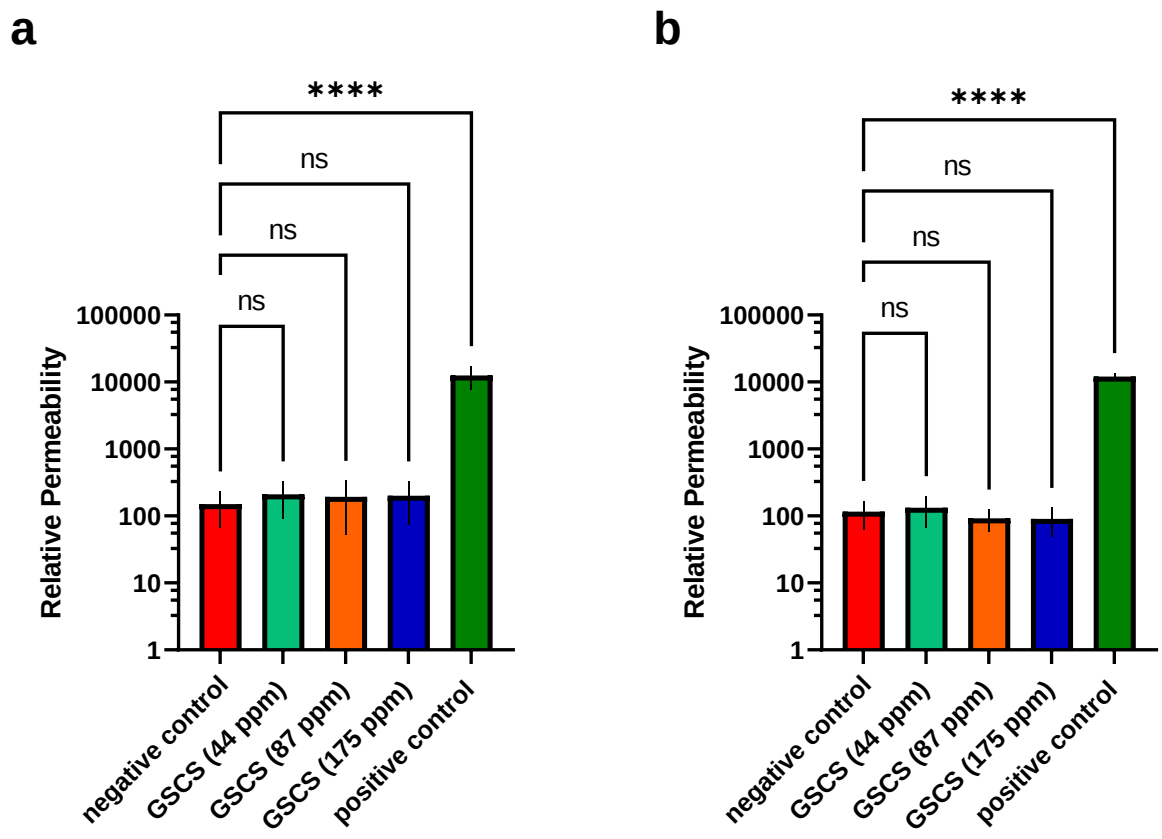


**Figure 2.4** Paracellular permeability of HNECs-ALI cultures derived from CRS and non-CRS control patients exposed to GSCS after two hours.

Fluorescein isothiocyanate (FITC)-dextran was quantified after a two-hour exposure of GSCS at 44, 87 and 175 ppm on HNECs-ALI cultures from (a) non-CRS control patients and (b) CRS patients. Negative and positive controls were medium and 10 % Triton X-100, respectively. The values are shown as means ± SEM for n = 6. ANOVA followed by Tukey HSD post hoc test. ****$p < 0.0001$.

**Cytotoxicity**

Cell viability was evaluated by quantification of LDH release in the medium of HNEC-ALI cultures as well as the enzymatic reduction of MTT to the blue MTT-formazan crystals after exposure to GSCS for 2 hours for the LDH assay as well as 15 minutes and 2 hours for MTT assay, respectively. No significant

difference in LDH levels and the absorbance of the MTT-formazan solution was seen compared to negative control in both CRS and non-CRS control patients (Figure 3.4).

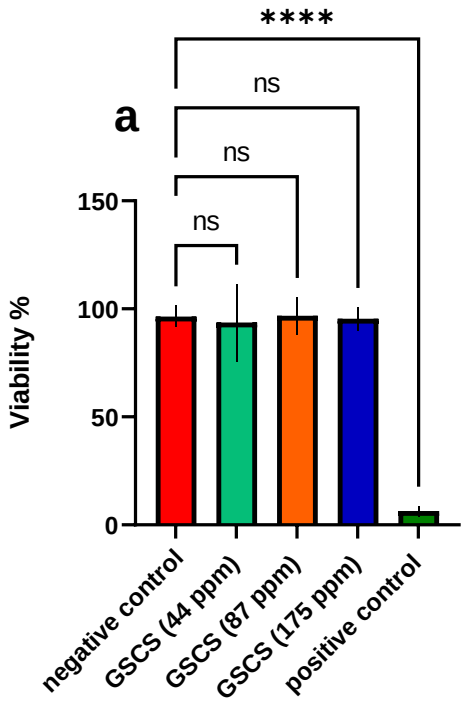
a
****
ns
ns
ns
Viability %
150
100
50
0
negative control
GSCS (44 ppm)
GSCS (87 ppm)
GSCS (175 ppm)
positive control

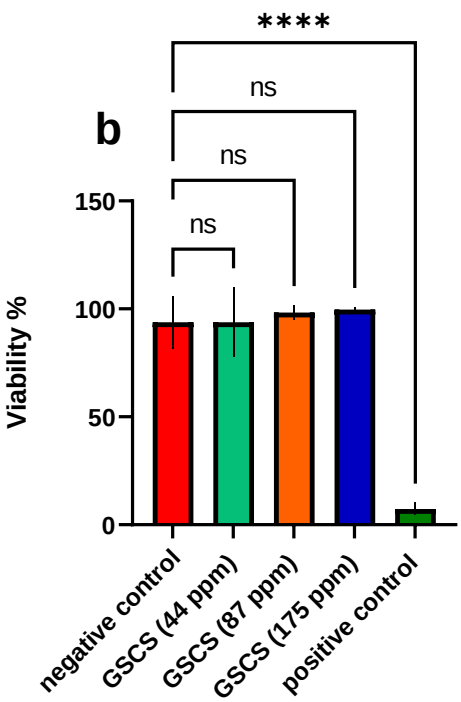
b
****
ns
ns
ns
Viability %
150
100
50
0
negative control
GSCS (44 ppm)
GSCS (87 ppm)
GSCS (175 ppm)
positive control

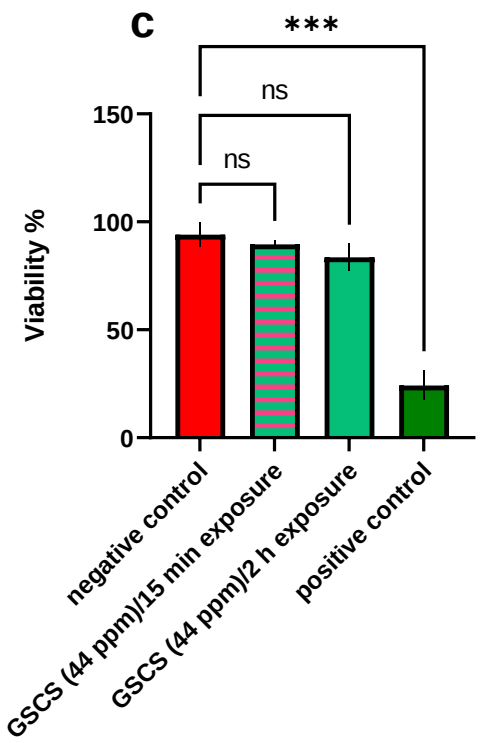
c
***
ns
ns
Viability %
150
100
50
0
negative control
GSCS (44 ppm)/15 min exposure
GSCS (44 ppm)/2 h exposure
positive control

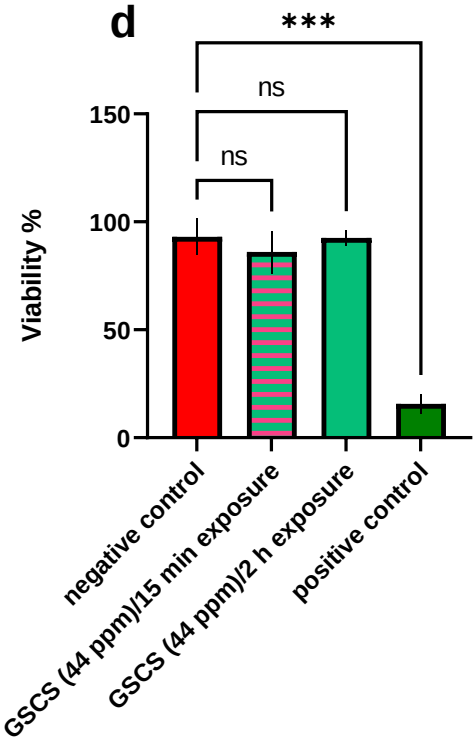
d
***
ns
ns
Viability %
150
100
50
0
negative control
GSCS (44 ppm)/15 min exposure
GSCS (44 ppm)/2 h exposure
positive control

**Figure 3.4** Lactate dehydrogenase secretion and MTT-formazan assay of HNEC-ALI cultures derived from CRS and non-CRS control patients exposed to GSCS for two hours and 15 minutes.

Lactate dehydrogenase was quantified after a two-hour exposure of GSCS at 44, 87 and 175 ppm on HNECs-ALI cultures from (a) non-CRS control and (b) CRS patients. The absorbance of formazan solution was measured after a two-hour and 15-minute exposure of GSCS at 44 ppm on HNECs-ALI cultures from (c) CRS and (d) non-CRS control patients. Negative and positive controls were medium and 10% Triton X-100, respectively. The values are shown as means ± SEM for n = 12 and 6, respectively. ANOVA followed by Tukey HSD post hoc test. ***p < 0.001; ****p < 0.0001.

**Interleukin 6 (IL-6) secretion**

Application of GSCS for 2 hours did not induce IL-6 protein secretion by HNECs-ALI cultures derived from either CRS or non-CRS control patients compared to the negative control (medium), measured 4 hours after application of the test compounds (Figure 4.4). In contrast, the positive control (10% Triton X-100 in medium) induced a significant increase in IL-6 protein levels when compared with the negative control.

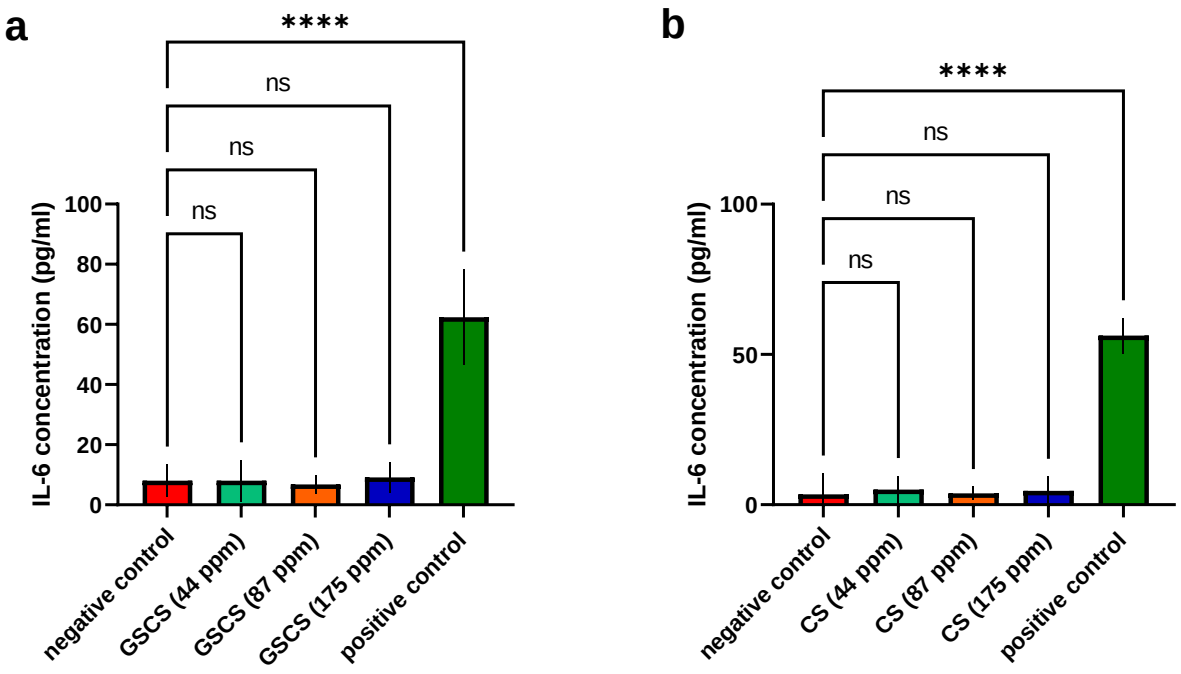


**Figure 4.4** Interleukin-6 secretion of HNECs-ALI cultures derived from CRS and non-CRS control patients exposed to GSCS for two hours.

Interleukin-6 was quantified after a two-hour exposure of GSCS at 44, 87 and 175 ppm on HNECs-ALI cultures from (a) non-CRS control patients and (b) CRS patients. Negative and positive controls were medium and 10 % Triton X-100, respectively. The values are shown as means ± SEM for n = 6. ANOVA followed by Tukey HSD post hoc test. ****$p < 0.0001$.

**Ciliary beat frequency**

HNEC-ALI cultures were treated with different concentrations of GSCS, medium (negative control) and 10% Triton X-100 in medium (positive control) for two hours (Figure 5.4). The cilia beat frequency (CBF) was assessed at different time points (0, 10, 20, 30, 40, 50 minutes, 1, 1.5 and 2 hours). There was no significant difference in CBF compared to the negative control for any of the test solutions at any of the time points. In contrast, the positive control induced a significant reduction in CBF compared to negative control at all-time points when compared with time 0.

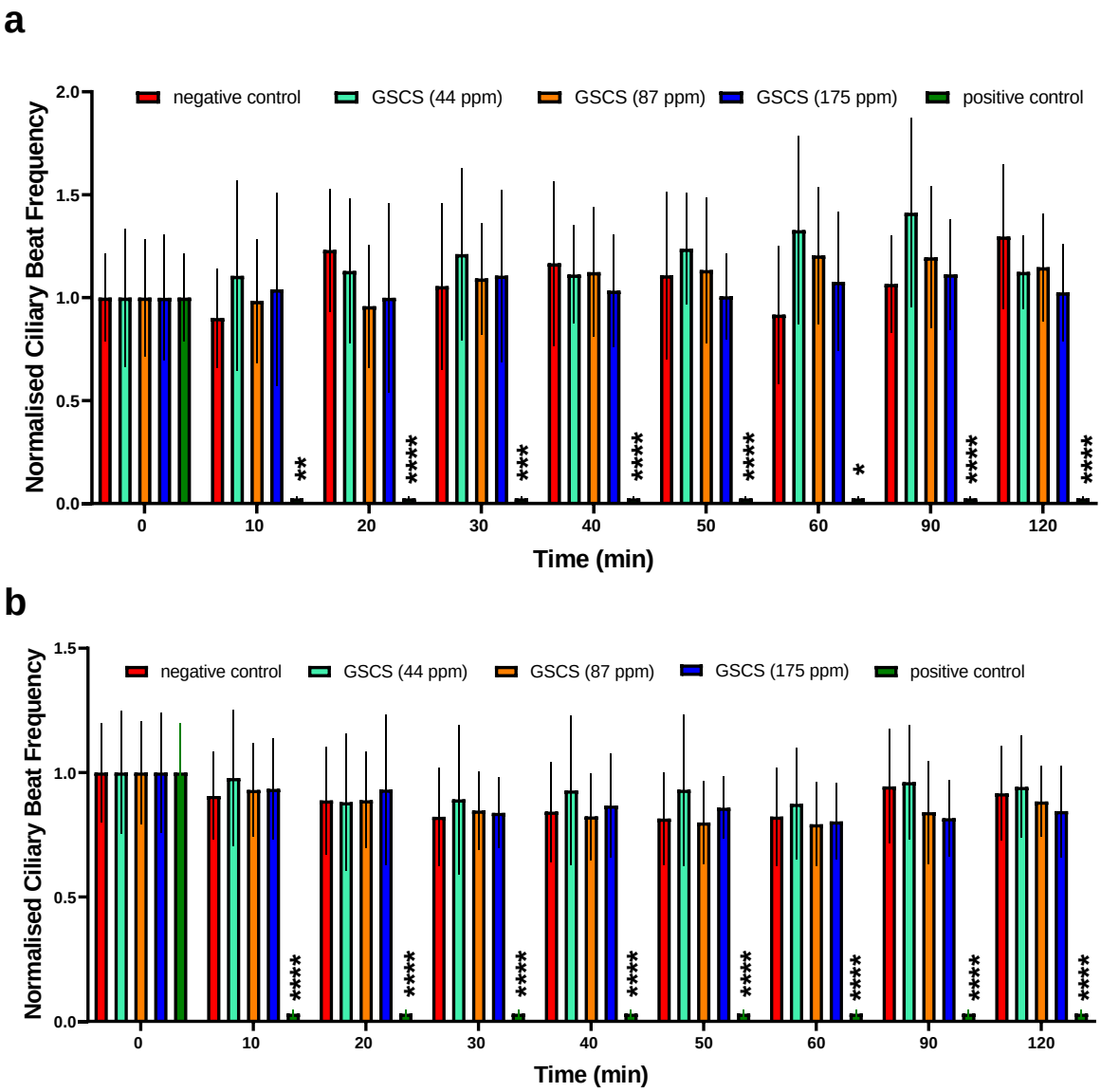


**Figure 5.4** Ciliary Beat Frequency of HNECs-ALI cultures derived from CRS and non-CRS control patients exposed to GSCS after two hours.

Ciliary Beat Frequency was measured after a two-hour exposure of GSCS at 44, 87 and 175 ppm on HNEC-ALI cultures from (a) non-CRS control patients and (b) CRS patients. Negative and positive controls were medium and 10 % Triton X-100, respectively. The values are shown as means ± SEM for n=6. ANOVA followed by Tukey HSD post hoc test. * $p < 0.05$; **, $p < 0.01$; ***, $p < 0.001$; ****$p < 0.0001$.

**Ultrastructure of GSCS and HNEC-ALI cultures exposed o GSCS**

TEM images showed the presence of spherical GSCS (Figure 6.4a). Moreover, GSCS had no impact on morphology, cilia structure and tight junctions in treatment groups of HNECs derived from both control

(Figure 6.4c and d) and CRS (Figure 6.4g and h) patients in comparison to the negative control (Figure 6.4b and f). In contrast, in positive control samples, (Figure 6.4e and i) there was evidence of plasma membrane disruption and cell morphological changes. Furthermore, no GSCS was detected on the apical side (Figure 6.4l, n, t and v) and intercellular space (Figure 6.4m, o, u and w) of HNEC-ALI cultures exposed to GSCS for 15 min and 2 h.

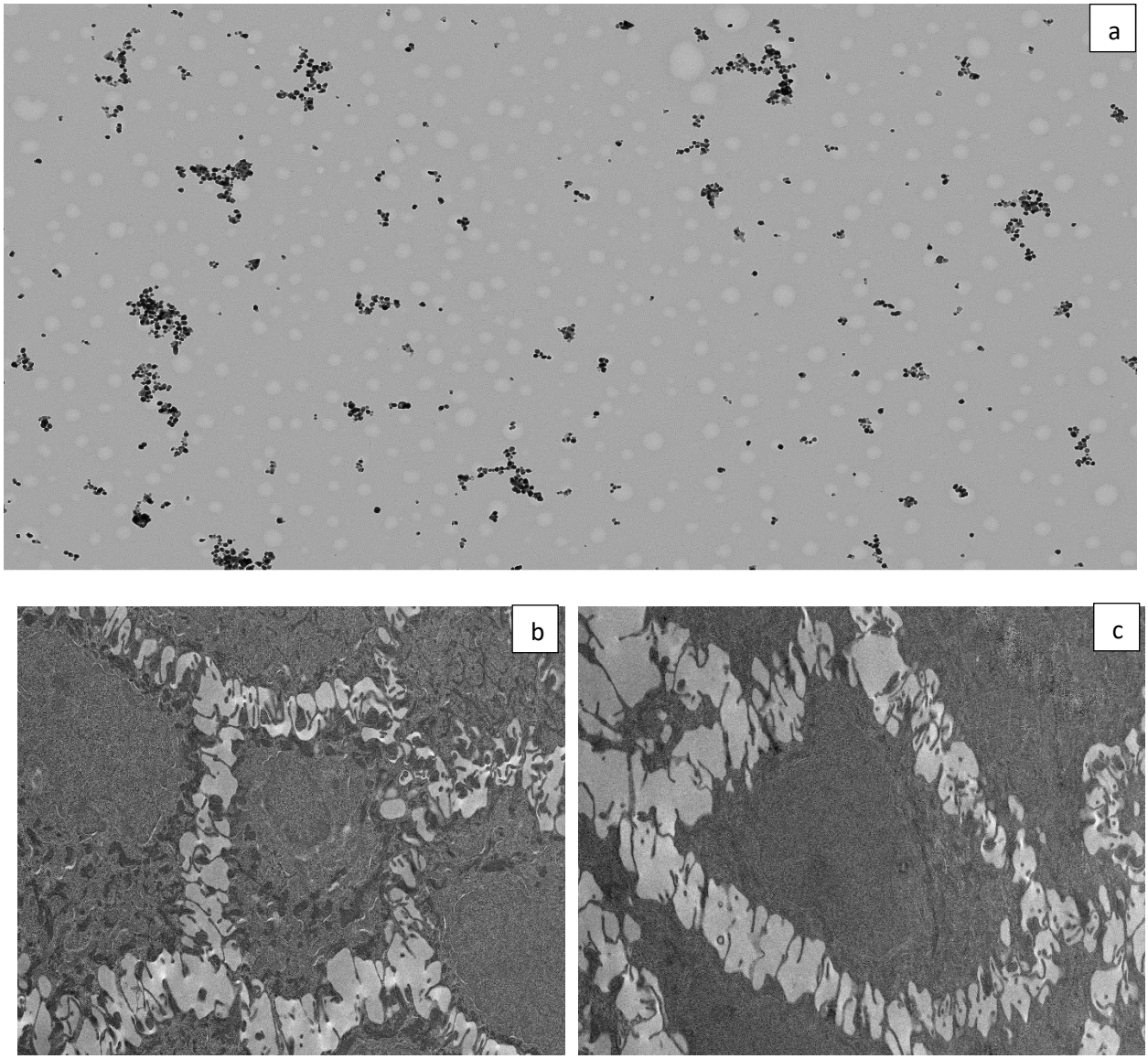

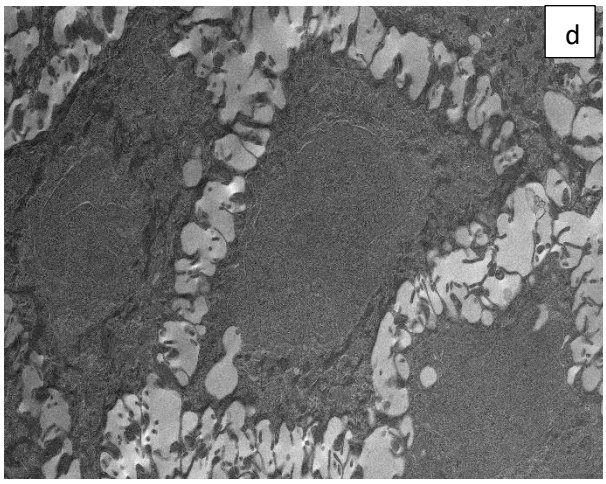
d

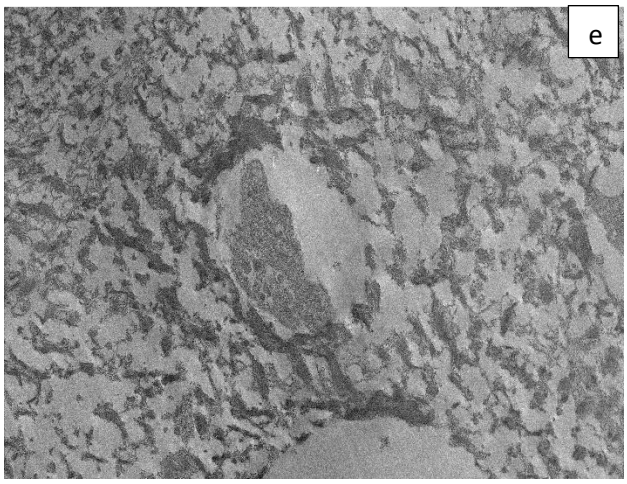
e

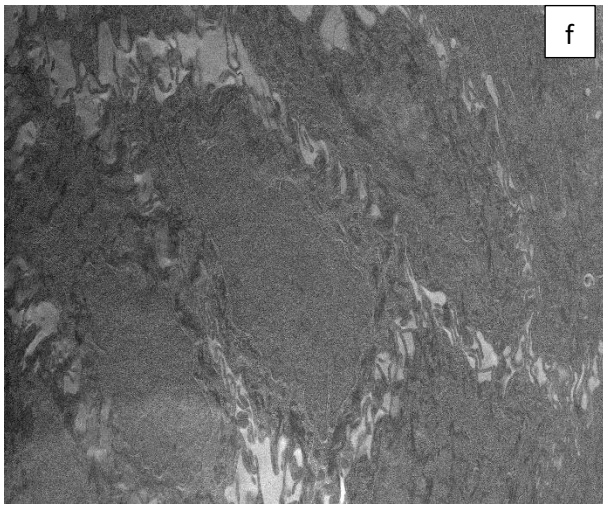
f

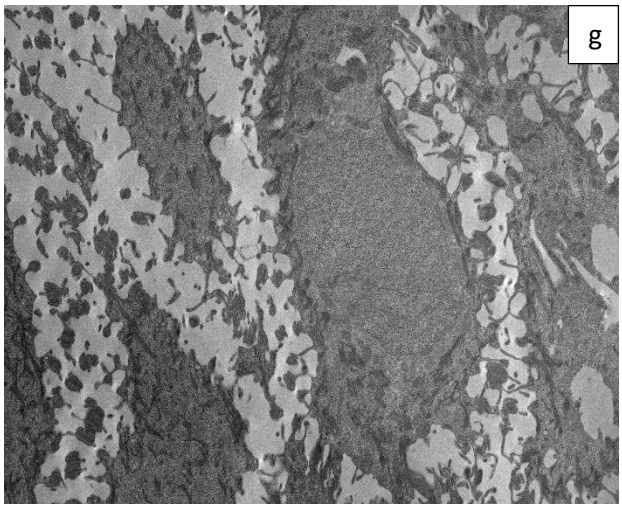
g

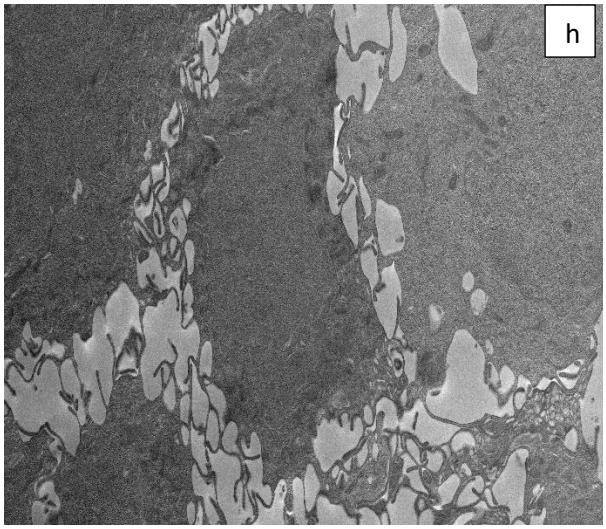
h

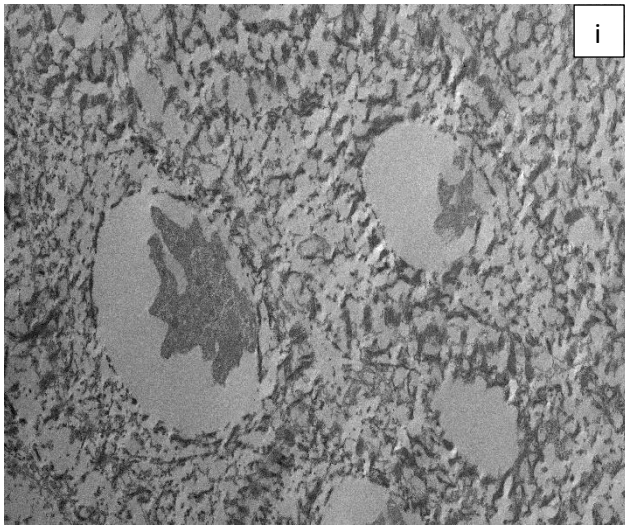
i

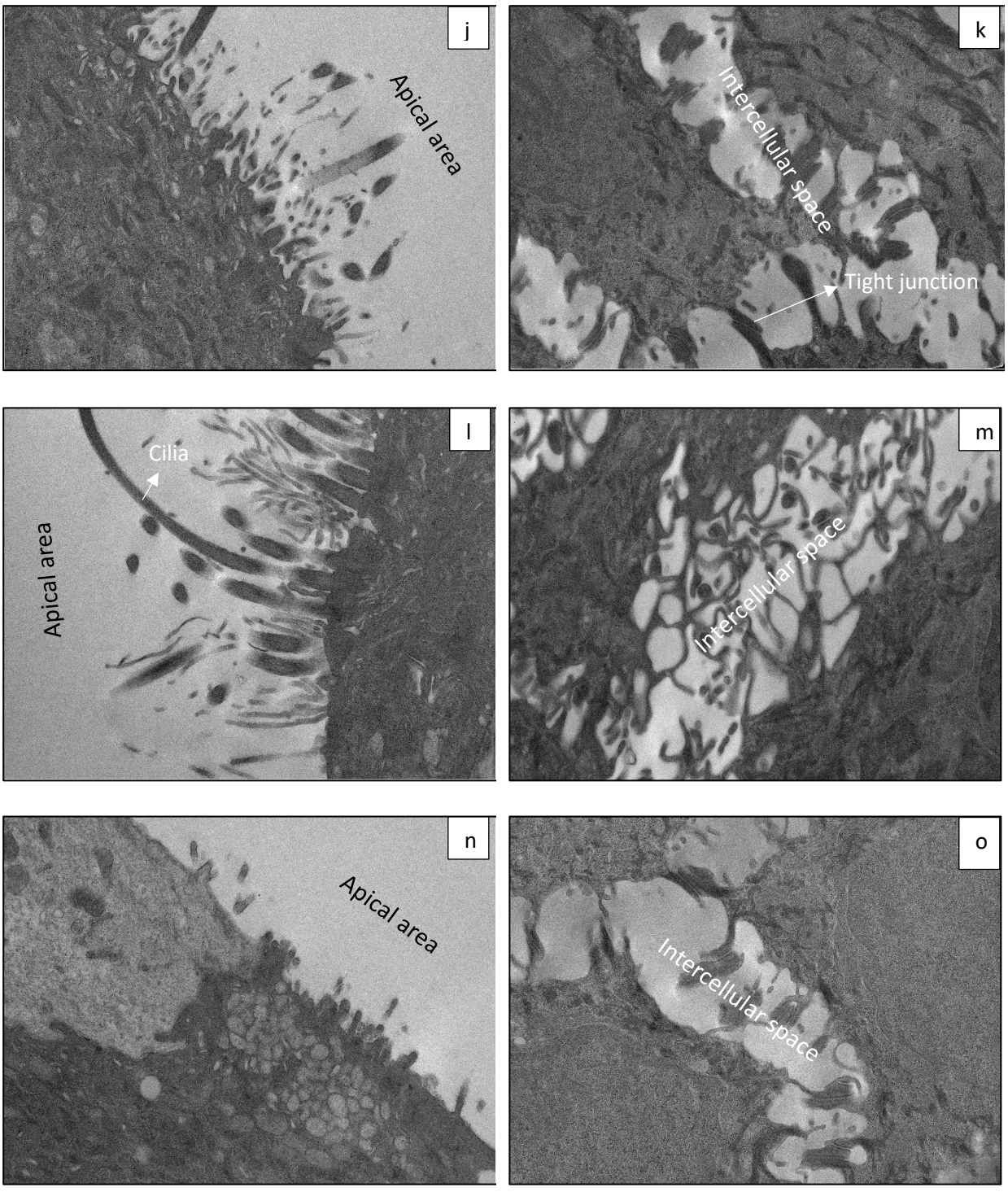
j
Apical area
k
Intercellular space
Tight junction
l
Cilia
Apical area
m
Intercellular space
n
Apical area
o
Intercellular space

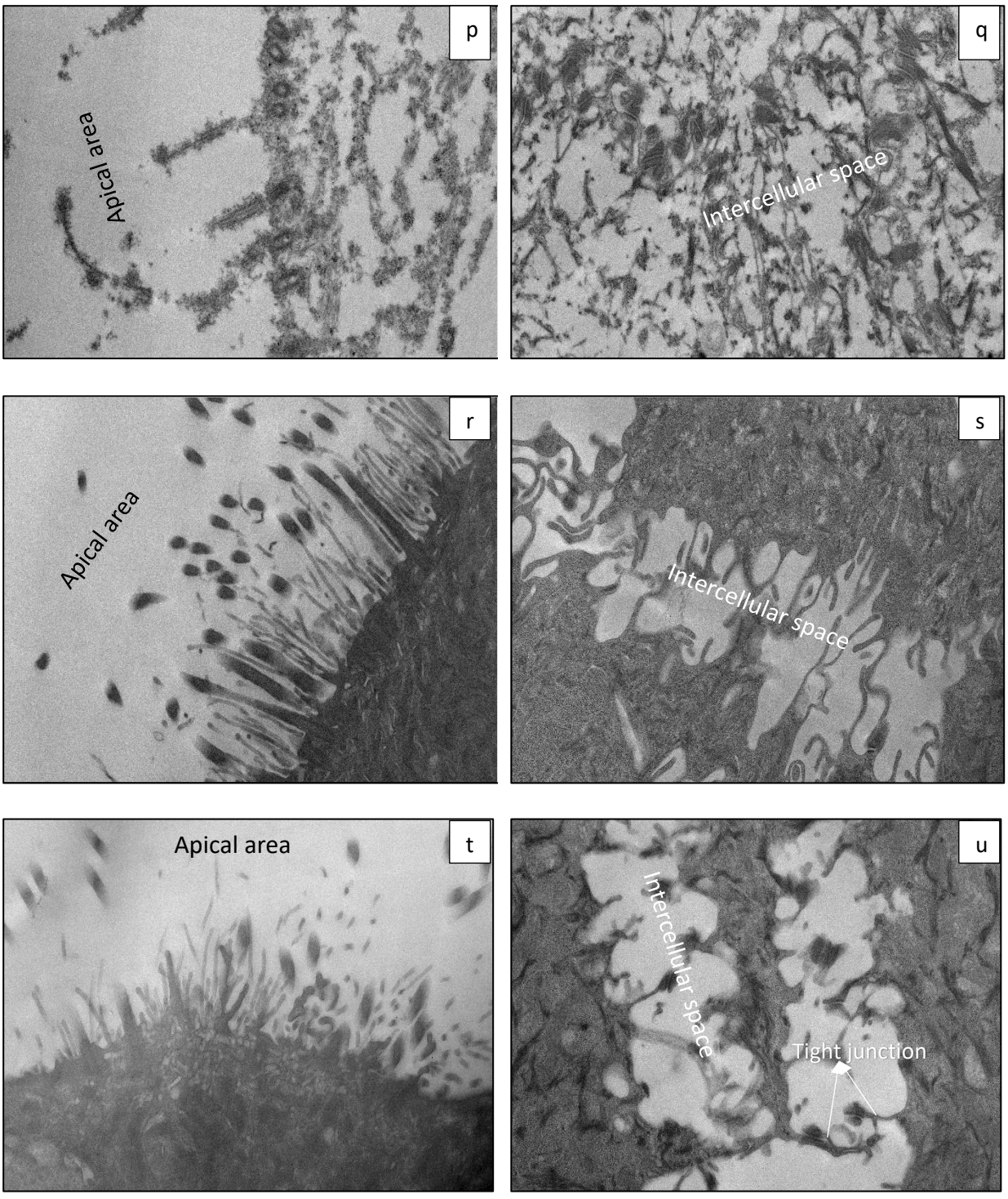
p
Apical area
q
Intercellular space
r
Apical area
s
Intercellular space
t
Apical area
u
Intercellular space
Tight junction

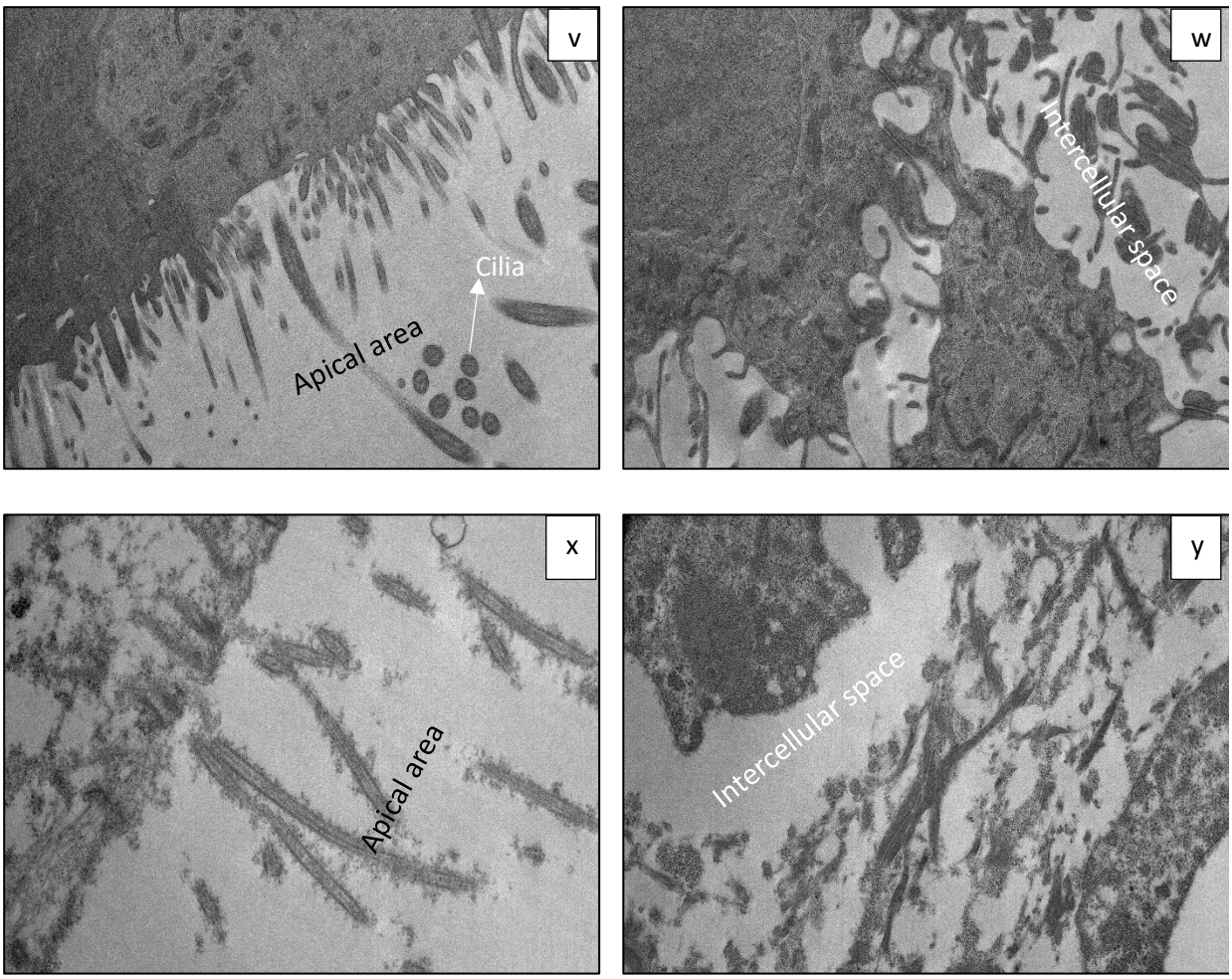


**Figure 6.4** Morphology and size of GSCS, the morphology of HNECs exposed to GSCS and the distribution of GSCS in apical and intercellular space of HNECs.

Transmission electron microscopy (TEM) images of (a) GSCS, morphology of the HNECs derived from control patient exposed to (b) media (negative control), (c) GSCS (15 min), (d) GSCS (2 h) and (e) 10% Triton X-100 (negative control), and the HNECs derived from CRS patient exposed to (f) media (negative control), (g) GSCS (15 min), (h) GSCS (2 h) and (i) 10% Triton X-100 (negative control), apical area of HNECs derived from control patient exposed to (j) media (negative control), (k) GSCS (15 min), (l) GSCS (2 h) and (m) 10% Triton X-100 (negative control), intercellular space of HNECs derived from control patient exposed to (n) media (negative control), (o) GSCS (15 min), (p) GSCS (2 h) and (q) 10% Triton X-100 (negative control), apical area of HNECs derived from CRS patient exposed to (r) media (negative control), (s) GSCS (15 min), (t) GSCS (2 h) and (u) 10% Triton X-100 (negative control), intercellular space of HNECs derived from CRS patient exposed to (v) media (negative control), (w) GSCS (15 min), (x) GSCS (2 h) and (y) 10% Triton X-100 (negative control).

**The presence of GSCS in the basal chamber**

Primary human nasal epithelial cell air liquid interface (HNEC-ALI) cultures were established from 3 CRS and 3 non-CRS control patients. After incubation of HNECs with different treatment groups, the presence of GSCS was evaluated by ICP-MS in the samples taken from the basal chamber (Table 1.4). Based on the results, the presence of GSCS in the treatment groups is not significant in comparison to the negative control (Figure 7.4).

**Table 1.4** Inductively coupled plasma-mass-spectrometry (ICP-MS) analysis of GSCS.

| Patient diagnosis | Patient ID | Treatment groups | GSCS concentration (ppb) |
|---|---|---|---|
| CRS | 8339 | Negative control | less than 0.1 |
| | | GSCS 15 min | 0 |
| | | GSCS 2h | 0.32 |
| | 8341 | Negative control | 1.4 |
| | | GSCS 15 min | 0.2 |
| | | GSCS 2h | 0.43 |
| | 8344 | Negative control | less than 0.1 |
| | | GSCS 15 min | 0.15 |
| | | GSCS 2h | 0.45 |
| Control | 8345 | Negative control | 0.2 |
| | | GSCS 15 min | 0.1 |
| | | GSCS 2h | 0.61 |
| | 8346 | Negative control | 0 |
| | | GSCS 15 min | 0 |
| | | GSCS 2h | 0.3 |
| | 8351 | Negative control | 0.1 |
| | | GSCS 15 min | less than 0.1 |
| | | GSCS 2h | 0.27 |

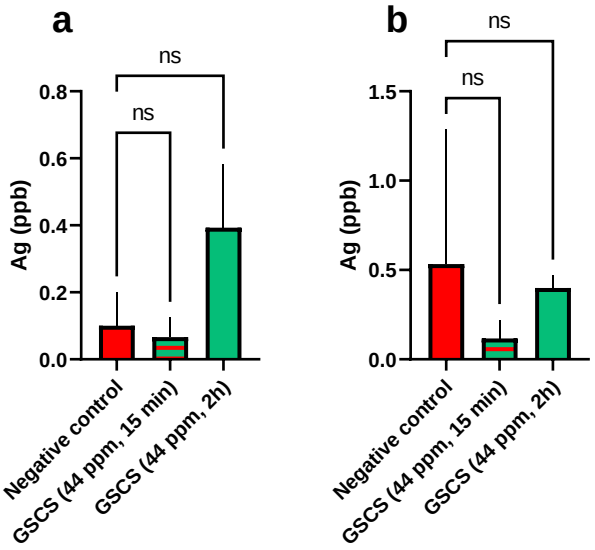


**Figure 7.4** Inductively coupled plasma-mass-spectrometry (ICP-MS) analysis of GSCS.

The concentration of Ag was measured after 2 h incubation of HNECs with GSCS in the media collected from the basal chamber of ALI-culture plates from (a) non-CRS control and (b) CRS patients. The negative control was medium. The values are shown as means ± SEM for n = 3. ANOVA followed by Tukey HSD post hoc test.

## Discussion

This study assessed the effect of GSCS on the barrier and mucociliary function of HNECs in an air-liquid interface culture. The GSCS exposure of CRS and non-CRS control HNEC-ALI cultures resulted in a significant decrease in TEER values which was not accompanied by any significant change in paracellular permeability of FITC-dextran or alteration in mucociliary function. Furthermore, a 2-hour application of GSCS even at high 175 ppm concentrations was not toxic and did not enhance the secretion of the pro-inflammatory cytokine IL-6.

Due to mucociliary clearance, the drug retention time in the nasal cavity is maximum of 15 minutes [390]. Hence, a maximum exposure time of 2 hours of the GSCS was considered sufficient to evaluate the *in vitro* safety and effect on the barrier, as is common for *in vitro* safety testing of compounds to be used as topical applications to the nose and paranasal sinuses [390, 443]. Based on the results 44 ppm CS did not affect TEER after 10 mins exposure giving a stronger justification for the safety of 44 ppm CS which is going to be used in the clinical trial because of the efficacy results of this concentration against clinical isolates tested in our previous study [413].

Paracellular movements of charged and uncharged solutes at epithelial tight junctions is controlled by the size and charge-selective pores through two different mechanisms. In the first mechanism ions, small uncharged molecules and water pass through the high-capacity, charge-selective pore pathway which is regulated by the expression of the claudin family of proteins. In the second mechanism larger ions and molecules, regardless of charge are transferred via the low-capacity leak pathway which is controlled by cytoskeletal dynamics or cell homeostasis affecting agents [390, 444, 445]. The TEER is one of the methods measuring the permeability of both pathways and is a simple and rapid indicator of cellular barrier integrity to examine the toxicity of drugs. It can be influenced by various factors such as the electrodes used, temperature variations, the media, passage number of cells and cell culture age. The TEER value reduction, accompanied no change in paracellular permeability of 4 kDa dextran over a long period seen in this study could be due to enhanced passage of small molecules and ions over the HNECs-ALI cultures via the pore pathway [390]. This could be due to an effect on the molecular organization of tight junctions or the activation of ionic channels when exposed to GSCS and it is not considered a sign of toxicity [446]. Furthermore, it could be due to the high osmolality of CS as well as the size, concentration and charge of GSCS [390, 447].

Cytotoxicity of silver nanoparticles is determined by their size, shape, charge, concentration, solubility, surface functionalization, exposure time, environmental factors and cell type [448]. The smaller the particles, and the higher their concentration, the higher the probability of an increase in epithelial permeability and induction of toxicity. Additionally, the charge can influence toxicity as negatively charged silver nanoparticles can be trapped by mucus and agglomerate becoming less toxic [448]. Moreover, silver nanoparticle shape can influence the uptake mechanism via cells and affect toxicity. The GSCS in this study are spherical and are known to be less toxic than for example star shaped CS [358].

The interaction between GSCS and HNECs did not induce IL-6 release after two hours of contact with GSCS in either non-CRS control or CRS HNECs. IL-6 production by cells can be the result of cell necrosis or pro-inflammatory stimulation [449]. The lack of IL-6 release strengthens our finding of the absence of LDH release and indicates the absence of toxicity with no significant necrosis or inflammatory activation, in line with previous studies [450-453].

The clearance of the airway tract depends not only on appropriate mucus/periciliary fluid production but also on the coordinated ciliary activity of ciliated cells which requires efficient communication through junctional complexes in airway epithelia. Ciliary beat frequency (CBF) is an indication of mucociliary clearance effectiveness and the reflective of the respiratory mucosal function health. The safety of topical treatments and their potential for ciliotoxicity is demonstrated through the absence of effect on the CBF [390,

[454]. In this study, no significant difference was detected after exposure of HNECs to GSCS for up to two hours, supporting the absence of ciliotoxicity of GSCS [454].

It has been reported that inhaled nanoparticles can embed in olfactory epithelium which then can undergo transportation from the olfactory bulb to the brain and induce neurotoxicity [455, 456, 457, 458, 459, 460, 461, 462]. However, according to our results, GSCS did not cross HNEC-ALI cultures which are further in support of safety when used topically in the nose.

**Conclusion**

CRS and non-CRS control HNECs were exposed to green synthesized colloidal silver (GSCS) for up to two hours. Results showed no evidence of toxicity with preserved mucosal barrier structure and mucociliary function, even with the highest tested concentration of 175 ppm. Our results indicate the potential for GSCS to be used as a topical treatment for CRS infectious exacerbation.

## Chapter 5: Conclusion, future prospective and translational prospects

Over the past decades, the emergence and spread of antibiotic-resistant bacteria have had major implications for society, the economy and medicine, threatening human health and imposing a high burden on the healthcare system around the world. The already existed antibiotics contain few molecules with a novel mode of action requiring the development of new antimicrobial agents. These antimicrobial agents should also be able to eradicate biofilms as they play an important role in infectious disease and are resistant to antibiotics up to 1000-fold. Different materials have been suggested to be used as a treatment for the eradication of infection so far, however, only 20% of those materials which enter phase one clinical trials are approved to be used in patients [463]. The success of the drugs depends on different factors such as delivery approach, disease severity, antimicrobial susceptibility and evasion mechanism of pathogens, suitability for clinical trial and the possibility of commercialization. Therefore, there is an unmet need for the development of antimicrobial agents which can overcome those challenges. Colloidal silver (CS) has been recognized as a good bactericidal agent. It can offer the best treatment for bacterial infectious diseases and be applied topically to reduce side effects, increase the dose of CS at the site of infection. However, their slow production of them limit their application. The CS further can alter the susceptibility of bacteria to antibiotics and overcome the antibiotic resistance crisis in the treatment of infectious diseases. In this thesis, a single 15-minute fabrication method of CS was developed using *Corymbia maculata* aqueous leaf extract. The CS was spherical, 40 nm in size and stable for over one year. They demonstrated efficacy against planktonic and biofilm of gram-positive and gram-negative clinical isolates from chronic rhinosinusitis (CRS) patients *in vitro* and in an *in vivo C. elegans* model. More spesifically, the CS showed higher efficacy against *P. aeruginosa* which may be due to the the higher production of ROS in gram-negative in comparison to the gram-positive bacteria [464]. They revealed a non-toxic effect against airway epithelial cells (Nuli-1) *in vitro* and *in vivo C. elegans* model. The combination of CS and antibiotics improved the efficacy of the antibiotic bactericidal activity. The CS and antibiotic combination did not interfere with antibiotics through antagonistic mechanisms. The CS enhanced the biofilm eradication capability of gentamicin through synergism. These findings provide the possibility of conducting a human trial to assess the efficacy of CS in which the CS will be used as a sinonasal rinse to reduce infection in CRS patients. However, evaluating the safety on the mucosal barrier structure and function is essential before conducting human trials. Consequently, CRS and non-CRS control human nasal epithelial cells were exposed to CS and the results showed no evidence of toxicity with preserved mucosal barrier structure and mucociliary function. The outcomes indicate the potential for the CS to be used as a topical treatment for CRS infectious exacerbation. A phase one clinical trial is going to be carried out at the Queen Elizabeth Hospital, Woodville, SA, Australia. The CS will be produced under the Good Laboratory Practice procedure at the Basil Hetzel Institute for Translational Health Research/the University of Adelaide. The CS is going to be used as a nasal rinse by patients suffering from chronic rhinosinusitis to eradicate infection. This treatment

may be beneficial for the life of almost 3 million Australians suffering from chronic rhinosinusitis. Finally, the CS can be used topically for other infections such as wound infection and burn wounds.

## References


1. Bachert, C.; Marple, B.; Schlosser, R. J.; Hopkins, C.; Schleimer, R. P.; Lambrecht, B. N.; Bröker, B. M.; Laidlaw, T.; Song, W.-J., Adult chronic rhinosinusitis. *Nature Reviews Disease Primers* **2020,** *6* (1), 86.
2. Niederfuhr, A.; Kirsche, H.; Riechelmann, H.; Wellinghausen, N., The bacteriology of chronic rhinosinusitis with and without nasal polyps. *Archives of Otolaryngology–Head & Neck Surgery* **2009,** *135* (2), 131-136.
3. Wald, E. R.; Applegate, K. E.; Bordley, C.; Darrow, D. H.; Glode, M. P.; Marcy, S. M.; Nelson, C. E.; Rosenfeld, R. M.; Shaikh, N.; Smith, M. J., Clinical practice guideline for the diagnosis and management of acute bacterial sinusitis in children aged 1 to 18 years. *Pediatrics* **2013,** *132* (1), e262-e280.
4. Falagas, M. E.; Giannopoulou, K. P.; Vardakas, K. Z.; Dimopoulos, G.; Karageorgopoulos, D. E., Comparison of antibiotics with placebo for treatment of acute sinusitis: a meta-analysis of randomised controlled trials. *The Lancet infectious diseases* **2008,** *8* (9), 543-552.
5. Bachert, C.; Pawankar, R.; Zhang, L.; Bunnag, C.; Fokkens, W. J.; Hamilos, D. L.; Jirapongsananuruk, O.; Kern, R.; Meltzer, E. O.; Mullol, J., ICON: chronic rhinosinusitis. *World Allergy Organization Journal* **2014,** *7* (1), 1-28.
6. Banerji, A.; Piccirillo, J. F.; Thawley, S. E.; Levitt, R. G.; Schechtman, K. B.; Kramper, M. A.; Hamilos, D. L., Chronic rhinosinusitis patients with polyps or polypoid mucosa have a greater burden of illness. *American journal of rhinology* **2007,** *21* (1), 19-26.
7. Khan, A.; Vandeplas, G.; Thi, M. T. H.; Joish, V. N.; Mannent, L.; Tomassen, P.; Van Zele, T.; Cardell, L. O.; Arebro, J.; Olze, H., The Global Allergy and Asthma European Network (GALEN) rhinosinusitis cohort: a large European cross-sectional study of chronic rhinosinusitis patients with and without nasal polyps. *Rhinology* **2019,** *57* (1), 32-42.
8. Bachert, C.; Zhang, L.; Gevaert, P., Current and future treatment options for adult chronic rhinosinusitis: focus on nasal polyposis. *Journal of Allergy and Clinical Immunology* **2015,** *136* (6), 1431-1440.
9. Fokkens, W. J.; Lund, V. J.; Mullol, J.; Bachert, C.; Alobid, I.; Baroody, F.; Cohen, N.; Cervin, A.; Douglas, R.; Gevaert, P., EPOS 2012: European position paper on rhinosinusitis and nasal polyps 2012. A summary for otorhinolaryngologists. *Rhinology* **2012,** *50* (1), 1-12.
10. Chen, Y.; Dales, R.; Lin, M., The epidemiology of chronic rhinosinusitis in Canadians. *The Laryngoscope* **2003,** *113* (7), 1199-1205.
11. Halawi, A. M.; Shintani Smith, S.; Chandra, R. K. In *Chronic rhinosinusitis: epidemiology and cost*, Allergy & Asthma Proceedings, 2013.
12. Hastan, D.; Fokkens, W.; Bachert, C.; Newson, R.; Bislimovska, J.; Bockelbrink, A.; Bousquet, P.; Brozek, G.; Bruno, A.; Dahlén, S., Chronic rhinosinusitis in Europe–an underestimated disease. A GA2LEN study. *Allergy* **2011,** *66* (9), 1216-1223.
13. Blackwell, D. L.; Lucas, J. W.; Clarke, T. C., Summary health statistics for US adults: national health interview survey, 2012. *Vital and health statistics. Series 10, Data from the National Health Survey* **2014,** (260), 1-161.
14. Cooke, G.; Valenti, L.; Glasziou, P.; Britt, H., Common general practice presentations and publication frequency. *Australian Family Physician* **2013,** *42* (1/2), 65-68.
15. Statistics, A. B. o., Australian health survey: first results, 2011–12. ABS Canberra: 2012.
16. Johnson, P. S.; Ohlsson, B.; von Buchwald, C.; Jannert, M.; Ahlner-Elmqvist, M., A multi-centre study on quality of life and absenteeism in patients with CRS referred for endoscopic surgery. *Rhinology* **2011,** *49* (4), 420-428.
17. Bhattacharyya, N., Functional limitations and workdays lost associated with chronic rhinosinusitis and allergic rhinitis. *American journal of rhinology & allergy* **2012,** *26* (2), 120-122.

18. Stankiewicz, J.; Tami, T.; Truitt, T.; Atkins, J.; Winegar, B.; Cink, P.; Schaeffer, B. T.; Raviv, J.; Henderson, D.; Duncavage, J. In *Impact of chronic rhinosinusitis on work productivity through one-year follow-up after balloon dilation of the ethmoid infundibulum*, International forum of allergy & rhinology, Wiley Online Library: 2011; pp 38-45.
19. Rudmik, L., Economics of chronic rhinosinusitis. *Current allergy and asthma reports* **2017,** *17* (4), 20.
20. Alt, J. A.; Smith, T. L.; Mace, J. C.; Soler, Z. M., Sleep quality and disease severity in patients with chronic rhinosinusitis. *The laryngoscope* **2013,** *123* (10), 2364-2370.
21. Chester, A. C.; Sindwani, R.; Smith, T. L.; Bhattacharyya, N., Fatigue improvement following endoscopic sinus surgery: a systematic review and meta-analysis. *The Laryngoscope* **2008,** *118* (4), 730-739.
22. Chester, A. C.; Sindwani, R.; Smith, T. L.; Bhattacharyya, N., Systematic review of change in bodily pain after sinus surgery. *Otolaryngology—Head and Neck Surgery* **2008,** *139* (6), 759-765.
23. Brandsted, R.; Sindwani, R., Impact of depression on disease-specific symptoms and quality of life in patients with chronic rhinosinusitis. *American journal of rhinology* **2007,** *21* (1), 50-54.
24. Litvack, J. R.; Mace, J.; Smith, T. L., Role of depression in outcomes of endoscopic sinus surgery. *Otolaryngology--Head and Neck Surgery* **2011,** *144* (3), 446-451.
25. Wasan, A.; Fernandez, E.; Jamison, R. N.; Bhattacharyya, N., Association of anxiety and depression with reported disease severity in patients undergoing evaluation for chronic rhinosinusitis. *Annals of Otology, Rhinology & Laryngology* **2007,** *116* (7), 491-497.
26. Gliklich, R. E.; Metson, R., The health impact of chronic sinusitis in patients seeking otolaryngologic care. *Otolaryngology—Head and Neck Surgery* **1995,** *113* (1), 104-109.
27. Soler, Z. M.; Wittenberg, E.; Schlosser, R. J.; Mace, J. C.; Smith, T. L., Health state utility values in patients undergoing endoscopic sinus surgery. *The Laryngoscope* **2011,** *121* (12), 2672-2678.
28. Remenschneider, A. K.; D'Amico, L.; Gray, S. T.; Holbrook, E. H.; Gliklich, R. E.; Metson, R., The EQ-5D: a new tool for studying clinical outcomes in chronic rhinosinusitis. *The Laryngoscope* **2015,** *125* (1), 7-15.
29. Avila, P. C.; Schleimer, R. P., Airway epithelium. In *Allergy and Allergic Diseases, Second Edition*, Wiley-Blackwell: 2009; pp 366-397.
30. Schleimer, R. P.; Kato, A.; Kern, R.; Kuperman, D.; Avila, P. C., Epithelium: at the interface of innate and adaptive immune responses. *Journal of Allergy and Clinical Immunology* **2007,** *120* (6), 1279-1284.
31. Man, W. H.; de Steenhuijsen Piters, W. A.; Bogaert, D., The microbiota of the respiratory tract: gatekeeper to respiratory health. *Nature Reviews Microbiology* **2017,** *15* (5), 259-270.
32. Sousa, A. M.; Pereira, M. O., A prospect of current microbial diagnosis methods. **2013**.
33. Baroody, F. M.; Mucha, S. M.; Detineo, M.; Naclerio, R. M., Nasal challenge with allergen leads to maxillary sinus inflammation. *Journal of allergy and clinical immunology* **2008,** *121* (5), 1126-1132. e7.
34. Platt, M. P.; Soler, Z.; Metson, R.; Stankovic, K. M., Pathways analysis of molecular markers in chronic sinusitis with polyps. *Otolaryngology--Head and Neck Surgery* **2011,** *144* (5), 802-808.
35. Lam, K.; Schleimer, R.; Kern, R. C., The etiology and pathogenesis of chronic rhinosinusitis: a review of current hypotheses. *Current allergy and asthma reports* **2015,** *15* (7), 1-10.
36. Paramasivan, S.; Bassiouni, A.; Shiffer, A.; Dillon, M. R.; Cope, E. K.; Cooksley, C.; Ramezanpour, M.; Moraitis, S.; Ali, M. J.; Bleier, B., The international sinonasal microbiome study: A multicentre, multinational characterization of sinonasal bacterial ecology. *Allergy* **2020,** *75* (8), 2037-2049.
37. Abreu, N. A.; Nagalingam, N. A.; Song, Y.; Roediger, F. C.; Pletcher, S. D.; Goldberg, A. N.; Lynch, S. V., Sinus microbiome diversity depletion and Corynebacterium tuberculostearicum enrichment mediates rhinosinusitis. *Science translational medicine* **2012,** *4* (151), 151ra124-151ra124.
38. Bordin, A.; Sidjabat, H. E.; Cottrell, K.; Cervin, A., Chronic rhinosinusitis: a microbiome in dysbiosis and the search for alternative treatment options. *Microbiology Australia* **2016,** *37* (3), 149-152.

39. Hoggard, M.; Wagner Mackenzie, B.; Jain, R.; Taylor, M. W.; Biswas, K.; Douglas, R. G., Chronic rhinosinusitis and the evolving understanding of microbial ecology in chronic inflammatory mucosal disease. *Clinical microbiology reviews* **2017,** *30* (1), 321-348.
40. Aurora, R.; Chatterjee, D.; Hentzleman, J.; Prasad, G.; Sindwani, R.; Sanford, T., Contrasting the microbiomes from healthy volunteers and patients with chronic rhinosinusitis. *JAMA otolaryngology–head & neck surgery* **2013,** *139* (12), 1328-1338.
41. Choi, E. B.; Hong, S. W.; Kim, D. K.; Jeon, S.; Kim, K. R.; Cho, S. H.; Gho, Y.; Jee, Y. K.; Kim, Y. K., Decreased diversity of nasal microbiota and their secreted extracellular vesicles in patients with chronic rhinosinusitis based on a metagenomic analysis. *Allergy* **2014,** *69* (4), 517-526.
42. Biswas, K.; Hoggard, M.; Jain, R.; Taylor, M. W.; Douglas, R. G., The nasal microbiota in health and disease: variation within and between subjects. *Frontiers in microbiology* **2015,** *6*, 134.
43. Cleland, E. J.; Bassiouni, A.; Vreugde, S.; Wormald, P.-J., The bacterial microbiome in chronic rhinosinusitis: richness, diversity, postoperative changes, and patient outcomes. *American journal of rhinology & allergy* **2016,** *30* (1), 37-43.
44. Ramakrishnan, V. R.; Hauser, L. J.; Feazel, L. M.; Ir, D.; Robertson, C. E.; Frank, D. N., Sinus microbiota varies among chronic rhinosinusitis phenotypes and predicts surgical outcome. *Journal of Allergy and Clinical Immunology* **2015,** *136* (2), 334-342. e1.
45. Wagner Mackenzie, B.; Waite, D. W.; Hoggard, M.; Douglas, R. G.; Taylor, M. W.; Biswas, K., Bacterial community collapse: a meta-analysis of the sinonasal microbiota in chronic rhinosinusitis. *Environmental microbiology* **2017,** *19* (1), 381-392.
46. Cervin, A. U., The potential for topical probiotic treatment of chronic rhinosinusitis, a personal perspective. *Frontiers in cellular and infection microbiology* **2018,** *7*, 530.
47. Boase, S.; Foreman, A.; Cleland, E.; Tan, L.; Melton-Kreft, R.; Pant, H.; Hu, F. Z.; Ehrlich, G. D.; Wormald, P.-J., The microbiome of chronic rhinosinusitis: culture, molecular diagnostics and biofilm detection. *BMC infectious diseases* **2013,** *13* (1), 1-9.
48. Cleland, E. J.; Bassiouni, A.; Wormald, P. J. In *The bacteriology of chronic rhinosinusitis and the pre-eminence of Staphylococcus aureus in revision patients*, International forum of allergy & rhinology, Wiley Online Library: 2013; pp 642-646.
49. Nadel, D. M.; Lanza, D. C.; Kennedy, D. W., Endoscopically guided cultures in chronic sinusitis. *American journal of rhinology* **1998,** *12* (4), 233-242.
50. Bendouah, Z.; Barbeau, J.; Hamad, W. A.; Desrosiers, M., Biofilm formation by Staphylococcus aureus and Pseudomonas aeruginosa is associated with an unfavorable evolution after surgery for chronic sinusitis and nasal polyposis. *Otolaryngology—Head and Neck Surgery* **2006,** *134* (6), 991-996.
51. Jervis-Bardy, J.; Foreman, A.; Field, J.; Wormald, P. J., Impaired mucosal healing and infection associated with Staphylococcus aureus after endoscopic sinus surgery. *American journal of rhinology & allergy* **2009,** *23* (5), 549-552.
52. Bhattacharyya, N.; Gopal, H. V.; Lee, K. H., Bacterial infection after endoscopic sinus surgery: a controlled prospective study. *The Laryngoscope* **2004,** *114* (4), 765-767.
53. Bhattacharyya, N.; Kepnes, L. J., The microbiology of recurrent rhinosinusitis after endoscopic sinus surgery. *Archives of otolaryngology–head & neck surgery* **1999,** *125* (10), 1117-1120.
54. Singhal, D.; Foreman, A.; Bardy, J. J.; Wormald, P. J., Staphylococcus aureus biofilms: Nemesis of endoscopic sinus surgery. *The Laryngoscope* **2011,** *121* (7), 1578-1583.
55. Tan, N. C. W.; Foreman, A.; Jardeleza, C.; Douglas, R.; Vreugde, S.; Wormald, P. J. In *Intracellular Staphylococcus aureus: the Trojan horse of recalcitrant chronic rhinosinusitis?*, International forum of allergy & rhinology, Wiley Online Library: 2013; pp 261-266.
56. Jensen, P. Ø.; Givskov, M.; Bjarnsholt, T.; Moser, C., The immune system vs. Pseudomonas aeruginosa biofilms. *FEMS Immunology & Medical Microbiology* **2010,** *59* (3), 292-305.
57. Sanclement, J. A.; Webster, P.; Thomas, J.; Ramadan, H. H., Bacterial biofilms in surgical specimens of patients with chronic rhinosinusitis. *The Laryngoscope* **2005,** *115* (4), 578-582.
58. Costerton, J. W.; Stewart, P. S.; Greenberg, E. P., Bacterial biofilms: a common cause of persistent infections. *Science* **1999,** *284* (5418), 1318-1322.

59. Foreman, A.; Psaltis, A. J.; Tan, L. W.; Wormald, P.-J., Characterization of bacterial and fungal biofilms in chronic rhinosinusitis. *American journal of rhinology & allergy* **2009,** *23* (6), 556-561.
60. Tan, N. W.; Cooksley, C.; Roscioli, E.; Drilling, A.; Douglas, R.; Wormald, P. J.; Vreugde, S., Small-colony variants and phenotype switching of intracellular S taphylococcus aureus in chronic rhinosinusitis. *Allergy* **2014,** *69* (10), 1364-1371.
61. von Eiff, C.; Heilmann, C.; Proctor, R. A.; Woltz, C.; Peters, G.; Götz, F., A site-directed Staphylococcus aureus hemB mutant is a small-colony variant which persists intracellularly. *Journal of bacteriology* **1997,** *179* (15), 4706-4712.
62. Boase, S.; Valentine, R.; Singhal, D.; Tan, L. W.; Wormald, P. J. In *A sheep model to investigate the role of fungal biofilms in sinusitis: fungal and bacterial synergy*, International forum of allergy & rhinology, Wiley Online Library: 2011; pp 340-347.
63. Boase, S.; Jervis-Bardy, J.; Cleland, E.; Pant, H.; Tan, L.; Wormald, P. J. In *Bacterial-induced epithelial damage promotes fungal biofilm formation in a sheep model of sinusitis*, International forum of allergy & rhinology, Wiley Online Library: 2013; pp 341-348.
64. Ramsey, M. M.; Freire, M. O.; Gabrilska, R. A.; Rumbaugh, K. P.; Lemon, K. P., Staphylococcus aureus shifts toward commensalism in response to Corynebacterium species. *Frontiers in microbiology* **2016,** *7*, 1230.
65. Ricciardi, B. F.; Muthukrishnan, G.; Masters, E.; Ninomiya, M.; Lee, C. C.; Schwarz, E. M., Staphylococcus aureus evasion of host immunity in the setting of prosthetic joint infection: biofilm and beyond. *Current reviews in musculoskeletal medicine* **2018,** *11* (3), 389-400.
66. d'Hérelle, F., On an invisible microbe antagonistic toward dysenteric bacilli: brief note by Mr. F. D'Herelle, presented by Mr. Roux. 1917. *Research in microbiology* **2007,** *158* (7), 553-554.
67. Golkar, Z.; Bagasra, O.; Pace, D. G., Bacteriophage therapy: a potential solution for the antibiotic resistance crisis. *The Journal of Infection in Developing Countries* **2014,** *8* (02), 129-136.
68. Vilas Boas, D.; Almeida, C.; Sillankorva, S.; Nicolau, A.; Azeredo, J.; Azevedo, N. F., Discrimination of bacteriophage infected cells using locked nucleic acid fluorescent in situ hybridization (LNA-FISH). *Biofouling* **2016,** *32* (2), 179-190.
69. Fong, S. A.; Drilling, A.; Morales, S.; Cornet, M. E.; Woodworth, B. A.; Fokkens, W. J.; Psaltis, A. J.; Vreugde, S.; Wormald, P.-J., Activity of bacteriophages in removing biofilms of Pseudomonas aeruginosa isolates from chronic rhinosinusitis patients. *Frontiers in cellular and infection microbiology* **2017,** *7*, 418.
70. Uyttebroek, S.; Onsea, J.; Metsemakers, W.-J.; Dupont, L.; Devolder, D.; Wagemans, J.; Lavigne, R.; Spriet, I.; Van Gerven, L., The Potential Role of Bacteriophages in the Treatment of Recalcitrant Chronic Rhinosinusitis. *Antibiotics* **2021,** *10* (6), 675.
71. Drilling, A.; Morales, S.; Jardeleza, C.; Vreugde, S.; Speck, P.; Wormald, P.-J., Bacteriophage reduces biofilm of Staphylococcus aureus ex vivo isolates from chronic rhinosinusitis patients. *American journal of rhinology & allergy* **2014,** *28* (1), 3-11.
72. Drilling, A. J.; Cooksley, C.; Chan, C.; Wormald, P. J.; Vreugde, S. In *Fighting sinus-derived Staphylococcus aureus biofilms in vitro with a bacteriophage-derived muralytic enzyme*, International forum of allergy & rhinology, Wiley Online Library: 2016; pp 349-355.
73. Drilling, A. J.; Ooi, M. L.; Miljkovic, D.; James, C.; Speck, P.; Vreugde, S.; Clark, J.; Wormald, P.-J., Long-term safety of topical bacteriophage application to the frontal sinus region. *Frontiers in cellular and infection microbiology* **2017,** *7*, 49.
74. Bachert, C.; Holtappels, G.; Merabishvili, M.; Meyer, T.; Murr, A.; Zhang, N.; Van Crombruggen, K.; Gevaert, E.; Völker, U.; Bröker, B., Staphylococcus aureus controls interleukin-5 release in upper airway inflammation. *Journal of proteomics* **2018,** *180*, 53-60.
75. Zhang, G.; Zhao, Y.; Paramasivan, S.; Richter, K.; Morales, S.; Wormald, P. J.; Vreugde, S. In *Bacteriophage effectively kills multidrug resistant Staphylococcus aureus clinical isolates from chronic rhinosinusitis patients*, International forum of allergy & rhinology, Wiley Online Library: 2018; pp 406-414.

76. Szaleniec, J.; Gibała, A.; Pobiega, M.; Parasion, S.; Składzień, J.; Stręk, P.; Gosiewski, T.; Szaleniec, M., Exacerbations of chronic rhinosinusitis—microbiology and perspectives of phage therapy. *Antibiotics* **2019,** *8* (4), 175.
77. Ooi, M. L.; Drilling, A. J.; Morales, S.; Fong, S.; Moraitis, S.; Macias-Valle, L.; Vreugde, S.; Psaltis, A. J.; Wormald, P.-J., Safety and tolerability of bacteriophage therapy for chronic rhinosinusitis due to Staphylococcus aureus. *JAMA Otolaryngology–Head & Neck Surgery* **2019,** *145* (8), 723-729.
78. Fenton, M.; Casey, P. G.; Hill, C.; Gahan, C. G.; McAuliffe, O.; O'Mahony, J.; Maher, F.; Coffey, A., The truncated phage lysin CHAPk eliminates Staphylococcus aureus in the nares of mice. *Bioengineered bugs* **2010,** *1* (6), 404-407.
79. Drilling, A.; Morales, S.; Boase, S.; Jervis-Bardy, J.; James, C.; Jardeleza, C.; Tan, N. C. W.; Cleland, E.; Speck, P.; Vreugde, S. In *Safety and efficacy of topical bacteriophage and ethylenediaminetetraacetic acid treatment of Staphylococcus aureus infection in a sheep model of sinusitis*, International forum of allergy & rhinology, Wiley Online Library: 2014; pp 176-186.
80. Mills, E. A., Staphylococcus bacteriophage lysate aerosol therapy of sinusitis. *Laryngoscope* **1956,** *66*, 846–858.
81. Weber-Dąbrowska, B.; Mulczyk, M.; Górski, A., Bacteriophage therapy of bacterial infections: an update of our institute's experience. *Inflammation* **2001**, 201-209.
82. McCallin, S.; Sarker, S. A.; Sultana, S.; Oechslin, F.; Brüssow, H., Metagenome analysis of Russian and Georgian Pyophage cocktails and a placebo-controlled safety trial of single phage versus phage cocktail in healthy Staphylococcus aureus carriers. *Environmental microbiology* **2018,** *20* (9), 3278-3293.
83. Kryukov, A.; Gurov, A.; Izotova, G.; Lapenko, E., Results of the observational (non-interventional) research'Analysis of therapeutic efficiency of the polyvalent Piobacteriophag (Secstaphag) in the treatment of acute sinusitis'. *Vestnik otorinolaringologii* **2019,** *84* (5), 55-60.
84. Łusiak-Szelachowska, M.; Międzybrodzki, R.; Fortuna, W.; Borysowski, J.; Górski, A., Anti-phage serum antibody responses and the outcome of phage therapy. *Folia microbiologica* **2021,** *66* (1), 127-131.
85. Zajac, A. E.; Adams, A. S.; Turner, J. H. In *A systematic review and meta-analysis of probiotics for the treatment of allergic rhinitis*, International forum of allergy & rhinology, Wiley Online Library: 2015; pp 524-532.
86. Habermann, W.; Zimmermann, K.; Skarabis, H.; Kunze, R.; Rusch, V., Verminderung der Rezidivhäufigkeit bei Patienten mit chronisch rezidivierender hypertrophischer Sinusitis unter Behandlung mit einem bakteriellen Immunstimulans (Enterococcus faecalis-Bakterien humaner Herkunft). *Arzneimittelforschung* **2002,** *52* (08), 622-627.
87. Mukerji, S. S.; Pynnonen, M. A.; Kim, H. M.; Singer, A.; Tabor, M.; Terrell, J. E., Probiotics as adjunctive treatment for chronic rhinosinusitis: a randomized controlled trial. *Otolaryngology—Head and Neck Surgery* **2009,** *140* (2), 202-208.
88. Mårtensson, A.; Abolhalaj, M.; Lindstedt, M.; Mårtensson, A.; Olofsson, T. C.; Vásquez, A.; Greiff, L.; Cervin, A., Clinical efficacy of a topical lactic acid bacterial microbiome in chronic rhinosinusitis: a randomized controlled trial. *Laryngoscope investigative otolaryngology* **2017,** *2* (6), 410-416.
89. Niaz, K.; Maqbool, F.; Bahadar, H.; Abdollahi, M., Health benefits of manuka honey as an essential constituent for tissue regeneration. *Current drug metabolism* **2017,** *18* (10), 881-892.
90. Mavric, E.; Wittmann, S.; Barth, G.; Henle, T., Identification and quantification of methylglyoxal as the dominant antibacterial constituent of Manuka (Leptospermum scoparium) honeys from New Zealand. *Molecular nutrition & food research* **2008,** *52* (4), 483-489.
91. Kwakman, P. H.; Te Velde, A. A.; De Boer, L.; Vandenbroucke-Grauls, C. M.; Zaat, S. A., Two major medicinal honeys have different mechanisms of bactericidal activity. *PloS one* **2011,** *6* (3), e17709.
92. Kilty, S. J.; AlMutari, D.; Duval, M.; Groleau, M. A.; De Nanassy, J.; Gomes, M. M., Manuka honey: histological effect on respiratory mucosa. *American journal of rhinology & allergy* **2010,** *24* (2), e63-e66.
93. Jervis-Bardy, J.; Foreman, A.; Bray, S.; Tan, L.; Wormald, P. J., Methylglyoxal-infused honey mimics the anti-Staphylococcus aureus biofilm activity of manuka honey: potential implication in chronic rhinosinusitis. *The Laryngoscope* **2011,** *121* (5), 1104-1107.

94. Liu, M. Y.; Cokcetin, N. N.; Lu, J.; Turnbull, L.; Carter, D. A.; Whitchurch, C. B.; Harry, E. J., Rifampicin-manuka honey combinations are superior to other antibiotic-manuka honey combinations in eradicating Staphylococcus aureus biofilms. *Frontiers in microbiology* **2018,** *8*, 2653.
95. Molan, P. C., The evidence supporting the use of honey as a wound dressing. *The international journal of lower extremity wounds* **2006,** *5* (1), 40-54.
96. Orlandi, R. R.; Kingdom, T. T.; Hwang, P. H. In *International consensus statement on allergy and rhinology: rhinosinusitis executive summary*, International forum of allergy & rhinology, Wiley Online Library: 2016; pp S3-S21.
97. Alandejani, T.; Marsan, J.; Ferris, W.; Slinger, R.; Chan, F., Effectiveness of honey on Staphylococcus aureus and Pseudomonas aeruginosa biofilms. *Otolaryngology—Head and Neck Surgery* **2009,** *141* (1), 114-118.
98. Chang, E. H.; Alandejani, T.; Akbari, E.; Ostry, A.; Javer, A., Double-blinded, randomized, controlled trial of medicated versus nonmedicated merocel sponges for functional endoscopic sinus surgery. *J Otolaryngol Head Neck Surg* **2011,** *40* (Suppl 1), S14-S19.
99. Thamboo, A.; Thamboo, A.; Philpott, C.; Javer, A.; Clark, A.; Bent, J.; Kuhn, F.; Molan, P.; White, R.; Cooper, R., Single-blind study of manuka honey in allergic fungal rhinosinusitis. *Journal of Otolaryngology-Head and Neck Surgery* **2011,** *40* (3), 238.
100. Lee, V. S.; Humphreys, I. M.; Purcell, P. L.; Davis, G. E. In *Manuka honey sinus irrigation for the treatment of chronic rhinosinusitis: a randomized controlled trial*, International forum of allergy & rhinology, Wiley Online Library: 2017; pp 365-372.
101. Manji, J.; Thamboo, A.; Sunkaraneni, V.; Singh, A.; Tebbutt, S.; Garnis, C.; Javer, A., The association of Leptospermum honey with cytokine expression in the sinonasal epithelium of chronic rhinosinusitis patients. *World journal of otorhinolaryngology-head and neck surgery* **2019,** *5* (1), 19-25.
102. Numata, M.; Chu, H. W.; Dakhama, A.; Voelker, D. R., Pulmonary surfactant phosphatidylglycerol inhibits respiratory syncytial virus–induced inflammation and infection. *Proceedings of the National Academy of Sciences* **2010,** *107* (1), 320-325.
103. Rosen, P. L.; Palmer, J. N.; O'Malley Jr, B. W.; Cohen, N. A., Surfactants in the management of rhinopathologies. *American journal of rhinology & allergy* **2013,** *27* (3), 177-180.
104. Chiu, A. G.; Palmer, J. N.; Woodworth, B. A.; Doghramji, L.; Cohen, M. B.; Prince, A.; Cohen, N. A., Baby shampoo nasal irrigations for the symptomatic post-functional endoscopic sinus surgery patient. *American journal of rhinology* **2008,** *22* (1), 34-37.
105. Farag, A. A.; Deal, A. M.; McKinney, K. A.; Thorp, B. D.; Senior, B. A.; Ebert Jr, C. S.; Zanation, A. M. In *Single-blind randomized controlled trial of surfactant vs hypertonic saline irrigation following endoscopic endonasal surgery*, International forum of allergy & rhinology, Wiley Online Library: 2013; pp 276-280.
106. Isaacs, S.; Fakhri, S.; Luong, A.; Whited, C.; Citardi, M. J., The effect of dilute baby shampoo on nasal mucociliary clearance in healthy subjects. *American journal of rhinology & allergy* **2011,** *25* (1), e27-e29.
107. Turner, J. H.; Wu, J.; Dorminy, C. A.; Chandra, R. K. In *Safety and tolerability of surfactant nasal irrigation*, International forum of allergy & rhinology, Wiley Online Library: 2017; pp 809-812.
108. Johnson, E. E.; Wessling-Resnick, M., Iron metabolism and the innate immune response to infection. *Microbes and infection* **2012,** *14* (3), 207-216.
109. Weinberg, E. D., Iron availability and infection. *Biochimica et Biophysica Acta (BBA)-General Subjects* **2009,** *1790* (7), 600-605.
110. Stojiljkovic, I.; Kumar, V.; Srinivasan, N., Non-iron metalloporphyrins: potent antibacterial compounds that exploit haem/Hb uptake systems of pathogenic bacteria. *Molecular microbiology* **1999,** *31* (2), 429-442.
111. Richter, K.; Thomas, N.; Zhang, G.; Prestidge, C. A.; Coenye, T.; Wormald, P.-J.; Vreugde, S., Deferiprone and gallium-protoporphyrin have the capacity to potentiate the activity of antibiotics in Staphylococcus aureus small colony variants. *Frontiers in cellular and infection microbiology* **2017,** *7*, 280.

112. Ooi, M. L.; Richter, K.; Drilling, A. J.; Thomas, N.; Prestidge, C. A.; James, C.; Moratti, S.; Vreugde, S.; Psaltis, A. J.; Wormald, P.-J., Safety and efficacy of topical chitogel-deferiprone-gallium protoporphyrin in sheep model. *Frontiers in microbiology* **2018,** *9*, 917.
113. Usacheva, M. N.; Teichert, M. C.; Biel, M. A., Comparison of the methylene blue and toluidine blue photobactericidal efficacy against gram-positive and gram-negative microorganisms. *Lasers in Surgery and Medicine: The Official Journal of the American Society for Laser Medicine and Surgery* **2001,** *29* (2), 165-173.
114. Usacheva, M. N.; Teichert, M. C.; Sievert, C. E.; Biel, M. A., Effect of Ca+ on the photobactericidal efficacy of methylene blue and toluidine blue against gram-negative bacteria and the dye affinity for lipopolysaccharides. *Lasers in Surgery and Medicine: The Official Journal of the American Society for Laser Medicine and Surgery* **2006,** *38* (10), 946-954.
115. Wainwright, M.; Phoenix, D. A.; Nickson, P. B.; Morton, G., The use of new methylene blue in Pseudomonas aeruginosa biofilm destruction. **2002**.
116. Usacheva, M.; Teichert, M.; Usachev, Y.; Sievert, C.; Biel, M., Interaction of the photobactericides methylene blue and toluidine blue with a fluorophore in Pseudomonas aeruginosa cells. *Lasers in Surgery and Medicine: The Official Journal of the American Society for Laser Medicine and Surgery* **2008,** *40* (1), 55-61.
117. Usacheva, M. N.; Teichert, M. C.; Biel, M. A., The role of the methylene blue and toluidine blue monomers and dimers in the photoinactivation of bacteria. *Journal of Photochemistry and Photobiology B: Biology* **2003,** *71* (1-3), 87-98.
118. Jori, G.; Fabris, C.; Soncin, M.; Ferro, S.; Coppellotti, O.; Dei, D.; Fantetti, L.; Chiti, G.; Roncucci, G., Photodynamic therapy in the treatment of microbial infections: basic principles and perspective applications. *Lasers in Surgery and Medicine: The Official Journal of the American Society for Laser Medicine and Surgery* **2006,** *38* (5), 468-481.
119. Hamblin, M. R.; Hasan, T., Photodynamic therapy: a new antimicrobial approach to infectious disease? *Photochemical & Photobiological Sciences* **2004,** *3* (5), 436-450.
120. Wainwright, M.; Phoenix, D.; Laycock, S.; Wareing, D.; Wright, P., Photobactericidal activity of phenothiazinium dyes against methicillin-resistant strains of Staphylococcus aureus. *FEMS microbiology letters* **1998,** *160* (2), 177-181.
121. Biel, M. A.; Sievert, C.; Usacheva, M.; Teichert, M.; Balcom, J. In *Antimicrobial photodynamic therapy treatment of chronic recurrent sinusitis biofilms*, International forum of allergy & rhinology, Wiley Online Library: 2011; pp 329-334.
122. Biel, M. A.; Jones, J. W.; Pedigo, L.; Gibbs, A.; Loebel, N., The effect of antimicrobial photodynamic therapy on human ciliated respiratory mucosa. *The Laryngoscope* **2012,** *122* (12), 2628-2631.
123. Biel, M. A.; Pedigo, L.; Gibbs, A.; Loebel, N. In *Photodynamic therapy of antibiotic-resistant biofilms in a maxillary sinus model*, International forum of allergy & rhinology, Wiley Online Library: 2013; pp 468-473.
124. Bryce, E.; Wong, T.; Forrester, L.; Masri, B.; Jeske, D.; Barr, K.; Errico, S.; Roscoe, D., Nasal photodisinfection and chlorhexidine wipes decrease surgical site infections: a historical control study and propensity analysis. *Journal of Hospital Infection* **2014,** *88* (2), 89-95.
125. Myers, E. N.; Runer, T.; Cervin, A.; Lindberg, S.; Uddman, R., Nitric oxide is a regulator of mucociliary activity in the upper respiratory tract. *Otolaryngology—Head and Neck Surgery* **1998,** *119* (3), 278-287.
126. Lee, R. J.; Xiong, G.; Kofonow, J. M.; Chen, B.; Lysenko, A.; Jiang, P.; Abraham, V.; Doghramji, L.; Adappa, N. D.; Palmer, J. N., T2R38 taste receptor polymorphisms underlie susceptibility to upper respiratory infection. *The Journal of clinical investigation* **2012,** *122* (11), 4145-4159.
127. Bogdan, C., Nitric oxide and the immune response. *Nature immunology* **2001,** *2* (10), 907-916.
128. Lee, J. M.; McKnight, C. L.; Aves, T.; Yip, J.; Grewal, A. S.; Gupta, S. In *Nasal nitric oxide as a marker of sinus mucosal health in patients with nasal polyposis*, International forum of allergy & rhinology, Wiley Online Library: 2015; pp 894-899.

129. Colantonio, D.; Brouillette, L.; Parikh, A.; Scadding, G., Paradoxical low nasal nitric oxide in nasal polyposis. *Clinical & Experimental Allergy* **2002,** *32* (5), 698-701.
130. Arnal, J.; Flores, P.; Rami, J.; Murris-Espin, M.; Bremont, F.; Aguilla, I. P.; Serrano, E.; Didier, A., Nasal nitric oxide concentration in paranasal sinus inflammatory diseases. *European Respiratory Journal* **1999,** *13* (2), 307-312.
131. Ragab, S.; Lund, V.; Saleh, H.; Scadding, G., Nasal nitric oxide in objective evaluation of chronic rhinosinusitis therapy. *Allergy* **2006,** *61* (6), 717-724.
132. Lanz, M. J.; Prendes, S.; Peyrou, N.; Toledo, G.; Ferrer, C. M., Nasal nitric oxide as a noninvasive marker in the antibiotic treatment of acute bacterial sinusitis. *Journal of Allergy and Clinical Immunology* **2008,** *121* (2), 530.
133. Schlag, S.; Nerz, C.; Birkenstock, T. A.; Altenberend, F.; Götz, F., Inhibition of staphylococcal biofilm formation by nitrite. *Journal of bacteriology* **2007,** *189* (21), 7911-7919.
134. Jardeleza, C.; Foreman, A.; Baker, L.; Paramasivan, S.; Field, J.; Tan, L. W.; Wormald, P. J. In *The effects of nitric oxide on Staphylococcus aureus biofilm growth and its implications in chronic rhinosinusitis*, International forum of allergy & rhinology, Wiley Online Library: 2011; pp 438-444.
135. Jardeleza, C.; Rao, S.; Thierry, B.; Gajjar, P.; Vreugde, S.; Prestidge, C. A.; Wormald, P.-J., Liposome-encapsulated ISMN: a novel nitric oxide-based therapeutic agent against Staphylococcus aureus biofilms. *PloS one* **2014,** *9* (3), e92117.
136. Jardeleza, C.; Thierry, B.; Rao, S.; Rajiv, S.; Drilling, A.; Miljkovic, D.; Paramasivan, S.; James, C.; Dong, D.; Thomas, N., An in vivo safety and efficacy demonstration of a topical liposomal nitric oxide donor treatment for Staphylococcus aureus biofilm–associated rhinosinusitis. *Translational Research* **2015,** *166* (6), 683-692.
137. Abuzeid, W. M.; Girish, V. M.; Fastenberg, J. H.; Draganski, A. R.; Lee, A. Y.; Nosanchuk, J. D.; Friedman, J. M. In *Nitric oxide-releasing microparticles as a potent antimicrobial therapeutic against chronic rhinosinusitis bacterial isolates*, International forum of allergy & rhinology, Wiley Online Library: 2018; pp 1190-1198.
138. Miyake, M. M.; Bleier, B. S. In *Future topical medications in chronic rhinosinusitis*, International forum of allergy & rhinology, Wiley Online Library: 2019; pp S32-S46.
139. Zabner, J.; Seiler, M. P.; Launspach, J. L.; Karp, P. H.; Kearney, W. R.; Look, D. C.; Smith, J. J.; Welsh, M. J., The osmolyte xylitol reduces the salt concentration of airway surface liquid and may enhance bacterial killing. *Proceedings of the National Academy of Sciences* **2000,** *97* (21), 11614-11619.
140. Brown, C. L.; Graham, S. M.; Cable, B. B.; Ozer, E. A.; Taft, P. J.; Zabner, J., Xylitol enhances bacterial killing in the rabbit maxillary sinus. *The Laryngoscope* **2004,** *114* (11), 2021-2024.
141. Lin, L.; Tang, X.; Wei, J.; Dai, F.; Sun, G., Xylitol nasal irrigation in the treatment of chronic rhinosinusitis. *American journal of otolaryngology* **2017,** *38* (4), 383-389.
142. Huttenhower, C.; Gevers, D.; Knight, R.; Abubucker, S.; Badger, J. H.; Chinwalla, A. T.; Creasy, H. H.; Earl, A. M.; FitzGerald, M. G.; Fulton, R. S., Structure, function and diversity of the healthy human microbiome. *nature* **2012,** *486* (7402), 207.
143. Lee, R. J.; Kofonow, J. M.; Rosen, P. L.; Siebert, A. P.; Chen, B.; Doghramji, L.; Xiong, G.; Adappa, N. D.; Palmer, J. N.; Kennedy, D. W., Bitter and sweet taste receptors regulate human upper respiratory innate immunity. *The Journal of clinical investigation* **2014,** *124* (3), 1393-1405.
144. Lee, R. J.; Cohen, N. A., Role of the bitter taste receptor T2R38 in upper respiratory infection and chronic rhinosinusitis. *Current opinion in allergy and clinical immunology* **2015,** *15* (1), 14.
145. Maina, I. W.; Workman, A. D.; Cohen, N. A., The role of bitter and sweet taste receptors in upper airway innate immunity: recent advances and future directions. *World journal of otorhinolaryngology-head and neck surgery* **2018,** *4* (3), 200-208.
146. Banks, C.; Freeman, L.; Woodworth, B. A., Acquired cystic fibrosis transmembrane conductance regulator dysfunction. *World journal of otorhinolaryngology-head and neck surgery* **2018,** *4* (3), 193-199.
147. Accurso, F. J.; Rowe, S. M.; Clancy, J.; Boyle, M. P.; Dunitz, J. M.; Durie, P. R.; Sagel, S. D.; Hornick, D. B.; Konstan, M. W.; Donaldson, S. H., Effect of VX-770 in persons with cystic fibrosis and the G551D-CFTR mutation. *New England Journal of Medicine* **2010,** *363* (21), 1991-2003.

148. Dilokthornsakul, P.; Hansen, R. N.; Campbell, J. D., Forecasting US ivacaftor outcomes and cost in cystic fibrosis patients with the G551D mutation. *European Respiratory Journal* **2016,** *47* (6), 1697-1705.
149. Cho, D. Y.; Lim, D. J.; Mackey, C.; Weeks, C. G.; Garcia, J. A. P.; Skinner, D.; Zhang, S.; McCormick, J.; Woodworth, B. A. In *In-vitro evaluation of a ciprofloxacin-and ivacaftor-coated sinus stent against Pseudomonas aeruginosa biofilms*, International forum of allergy & rhinology, Wiley Online Library: 2019; pp 486-492.
150. Cho, D. Y.; Lim, D. J.; Mackey, C.; Weeks, C. G.; Peña Garcia, J. A.; Skinner, D.; Grayson, J. W.; Hill, H. S.; Alexander, D. K.; Zhang, S. In *l-methionine anti-biofilm activity against Pseudomonas aeruginosa is enhanced by the cystic fibrosis transmembrane conductance regulator potentiator, ivacaftor*, International forum of allergy & rhinology, Wiley Online Library: 2018; pp 577-583.
151. Cho, D. Y.; Skinner, D.; Zhang, S.; Fortenberry, J.; Sorscher, E. J.; Dean, N. R.; Woodworth, B. A. In *Cystic fibrosis transmembrane conductance regulator activation by the solvent ethanol: implications for topical drug delivery*, International forum of allergy & rhinology, Wiley Online Library: 2016; pp 178-184.
152. Cho, D. Y.; Zhang, S.; Lazrak, A.; Grayson, J. W.; Peña Garcia, J. A.; Skinner, D. F.; Lim, D. J.; Mackey, C.; Banks, C.; Matalon, S. In *Resveratrol and ivacaftor are additive G551D CFTR-channel potentiators: therapeutic implications for cystic fibrosis sinus disease*, International forum of allergy & rhinology, Wiley Online Library: 2019; pp 100-105.
153. Cho, D.-Y.; Lim, D. J.; Mackey, C.; Skinner, D.; Zhang, S.; McCormick, J.; Woodworth, B. A., Ivacaftor, a cystic fibrosis transmembrane conductance regulator potentiator, enhances ciprofloxacin activity against Pseudomonas aeruginosa. *American journal of rhinology & allergy* **2019,** *33* (2), 129-136.
154. Parikh, A.; Anand, U.; Ugwu, M. C.; Feridooni, T.; Massoud, E.; Agu, R. U., Drug-eluting nasal implants: formulation, characterization, clinical applications and challenges. *Pharmaceutics* **2014,** *6* (2), 249-267.
155. Cho, D. Y.; Hoffman, K.; Skinner, D.; Mackey, C.; Lim, D. J.; Alexander, G. C.; Bae, C. Y.; Han, D. K.; Jun, H. W.; Woodworth, B. A. In *Tolerance and pharmacokinetics of a ciprofloxacin-coated sinus stent in a preclinical model*, International forum of allergy & rhinology, Wiley Online Library: 2017; pp 352-358.
156. Cho, D. Y.; Lim, D. J.; Mackey, C.; Skinner, D.; Weeks, C.; Gill, G. S.; Hergenrother, R. W.; Swords, W. E.; Woodworth, B. A. In *Preclinical therapeutic efficacy of the ciprofloxacin-eluting sinus stent for Pseudomonas aeruginosa sinusitis*, International forum of allergy & rhinology, Wiley Online Library: 2018; pp 482-489.
157. Walker, A.; Philpott, C.; Hopkins, C., What is the most appropriate treatment for chronic rhinosinusitis? *Postgraduate medical journal* **2019,** *95* (1127), 493-496.
158. Orlandi, R. R.; Kingdom, T. T.; Hwang, P. H.; Smith, T. L.; Alt, J. A.; Baroody, F. M.; Batra, P. S.; Bernal-Sprekelsen, M.; Bhattacharyya, N.; Chandra, R. K. In *International consensus statement on allergy and rhinology: rhinosinusitis*, International forum of allergy & rhinology, Wiley Online Library: 2016; pp S22-S209.
159. Head, K.; Chong, L. Y.; Piromchai, P.; Hopkins, C.; Philpott, C.; Schilder, A. G.; Burton, M. J., Systemic and topical antibiotics for chronic rhinosinusitis. *Cochrane Database of Systematic Reviews* **2016,** (4).
160. Cervin, A.; Wallwork, B., Macrolide therapy of chronic rhinosinusitis. *Rhinology* **2007,** *45* (4), 259.
161. Kaplan, W.; Laing, R., *Priority medicines for Europe and the world*. World Health Organization Geneva: 2004.
162. Davies, S.; Gibbens, N., UK five year antimicrobial resistance strategy 2013 to 2018. *London: Department of Health* **2013**.
163. Jervis-Bardy, J.; Boase, S.; Psaltis, A.; Foreman, A.; Wormald, P. J., A randomized trial of mupirocin sinonasal rinses versus saline in surgically recalcitrant staphylococcal chronic rhinosinusitis. *The Laryngoscope* **2012,** *122* (10), 2148-2153.
164. Jervis-Bardy, J.; Wormald, P. J. In *Microbiological outcomes following mupirocin nasal washes for symptomatic, Staphylococcus aureus–positive chronic rhinosinusitis following endoscopic sinus surgery*, International forum of allergy & rhinology, Wiley Online Library: 2012; pp 111-115.

165. Antunes, M. B.; Feldman, M. D.; Cohen, N. A.; Chiu, A. G., Dose-dependent effects of topical tobramycin in an animal model of Pseudomonas sinusitis. *American journal of rhinology* **2007,** *21* (4), 423-427.
166. Carlton, D. A.; Beahm, D. D.; Chiu, A. G. In *Topical antibiotic therapy in chronic rhinosinusitis: an update*, International forum of allergy & rhinology, Wiley Online Library: 2019; pp S27-S31.
167. Mainz, J. G.; Schädlich, K.; Schien, C.; Michl, R.; Schelhorn-Neise, P.; Koitschev, A.; Koitschev, C.; Keller, P. M.; Riethmüller, J.; Wiedemann, B., Sinonasal inhalation of tobramycin vibrating aerosol in cystic fibrosis patients with upper airway Pseudomonas aeruginosa colonization: results of a randomized, double-blind, placebo-controlled pilot study. *Drug design, development and therapy* **2014,** *8*, 209.
168. Ezzat, W.; Fawaz, S.; Rabie, H.; Hamdy, T.; Shokry, Y., Effect of topical ofloxacin on bacterial biofilms in refractory post-sinus surgery rhino-sinusitis. *European Archives of Oto-Rhino-Laryngology* **2015,** *272* (9), 2355-2361.
169. Kim, J. S.; Kwon, S. H., Mupirocin in the treatment of staphylococcal infections in chronic rhinosinusitis: a meta-analysis. *PloS one* **2016,** *11* (12), e0167369.
170. Rudmik, L.; Soler, Z. M., Medical therapies for adult chronic sinusitis: a systematic review. *Jama* **2015,** *314* (9), 926-939.
171. Lee, V. S.; Davis, G. E., Culture-directed topical antibiotic treatment for chronic rhinosinusitis. *American journal of rhinology & allergy* **2016,** *30* (6), 414-417.
172. Carr, T. F.; Hill, J. L.; Chiu, A.; Chang, E. H., Alteration in bacterial culture after treatment with topical mupirocin for recalcitrant chronic rhinosinusitis. *JAMA Otolaryngology–Head & Neck Surgery* **2016,** *142* (2), 138-142.
173. Xaubet, A.; Mullol, J.; Lopez, E.; Roca-Ferrer, J.; Rozman, M.; CARRIÖN, T.; Fabra, J.; Picado, C., Comparison of the role of nasal polyp and normal nasal mucosal epithelial cells on in vitro eosinophil survival. Mediation by GM–CSF and inhibition by dexamethasone. *Clinical & Experimental Allergy* **1994,** *24* (4), 307-317.
174. Mullol, J.; Xaubet, A.; Lopez, E.; Roca-Ferrer, J.; Picado, C., Comparative study of the effects of different glucocorticosteroids on eosinophil survival primed by cultured epithelial cell supernatants obtained from nasal mucosa and nasal polyps. *Thorax* **1995,** *50* (3), 270-274.
175. Mullol, J.; Lopez, E.; Roca-Ferrer, J.; Xaubet, A.; Pujols, L.; Fernandez-Morata, J.; Fabra, J.; Picado, C., Effects of topical anti-inflammatory drugs on eosinophil survival primed by epithelial cells. Additive effect of glucocorticoids and nedocromil sodium. *Clinical & Experimental Allergy* **1997,** *27* (12), 1432-1441.
176. Mullou, J.; Xaubet, A.; Gaya, A.; Roca-Ferrer, J.; Lopez, E.; Fernandez, J.; Fernandez, M.; Picado, C., Cytokine gene expression and release from epithelial cells. A comparison study between healthy nasal mucosa and nasal polyps. *Clinical & Experimental Allergy* **1995,** *25* (7), 607-615.
177. Xaubet, A.; Mullol, J.; Roca-Ferrer, J.; Pujols, L.; Fuentes, M.; Perez, M.; Fabra, J.; Picado, C., Effect of budesonide and nedocromil sodium on IL-6 and IL-8 release from human nasal mucosa and polyp epithelial cells. *Respiratory medicine* **2001,** *95* (5), 408-414.
178. Lal, D.; Hwang, P. H. In *Oral corticosteroid therapy in chronic rhinosinusitis without polyposis: a systematic review*, International forum of allergy & rhinology, Wiley Online Library: 2011; pp 136-143.
179. Head, K.; Chong, L. Y.; Hopkins, C.; Philpott, C.; Schilder, A. G.; Burton, M. J., Short-course oral steroids as an adjunct therapy for chronic rhinosinusitis. *Cochrane Database of Systematic Reviews* **2016,** (4).
180. Arya, S. S.; Sharma, M. M.; Das, R. K.; Rookes, J.; Cahill, D.; Lenka, S. K., Vanillin mediated green synthesis and application of gold nanoparticles for reversal of antimicrobial resistance in Pseudomonas aeruginosa clinical isolates. *Heliyon* **2019,** *5* (7), e02021.
181. Schexnailder, P.; Schmidt, G., Nanocomposite polymer hydrogels. *Colloid and Polymer Science* **2009,** *287* (1), 1-11.
182. Valodkar, M.; Modi, S.; Pal, A.; Thakore, S., Synthesis and anti-bacterial activity of Cu, Ag and Cu–Ag alloy nanoparticles: a green approach. *Materials Research Bulletin* **2011,** *46* (3), 384-389.

183. Albanese, A.; Tang, P. S.; Chan, W. C., The effect of nanoparticle size, shape, and surface chemistry on biological systems. *Annual review of biomedical engineering* **2012,** *14*, 1-16.
184. Jeevanandam, J.; Barhoum, A.; Chan, Y. S.; Dufresne, A.; Danquah, M. K., Review on nanoparticles and nanostructured materials: history, sources, toxicity and regulations. *Beilstein journal of nanotechnology* **2018,** *9* (1), 1050-1074.
185. Karthick, V.; Ganesh Kumar, V.; Maiyalagan, T.; Deepa, R.; Govindaraju, K.; Rajeswari, A.; Stalin Dhas, T., Green synthesis of well dispersed nanoparticles using leaf extract of medicinally useful Adhatoda vasica nees. *Micro and Nanosystems* **2012,** *4* (3), 192-198.
186. Cookson, J., The preparation of palladium nanoparticles. *Platinum Metals Review* **2012,** *56* (2), 83-98.
187. Haider, A.; Kang, I.-K., Preparation of silver nanoparticles and their industrial and biomedical applications: a comprehensive review. *Advances in materials science and engineering* **2015,** *2015*.
188. Abbasi, E.; Milani, M.; Fekri Aval, S.; Kouhi, M.; Akbarzadeh, A.; Tayefi Nasrabadi, H.; Nikasa, P.; Joo, S. W.; Hanifehpour, Y.; Nejati-Koshki, K., Silver nanoparticles: synthesis methods, bio-applications and properties. *Critical reviews in microbiology* **2016,** *42* (2), 173-180.
189. Mittal, A. K.; Chisti, Y.; Banerjee, U. C., Synthesis of metallic nanoparticles using plant extracts. *Biotechnology advances* **2013,** *31* (2), 346-356.
190. Dhas, T. S.; Kumar, V. G.; Karthick, V.; Angel, K. J.; Govindaraju, K., Facile synthesis of silver chloride nanoparticles using marine alga and its antibacterial efficacy. *Spectrochimica Acta Part A: Molecular and Biomolecular Spectroscopy* **2014,** *120*, 416-420.
191. Rai, M.; Yadav, A.; Gade, A., Silver nanoparticles as a new generation of antimicrobials. *Biotechnology advances* **2009,** *27* (1), 76-83.
192. Atiyeh, B. S.; Costagliola, M.; Hayek, S. N.; Dibo, S. A., Effect of silver on burn wound infection control and healing: review of the literature. *burns* **2007,** *33* (2), 139-148.
193. Chernousova, S.; Epple, M., Silver as antibacterial agent: ion, nanoparticle, and metal. *Angewandte Chemie International Edition* **2013,** *52* (6), 1636-1653.
194. Edwards-Jones, V., The benefits of silver in hygiene, personal care and healthcare. *Letters in applied microbiology* **2009,** *49* (2), 147-152.
195. Chung, I. S.; Lee, M. Y.; Shin, D. H.; Jung, H. R., Three systemic argyria cases after ingestion of colloidal silver solution. *International journal of dermatology* **2010,** *49* (10), 1175-1177.
196. Schrauben, S. J.; Bhanusali, D. G.; Sheets, S.; Sinha, A. A., CUTIS Do Not Copy. *Cutis* **2012,** *89*, 221-224.
197. Foreman, A.; Wormald, P. J., Different biofilms, different disease? A clinical outcomes study. *The Laryngoscope* **2010,** *120* (8), 1701-1706.
198. Richter, K.; Facal, P.; Thomas, N.; Vandecandelaere, I.; Ramezanpour, M.; Cooksley, C.; Prestidge, C. A.; Coenye, T.; Wormald, P.-J.; Vreugde, S., Taking the silver bullet colloidal silver particles for the topical treatment of biofilm-related infections. *ACS applied materials & interfaces* **2017,** *9* (26), 21631-21638.
199. Zhang, X.-F.; Liu, Z.-G.; Shen, W.; Gurunathan, S., Silver nanoparticles: synthesis, characterization, properties, applications, and therapeutic approaches. *International journal of molecular sciences* **2016,** *17* (9), 1534.
200. Balazs, D.; Triandafillu, K.; Wood, P.; Chevolot, Y.; Van Delden, C.; Harms, H.; Hollenstein, C.; Mathieu, H., Inhibition of bacterial adhesion on PVC endotracheal tubes by RF-oxygen glow discharge, sodium hydroxide and silver nitrate treatments. *Biomaterials* **2004,** *25* (11), 2139-2151.
201. Goggin, R.; Jardeleza, C.; Wormald, P. J.; Vreugde, S. In *Colloidal silver: a novel treatment for Staphylococcus aureus biofilms?*, International forum of allergy & rhinology, Wiley Online Library: 2014; pp 171-175.
202. Feng, Q. L.; Wu, J.; Chen, G. Q.; Cui, F.; Kim, T.; Kim, J., A mechanistic study of the antibacterial effect of silver ions on Escherichia coli and Staphylococcus aureus. *Journal of biomedical materials research* **2000,** *52* (4), 662-668.

203. Rajiv, S.; Drilling, A.; Bassiouni, A.; James, C.; Vreugde, S.; Wormald, P. J. In *Topical colloidal silver as an anti-biofilm agent in a Staphylococcus aureus chronic rhinosinusitis sheep model*, International Forum of Allergy & Rhinology, Wiley Online Library: 2015; pp 283-288.
204. Ooi, M. L.; Richter, K.; Bennett, C.; Macias-Valle, L.; Vreugde, S.; Psaltis, A. J.; Wormald, P.-J., Topical colloidal silver for the treatment of recalcitrant chronic rhinosinusitis. *Frontiers in microbiology* **2018,** *9*, 720.
205. Scott, J. R.; Krishnan, R.; Rotenberg, B. W.; Sowerby, L. J., The effectiveness of topical colloidal silver in recalcitrant chronic rhinosinusitis: a randomized crossover control trial. *Journal of Otolaryngology-Head & Neck Surgery* **2017,** *46* (1), 64.
206. Salomoni, R.; Léo, P.; Montemor, A.; Rinaldi, B.; Rodrigues, M., Antibacterial effect of silver nanoparticles in Pseudomonas aeruginosa. *Nanotechnology, science and applications* **2017,** *10*, 115.
207. Bresee, J.; Bond, C. M.; Worthington, R. J.; Smith, C. A.; Gifford, J. C.; Simpson, C. A.; Carter, C. J.; Wang, G.; Hartman, J.; Osbaugh, N. A., Nanoscale structure–activity relationships, mode of action, and biocompatibility of gold nanoparticle antibiotics. *Journal of the American Chemical Society* **2014,** *136* (14), 5295-5300.
208. Fan, W.; Yung, B.; Huang, P.; Chen, X., Nanotechnology for multimodal synergistic cancer therapy. *Chemical reviews* **2017,** *117* (22), 13566-13638.
209. Brigger, I.; Dubernet, C.; Couvreur, P., Nanoparticles in cancer therapy and diagnosis. *Advanced drug delivery reviews* **2012,** *64*, 24-36.
210. Supraja, N.; Prasad, T.; Soundariya, M.; Babujanarthanam, R., Synthesis, characterization and dose dependent antimicrobial and anti-cancerous activity of phycogenic silver nanoparticles against human hepatic carcinoma (HepG2) cell line. *AIMS Bioeng* **2016,** *3* (4), 425-440.
211. Baptista, P. V.; McCusker, M. P.; Carvalho, A.; Ferreira, D. A.; Mohan, N. M.; Martins, M.; Fernandes, A. R., Nano-strategies to fight multidrug resistant bacteria—"A Battle of the Titans". *Frontiers in microbiology* **2018,** *9*, 1441.
212. Hajipour, M. J.; Fromm, K. M.; Ashkarran, A. A.; de Aberasturi, D. J.; de Larramendi, I. R.; Rojo, T.; Serpooshan, V.; Parak, W. J.; Mahmoudi, M., Antibacterial properties of nanoparticles. *Trends in biotechnology* **2012,** *30* (10), 499-511.
213. Sre, P. R.; Reka, M.; Poovazhagi, R.; Kumar, M. A.; Murugesan, K., Antibacterial and cytotoxic effect of biologically synthesized silver nanoparticles using aqueous root extract of Erythrina indica lam. *Spectrochimica Acta Part A: Molecular and Biomolecular Spectroscopy* **2015,** *135*, 1137-1144.
214. Braithwaite, M. C.; Tyagi, C.; Tomar, L. K.; Kumar, P.; Choonara, Y. E.; Pillay, V., Nutraceutical-based therapeutics and formulation strategies augmenting their efficiency to complement modern medicine: An overview. *Journal of Functional Foods* **2014,** *6*, 82-99.
215. Bose, D.; Chatterjee, S., Biogenic synthesis of silver nanoparticles using guava (Psidium guajava) leaf extract and its antibacterial activity against Pseudomonas aeruginosa. *Applied Nanoscience* **2016,** *6* (6), 895-901.
216. Nagajyothi, P.; Lee, K., Synthesis of plant-mediated silver nanoparticles using Dioscorea batatas rhizome extract and evaluation of their antimicrobial activities. *Journal of nanomaterials* **2011,** *2011*.
217. Silvero C, M. J. n.; Rocca, D. M.; de la Villarmois, E. A.; Fournier, K.; Lanterna, A. E.; Perez, M. F.; Becerra, M. C.; Scaiano, J. C., Selective photoinduced antibacterial activity of amoxicillin-coated gold nanoparticles: from one-step synthesis to in vivo cytocompatibility. *ACS omega* **2018,** *3* (1), 1220-1230.
218. Dakal, T. C.; Kumar, A.; Majumdar, R. S.; Yadav, V., Mechanistic basis of antimicrobial actions of silver nanoparticles. *Frontiers in microbiology* **2016,** *7*, 1831.
219. Abbaszadegan, A.; Ghahramani, Y.; Gholami, A.; Hemmateenejad, B.; Dorostkar, S.; Nabavizadeh, M.; Sharghi, H., The effect of charge at the surface of silver nanoparticles on antimicrobial activity against gram-positive and gram-negative bacteria: a preliminary study. *Journal of Nanomaterials* **2015,** *2015*.
220. Nalwade, A. R.; Jadhav, A., Biosynthesis of silver nanoparticles using leaf extract of Daturaalba Nees. and evaluation of their antibacterial activity. *Arch. Appl. Sci. Res* **2013,** *5*, 45-49.

221. Raffi, M.; Hussain, F.; Bhatti, T.; Akhter, J.; Hameed, A.; Hasan, M., Antibacterial characterization of silver nanoparticles against E. coli ATCC-15224. *Journal of materials science and technology* **2008,** *24* (2), 192-196.
222. Sondi, I.; Salopek-Sondi, B., Silver nanoparticles as antimicrobial agent: a case study on E. coli as a model for Gram-negative bacteria. *Journal of colloid and interface science* **2004,** *275* (1), 177-182.
223. Ghosh, S.; Patil, S.; Ahire, M.; Kitture, R.; Kale, S.; Pardesi, K.; Cameotra, S. S.; Bellare, J.; Dhavale, D. D.; Jabgunde, A., Synthesis of silver nanoparticles using Dioscorea bulbifera tuber extract and evaluation of its synergistic potential in combination with antimicrobial agents. *International journal of nanomedicine* **2012,** *7*, 483.
224. Schreurs, W.; Rosenberg, H., Effect of silver ions on transport and retention of phosphate by Escherichia coli. *Journal of bacteriology* **1982,** *152* (1), 7-13.
225. Kim, S.-H.; Lee, H.-S.; Ryu, D.-S.; Choi, S.-J.; Lee, D.-S., Antibacterial activity of silver-nanoparticles against Staphylococcus aureus and Escherichia coli. *Microbiology and Biotechnology Letters* **2011,** *39* (1), 77-85.
226. Rai, M.; Deshmukh, S.; Ingle, A.; Gade, A., Silver nanoparticles: the powerful nanoweapon against multidrug-resistant bacteria. *Journal of applied microbiology* **2012,** *112* (5), 841-852.
227. Pal, S., YK Tak JM Song 2007 Does the antibacterial activity of silver nanoparticles depend on the shape of the nanoparticle? A study of the Gram-negative bacterium Escherichia coli Appl. *Environ. Microbiol*, 1712-1720.
228. Habash, M. B.; Park, A. J.; Vis, E. C.; Harris, R. J.; Khursigara, C. M., Synergy of silver nanoparticles and aztreonam against Pseudomonas aeruginosa PAO1 biofilms. *Antimicrobial agents and chemotherapy* **2014,** *58* (10), 5818-5830.
229. Singh, B. R.; Singh, B. N.; Singh, A.; Khan, W.; Naqvi, A. H.; Singh, H. B., Mycofabricated biosilver nanoparticles interrupt Pseudomonas aeruginosa quorum sensing systems. *Scientific reports* **2015,** *5* (1), 1-14.
230. Li, X.-Z.; Nikaido, H.; Williams, K. E., Silver-resistant mutants of Escherichia coli display active efflux of Ag+ and are deficient in porins. *Journal of bacteriology* **1997,** *179* (19), 6127-6132.
231. Morones, J. R.; Elechiguerra, J. L.; Camacho, A.; Holt, K.; Kouri, J. B.; Ramírez, J. T.; Yacaman, M. J., The bactericidal effect of silver nanoparticles. *Nanotechnology* **2005,** *16* (10), 2346.
232. Jung, W. K.; Koo, H. C.; Kim, K. W.; Shin, S.; Kim, S. H.; Park, Y. H., Antibacterial activity and mechanism of action of the silver ion in Staphylococcus aureus and Escherichia coli. *Applied and environmental microbiology* **2008,** *74* (7), 2171-2178.
233. Klueh, U.; Wagner, V.; Kelly, S.; Johnson, A.; Bryers, J., Efficacy of silver-coated fabric to prevent bacterial colonization and subsequent device-based biofilm formation. *Journal of Biomedical Materials Research: An Official Journal of The Society for Biomaterials, The Japanese Society for Biomaterials, and The Australian Society for Biomaterials and the Korean Society for Biomaterials* **2000,** *53* (6), 621-631.
234. Lok, C.-N.; Ho, C.-M.; Chen, R.; He, Q.-Y.; Yu, W.-Y.; Sun, H.; Tam, P. K.-H.; Chiu, J.-F.; Che, C.-M., Proteomic analysis of the mode of antibacterial action of silver nanoparticles. *Journal of proteome research* **2006,** *5* (4), 916-924.
235. Steuber, J.; Krebs, W.; Dimroth, P., The Na+-translocating NADH: ubiquinone oxidoreductase from Vibrio alginolyticus: redox states of the FAD prosthetic group and mechanism of Ag+ inhibition. *European journal of biochemistry* **1997,** *249* (3), 770-776.
236. Bhattacharya, R.; Mukherjee, P., Biological properties of "naked" metal nanoparticles. *Advanced drug delivery reviews* **2008,** *60* (11), 1289-1306.
237. Hsueh, Y.-H.; Lin, K.-S.; Ke, W.-J.; Hsieh, C.-T.; Chiang, C.-L.; Tzou, D.-Y.; Liu, S.-T., The antimicrobial properties of silver nanoparticles in Bacillus subtilis are mediated by released Ag+ ions. *PloS one* **2015,** *10* (12), e0144306.
238. Kumar, N.; Das, S.; Jyoti, A.; Kaushik, S., Synergistic effect of silver nanoparticles with doxycycline against Klebsiella pneumoniae. *Int J Pharm Pharm Sci* **2016,** *8* (7), 183-186.

239. Radzig, M.; Nadtochenko, V.; Koksharova, O.; Kiwi, J.; Lipasova, V.; Khmel, I., Antibacterial effects of silver nanoparticles on gram-negative bacteria: influence on the growth and biofilms formation, mechanisms of action. *Colloids and Surfaces B: Biointerfaces* **2013,** *102*, 300-306.
240. Monteiro, D. R.; Gorup, L. F.; Takamiya, A. S.; de Camargo, E. R.; Filho, A. C. R.; Barbosa, D. B., Silver distribution and release from an antimicrobial denture base resin containing silver colloidal nanoparticles. *Journal of Prosthodontics: Implant, Esthetic and Reconstructive Dentistry* **2012,** *21* (1), 7-15.
241. Kim, J.-Y.; Kim, S.-E.; Kim, J.-E.; Lee, J.-C.; Yoon, J.-Y., The biocidal activity of nano-sized silver particles comparing with silver ion. *Journal of Korean Society of Environmental Engineers* **2005,** *27* (7), 771-776.
242. Kim, J. S.; Kuk, E.; Yu, K. N.; Kim, J.-H.; Park, S. J.; Lee, H. J.; Kim, S. H.; Park, Y. K.; Park, Y. H.; Hwang, C.-Y., Antimicrobial effects of silver nanoparticles. *Nanomedicine: Nanotechnology, biology and medicine* **2007,** *3* (1), 95-101.
243. Pellieux, C.; Dewilde, A.; Pierlot, C.; Aubry, J.-M., Bactericidal and virucidal activities of singlet oxygen generated by thermolysis of naphthalene endoperoxides. *Methods in enzymology* **2000,** *319*, 197-207.
244. Wu, D.; Fan, W.; Kishen, A.; Gutmann, J. L.; Fan, B., Evaluation of the antibacterial efficacy of silver nanoparticles against Enterococcus faecalis biofilm. *Journal of endodontics* **2014,** *40* (2), 285-290.
245. Friedman, A., Nanotechnology and the diagnosis of dermatological infectious disease. *Journal of drugs in dermatology: JDD* **2012,** *11* (7), 846-851.
246. Belluco, S.; Losasso, C.; Patuzzi, I.; Rigo, L.; Conficoni, D.; Gallocchio, F.; Cibin, V.; Catellani, P.; Segato, S.; Ricci, A., Silver as antibacterial toward Listeria monocytogenes. *Frontiers in microbiology* **2016,** *7*, 307.
247. Howden, P. J.; Faux, S. P., Fibre-induced lipid peroxidation leads to DNA adduct formation in Salmonella typhimurium TA104 and rat lung fibroblasts. *Carcinogenesis* **1996,** *17* (3), 413-419.
248. Huang, C.-C.; Aronstam, R. S.; Chen, D.-R.; Huang, Y.-W., Oxidative stress, calcium homeostasis, and altered gene expression in human lung epithelial cells exposed to ZnO nanoparticles. *Toxicology in vitro* **2010,** *24* (1), 45-55.
249. Deutscher, J.; Saier Jr, M. H., Ser/Thr/Tyr protein phosphorylation in bacteria–for long time neglected, now well established. *Journal of molecular microbiology and biotechnology* **2005,** *9* (3-4), 125-131.
250. Kirstein, J.; Turgay, K., A new tyrosine phosphorylation mechanism involved in signal transduction in Bacillus subtilis. *Journal of molecular microbiology and biotechnology* **2005,** *9* (3-4), 182-188.
251. Mijakovic, I.; Petranovic, D.; Bottini, N.; Deutscher, J.; Jensen, P. R., Protein-tyrosine phosphorylation in Bacillus subtilis. *Journal of molecular microbiology and biotechnology* **2005,** *9* (3-4), 189-197.
252. Mijakovic, I.; Petranovic, D.; Macek, B.; Cepo, T.; Mann, M.; Davies, J.; Jensen, P. R.; Vujaklija, D., Bacterial single-stranded DNA-binding proteins are phosphorylated on tyrosine. *Nucleic acids research* **2006,** *34* (5), 1588-1596.
253. Mijakovic, I.; Poncet, S.; Boël, G.; Mazé, A.; Gillet, S.; Jamet, E.; Decottignies, P.; Grangeasse, C.; Doublet, P.; Le Maréchal, P., Transmembrane modulator-dependent bacterial tyrosine kinase activates UDP-glucose dehydrogenases. *The EMBO Journal* **2003,** *22* (18), 4709-4718.
254. Iniesta, A. A.; McGrath, P. T.; Reisenauer, A.; McAdams, H. H.; Shapiro, L., A phospho-signaling pathway controls the localization and activity of a protease complex critical for bacterial cell cycle progression. *Proceedings of the National Academy of Sciences* **2006,** *103* (29), 10935-10940.
255. Grangeasse, C.; Obadia, B.; Mijakovic, I.; Deutscher, J.; Cozzone, A. J.; Doublet, P., Autophosphorylation of the Escherichia coli protein kinase Wzc regulates tyrosine phosphorylation of Ugd, a UDP-glucose dehydrogenase. *Journal of Biological Chemistry* **2003,** *278* (41), 39323-39329.
256. Shrivastava, S., Nanomedicine: physiological principle of distribution. *Dig. J. Nanomater. Bios* **2008,** *3*, 303-308.

257. Shrivastava, S.; Bera, T.; Roy, A.; Singh, G.; Ramachandrarao, P.; Dash, D., Characterization of enhanced antibacterial effects of novel silver nanoparticles. *Nanotechnology* **2007,** *18* (22), 225103.
258. Costerton, J. W.; Geesey, G. G.; Cheng, K.-J., How bacteria stick. *Scientific American* **1978,** *238* (1), 86-95.
259. Coenye, T., Response of sessile cells to stress: from changes in gene expression to phenotypic adaptation. *FEMS Immunology & Medical Microbiology* **2010,** *59* (3), 239-252.
260. Davies, D., Understanding biofilm resistance to antibacterial agents. *Nature reviews Drug discovery* **2003,** *2* (2), 114-122.
261. Sahu, S. C.; Zheng, J.; Graham, L.; Chen, L.; Ihrie, J.; Yourick, J. J.; Sprando, R. L., Comparative cytotoxicity of nanosilver in human liver HepG2 and colon Caco2 cells in culture. *Journal of Applied Toxicology* **2014,** *34* (11), 1155-1166.
262. Gurunathan, S.; Park, J. H.; Han, J. W.; Kim, J.-H., Comparative assessment of the apoptotic potential of silver nanoparticles synthesized by Bacillus tequilensis and Calocybe indica in MDA-MB-231 human breast cancer cells: targeting p53 for anticancer therapy. *International journal of nanomedicine* **2015,** *10*, 4203.
263. He, D.; Dorantes-Aranda, J. J.; Waite, T. D., Silver Nanoparticle・Algae Interactions: Oxidative Dissolution, Reactive Oxygen Species Generation and Synergistic Toxic Effects. *Environmental science & technology* **2012,** *46* (16), 8731-8738.
264. Miethling-Graff, R.; Rumpker, R.; Richter, M.; Verano-Braga, T.; Kjeldsen, F.; Brewer, J.; Hoyland, J.; Rubahn, H.-G.; Erdmann, H., Exposure to silver nanoparticles induces size-and dose-dependent oxidative stress and cytotoxicity in human colon carcinoma cells. *Toxicology in vitro* **2014,** *28* (7), 1280-1289.
265. De Gusseme, B.; Hennebel, T.; Christiaens, E.; Saveyn, H.; Verbeken, K.; Fitts, J. P.; Boon, N.; Verstraete, W., Virus disinfection in water by biogenic silver immobilized in polyvinylidene fluoride membranes. *Water research* **2011,** *45* (4), 1856-1864.
266. AshaRani, P.; Low Kah Mun, G.; Hande, M. P.; Valiyaveettil, S., Cytotoxicity and genotoxicity of silver nanoparticles in human cells. *ACS nano* **2009,** *3* (2), 279-290.
267. Li, Y.; Guo, M.; Lin, Z.; Zhao, M.; Xiao, M.; Wang, C.; Xu, T.; Chen, T.; Zhu, B., Polyethylenimine-functionalized silver nanoparticle-based co-delivery of paclitaxel to induce HepG2 cell apoptosis. *International journal of nanomedicine* **2016,** *11*, 6693.
268. Li, P.; Nijhawan, D.; Budihardjo, I.; Srinivasula, S. M.; Ahmad, M.; Alnemri, E. S.; Wang, X., Cytochrome c and dATP-dependent formation of Apaf-1/caspase-9 complex initiates an apoptotic protease cascade. *cell* **1997,** *91* (4), 479-489.
269. Chen, S.-Y.; Huang, M.-T.; Pender, S. L.; Ruslin, M.; Chou, H.-H.; Ou, K.-L., The application of silver nano-particles on developing potential treatment for chronic rhinosinusitis: Antibacterial action and cytotoxicity effect on human nasal epithelial cell model. *Materials Science and Engineering: C* **2017,** *80*, 624-630.
270. Psaltis, A. J.; Ha, K. R.; Beule, A. G.; Tan, L. W.; Wormald, P. J., Confocal scanning laser microscopy evidence of biofilms in patients with chronic rhinosinusitis. *The Laryngoscope* **2007,** *117* (7), 1302-1306.
271. Chen, H.-H.; Liu, X.; Ni, C.; Lu, Y.-P.; Xiong, G.-Y.; Lu, Y.-Y.; Wang, S.-Q., Bacterial biofilms in chronic rhinosinusitis and their relationship with inflammation severity. *Auris Nasus Larynx* **2012,** *39* (2), 169-174.
272. Stoodley, P.; DeBeer, D.; Lewandowski, Z., Liquid flow in biofilm systems. *Appl. Environ. Microbiol.* **1994,** *60* (8), 2711-2716.
273. Donlan, R. M.; Costerton, J. W., Biofilms: survival mechanisms of clinically relevant microorganisms. *Clinical microbiology reviews* **2002,** *15* (2), 167-193.
274. Foreman, A.; Jervis-Bardy, J.; Wormald, P. J., Do biofilms contribute to the initiation and recalcitrance of chronic rhinosinusitis? *The Laryngoscope* **2011,** *121* (5), 1085-1091.
275. Fastenberg, J. H.; Hsueh, W. D.; Mustafa, A.; Akbar, N. A.; Abuzeid, W. M., Biofilms in chronic rhinosinusitis: pathophysiology and therapeutic strategies. *World journal of otorhinolaryngology-head and neck surgery* **2016,** *2* (4), 219-229.

276. Fulaz, S.; Vitale, S.; Quinn, L.; Casey, E., Nanoparticle–biofilm interactions: the role of the EPS matrix. *Trends in microbiology* **2019,** *27* (11), 915-926.
277. Davies, D. G.; Parsek, M. R.; Pearson, J. P.; Iglewski, B. H.; Costerton, J. W.; Greenberg, E. P., The involvement of cell-to-cell signals in the development of a bacterial biofilm. *Science* **1998,** *280* (5361), 295-298.
278. Parsek, M. R.; Greenberg, E., Sociomicrobiology: the connections between quorum sensing and biofilms. *Trends in microbiology* **2005,** *13* (1), 27-33.
279. Flemming, H.-C.; Wingender, J., The biofilm matrix. *Nature reviews microbiology* **2010,** *8* (9), 623-633.
280. Hall-Stoodley, L.; Costerton, J. W.; Stoodley, P., Bacterial biofilms: from the natural environment to infectious diseases. *Nature reviews microbiology* **2004,** *2* (2), 95-108.
281. Hall-Stoodley, L.; Stoodley, P., Biofilm formation and dispersal and the transmission of human pathogens. *Trends in microbiology* **2005,** *13* (1), 7-10.
282. Sauer, K.; Cullen, M.; Rickard, A.; Zeef, L.; Davies, D. G.; Gilbert, P., Characterization of nutrient-induced dispersion in Pseudomonas aeruginosa PAO1 biofilm. *Journal of bacteriology* **2004,** *186* (21), 7312-7326.
283. Ikuma, K.; Decho, A. W.; Lau, B. L., When nanoparticles meet biofilms—interactions guiding the environmental fate and accumulation of nanoparticles. *Frontiers in microbiology* **2015,** *6*, 591.
284. Westmeier, D.; Hahlbrock, A.; Reinhardt, C.; Fröhlich-Nowoisky, J.; Wessler, S.; Vallet, C.; Pöschl, U.; Knauer, S.; Stauber, R., Nanomaterial–microbe cross-talk: physicochemical principles and (patho) biological consequences. *Chemical Society Reviews* **2018,** *47* (14), 5312-5337.
285. Peulen, T.-O.; Wilkinson, K. J., Diffusion of nanoparticles in a biofilm. *Environmental science & technology* **2011,** *45* (8), 3367-3373.
286. Flemming, H., Cohesiveness in biofilm matrix polymers. *Community structure and cooperation in biofilms* **2000**, 87-105.
287. Miller, K. P.; Wang, L.; Benicewicz, B. C.; Decho, A. W., Inorganic nanoparticles engineered to attack bacteria. *Chemical Society Reviews* **2015,** *44* (21), 7787-7807.
288. Lerner, R. N.; Lu, Q.; Zeng, H.; Liu, Y., The effects of biofilm on the transport of stabilized zerovalent iron nanoparticles in saturated porous media. *Water research* **2012,** *46* (4), 975-985.
289. Chen, J.; Andler, S. M.; Goddard, J. M.; Nugen, S. R.; Rotello, V. M., Integrating recognition elements with nanomaterials for bacteria sensing. *Chemical Society Reviews* **2017,** *46* (5), 1272-1283.
290. Koo, H.; Allan, R. N.; Howlin, R. P.; Stoodley, P.; Hall-Stoodley, L., Targeting microbial biofilms: current and prospective therapeutic strategies. *Nature Reviews Microbiology* **2017,** *15* (12), 740-755.
291. Benoit, D. S.; Koo, H., Targeted, triggered drug delivery to tumor and biofilm microenvironments. Future Medicine: 2016.
292. Barros, C. H.; Fulaz, S.; Stanisic, D.; Tasic, L., Biogenic nanosilver against multidrug-resistant bacteria (MDRB). *Antibiotics* **2018,** *7* (3), 69.
293. Tang, S.; Zheng, J., Antibacterial activity of silver nanoparticles: structural effects. *Advanced healthcare materials* **2018,** *7* (13), 1701503.
294. Ballottin, D.; Fulaz, S.; Cabrini, F.; Tsukamoto, J.; Duran, N.; Alves, O. L.; Tasic, L., Antimicrobial textiles: Biogenic silver nanoparticles against Candida and Xanthomonas. *Materials Science and Engineering: C* **2017,** *75*, 582-589.
295. Ballottin, D.; Fulaz, S.; Souza, M. L.; Corio, P.; Rodrigues, A. G.; Souza, A. O.; Gaspari, P. M.; Gomes, A. F.; Gozzo, F.; Tasic, L., Elucidating protein involvement in the stabilization of the biogenic silver nanoparticles. *Nanoscale research letters* **2016,** *11* (1), 1-9.
296. Fabrega, J.; Renshaw, J. C.; Lead, J. R., Interactions of silver nanoparticles with Pseudomonas putida biofilms. *Environmental science & technology* **2009,** *43* (23), 9004-9009.
297. Choi, O.; Yu, C.-P.; Fernández, G. E.; Hu, Z., Interactions of nanosilver with Escherichia coli cells in planktonic and biofilm cultures. *Water research* **2010,** *44* (20), 6095-6103.
298. Sheng, Z.; Liu, Y., Effects of silver nanoparticles on wastewater biofilms. *Water research* **2011,** *45* (18), 6039-6050.

299. Gliga, A. R.; Skoglund, S.; Wallinder, I. O.; Fadeel, B.; Karlsson, H. L., Size-dependent cytotoxicity of silver nanoparticles in human lung cells: the role of cellular uptake, agglomeration and Ag release. *Particle and fibre toxicology* **2014,** *11* (1), 1-17.
300. Carlson, C.; Hussain, S. M.; Schrand, A. M.; K. Braydich-Stolle, L.; Hess, K. L.; Jones, R. L.; Schlager, J. J., Unique cellular interaction of silver nanoparticles: size-dependent generation of reactive oxygen species. *The journal of physical chemistry B* **2008,** *112* (43), 13608-13619.
301. Chen, S.-F.; Zhang, H., Aggregation kinetics of nanosilver in different water conditions. *Advances in natural sciences: nanoscience and nanotechnology* **2012,** *3* (3), 035006.
302. Britto, J.; Gracelin, D.; Kumar, P., Antibacterial activity of silver nanoparticles synthesized from a few medicinal ferns. *Int J Pharm Res Dev* **2014,** *6*, 25-9.
303. Sharma, V. K., Aggregation and toxicity of titanium dioxide nanoparticles in aquatic environment—a review. *Journal of Environmental Science and Health Part A* **2009,** *44* (14), 1485-1495.
304. Oberdörster, E., Manufactured nanomaterials (fullerenes, C60) induce oxidative stress in the brain of juvenile largemouth bass. *Environmental health perspectives* **2004,** *112* (10), 1058-1062.
305. Jiang, Z.-J.; Liu, C.-Y.; Sun, L.-W., Catalytic properties of silver nanoparticles supported on silica spheres. *The Journal of Physical Chemistry B* **2005,** *109* (5), 1730-1735.
306. Petosa, A. R.; Jaisi, D. P.; Quevedo, I. R.; Elimelech, M.; Tufenkji, N., Aggregation and deposition of engineered nanomaterials in aquatic environments: role of physicochemical interactions. *Environmental science & technology* **2010,** *44* (17), 6532-6549.
307. Liu, W.; Wu, Y.; Wang, C.; Li, H. C.; Wang, T.; Liao, C. Y.; Cui, L.; Zhou, Q. F.; Yan, B.; Jiang, G. B., Impact of silver nanoparticles on human cells: effect of particle size. *Nanotoxicology* **2010,** *4* (3), 319-330.
308. Nel, A.; Xia, T.; Mädler, L.; Li, N., Toxic potential of materials at the nanolevel. *science* **2006,** *311* (5761), 622-627.
309. Akter, M.; Sikder, M. T.; Rahman, M. M.; Ullah, A. A.; Hossain, K. F. B.; Banik, S.; Hosokawa, T.; Saito, T.; Kurasaki, M., A systematic review on silver nanoparticles-induced cytotoxicity: Physicochemical properties and perspectives. *Journal of advanced research* **2018,** *9*, 1-16.
310. Mishra, A. R.; Zheng, J.; Tang, X.; Goering, P. L., Silver nanoparticle-induced autophagic-lysosomal disruption and NLRP3-inflammasome activation in HepG2 cells is size-dependent. *Toxicological Sciences* **2016,** *150* (2), 473-487.
311. Kaba, S. I.; Egorova, E. M., In vitro studies of the toxic effects of silver nanoparticles on HeLa and U937 cells. *Nanotechnology, science and applications* **2015,** *8*, 19.
312. Greulich, C.; Kittler, S.; Epple, M.; Muhr, G.; Köller, M., Studies on the biocompatibility and the interaction of silver nanoparticles with human mesenchymal stem cells (hMSCs). *Langenbeck's Archives of Surgery* **2009,** *394* (3), 495-502.
313. Park, E.-J.; Yi, J.; Kim, Y.; Choi, K.; Park, K., Silver nanoparticles induce cytotoxicity by a Trojan-horse type mechanism. *Toxicology in vitro* **2010,** *24* (3), 872-878.
314. Lankoff, A.; Sandberg, W. J.; Wegierek-Ciuk, A.; Lisowska, H.; Refsnes, M.; Sartowska, B.; Schwarze, P. E.; Meczynska-Wielgosz, S.; Wojewodzka, M.; Kruszewski, M., The effect of agglomeration state of silver and titanium dioxide nanoparticles on cellular response of HepG2, A549 and THP-1 cells. *Toxicology letters* **2012,** *208* (3), 197-213.
315. Le, A.-T.; Huy, P.; Tam, P. D.; Huy, T. Q.; Cam, P. D.; Kudrinskiy, A.; Krutyakov, Y. A., Green synthesis of finely-dispersed highly bactericidal silver nanoparticles via modified Tollens technique. *Current Applied Physics* **2010,** *10* (3), 910-916.
316. Arora, S.; Jain, J.; Rajwade, J.; Paknikar, K., Interactions of silver nanoparticles with primary mouse fibroblasts and liver cells. *Toxicology and applied pharmacology* **2009,** *236* (3), 310-318.
317. Sriram, M. I.; Kalishwaralal, K.; Barathmanikanth, S.; Gurunathani, S., Size-based cytotoxicity of silver nanoparticles in bovine retinal endothelial cells. *Nanoscience Methods* **2012,** *1* (1), 56-77.
318. Kaur, J.; Tikoo, K., Evaluating cell specific cytotoxicity of differentially charged silver nanoparticles. *Food and Chemical Toxicology* **2013,** *51*, 1-14.

319. Foldbjerg, R.; Dang, D. A.; Autrup, H., Cytotoxicity and genotoxicity of silver nanoparticles in the human lung cancer cell line, A549. *Archives of toxicology* **2011,** *85* (7), 743-750.
320. Kim, T. H.; Kim, M.; Park, H. S.; Shin, U. S.; Gong, M. S.; Kim, H. W., Size-dependent cellular toxicity of silver nanoparticles. *Journal of biomedical materials research Part A* **2012,** *100* (4), 1033-1043.
321. Arora, S.; Jain, J.; Rajwade, J.; Paknikar, K., Cellular responses induced by silver nanoparticles: in vitro studies. *Toxicology letters* **2008,** *179* (2), 93-100.
322. Kim, S.; Choi, J. E.; Choi, J.; Chung, K.-H.; Park, K.; Yi, J.; Ryu, D.-Y., Oxidative stress-dependent toxicity of silver nanoparticles in human hepatoma cells. *Toxicology in vitro* **2009,** *23* (6), 1076-1084.
323. Park, E.-J.; Yi, J.; Chung, K.-H.; Ryu, D.-Y.; Choi, J.; Park, K., Oxidative stress and apoptosis induced by titanium dioxide nanoparticles in cultured BEAS-2B cells. *Toxicology letters* **2008,** *180* (3), 222-229.
324. Stoehr, L. C.; Gonzalez, E.; Stampfl, A.; Casals, E.; Duschl, A.; Puntes, V.; Oostingh, G. J., Shape matters: effects of silver nanospheres and wires on human alveolar epithelial cells. *Particle and fibre toxicology* **2011,** *8* (1), 1-15.
325. Singh, R. P.; Ramarao, P., Cellular uptake, intracellular trafficking and cytotoxicity of silver nanoparticles. *Toxicology letters* **2012,** *213* (2), 249-259.
326. Hamilton, R. F.; Buckingham, S.; Holian, A., The effect of size on Ag nanosphere toxicity in macrophage cell models and lung epithelial cell lines is dependent on particle dissolution. *International journal of molecular sciences* **2014,** *15* (4), 6815-6830.
327. Piao, M. J.; Kang, K. A.; Lee, I. K.; Kim, H. S.; Kim, S.; Choi, J. Y.; Choi, J.; Hyun, J. W., Silver nanoparticles induce oxidative cell damage in human liver cells through inhibition of reduced glutathione and induction of mitochondria-involved apoptosis. *Toxicology letters* **2011,** *201* (1), 92-100.
328. Kittler, S.; Greulich, C.; Diendorf, J.; Koller, M.; Epple, M., Toxicity of silver nanoparticles increases during storage because of slow dissolution under release of silver ions. *Chemistry of materials* **2010,** *22* (16), 4548-4554.
329. Carrola, J.; Bastos, V.; Jarak, I.; Oliveira-Silva, R.; Malheiro, E.; Daniel-da-Silva, A. L.; Oliveira, H.; Santos, C.; Gil, A. M.; Duarte, I. F., Metabolomics of silver nanoparticles toxicity in HaCaT cells: structure–activity relationships and role of ionic silver and oxidative stress. *Nanotoxicology* **2016,** *10* (8), 1105-1117.
330. Aueviriyavit, S.; Phummiratch, D.; Maniratanachote, R., Mechanistic study on the biological effects of silver and gold nanoparticles in Caco-2 cells–induction of the Nrf2/HO-1 pathway by high concentrations of silver nanoparticles. *Toxicology letters* **2014,** *224* (1), 73-83.
331. Jiao, Z.-H.; Li, M.; Feng, Y.-X.; Shi, J.-C.; Zhang, J.; Shao, B., Hormesis effects of silver nanoparticles at non-cytotoxic doses to human hepatoma cells. *PloS one* **2014,** *9* (7), e102564.
332. Yilma, A. N.; Singh, S. R.; Dixit, S.; Dennis, V. A., Anti-inflammatory effects of silver-polyvinyl pyrrolidone (Ag-PVP) nanoparticles in mouse macrophages infected with live Chlamydia trachomatis. *International Journal of Nanomedicine* **2013,** *8*, 2421.
333. Kalishwaralal, K.; Banumathi, E.; Pandian, S. R. K.; Deepak, V.; Muniyandi, J.; Eom, S. H.; Gurunathan, S., Silver nanoparticles inhibit VEGF induced cell proliferation and migration in bovine retinal endothelial cells. *Colloids and Surfaces B: Biointerfaces* **2009,** *73* (1), 51-57.
334. Wang, J.; Rahman, M. F.; Duhart, H. M.; Newport, G. D.; Patterson, T. A.; Murdock, R. C.; Hussain, S. M.; Schlager, J. J.; Ali, S. F., Expression changes of dopaminergic system-related genes in PC12 cells induced by manganese, silver, or copper nanoparticles. *Neurotoxicology* **2009,** *30* (6), 926-933.
335. Haase, A.; Tentschert, J.; Jungnickel, H.; Graf, P.; Mantion, A.; Draude, F.; Plendl, J.; Goetz, M.; Galla, S.; Mašić, A. In *Toxicity of silver nanoparticles in human macrophages: uptake, intracellular distribution and cellular responses*, Journal of Physics: Conference Series, IOP Publishing: 2011; p 012030.
336. Mytych, J.; Zebrowski, J.; Lewinska, A.; Wnuk, M., Prolonged effects of silver nanoparticles on p53/p21 pathway-mediated proliferation, DNA damage response, and methylation parameters in HT22 hippocampal neuronal cells. *Molecular neurobiology* **2017,** *54* (2), 1285-1300.
337. Park, M. V.; Neigh, A. M.; Vermeulen, J. P.; de la Fonteyne, L. J.; Verharen, H. W.; Briedé, J. J.; van Loveren, H.; de Jong, W. H., The effect of particle size on the cytotoxicity, inflammation, developmental toxicity and genotoxicity of silver nanoparticles. *Biomaterials* **2011,** *32* (36), 9810-9817.

338. Travan, A.; Pelillo, C.; Donati, I.; Marsich, E.; Benincasa, M.; Scarpa, T.; Semeraro, S.; Turco, G.; Gennaro, R.; Paoletti, S., Non-cytotoxic silver nanoparticle-polysaccharide nanocomposites with antimicrobial activity. *Biomacromolecules* **2009,** *10* (6), 1429-1435.
339. Teeguarden, J. G.; Hinderliter, P. M.; Orr, G.; Thrall, B. D.; Pounds, J. G., Particokinetics in vitro: dosimetry considerations for in vitro nanoparticle toxicity assessments. *Toxicological sciences* **2007,** *95* (2), 300-312.
340. Lison, D.; Thomassen, L. C.; Rabolli, V.; Gonzalez, L.; Napierska, D.; Seo, J. W.; Kirsch-Volders, M.; Hoet, P.; Kirschhock, C. E.; Martens, J. A., Nominal and effective dosimetry of silica nanoparticles in cytotoxicity assays. *Toxicological sciences* **2008,** *104* (1), 155-162.
341. Lundqvist, M.; Stigler, J.; Elia, G.; Lynch, I.; Cedervall, T.; Dawson, K. A., Nanoparticle size and surface properties determine the protein corona with possible implications for biological impacts. *Proceedings of the National Academy of Sciences* **2008,** *105* (38), 14265-14270.
342. Ehrenberg, M. S.; Friedman, A. E.; Finkelstein, J. N.; Oberdörster, G.; McGrath, J. L., The influence of protein adsorption on nanoparticle association with cultured endothelial cells. *Biomaterials* **2009,** *30* (4), 603-610.
343. Kittler, S.; Greulich, C.; Gebauer, J.; Diendorf, J.; Treuel, L.; Ruiz, L.; Gonzalez-Calbet, J.; Vallet-Regi, M.; Zellner, R.; Köller, M., The influence of proteins on the dispersability and cell-biological activity of silver nanoparticles. *Journal of Materials Chemistry* **2010,** *20* (3), 512-518.
344. Bae, E.; Lee, B.-C.; Kim, Y.; Choi, K.; Yi, J., Effect of agglomeration of silver nanoparticle on nanotoxicity depression. *Korean Journal of Chemical Engineering* **2013,** *30* (2), 364-368.
345. Liu, H. H.; Surawanvijit, S.; Rallo, R.; Orkoulas, G.; Cohen, Y., Analysis of nanoparticle agglomeration in aqueous suspensions via constant-number Monte Carlo simulation. *Environmental science & technology* **2011,** *45* (21), 9284-9292.
346. Durán, N.; Silveira, C. P.; Durán, M.; Martinez, D. S. T., Silver nanoparticle protein corona and toxicity: a mini-review. *Journal of nanobiotechnology* **2015,** *13* (1), 1-17.
347. Yin, N.; Liu, Q.; Liu, J.; He, B.; Cui, L.; Li, Z.; Yun, Z.; Qu, G.; Liu, S.; Zhou, Q., Silver nanoparticle exposure attenuates the viability of rat cerebellum granule cells through apoptosis coupled to oxidative stress. *Small* **2013,** *9* (9-10), 1831-1841.
348. Braydich-Stolle, L.; Hussain, S.; Schlager, J. J.; Hofmann, M.-C., In vitro cytotoxicity of nanoparticles in mammalian germline stem cells. *Toxicological sciences* **2005,** *88* (2), 412-419.
349. Navya, P.; Daima, H. K., Rational engineering of physicochemical properties of nanomaterials for biomedical applications with nanotoxicological perspectives. *Nano Convergence* **2016,** *3* (1), 1-14.
350. Lesniak, A.; Fenaroli, F.; Monopoli, M. P.; Åberg, C.; Dawson, K. A.; Salvati, A., Effects of the presence or absence of a protein corona on silica nanoparticle uptake and impact on cells. *ACS nano* **2012,** *6* (7), 5845-5857.
351. Murugan, K.; Choonara, Y. E.; Kumar, P.; Bijukumar, D.; du Toit, L. C.; Pillay, V., Parameters and characteristics governing cellular internalization and trans-barrier trafficking of nanostructures. *International journal of nanomedicine* **2015,** *10*, 2191.
352. Jiang, X.; Foldbjerg, R.; Miclaus, T.; Wang, L.; Singh, R.; Hayashi, Y.; Sutherland, D.; Chen, C.; Autrup, H.; Beer, C., Multi-platform genotoxicity analysis of silver nanoparticles in the model cell line CHO-K1. *Toxicology letters* **2013,** *222* (1), 55-63.
353. van Aerle, R.; Lange, A.; Moorhouse, A.; Paszkiewicz, K.; Ball, K.; Johnston, B. D.; de-Bastos, E.; Booth, T.; Tyler, C. R.; Santos, E. M., Molecular mechanisms of toxicity of silver nanoparticles in zebrafish embryos. *Environmental science & technology* **2013,** *47* (14), 8005-8014.
354. Harvey, R. J.; Lund, V. J., Biofilms and chronic rhinosinusitis: systematic review of evidence, current concepts and directions for research. *Rhinology* **2007,** *45* (1), 3.
355. Behravan, M.; Panahi, A. H.; Naghizadeh, A.; Ziaee, M.; Mahdavi, R.; Mirzapour, A., Facile green synthesis of silver nanoparticles using Berberis vulgaris leaf and root aqueous extract and its antibacterial activity. *International journal of biological macromolecules* **2019,** *124*, 148-154.

356. Nilavukkarasi, M.; Vijayakumar, S.; Kumar, S. P., Biological synthesis and characterization of silver nanoparticles with Capparis zeylanica L. leaf extract for potent antimicrobial and anti proliferation efficiency. *Materials Science for Energy Technologies* **2020,** *3*, 371-376.
357. Hekmati, M.; Hasanirad, S.; Khaledi, A.; Esmaeili, D., Green synthesis of silver nanoparticles using extracts of Allium rotundum l, Falcaria vulgaris Bernh, and Ferulago angulate Boiss, and their antimicrobial effects in vitro. *Gene Reports* **2020,** *19*, 100589.
358. Richter, K.; Facal, P.; Thomas, N.; Vandecandelaere, I.; Ramezanpour, M.; Cooksley, C.; Prestidge, C. A.; Coenye, T.; Wormald, P.-J.; Vreugde, S. J. A. a. m.; interfaces, Taking the silver bullet colloidal silver particles for the topical treatment of biofilm-related infections. **2017,** *9* (26), 21631-21638.
359. Das, C. A.; Kumar, V. G.; Dhas, T. S.; Karthick, V.; Govindaraju, K.; Joselin, J. M.; Baalamurugan, J., Antibacterial activity of silver nanoparticles (biosynthesis): A short review on recent advances. *Biocatalysis and Agricultural Biotechnology* **2020**, 101593.
360. Siddiqi, K. S.; Husen, A.; Rao, R. A., A review on biosynthesis of silver nanoparticles and their biocidal properties. *Journal of nanobiotechnology* **2018,** *16* (1), 14.
361. Guzman, M.; Dille, J.; Godet, S., Synthesis and antibacterial activity of silver nanoparticles against gram-positive and gram-negative bacteria. *Nanomedicine: Nanotechnology, Biology and Medicine* **2012,** *8* (1), 37-45.
362. Alshehri, M. A.; Trivedi, S.; Alanazi, N. A.; Panneerselvam, C.; Baeshen, R.; Alatawi, A., One-step synthesis of ag nanoparticles using aqueous extracts from sundarbans mangroves revealed high toxicity on major mosquito vectors and microbial pathogens. *Journal of Cluster Science* **2020,** *31* (1), 177-184.
363. Kannan, R. R. R.; Arumugam, R.; Ramya, D.; Manivannan, K.; Anantharaman, P., Green synthesis of silver nanoparticles using marine macroalga Chaetomorpha linum. *Applied Nanoscience* **2013,** *3* (3), 229-233.
364. Wrótniak-Drzewiecka, W.; Gaikwad, S.; Laskowski, D.; Dahm, H.; Niedojadło, J.; Gade, A.; Rai, M., Novel approach towards synthesis of silver nanoparticles from Myxococcus virescens and their lethality on pathogenic bacterial cells. *Austin J Biotechnol Bioeng* **2014,** *1* (1), 7.
365. Hou, X.; Amais, R. S.; Jones, B. T.; Donati, G. L., Inductively coupled plasma optical emission spectrometry. *Encyclopedia of Analytical Chemistry: Applications, Theory and Instrumentation* **2006**, 1-25.
366. Okafor, F.; Janen, A.; Kukhtareva, T.; Edwards, V.; Curley, M., Green synthesis of silver nanoparticles, their characterization, application and antibacterial activity. *International journal of environmental research and public health* **2013,** *10* (10), 5221-5238.
367. Marinova, D.; Ribarova, F.; Atanassova, M., Total phenolics and total flavonoids in Bulgarian fruits and vegetables. *Journal of the university of chemical technology and metallurgy* **2005,** *40* (3), 255-260.
368. Beketov, E.; Pakhomov, V.; Nesterova, O., Improved method of flavonoid extraction from bird cherry fruits. *Pharmaceutical Chemistry Journal* **2005,** *39* (6), 316-318.
369. Albalasmeh, A. A.; Berhe, A. A.; Ghezzehei, T. A., A new method for rapid determination of carbohydrate and total carbon concentrations using UV spectrophotometry. *Carbohydrate polymers* **2013,** *97* (2), 253-261.
370. Palethorpe, H. M.; Drew, P. A.; Smith, E., Androgen signaling in esophageal adenocarcinoma cell lines in vitro. *Digestive diseases and sciences* **2017,** *62* (12), 3402-3414.
371. Clinical; Institute, L. S., Methods for dilution antimicrobial susceptibility tests for bacteria that grow aerobically. Clinical and Laboratory Standards Institute Wayne, PA: 2006.
372. Plum, G., Haemophilus influenzae Protocols. Methods in Molecular Medicine. *International Journal of Medical Microbiology* **2003,** *293* (4), 250.
373. Paseban, N.; Ghadam, P.; Pourhosseini, P. S., The Fluorescence Behavior and Stability of AgNPs Synthesized by Juglans Regia Green Husk Aqueous Extract. *International Journal of Nanoscience and Nanotechnology* **2019,** *15* (2), 117-126.
374. Ajitha, B.; Reddy, Y. A. K.; Reddy, P. S.; Jeon, H.-J.; Ahn, C. W., Role of capping agents in controlling silver nanoparticles size, antibacterial activity and potential application as optical hydrogen peroxide sensor. *RSC Advances* **2016,** *6* (42), 36171-36179.

375. Ravichandran, V.; Vasanthi, S.; Shalini, S.; Shah, S. A. A.; Tripathy, M.; Paliwal, N., Green synthesis, characterization, antibacterial, antioxidant and photocatalytic activity of Parkia speciosa leaves extract mediated silver nanoparticles. *Results in Physics* **2019,** *15*, 102565.
376. Pereira, T. M.; Polez, V. L. P.; Sousa, M. H.; Silva, L. P., Modulating physical, chemical, and biological properties of silver nanoparticles obtained by green synthesis using different parts of the tree Handroanthus heptaphyllus (Vell.) Mattos. *Colloid and Interface Science Communications* **2020,** *34*, 100224.
377. Cainelli, G.; Cardillo, G., *Chromium oxidations in organic chemistry*. Springer Science & Business Media: 2012; Vol. 19.
378. Wang, K.; Liu, Y.; Jin, X.; Chen, Z., Characterization of iron nanoparticles/reduced graphene oxide composites synthesized by one step eucalyptus leaf extract. *Environmental pollution* **2019,** *250*, 8-13.
379. Vecchio, M. G.; Loganes, C.; Minto, C., Beneficial and healthy properties of Eucalyptus plants: A great potential use. *The Open Agriculture Journal* **2016,** *10* (1).
380. Van Wyk, B.-E.; Wink, M., *Medicinal plants of the world*. CABI: 2018.
381. Valeriano, C.; De Oliveira, T. L. C.; De Carvalho, S. M.; das Graças Cardoso, M.; Alves, E.; Piccoli, R. H., The sanitizing action of essential oil-based solutions against Salmonella enterica serotype Enteritidis S64 biofilm formation on AISI 304 stainless steel. *Food Control* **2012,** *25* (2), 673-677.
382. Sebei, K.; Sakouhi, F.; Herchi, W.; Khouja, M. L.; Boukhchina, S., Chemical composition and antibacterial activities of seven Eucalyptus species essential oils leaves. *Biological research* **2015,** *48* (1), 7.
383. Silva, S. M.; Abe, S. Y.; Murakami, F. S.; Frensch, G.; Marques, F. A.; Nakashima, T., Essential oils from different plant parts of Eucalyptus cinerea F. Muell. ex Benth.(Myrtaceae) as a source of 1, 8-cineole and their bioactivities. *Pharmaceuticals* **2011,** *4* (12), 1535-1550.
384. Salehi, B.; Sharifi-Rad, J.; Quispe, C.; Llaique, H.; Villalobos, M.; Smeriglio, A.; Trombetta, D.; Ezzat, S. M.; Salem, M. A.; Zayed, A. M., Insights into Eucalyptus genus chemical constituents, biological activities and health-promoting effects. *Trends in Food Science & Technology* **2019**.
385. Feizi, S.; Taghipour, E.; Ghadam, P.; Mohammadi, P., Antifungal, antibacterial, antibiofilm and colorimetric sensing of toxic metals activities of eco friendly, economical synthesized Ag/AgCl nanoparticles using Malva sylvestris leaf extracts. *Microbial pathogenesis* **2018,** *125*, 33-42.
386. Frenking, G.; Tonner, R.; Klein, S.; Takagi, N.; Shimizu, T.; Krapp, A.; Pandey, K. K.; Parameswaran, P., New bonding modes of carbon and heavier group 14 atoms Si–Pb. *Chemical Society Reviews* **2014,** *43* (14), 5106-5139.
387. Badawy, A. M. E.; Luxton, T. P.; Silva, R. G.; Scheckel, K. G.; Suidan, M. T.; Tolaymat, T. M., Impact of environmental conditions (pH, ionic strength, and electrolyte type) on the surface charge and aggregation of silver nanoparticles suspensions. *Environmental science & technology* **2010,** *44* (4), 1260-1266.
388. Barhoum, A.; García-Betancourt, M. L.; Rahier, H.; Van Assche, G., Physicochemical characterization of nanomaterials: polymorph, composition, wettability, and thermal stability. In *Emerging Applications of Nanoparticles and Architecture Nanostructures*, Elsevier: 2018; pp 255-278.
389. Grosse, S.; Evje, L.; Syversen, T., Silver nanoparticle-induced cytotoxicity in rat brain endothelial cell culture. *Toxicology in vitro* **2013,** *27* (1), 305-313.
390. Ramezanpour, M.; Smith, J. L.; Psaltis, A. J.; Wormald, P. J.; Vreugde, S. In *In vitro safety evaluation of a povidone-iodine solution applied to human nasal epithelial cells*, International forum of allergy & rhinology, Wiley Online Library: 2020; pp 1141-1148.
391. Stoehr, L. C.; Gonzalez, E.; Stampfl, A.; Casals, E.; Duschl, A.; Puntes, V.; Oostingh, G. J., Shape matters: effects of silver nanospheres and wires on human alveolar epithelial cells. *Particle and fibre toxicology* **2011,** *8* (1), 36.
392. Khalandi, B.; Asadi, N.; Milani, M.; Davaran, S.; Abadi, A. J. N.; Abasi, E.; Akbarzadeh, A., A review on potential role of silver nanoparticles and possible mechanisms of their actions on bacteria. *Drug research* **2017,** *11* (02), 70-76.

393. Yun'an Qing, L. C.; Li, R.; Liu, G.; Zhang, Y.; Tang, X.; Wang, J.; Liu, H.; Qin, Y., Potential antibacterial mechanism of silver nanoparticles and the optimization of orthopedic implants by advanced modification technologies. *International journal of nanomedicine* **2018,** *13*, 3311.
394. Chatterjee, T.; Chatterjee, B. K.; Majumdar, D.; Chakrabarti, P., Antibacterial effect of silver nanoparticles and the modeling of bacterial growth kinetics using a modified Gompertz model. *Biochimica et Biophysica Acta (BBA)-General Subjects* **2015,** *1850* (2), 299-306.
395. Docter, D.; Westmeier, D.; Markiewicz, M.; Stolte, S.; Knauer, S.; Stauber, R., The nanoparticle biomolecule corona: lessons learned–challenge accepted? *Chemical Society Reviews* **2015,** *44* (17), 6094-6121.
396. Allison, D. G., *Community structure and co-operation in biofilms*. Cambridge University Press: 2000; Vol. 59.
397. Regiel-Futyra, A.; Dąbrowski, J. M.; Mazuryk, O.; Śpiewak, K.; Kyzioł, A.; Pucelik, B.; Brindell, M.; Stochel, G., Bioinorganic antimicrobial strategies in the resistance era. *Coordination Chemistry Reviews* **2017,** *351*, 76-117.
398. Hussain, A.; Alajmi, M. F.; Khan, M. A.; Pervez, S. A.; Ahmed, F.; Amir, S.; Husain, F. M.; Khan, M. S.; Shaik, G. M.; Hassan, I., Biosynthesized silver nanoparticle (AgNP) from Pandanus odorifer leaf extract exhibits anti-metastasis and anti-biofilm potentials. *Frontiers in microbiology* **2019,** *10*, 8.
399. Di Giulio, M.; Di Bartolomeo, S.; Di Campli, E.; Sancilio, S.; Marsich, E.; Travan, A.; Cataldi, A.; Cellini, L., The effect of a silver nanoparticle polysaccharide system on streptococcal and saliva-derived biofilms. *International journal of molecular sciences* **2013,** *14* (7), 13615-13625.
400. Singh, P.; Pandit, S.; Beshay, M.; Mokkapati, V.; Garnaes, J.; Olsson, M. E.; Sultan, A.; Mackevica, A.; Mateiu, R. V.; Lütken, H., Anti-biofilm effects of gold and silver nanoparticles synthesized by the Rhodiola rosea rhizome extracts. *Artificial cells, nanomedicine, and biotechnology* **2018,** *46* (sup3), S886-S899.
401. Liao, C.; Li, Y.; Tjong, S. C., Bactericidal and cytotoxic properties of silver nanoparticles. *International journal of molecular sciences* **2019,** *20* (2), 449.
402. Ferdous, Z.; Beegam, S.; Tariq, S.; Ali, B. H.; Nemmar, A., The in vitro effect of polyvinylpyrrolidone and citrate coated silver nanoparticles on erythrocytic oxidative damage and eryptosis. *Cellular Physiology and Biochemistry* **2018,** *49* (4), 1577-1588.
403. Hwang, I.-s.; Hwang, J. H.; Choi, H.; Kim, K.-J.; Lee, D. G., Synergistic effects between silver nanoparticles and antibiotics and the mechanisms involved. *Journal of medical microbiology* **2012,** *61* (12), 1719-1726.
404. Swami, A.; Mirlekar, K.; Baveja, S., Individual and Combined Efficacy of Silver Nanoparticles and Different Antibiotics against Multidrug-Resistant Clinical Isolates.
405. Venkatesan, J.; Kim, S.-K.; Shim, M. S., Antimicrobial, antioxidant, and anticancer activities of biosynthesized silver nanoparticles using marine algae Ecklonia cava. *Nanomaterials* **2016,** *6* (12), 235.
406. Rai, M. K.; Deshmukh, S.; Ingle, A.; Gade, A., Silver nanoparticles: the powerful nanoweapon against multidrug-resistant bacteria. *Journal of applied microbiology* **2012,** *112* (5), 841-852.
407. Mazur, P.; Skiba-Kurek, I.; Mrowiec, P.; Karczewska, E.; Drożdż, R., Synergistic ROS-Associated Antimicrobial Activity of Silver Nanoparticles and Gentamicin Against Staphylococcus epidermidis. *International Journal of Nanomedicine* **2020,** *15*, 3551-3562.
408. Vazquez-Muñoz, R.; Meza-Villezcas, A.; Fournier, P.; Soria-Castro, E.; Juarez-Moreno, K.; Gallego-Hernández, A.; Bogdanchikova, N.; Vazquez-Duhalt, R.; Huerta-Saquero, A., Enhancement of antibiotics antimicrobial activity due to the silver nanoparticles impact on the cell membrane. *PloS one* **2019,** *14* (11), e0224904.
409. Shahverdi, A. R.; Fakhimi, A.; Shahverdi, H. R.; Minaian, S., Synthesis and effect of silver nanoparticles on the antibacterial activity of different antibiotics against Staphylococcus aureus and Escherichia coli. *Nanomedicine: Nanotechnology, Biology and Medicine* **2007,** *3* (2), 168-171.
410. De Souza, A.; Mehta, D.; Leavitt, R., Bactericidal activity of combinations of Silver–Water Dispersion TM with 19 antibiotics against seven microbial strains. *Current Science* **2006**, 926-929.

411. Fayaz, A. M.; Balaji, K.; Girilal, M.; Yadav, R.; Kalaichelvan, P. T.; Venketesan, R., Biogenic synthesis of silver nanoparticles and their synergistic effect with antibiotics: a study against gram-positive and gram-negative bacteria. *Nanomedicine: Nanotechnology, Biology and Medicine* **2010,** *6* (1), 103-109.
412. Li, P.; Li, J.; Wu, C.; Wu, Q.; Li, J., Synergistic antibacterial effects of β-lactam antibiotic combined with silver nanoparticles. *Nanotechnology* **2005,** *16* (9), 1912.
413. Feizi, S.; Cooksley, C. M.; Bouras, G. S.; Prestidge, C. A.; Coenye, T.; Psaltis, A. J.; Wormald, P.-J.; Vreugde, S., Colloidal silver combating pathogenic Pseudomonas aeruginosa and MRSA in chronic rhinosinusitis. *Colloids and Surfaces B: Biointerfaces* **2021**, 111675.
414. CLSI, W., Clinical and laboratory standards institute methods for dilution antimicrobial susceptibility tests for bacteria that grow aerobically. *Approve Standard M7-A7, CLSI, seventh ed, PA, USA* **2006**.
415. Richter, K.; Ramezanpour, M.; Thomas, N.; Prestidge, C. A.; Wormald, P. J.; Vreugde, S. In *Mind "De GaPP": in vitro efficacy of deferiprone and gallium-protoporphyrin against Staphylococcus aureus biofilms*, International forum of allergy & rhinology, Wiley Online Library: 2016; pp 737-743.
416. Sueke, H.; Kaye, S. B.; Neal, T.; Hall, A.; Tuft, S.; Parry, C. M., An in vitro investigation of synergy or antagonism between antimicrobial combinations against isolates from bacterial keratitis. *Investigative ophthalmology & visual science* **2010,** *51* (8), 4151-4155.
417. Rajkumari, N.; Mathur, P.; Bhardwaj, N.; Gupta, G.; Dahiya, R.; Behera, B.; Misra, M. C., Resistance pattern of mupirocin in methicillin-resistant Staphylococcus aureus in trauma patients and comparison between disc diffusion and E-test for better detection of resistance in low resource countries. *Journal of laboratory physicians* **2014,** *6* (2), 91.
418. Panáček, A.; Smékalová, M.; Večeřová, R.; Bogdanová, K.; Röderová, M.; Kolář, M.; Kilianová, M.; Hradilová, Š.; Froning, J. P.; Havrdová, M., Silver nanoparticles strongly enhance and restore bactericidal activity of inactive antibiotics against multiresistant Enterobacteriaceae. *Colloids and Surfaces B: Biointerfaces* **2016,** *142*, 392-399.
419. Thomas, R.; Jishma, P.; Snigdha, S.; Soumya, K.; Mathew, J.; Radhakrishnan, E., Enhanced antimicrobial efficacy of biosynthesized silver nanoparticle based antibiotic conjugates. *Inorganic Chemistry Communications* **2020,** *117*, 107978.
420. Sullivan, G. J.; Delgado, N. N.; Maharjan, R.; Cain, A. K., How antibiotics work together: Molecular mechanisms behind combination therapy. *Current Opinion in Microbiology* **2020,** *57*, 31-40.
421. Hashim, N.; Paramasivam, M.; Tan, J. S.; Kernain, D.; Hussin, M. H.; Brosse, N.; Gambier, F.; Raja, P. B., Green mode synthesis of silver nanoparticles using Vitis vinifera's tannin and screening its antimicrobial activity/apoptotic potential versus cancer cells. *Materials Today Communications* **2020,** *25*, 101511.
422. Kalyani, R. L.; Vijaykumar, P.; Pammi, S.; Rajkumar, M.; Swamy, P.; Murthy, K., Biosynthesis of Silver Nanoparticles using Annona squamosa Leaf Extract with Synergistic Antibacterial Activity. *Indian Journal of Pharmaceutical Sciences* **2019,** *81* (6), 1036-1044.
423. Habash, M. B.; Goodyear, M. C.; Park, A. J.; Surette, M. D.; Vis, E. C.; Harris, R. J.; Khursigara, C. M., Potentiation of tobramycin by silver nanoparticles against Pseudomonas aeruginosa biofilms. *Antimicrobial agents and chemotherapy* **2017,** *61* (11).
424. Morones-Ramirez, J. R.; Winkler, J. A.; Spina, C. S.; Collins, J. J., Silver enhances antibiotic activity against gram-negative bacteria. *Science translational medicine* **2013,** *5* (190), 190ra81-190ra81.
425. Thirumurugan, G.; Seshagiri Rao, J. V.; Dhanaraju, M. D., Elucidating pharmacodynamic interaction of silver nanoparticle - topical deliverable antibiotics. *Sci Rep* **2016,** *6*, 29982.
426. Siddique, M. H.; Aslam, B.; Imran, M.; Ashraf, A.; Nadeem, H.; Hayat, S.; Khurshid, M.; Afzal, M.; Malik, I. R.; Shahzad, M., Effect of Silver Nanoparticles on Biofilm Formation and EPS Production of Multidrug-Resistant Klebsiella pneumoniae. *BioMed Research International* **2020,** *2020*.
427. Katva, S.; Das, S.; Moti, H. S.; Jyoti, A.; Kaushik, S., Antibacterial synergy of silver nanoparticles with gentamicin and chloramphenicol against Enterococcus faecalis. *Pharmacognosy magazine* **2017,** *13* (Suppl 4), S828.

428. Cho, D.-Y.; Hunter, R. C.; Ramakrishnan, V. R., The Microbiome and Chronic Rhinosinusitis. *Immunology and Allergy Clinics* **2020,** *40* (2), 251-263.
429. Ferdous, Z.; Nemmar, A., Health Impact of Silver Nanoparticles: A Review of the Biodistribution and Toxicity Following Various Routes of Exposure. *International Journal of Molecular Sciences* **2020,** *21* (7), 2375.
430. Lee, Y. S.; Kim, D. W.; Lee, Y. H.; Oh, J. H.; Yoon, S.; Choi, M. S.; Lee, S. K.; Kim, J. W.; Lee, K.; Song, C.-W., Silver nanoparticles induce apoptosis and G2/M arrest via PKCζ-dependent signaling in A549 lung cells. *Archives of toxicology* **2011,** *85* (12), 1529-1540.
431. De Matteis, V.; Malvindi, M. A.; Galeone, A.; Brunetti, V.; De Luca, E.; Kote, S.; Kshirsagar, P.; Sabella, S.; Bardi, G.; Pompa, P. P., Negligible particle-specific toxicity mechanism of silver nanoparticles: the role of Ag+ ion release in the cytosol. *Nanomedicine: Nanotechnology, Biology and Medicine* **2015,** *11* (3), 731-739.
432. Wang, X.; Ji, Z.; Chang, C. H.; Zhang, H.; Wang, M.; Liao, Y. P.; Lin, S.; Meng, H.; Li, R.; Sun, B., Use of coated silver nanoparticles to understand the relationship of particle dissolution and bioavailability to cell and lung toxicological potential. *Small* **2014,** *10* (2), 385-398.
433. Gliga, A. R.; Di Bucchianico, S.; Lindvall, J.; Fadeel, B.; Karlsson, H. L., RNA-sequencing reveals long-term effects of silver nanoparticles on human lung cells. *Scientific reports* **2018,** *8* (1), 1-14.
434. Gaiser, B. K.; Hirn, S.; Kermanizadeh, A.; Kanase, N.; Fytianos, K.; Wenk, A.; Haberl, N.; Brunelli, A.; Kreyling, W. G.; Stone, V., Effects of silver nanoparticles on the liver and hepatocytes in vitro. *toxicological sciences* **2013,** *131* (2), 537-547.
435. Xue, Y.; Zhang, T.; Zhang, B.; Gong, F.; Huang, Y.; Tang, M., Cytotoxicity and apoptosis induced by silver nanoparticles in human liver HepG2 cells in different dispersion media. *Journal of Applied Toxicology* **2016,** *36* (3), 352-360.
436. Ramezanpour, M.; Bolt, H.; Psaltis, A. J.; Wormald, P.-J.; Vreugde, S., Primary human nasal epithelial cells: a source of poly (I: C) LMW-induced IL-6 production. *Scientific reports* **2018,** *8* (1), 1-8.
437. Bennett, C.; Ramezanpour, M.; Cooksley, C.; Vreugde, S.; Psaltis, A. J. In *Kappa-carrageenan sinus rinses reduce inflammation and intracellular Staphylococcus aureus infection in airway epithelial cells*, International forum of allergy & rhinology, Wiley Online Library: 2019; pp 918-925.
438. Panchatcharam, B. S.; Cooksley, C. M.; Ramezanpour, M.; Vediappan, R. S.; Bassiouni, A.; Wormald, P. J.; Psaltis, A. J.; Vreugde, S. In *Staphylococcus aureus biofilm exoproteins are cytotoxic to human nasal epithelial barrier in chronic rhinosinusitis*, International Forum of Allergy & Rhinology, Wiley Online Library: 2020.
439. Kao, S. S. T.; Ramezanpour, M.; Bassiouni, A.; Wormald, P. J.; Psaltis, A. J.; Vreugde, S. In *The effect of neutrophil serine proteases on human nasal epithelial cell barrier function*, International Forum of Allergy & Rhinology, Wiley Online Library: 2019; pp 1220-1226.
440. Murphy, J.; Ramezanpour, M.; Drilling, A.; Roscioli, E.; Psaltis, A. J.; Wormald, P. J.; Vreugde, S. In *In vitro characteristics of an airway barrier-disrupting factor secreted by Staphylococcus aureus*, International forum of allergy & rhinology, Wiley Online Library: 2019; pp 187-196.
441. Plumb, J., Cell sensitivity assays: the MTT assay. *Methods in molecular medicine* **1999,** *28*, 25-30.
442. Murphy, J.; Ramezanpour, M.; Stach, N.; Dubin, G.; Psaltis, A. J.; Wormald, P. J.; Vreugde, S., Staphylococcus Aureus V8 protease disrupts the integrity of the airway epithelial barrier and impairs IL-6 production in vitro. *The Laryngoscope* **2018,** *128* (1), E8-E15.
443. Ramezanpour, M.; Murphy, J.; Smith, J. L.; Vreugde, S.; Psaltis, A. J. In *In vitro safety evaluation of human nasal epithelial cell monolayers exposed to carrageenan sinus wash*, International forum of allergy & rhinology, Wiley Online Library: 2017; pp 1170-1177.
444. Van Itallie, C. M.; Holmes, J.; Bridges, A.; Gookin, J. L.; Coccaro, M. R.; Proctor, W.; Colegio, O. R.; Anderson, J. M., The density of small tight junction pores varies among cell types and is increased by expression of claudin-2. *Journal of cell science* **2008,** *121* (3), 298-305.
445. Anderson, J. M.; Van Itallie, C. M., Physiology and function of the tight junction. *Cold Spring Harbor perspectives in biology* **2009,** *1* (2), a002584.

446. Srinivasan, B.; Kolli, A. R.; Esch, M. B.; Abaci, H. E.; Shuler, M. L.; Hickman, J. J., TEER measurement techniques for in vitro barrier model systems. *Journal of laboratory automation* **2015,** *20* (2), 107-126.
447. Chin, E.; Goh, E., Blood–brain barrier on a chip. In *Methods in cell biology*, Elsevier: 2018; Vol. 146, pp 159-182.
448. Williams, K. M.; Gokulan, K.; Cerniglia, C. E.; Khare, S., Size and dose dependent effects of silver nanoparticle exposure on intestinal permeability in an in vitro model of the human gut epithelium. *Journal of nanobiotechnology* **2016,** *14* (1), 62.
449. Cohen, I.; Rider, P.; Carmi, Y.; Braiman, A.; Dotan, S.; White, M. R.; Voronov, E.; Martin, M. U.; Dinarello, C. A.; Apte, R. N., Differential release of chromatin-bound IL-1α discriminates between necrotic and apoptotic cell death by the ability to induce sterile inflammation. *Proceedings of the National Academy of Sciences* **2010,** *107* (6), 2574-2579.
450. David, L.; Moldovan, B.; Vulcu, A.; Olenic, L.; Perde-Schrepler, M.; Fischer-Fodor, E.; Florea, A.; Crisan, M.; Chiorean, I.; Clichici, S., Green synthesis, characterization and anti-inflammatory activity of silver nanoparticles using European black elderberry fruits extract. *Colloids and Surfaces B: Biointerfaces* **2014,** *122*, 767-777.
451. Lava, M.; Muddapur, U. M.; Basavegowda, N.; More, S. S.; More, V. S., Characterization, anticancer, antibacterial, anti-diabetic and anti-inflammatory activities of green synthesized silver nanoparticles using Justica wynaadensis leaves extract. *Materials Today: Proceedings* **2020**.
452. Krajewska, J. B.; Długosz, O.; Sałaga, M.; Banach, M.; Fichna, J., Silver nanoparticles based on blackcurrant extract show potent anti-inflammatory effect in vitro and in DSS-induced colitis in mice. *International journal of pharmaceutics* **2020,** *585*, 119549.
453. Hebeish, A.; El-Rafie, M.; El-Sheikh, M.; Seleem, A. A.; El-Naggar, M. E., Antimicrobial wound dressing and anti-inflammatory efficacy of silver nanoparticles. *International journal of biological macromolecules* **2014,** *65*, 509-515.
454. Tratnjek, L.; Kreft, M.; Kristan, K.; Kreft, M. E., Ciliary beat frequency of in vitro human nasal epithelium measured with the simple high-speed microscopy is applicable for safety studies of nasal drug formulations. *Toxicology in Vitro* **2020**, 104865.
455. Balasubramanian, S. K.; Poh, K.-W.; Ong, C.-N.; Kreyling, W. G.; Ong, W.-Y.; Liya, E. Y., The effect of primary particle size on biodistribution of inhaled gold nano-agglomerates. *Biomaterials* **2013,** *34* (22), 5439-5452.
456. Elder, A.; Gelein, R.; Silva, V.; Feikert, T.; Opanashuk, L.; Carter, J.; Potter, R.; Maynard, A.; Ito, Y.; Finkelstein, J., Translocation of inhaled ultrafine manganese oxide particles to the central nervous system. *Environmental health perspectives* **2006,** *114* (8), 1172-1178.
457. Hopkins, L. E.; Patchin, E. S.; Chiu, P.-L.; Brandenberger, C.; Smiley-Jewell, S.; Pinkerton, K. E., Nose-to-brain transport of aerosolised quantum dots following acute exposure. *Nanotoxicology* **2014,** *8* (8), 885-893.
458. Kao, Y.-Y.; Cheng, T.-J.; Yang, D.-M.; Wang, C.-T.; Chiung, Y.-M.; Liu, P.-S., Demonstration of an olfactory bulb–brain translocation pathway for ZnO nanoparticles in rodent cells in vitro and in vivo. *Journal of Molecular Neuroscience* **2012,** *48* (2), 464-471.
459. Moshkin, M. P.; Petrovski, D.; Akulov, A.; Romashchenko, A.; Gerlinskaya, L.; Ganimedov, V.; Muchnaya, M.; Sadovsky, A.; Koptyug, I.; Savelov, A., Nasal aerodynamics protects brain and lung from inhaled dust in subterranean diggers, Ellobius talpinus. *Proceedings of the Royal Society B: Biological Sciences* **2014,** *281* (1792), 20140919.
460. Oberdörster, G.; Sharp, Z.; Atudorei, V.; Elder, A.; Gelein, R.; Kreyling, W.; Cox, C., Translocation of inhaled ultrafine particles to the brain. *Inhalation toxicology* **2004,** *16* (6-7), 437-445.
461. Sunderman, F. W., Nasal toxicity, carcinogenicity, and olfactory uptake of metals. *Annals of Clinical & Laboratory Science* **2001,** *31* (1), 3-24.
462. Yu, L. E.; Lanry Yung, L.-Y.; Ong, C.-N.; Tan, Y.-L.; Suresh Balasubramaniam, K.; Hartono, D.; Shui, G.; Wenk, M. R.; Ong, W.-Y., Translocation and effects of gold nanoparticles after inhalation exposure in rats. *Nanotoxicology* **2007,** *1* (3), 235-242.

463. Hay, M.; Thomas, D. W.; Craighead, J. L.; Economides, C.; Rosenthal, J., Clinical development success rates for investigational drugs. *Nature biotechnology* **2014,** *32* (1), 40-51.
464. Domínguez, A. V.; Algaba, R. A.; Canturri, A. M.; Villodres, Á. R.; Smani, Y., Antibacterial activity of colloidal silver against gram-negative and gram-positive bacteria. *Antibiotics* **2020,** *9* (1).